Voltage Management of Networks with Distributed Generation.

James O'Donnell

A thesis submitted for the degree of Doctor of Philosophy.
The University of Edinburgh.
September 2007

Abstract

At present there is much debate about the impacts and benefits of increasing the amount of generation connected to the low voltage areas of the electricity distribution network. The UK government is under political pressure to diversify energy sources for environmental reasons, for long-term sustainability and to buffer the potential insecurity of uncertain international energy markets. UK Distribution Network Operators (DNOs) are processing large numbers of applications to connect significant amounts of Distributed Generation (DG). DNOs hold statutory responsibility to preserve supply quality and must screen the DG applications for their impact on the network. The DNOs often require network upgrades or DG curtailment, reducing the viability of proposed projects.

Many studies exist that identify barriers to the widespread connection of DG. Among them are: suitability of existing protection equipment; rating of existing lines and equipment; impact in terms of expanded voltage envelope and increased harmonic content; conflict with automatic voltage regulating equipment. These barriers can be overcome by expensive upgrades of the distribution network or the expensive deep connection of DG to the higher voltage, sub-transmission network.

This work identifies changes in network operating practice that could allow the connection of more DG without costly upgrades. The thesis reported is that adopting options for a more openly managed, actively controlled, distribution network can allow increased DG capacity without upgrades.

Simulations have been performed showing DG connected with wind farm production time series to a representative section of the Scottish distribution network. The simulations include modelling of voltage regulation by network equipment and/or new generation. The cost and effects of the consequent network behaviour evaluated in monetary terms are reported. Alternative control strategies are shown and recommended, to reduce DNO operation and maintenance costs and the cost of connection to the developer with no reduction in supply quality.

Declaration of originality

I hereby declare that the research recorded in this thesis and the thesis itself was composed and originated entirely by myself in the School of Engineering and Electronics at The University of Edinburgh.

James O’Donnell

Acknowledgements

I thank Professor Robin Wallace for his continual support and enthusiasm for this project and on a more personal level the moral support he provided. I thank Dr Gareth Harrison for his ability to focus my work and for his help in preparing this thesis. Also crucial was Dr Aristides Kiprakis with whom I discussed my work. Aristides provided a valuable sounding board for ideas at the early stages of the project.

Other members of the Institute for Energy Systems have provided key criticisms and support that have shaped the presentation and ensured the thoroughness of the work. These include Dr David Ingram, Prof. Janusz Bialek, Prof. Alan Murray, Dr Vengatesan Venugopal, Dr Sasa Djokic and Dr Alan Smaill.

I thank all colleagues at the Institute for creating a stimulating working environment, as well as for their friendship. In particular, for their discussion of my work and their own, I thank Ally Price, Dr Thomas Boehme, Dr Jo Zhou, Dr Panagis Vovos, Alasdair McDonald, Dr Mark Winskel, Dr Nando Ochoa, Dr Sarah Graham, Dr Simon Forrest and Dr Richard Loh.

Contents

List of figures

List of tables

Acronyms and abbreviations

The following are equivalent though ULTC is preferred in this text:

LTC	Load Tap Changer
ULTC	Under Load Tap Changer
OLTC	On Load Tap Changer
TCUL	Tap Changer Under Load
DNO	Distribution Network Operator
TSO	Transmission System Operator
GSP	Grid Supply Point
LV	Low Voltage ($<$33kV), alternatively used to denote the lower voltage side of a ULTC
MV	Medium Voltage (33kV$\geq$MV$<$132kV)
HV	High Voltage ($\geq$132kV), alternatively used to denote the higher voltage side of a ULTC
EHV	Extra High Voltage ($>$300kV)
FACTS	Flexible Alternating Current Transmission System
STATCOM	Static Synchronous Compensator
SVC	Static Var Compensator
AVR	Automatic Voltage Regulator
AVC	Automatic Voltage Control
CHP	Combined Heat and Power
DG	Distributed Generation
PSSE	Power System Simulator for Engineering
API	Application Programming Interface
ARMA	Auto-regressive moving-average
D&G	Dumfries and Galloway

Nomenclature and Glossary

N_{TC}	The number of tap-change operations.
$ULTC^{code}_{GSP/P}$	Under Load Tap Changer named by a code according to diagrams. GSP/P denotes a grid transformer/primary transformer respectively.
$X^{\pm}$	A power factor range between X leading and X lagging inclusive.
DG_{max}	The base scenario defining the amount of DG capacity connected to each feeder.
$DGfactor$	A factor applied to DG_{max} to vary the connected DG capacity.

Chapter 1
Introduction

1.1 Project motivation

This study was conceived during a period of debate about the desirability and means of connection of large amounts of renewable generation. The pressure for more renewable generation arises from many factors. The UK and Scottish parliaments both support renewable energy as part of a long-term strategy to deal with increasing UK and global energy demands [1] coupled with increasing awareness of the negative impacts of fossil-fuel based generation. The combustion of fossil-fuels inevitably release carbon dioxide (CO_2) into the atmosphere which has been linked to the negative consequences of global warming and associated sea-level rise and climate change [2]. An increased diversity of energy supply also helps insulate the UK from price variations of fuel imports.

Renewable generation thus attracts financial and trading concessions from the UK government and is currently seen as an excellent investment opportunity. Onshore wind generation is the majority source of new renewable projects. The environmental impact and perceived high profitability combines to create local resistance of not only the construction of the generation plant itself, but also to the upgrades in network infrastructure required to connect the new plant. Infrastructure upgrades also add to the total cost of the energy generated whether the cost is borne by the network operators or the electricity generators themselves.

By its nature, renewable energy resources are geographically dispersed and are often distant from the higher voltage transmission network that most efficiently carries the generated energy. Potential renewable plant is, however, often close to lower voltage lines which are part of the distribution network. These distribution networks are managed by Distribution Network Operators (DNOs) who hold statutory responsibility to preserve supply quality and must screen the new generator applications for their impact on the network. The DNOs often

require network upgrades or distributed generation (DG) curtailment, reducing the viability of proposed projects.

One of the objections to connection of DG at lower voltages is its effect on local voltage profiles and its impact on a network equipment used to control voltages at the distribution level, specifically the under-load tap-changing transformer (ULTC). There is a lack of published research that quantifies the real impact of DG on ULTCs and the resultant cost to the DNO in terms of equipment maintenance and in terms of voltage rise and fluctuations.

The work was inspired by two ongoing areas of work within the Institute for Energy Systems at the University of Edinburgh. The first was the use of optimal power flow techniques to study the maximal connection of generation in an example rural network [3, 4]. The second work designed and modelled a novel reactive power controller for a distributed generator to maximise the capacity that could be connected to existing networks without detriment to voltage quality [5, 6].

1.2 Project objectives

The project sought to increase understanding of the costs and operational changes associated with the connection of variable power output generation connected to the distribution network. With this increased knowledge, the use of existing equipment and lines can be maximised with the result of lower connection and use-of-system charges. With lower associated costs, more developments will become feasible allowing greater choice for developers and utilities regarding the best locations for plant; and where the market exists and planning authorities allow, a greater penetration of renewable plant.

The project objectives are summarised as follows:

- Create a method for the power-flow simulation of a distribution network over time.
- Estimate increased maintenance costs of transformers due to variable DG.
- Quantify effect of increased variable DG on voltage control.

- Identify strategies to maximise benefit of increased variable DG.

1.3 Thesis and contribution to knowledge

The thesis of this study was that the additional operation and cost to the network operator of ULTC voltage control as a result of increased distributed generation can be acceptably small using existing equipment and revised control of the DG.

The operation of selected DG in voltage control mode has been shown to be preferable to constant power factor mode. Importantly, the voltage control mode does not cause the currently perceived extent of conflict with transformer operation or result in dependency on the DG for voltage control. This allows the DNO the option to require or allow new DG in voltage control mode as part of its distribution network voltage control strategy.

In demonstrating the operation of ULTCs over time, a novel simulation method is reported allowing for future work to incorporate more complex components such as agent-based controllers and thermal constraint modelling.

The contributions to knowledge are summarised as follows:

- DG can be operated in PV mode with conflicating with ULTCs.
- PV mode operation of DG results in better voltage management than when in PQ mode.
- The maintenance cost due to increased operation of ULTCs due to time-varying DG is low relative to energy revenues and the capital cost of new equipment.

1.4 Thesis outline

Chapter 2 outlines the negative and positive impacts of increased renewable generation connected in the distribution network followed by a more detailed consideration of voltage control in the distribution network and tap-changing transformer operation. Chapter 3 describes how the operation of tap-changing transformers is modelled over time using a

combination of a commercial power flow solver and custom modules coded in Python. The outcomes of simulations are shown to match expected system behaviour in Chapter 4.

Chapters 5 and 6 demonstrate network behaviour and tap-changer operation in response to large amounts of distributed generation (DG). Chapter 5 employs DG in fixed power factor mode only whereas Chapter 6 uses active power control and voltage control algorithms to improve network voltages. The conclusions of this study are reported and discussed in Chapter 7 with a summary of findings with respect to the original thesis and a number of applications for the methods shown in this study in further research.

Chapter 2
Distributed Generation in Future Distribution Networks

This chapter highlights the reasons for the connection of generation in the distribution network and the negative and positive impacts it can have on network operation and control. The effect of distributed generation on voltage control is identified as a significant limitation on the amount of new capacity that can be connected. A summary of the types of generation and their impact on voltage is given. The Under-Load Tap-Changing transformer (ULTC) is currently the primary means of voltage control in the distribution network and strategies of its operation are detailed.

2.1 Increasing Distributed Generation

At present there is much attention being paid to the impacts of increasing amount of small-scale generation connected to the electricity supply network at the distribution level. The target for the amount of Scotland's generation to come from renewable resources by 2010 is set at 18% [7]. The Scottish Parliament in 2005 reported that exceeding this target of connecting new renewables would not be possible due to availability of connections with 950 MW of onshore wind already having consent [8]. Power providers worldwide have acknowledged there will be significant increased generation connected at low voltages [9] in the future.

This study focused on activities in Scotland and the UK but will reference papers relating to networks in other countries and has relevance to such networks.

2.1.1 Distributed Generation

The paradigm for the electricity supply network in the 20th century in most countries, such as the UK, is for large generators to be connected centrally to the high voltage transmission network [10, 11]. The transmission network is for bulk inter-regional transfer of electrical energy and is well interconnected.

Consumers are connected to the transmission network via lower voltage networks collectively called the distribution network. These low and medium voltage networks are largely connected to each other, connecting to the transmission network at a few grid supply points (GSPs) [12]. In general, the resistance of the distribution lines dominates its reactance as lower voltages and lighter lines are used towards the extremes of the network. This has implications for the effect of the amount of additional generation capacity that can be connected at this level; this is explored in Chapter 4.

Distributed Generation (DG) is that which is connected to the distribution network and will often be connected both geographically and electrically close to consumers. Economics of construction of the distribution network has resulted in lower demand towards the edges being met by progressively reducing conductor areas. This radially tapered distribution network exhibits increasing resistance per unit length towards its edges. As a consequence, real power flow has a greater proportional effect on bus voltages here than closer to the transmission network where larger conductors are used with consequently less resistance. DG has implications for voltage quality and the safe and proper functioning of the distribution network as discussed in section 2.2.

2.1.2 Benefits of Distributed Generation

There are a number of reasons for the present interest in distributed generation.

Deregulation

Competitive practices require that electrical energy and ancillary services are bought from any size energy supplier by open market trading or by negotiation. This allows any size of

Generator to sell its services according to the price it demands for the relevant service.

System Losses

Siting generation near points of demand can reduce the transmission and distribution losses caused by the resistance of the power lines, cables and transformers. Most demand is on the distribution network and thus connecting generation to a point nearby the load on the distribution network will tend to cause the least losses assuming the generation does not greatly exceed the local demand.

Figure 2.1 shows line losses for varying generation connected at a load bus of fixed load. Line losses are zero when the generation exactly supplies the load complex power. The curve is approximately quadratic as $LineLosses \propto I^2R$ and $I \propto S$ where: I is the line current; R is the resistance and S is the apparent power flowing through the line. Note the zero losses at 10 MVA generated as the generation matches the load.

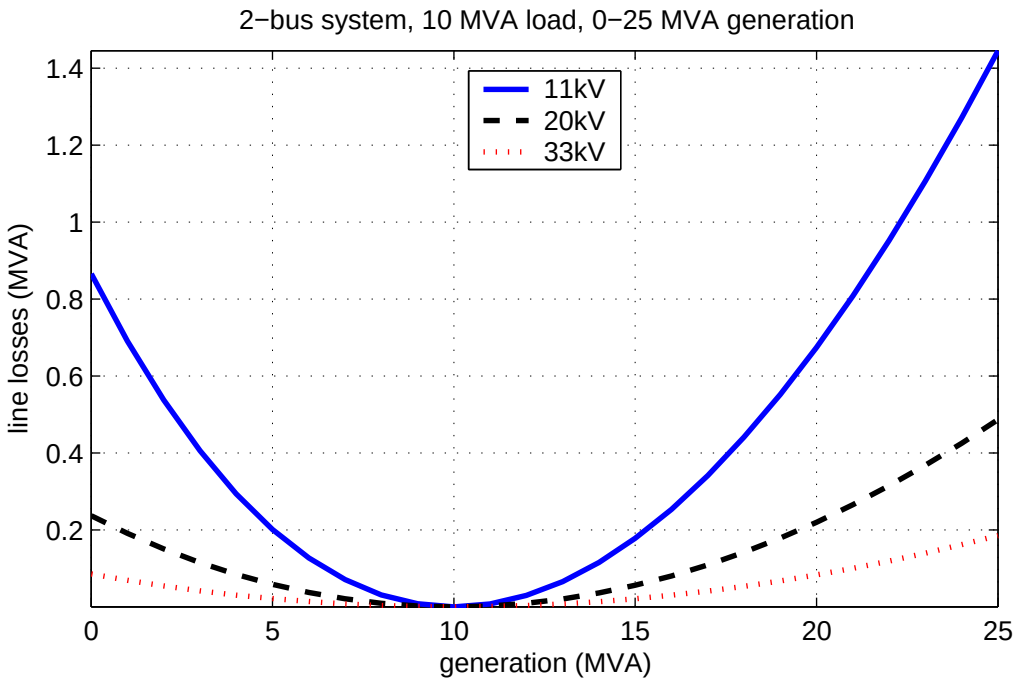

Figure 2.1: *Line losses between 2 buses separated by a 1km line with varying connected DG. Losses are shown for three voltage levels. From [6].*

Most losses occur on the distribution network with an average 6% of generated energy lost compared to 1.5% on the transmission network [2].

Small-scale CHP

The principle of combined heat and power (CHP) plants has been applied to units that operate so as to provide heat like conventional boilers and also electrical power. These units are designed to run in parallel to the electrical grid as the electrical power output is driven by heat as opposed to electrical demand. The efficiency of the unit is greater than a unit designed solely for heating. This is because the generation of the electricity using the same fuel at a centralised generation plant usually will not utilise its waste heat but will dump it into the air or into rivers or the sea. Despite the low electrical efficiency of smaller CHP units, the thermal output is equivalent to the thermal boilers they replace with the benefit of the electricity doing other useful work before resulting in heat energy.

The development of such devices, particularly micro-CHP units designed for homes, is tied to the de-regulation of the electricity market and the development of codes of practice for parallel operation of such devices with the electricity network.

CO_2 reduction

The reduction of CO_2 output by human activity is considered desirable and even essential. In the UK government targets exist for CO_2 emissions. Incentives and penalties exist for the electricity industry as a means by which the goal of reduced CO_2 will be achieved. Under the Renewables Obligations (Scotland) [7], Electricity providers are motivated to source a proportion of electricity supplied from renewable sources. These sources are considered low or zero CO_2 emission sources. Renewable plant is often relatively small and may be located far from the transmission network. For this reason it is more cheaply connected at lower voltages.

Diversification and security of supply

World economic and political pressures and ultimately the attainability of a particular fuel source has implications for its unit price and for any industry requiring that source. It is desirable that the electricity supply is diverse enough to be as independent as possible to the price fluctuations or increases of a particular fuel.

The fuel source for UK electricity generation is split mainly between nuclear, coal, gas and oil [13]. Increasing the generation portfolio to include sources not reliant on these fuels, reduces the risk to the electricity industry and of price increases for consumers. One large hydro project is under way in Glendoe, Inverness-shire with other options for alternative energy sources including wind, wave, tidal, small-scale hydro and biomass. Many of these options are well suited to small installations located away from the transmission network as above.

With growing demand in the UK combined with the position of many large generating plant nearing the end of their lifetimes, much more generating capacity is required to be built.

System security

With appropriate controls and restraints, a distributed generator can contribute to local system security similar to how larger generators deliver system support for a larger network. DG provides flexibility for reactive power support and voltage and power flow services [11, 14, 15]. Security of supply contributions of DG in the United Kingdom may be limited to firmer types of DG such as biomass or land fill-gas plant, combined heat and power plant and to some extent solar-photovoltaic installations [15].

For real power balancing, DG may be limited in the availability of its energy source, in the sophistication of its control strategy and its coordination with other generation in the local and higher voltage networks. By appropriate diversification of DG energy sources such as wind, wave and biomass plants, DG can however improve system-wide diversity of supply [16].

As these problems are current research interests and any solutions not implemented in the networks, DNOs and the electricity industry have in the past considered distributed generation

a detriment to system security [17].

Ease of finding sites

Planning guidelines, population location, historical and nature reserves and a strong community awareness of local developments means that siting large generating plant can mean a lengthy and expensive application process and even cause problems at the highest political level. Siting smaller plant could cause less problems leading to cost reductions in total project development costs [18]. Smaller plant is encouraged in new developments reducing planning and construction costs.

Low capital cost

Similarly to easier siting, a small plant requires less initial investment than a large one and hence less financial risk. Small plant can be added incrementally as required whereas large plant such as nuclear requires extensive planning and public enquiries. New large plant also requires major infrastructure investment, both in network equipment, in terms of supply of the energy source and in terms of staffing and training.

As discussed above, the cost of connection for DG tends to be lower than for plant connecting at the transmission level. In particular very small scale generation connected below 1 kV would have low connection costs. This type of generation could contribute up to 10% of average load in Europe by 2020 [9].

It is cheaper for smaller generators to connect at lower voltages as protection and switching equipment for lower voltage connection is cheaper than for high voltage connection [14]. Similarly generators restricted in their location by their energy source, such as a wind farm located in an area of high average wind speed, will tend to connect to the distribution network. In rural areas, lower voltage networks will usually be closer than higher voltage networks and thus the cost of lines to connect will be lower.

2.1.3 Types of plant

Types of generating plant can be distinguished by their effect on the distribution network and any benefits they bring the DNO.

Dispatchable

The power output of dispatchable plant can be controlled. Dispatchable DG is limited to small thermal plant and hydro schemes. The energy source for the prime mover of the generator must itself be available on demand. Examples of dispatchable DG are small biomass plant, small hydro with reservoir and electricity storage plant that stores electrical energy during times of excess generation. The speed at which plant can react to control commands varies with the technology.

Voltage control

Some plant may be available for voltage regulation. Automatic voltage regulation is usually only achieved with plant using synchronous generators. Regulation is achieved by adjusting the excitation of the synchronous generator. It is also possible to achieve the same effect with power electronic converters. Plant using such power converters such as asynchronous wind turbines, photo-voltaic installations and power storage could be employed to assist with voltage control [5].

Power factor control

Plant not available for voltage control will usually be required to operate at a strict power factor or within a small range. Indeed this is currently the case for all smaller plant [11] which are required to operate at unity power factor [17]. In the case of smaller synchronous generators, voltage control can lead to undesirable operating points in the machine [19]. The machine may become over-excited such that the field winding overheats or become under-excited such that the machine loses synchronisation with the network.

2.1.4 Technical impacts of increased Distributed Generation

There are several network impacts that are seen as a result of the connection of DG and can limit the capacity that can be accepted:

Reverse power flows

Reverse power flow describes the situation where a section of the network which previously experienced power flow in one direction, from high voltage sections to low voltage ones, sees power flow in the opposite direction. This is due to generating plant connected at low voltage where the amount of generation exceeds local demand. Reverse power flow is greatest at times of low local demand and high generating output.

Reverse power flow can be a problem for the Distribution Network Operator (DNO):

- The existing protection equipment may not allow reverse power flow or may not offer protection while it occurs.
- Existing transformers, in particular those with ULTCs, are likely to have assumed uni-directional power flow. They may not have the correct ratios or range of tap settings available for selections and reverse power flow may only be allowed at a lower value than the transformer rating [11].

Voltages

The connection of distributed generation can cause significant voltage rise in the local network substation unless it absorbs reactive power [12, 14, 20]. This approach has implications for charging for reactive power and may cause a change in voltage profile of the feeder requiring a review of voltage control on the feeder [21].

Connection of generation at the distribution level can also cause step voltages. When a generator starts, stops or is removed from the network quickly, it causes a step in the voltage profile of the local network. The size of the step is related to the transfer of active and reactive

power between the network and generator. Unless the generator is at unity power factor the size of the step is linked to the size of the generator.

The maximum step voltage a generator is allowed to cause is $\pm 3\%$ in the UK [22]. Thus the generator size is limited by, among other things, the step voltage it can cause in the local network [17].

Certain generating plant can degrade voltage quality [11]. Fast changing power output can cause corresponding changes in voltage level called flicker. Flicker due to wind turbines, for example, occurs as a result of changing wind speeds and also as a result of the tower shadow effect, the effect of wind turbine blades passing their supporting tower [23]. Plant connecting via an electronic inverter which uses switching to produce the AC output, can introduce undesirable harmonics in the voltage [24].

Fault level

The connection of synchronous generators contributes to the fault level in the network near the connection [10]. A majority of renewable generating sources, however, use induction generators or electronic convertors which have a relatively lower fault contribution [11]. The induction generator power output will drop to zero as the fault causes the induction generator to lose excitation [24].

In addition, distributed generation can change the behaviour of Under-Load Tap-Changing transformers (ULTCs). The impedance of a ULTC is related to tap position [25] and thus the fault level of the network near the ULTC. If reverse power flow, due to generation exceeding demand, raises the voltage below the ULTC then the impedance of the ULTC will be lower than if the generation was not there and thus can unacceptably raise the fault level. The variation of tap position accounts for a variation in transformer impedance of $\pm 10 - 15\%$ of the nominal impedance [26].

Current limit

The current carrying capacity of lines and transformers are limited by their resistance. Resistance causes electrical losses in the form of heat generated. The limit to the current a line can carry is dependent on the line and also on the ambient temperature of the air surrounding and cooling the line, leading to different line ratings depending on the season. Similarly, transformers differ in construction and will dissipate heat due to losses better with cooler exterior air temperatures. Ultimately the limit to the capacity is determined by a limit on the ability of the lines or transformers to dissipate heat and their maximum acceptable operating temperatures.

The introduction of generation in a radial rural distribution network for example, may lead to higher power export to the transmission network or higher voltage substation, than the power previously imported from it. The generation is limited then by the rating of the transformers and lines connecting to the higher voltage network minus the minimum local demand.

Protection

Other than potentially causing reverse power flow, DG may be limited by the protection equipment installed on the local network [27]:

- Island operation

  Connection of generation to the network is not allowed if the local network is disconnected from the entire network, for example when disconnected by breakers because of a fault. Thus loss of mains protection must be installed if not already present [10]. This will disallow the export of power from the generator during disconnection.

- Frequency

  Under or over frequency protection will disconnect feeders or individual generators if there is a mismatch or deviation in AC frequency. This limits the ability for generation to support the network in times of heavy demand which can reduce the frequency of the local network.

Location of connection	Maximum capacity (MW)
out on 11 kV network	1-2
11 kV substation busbar	8-10
out on 33 kV network	12-15
33 kV GSP substation busbar	25-30
on 132 kV network	30-60

Table 2.1: *Typical connection capacities at distribution voltages [29].*

- Voltage

  Under or over voltage protection can disconnect feeders or individual generators connected at distribution level if there the bus voltage is outwith $\pm 3\%$ [4] of nominal. This limit is part of Engineering Recommendation P28 and is more restrictive than the $\pm 6\%$ limit required by the Electricity Safety, Quality and Continuity Regulations 2002. It limits the ability of distribution generation to provide voltage support to the network.

The DNO ensures suitable equipment and protection is utilised and maintained in the distribution network and by connected generating plant. Power ratings of equipment must not be exceeded to minimise equipment failure and thus disconnection of the consumer. Protection should be sufficient to isolate faults locally, minimising the impact on the larger network and thus minimising consumer outages [28].

Table 2.1 shows possible capacities of DG that can be connected at different voltage levels [29] taking into account thermal limits and voltage rise problems.

Limits to system security contribution

DG is presently limited in its ability to provide energy and provide system security in particular it has limited ability for balancing the real power output of system generation with system demand. Most larger plant, some of which the DG might displace, is connected at the transmission level and can deliver a wide range of power outputs as required. Such plant is dispatchable, it can vary the real power output by the modification of the energy input into the

generator such as water flow or the rate of fossil fuel burning. DG varies in its dispatchability depending on its energy source and size.

Dispatchability of the plant is dependent on:

- Security of energy source: The control of energy input into the generator to be converted to electrical energy must be controllable. For example the flow of gas into a gas turbine can be controlled given a sufficient supply, whereas the wind for a wind turbine is not controlled. Hydro plant is dispatchable but will be subject to limits such as the total water in the reservoir.
- Output range of the electrical generator: A generator output could be from zero to its rated power. In practice, the efficiency of conversion to electrical power may limit how little it can produce economically.
- Control strategy: The design of some plant may not suit dispatch according to required power output. For example, although a combined heat and power plant is capable of operating to order, the efficiencies gained from using the waste heat are lost if the heat is not required and thus the plant is usually operated according to heat demand [24]. Nuclear plant is usually operated with a steady electrical power output as the process that provides the heat energy in older plants is not suited to frequent and rapid changes in output. Many coal plants are capable of rapid changes in power output as the steam used to rotate the turbine is buffered and the rate at which it is released can be changed very quickly. The rate of burning of the feedstock is then relatively rapidly adjusted to maintain the steam buffer.
- Capacity: The DNO or the Transmission System Operator (TSO) exerts varying levels of control to plant real power output. A small plant may be capable of the above services but larger plants tend to be used for real power balancing and frequency response as they can be more easily dispatched centrally to be in the required state of readiness or operation as required by the Transmission System Operator (TSO) [15]. With present techniques it is simplest to control a small number of larger plant for this purpose as this is easier than to control a large number of small ones [15]. For this reason a large number of small DG may not be dispatched centrally.

2.2 Traditional voltage management of the distribution network

The direction of power flow is historically from the transmission network down into the distribution network. Frequency and voltage are kept within statutory limits by the central control and dispatch of large generating plant by National Grid.

The DNO has the responsibility to connect the consumers demanding for electricity to its supply. Traditionally this has involved providing connection to the transmission network. All but the largest industrial consumers are connected at lower voltages than the transmission network. The DNO is obliged to maintain the voltage at all Low Voltage buses over 400V within $\pm 6\%$ and within $+10\%/-6\%$ for 400V buses [28].

Power is fed to the distribution network at the Grid Supply Point (GSP) which is a transformer or a number of parallel transformers feeding (usually) a 33 kV busbar. The high voltage side of the GSP transformer is kept within voltage limits by the actions of plant connected to the transmission network.

The voltage on the distribution side of the the GSP is regulated by the transformers which are ULTCs. These are described further in the next section. Voltage control in the distribution network, below each GSP, is largely automatic with predictable local control achieved by good planning; some automatic devices, such as ULTCs on the primary transformers and infrequent remote or on-site manual switching and adjustment.

The DNO may have contracts to connect generators to the distribution network. This generation may be used to maintain voltages in the network. Connected generation may also be used for frequency support, providing local demand for real power. The supply of these services is usually only possible from firmer generation with a controllable energy source such as a hydro scheme.

The most common automatic devices used for voltage control in the distribution network in Scotland are ULTCs [30]. The following sections describe the role and operation of the ULTC with a view to the simulation of its operation and ability to operate effectively and

economically with increased DG.

2.2.1 The voltage regulating transformer

The voltage regulating transformer or Under Load Tap Changer (ULTC) performs the role of stepping up or down the voltage between Medium Voltage (33 kV$<$MV$\leq$132 kV) circuits and High Voltage (HV$\geq$132 kV) circuits or between MV and Low Voltage (LV$<$33 kV) circuits or directly between LV and HV circuits. In addition to this it is able to vary the exact transformer ratio by small steps as detailed further in this section. The actions are determined by the Automatic Voltage Control relay (AVC). In this way it is able to manipulate the voltage of buses connected either directly or indirectly to the ULTC. In a similar way, the autotransformer can be used for voltage control between buses of similar nominal voltage [31].

Location

There are two roles the ULTC can perform. The first is to step down the voltage at the grid supply points (GSPs). Here the AVC acts to control the voltage of the lower voltage bus. The second is to step up the voltage from generating plant. The AVC then acts to keep the voltage of the higher voltage bus within limits.

In general then, the AVC seeks to control the voltage of the bus on the side closer to the consumer. None of the examples in this study will contain transformers connecting buses of similar nominal voltage.

Operation

The tap-changing ability of the ULTC is provided by a mechanism that connects more or less of either the low voltage (LV) or high voltage (HV) winding [32, 33]. The voltage on the LV winding is defined as:

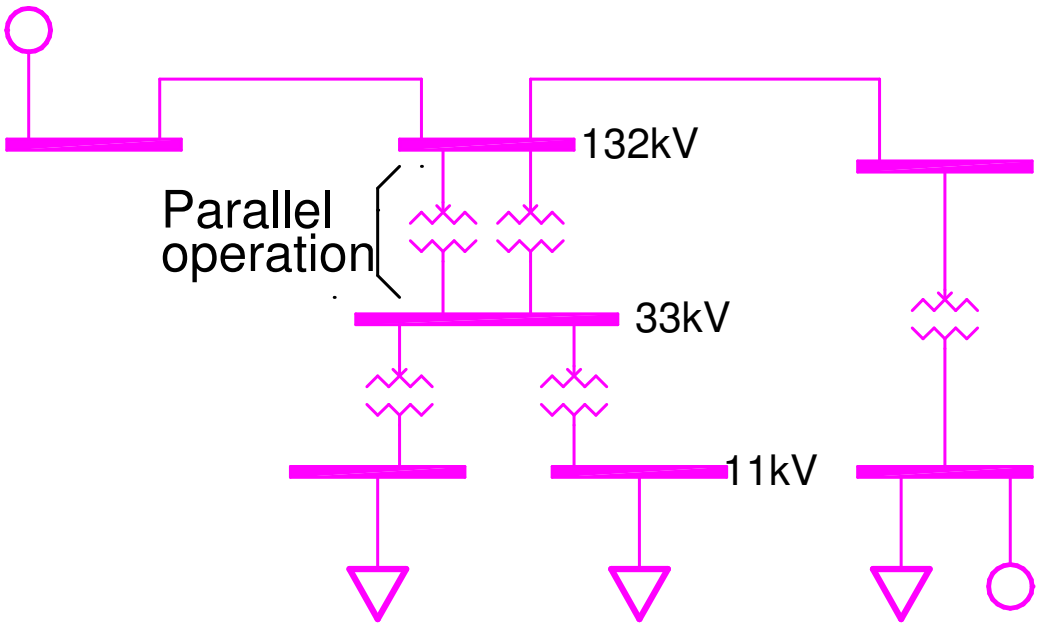

Figure 2.2: *Example placement of transformers in the distribution network.*

$$V_{LV} = V_{HV}\frac{N_{LV}}{N_{HV}} \tag{2.1}$$

where N is the number of turns on each winding. N_{HV}/N_{LV} defines the turns ratio.

The transformers in the network examined are of the type that changes the number of turns of the high voltage winding that are connected. In this case, connecting less of the high voltage winding, lowers the tap ratio and thus raises the voltage on the low voltage side. Connecting more will raise the tap ratio and thus lower the voltage on the low voltage side.

As a product of the construction of a two winding transformer, reducing the number of turns connected on the high voltage side is termed tapping up. A tap up raises the LV voltage and a tap down lowers the LV voltage. Figure 2.3.

In this study, the lowest number of connected turns is termed tap position 1, the highest number is termed tap position n where n is the number of taps. As a consequence of that definition, the term “tap up” refers to increasing the tap position and consequently increasing

the number of turns on the HV winding. The term "tap down" refers to decreasing the tap position and consequently decreasing the number of turns on the HV winding.

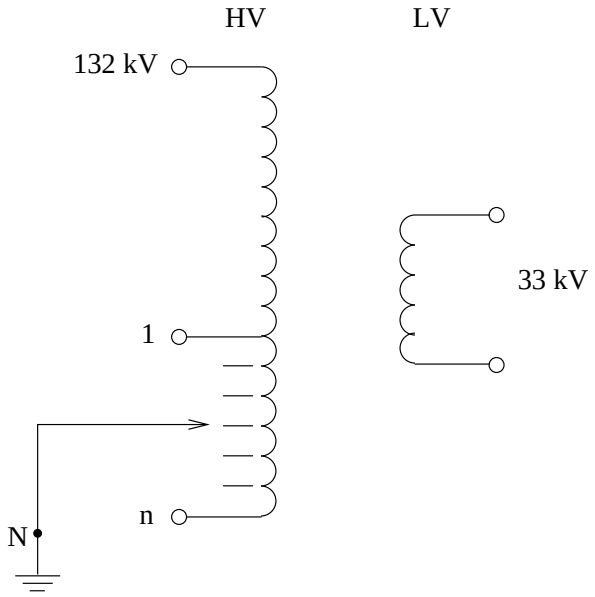

Figure 2.3: *Transformer windings with taps numbered as used in this study. The diagram is an edited copy from Harker [33]*

Note, however, that this is contrary to the practice of numbering the taps according to their physical arrangement in relation to the ground. Harker reports that the taps should be numbered 1 for the most turns connected and N for the least number of turns connected [33].

A single tap-changing operation, either up or down, takes a number of seconds to complete. A tapping operation involves mechanically making the connection to the next tap before breaking the connection the existing tap. A *divertor* resistor or inductor is placed in series with the short-circuited turns to prevent large short-circuit currents during this process [34]. On older devices the operation took in the order of 10 seconds [35]. Newer devices take between 1 and 5 seconds [36–38].

The time taken for a complete tap change is significant though it is smaller than the delay implemented by most existing and proposed AVCs as described in section 2.3.4.

Cost of ULTC Operation

More significant than the time taken for a tap change is the appreciation that a tap change has a cost associated to it as a result of the wear and tear on the mechanism [38, 39]. Maintenance of the LTCs can account for 40-50% of transformer maintenance costs [40].

A single transformer maintenance operation is approximated to be £18,000 by Handley in 2001 [41]. Such maintenance typically occurs either at 100,000 tap change operations and two to seven years [40–42] of operation, whichever is the earlier.

Not taking into consideration the results of condition monitoring techniques, Redfern and Handley, however, suggest a maintenance interval of only 40,000 tap operations [43]. This figure arises as the result of a trade-off between the cost of maintenance and the probability of failure multiplied by the cost of a failure.

The cost per tap operation is calculated as 50% of transformer maintenace costs. The transformer maintenance cost per tap operation is calculated by dividing the maintenance cost of a transformer by the expected number of tap operations between maintenance. This gives the following equation:

$$TMC = \frac{50}{100} \cdot \frac{MaintenanceCost}{OperationsBetweenMaintenance} = \frac{1}{2} \cdot \frac{18000}{40000} \tag{2.2}$$

resulting in a 22.5 pence *Tap Maintenance Cost* per tap operation.

To evaluate the system cost of ULTC tap operations, the number of tapping operations made by each ULTC over the period of the scenario is determined. The total tapping cost for that scenario is thus the number of tapping operations multiplied by the estimated cost of each individual operation. Note that when evaluating the cost to the system of a period of tap operation, the evaluation also includes the loss of generating opportunity costs associated with shutting down a ULTC for maintenance as described in section 3.6.1.

The capital cost of existing ULTCs are not included in the cost per tap change in this study. Connection costs attributable to transformers are available from Scottish Power and Scottish and Southern for Grid transformers. SP and SSE charge £500,000 and £1,250,000 respectively for a new 132/33 kV 30MVA transformer required due to connections as of April 2007 [44, 45], with the former quoting ongoing yearly charges of £56,000.

Transformer parameters

Apart from the power and voltage ratings of the transformer, a design decision has to be made as to the number and spacing of the winding taps needed to provide sufficient voltage control.

The step size determines how fine the adjustments to the control voltage are made by the transformer. A balance has to be struck between the following:

- The total number of taps.
- The range of required control.
- The allowed voltage limit on the control bus.
- The variability of the real and imaginary power flows through the transformer.

The exact relationship between the step width, number of taps and the total possible ratio adjustment is defined later in section 2.3.4. The steps are usually linear steps of between 1% and 5% [36, 39, 46–48].

Network evolution

The network changes over time. There are seasonal changes in average load, generation and line and equipment properties. In addition load patterns change, generation requirements change and new plant and equipment is installed. Such changes can require an adjustment of the control parameters of the AVC. Many of these changes are effected manually at the location of the ULTC.

2.3 ULTC Development

There are many types of AVC installed today. The controllers have become increasingly sophisticated as problems in their operation have been observed in the field, and predicted by research.

2.3.1 Digital control

Programmable logic circuits and microprocessors have been used to improve the ease of adjustment of ULTC AVCs as compared to previous analogue designs [49–51]. In addition, most of the subsequent control strategies rely on the digital controllers for ease of implementation. Quoting Harlow [50]:

> It is recognized that being able to mathematically define the desired operation is tantamount to its implementation when considering digital control.

2.3.2 Communication

Control units can be linked to each other or to central control stations for remote adjustment such as with the GenAVC ULTC AVC [52] as shown in Figure 2.4. Quoting [52], "GenAVC^{TM} operates by making an estimation of the voltages on the network controlled by a primary substation transformer, using information about the state of the network collected from remote measurement units." Communication also allows for certain strategies to improve ULTC behaviour such as serial and parallel operation. This is discussed in section 2.3.5.

The benefits obtained from control strategies involving communication must be balanced against capital and installation costs of communications equipment. Typical costs to modify an AVC relay and install a remote voltage sensor are £2000 for the relay and £1000 for each remote voltage sensor [31]. In addition, such units are capable of communicating alarm signals and other operating data to the control station.

2.3.3 Periodic change

The pattern of electricity use and supply changes over time. There exist ULTC control units that have been manufactured to change the way in which they operate according to the time of day and day of the week.

Figure 2.5 demonstrates the seasonal variability of real power demand in the Scottish Power

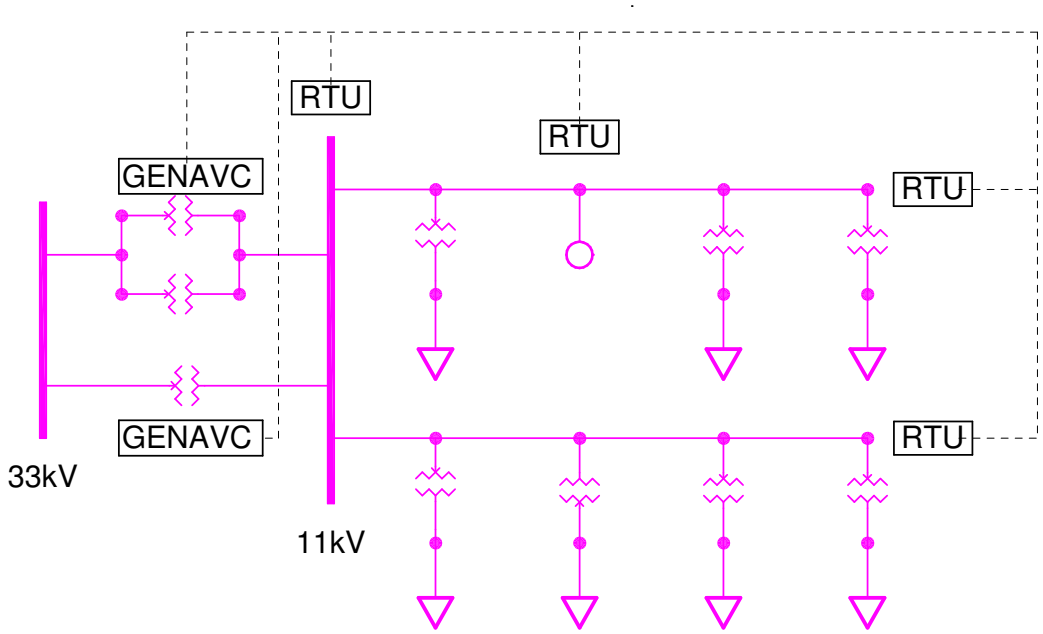

Figure 2.4: *The GenAVC uses remote measurements to make tapping decisions.*

area.

The difference in variation of real power translates into different requirements on voltage regulating equipment to maintain acceptable voltage levels at consumer busbars.

2.3.4 Control strategies

Control strategies started with simple voltage regulation of one of the connected buses. Increased sophistication has allowed the AVC to take into account a number of other factors:

- The actual or estimated voltage at remote points in the network.
- The operation of parallel ULTCs.
- The power flow through the ULTC.
- The operation of other voltage regulating devices.

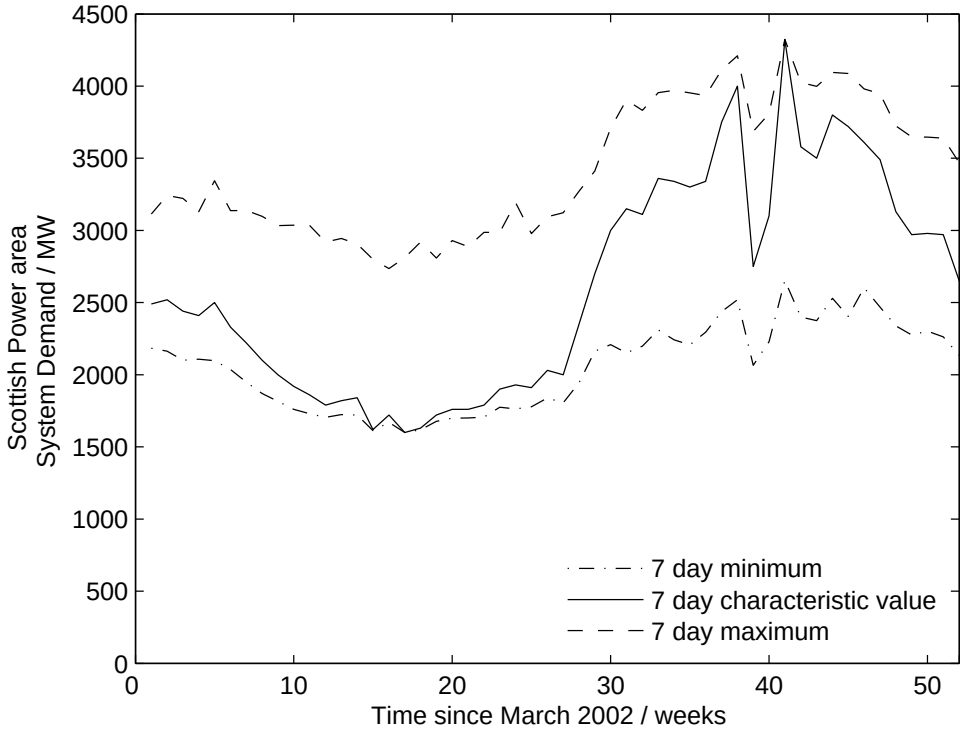

Figure 2.5: *Real power demand depends on the time of year.*

The next section starts with the most basic AVC strategy. The following sections describe further developments that have been implemented or simulated.

Basic voltage regulator

This section describes the operation of the basic voltage regulating strategy for tap-changers such as those used in the Scottish Power area [53]. The method has evolved to work well in networks where power is supplied at high voltage and consumed at low voltages. Its goal is to minimise voltage error from a set-point. Its actions are to tap-up, tap-down or stay put.

A common mode for the tap changer is to control the voltage on the lower voltage busbar to which it is connected. Some of the rules that have evolved to determine the stepping actions are described [31].

- The most basic rule by which a tap-changer operates is that if the controlled voltage is lower than the set-point, the turns ratio is reduced and vice versa. The tap changer

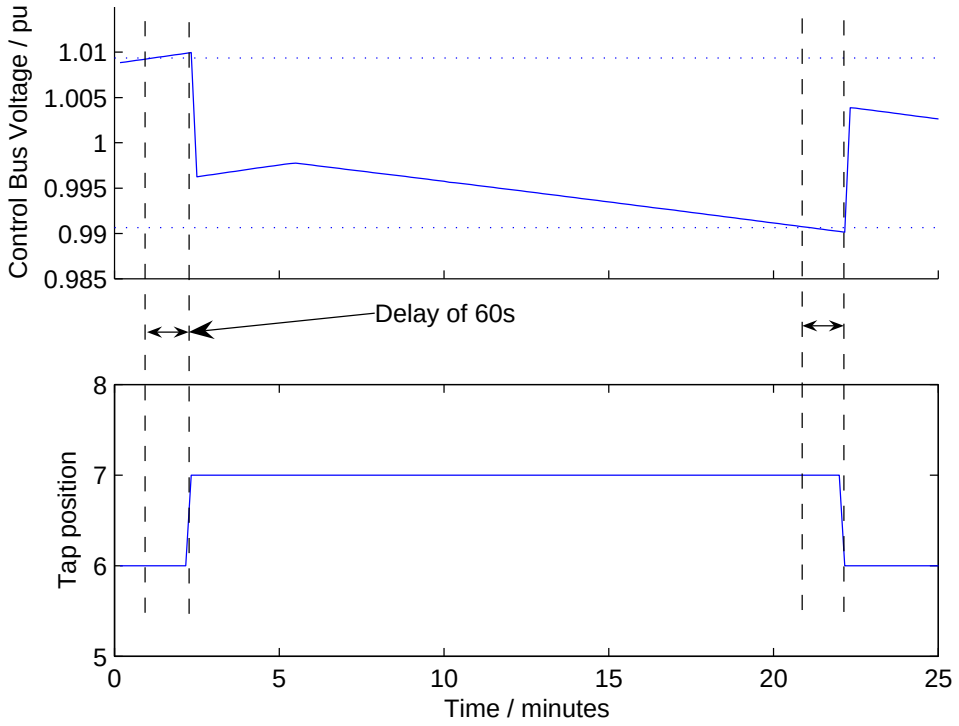

Figure 2.6: *Tapping operations due to the control voltage being outwith limits for a period of time.*

changes the transformer turns ratio in fixed steps. There is a limit to how much the turns ratio can be adjusted.

- The next most important rule is that the tapping action should only occur when the voltage violation, measured per-unit, is at least unity ± 0.00625. This is half that of the step-size per-unit of a typical ULTC. This avoids the situation called hunting, where the tap-changer continually switches between two settings as both result in a voltage violation.

- To avoid frequent operation, the tap-changer will only act after voltage exceeds the dead-band for a given delay, typically 45 to 60 seconds [53]. Increased sophistication has been achieved by reducing or cancelling the delay in situations where more than one tap change is required to correct the voltage [54]. Another method is to change the delay as a function of voltage as described in section 2.3.4.

- To allow rapid adjustment due to large voltage violations, an inter-tap delay which is

lower than the normal delay, is allowed if the tap operation fails to bring the voltage error within the dead-band.

Refinements of the basic voltage controller.

Direct control of tap-changer.

The operation of more than one transformer in parallel requires a method to avoid them working against each other. Both of the following methods need continuous communication between the transformers in parallel.

Parallel operation can be achieved where communication is possible between the transformers and they can be operated in master-follower mode. The assumption of this method is that the tap position for each transformer should always be identical. A rule of thumb suggested is that the transformer impedances must be matched to within 7.5% of each other and have the same tapping ratios [51].

Parallel transformers can be biased to tend towards equal settings with a difference in tap setting no more than one step. This can be achieved by measuring any circulating current between the transformers as a result of their relative tap position [55, 56]. This method requires a signal between the parallel transformers reflecting the circulating current sensed by a "'balancer"' circuit [57].

Input voltage manipulation.

Improved accuracy of control under varying power flow can be achieved by adjusting the measured voltage at the terminals of the secondary winding according to the product of current and reactance of the line between the transformer and the point for which voltage is controlled [58]. This is Line Drop Compensation.

This method relies on accurate adjustment of the measured voltage to reflect the properties of the line. An incorrect adjustment can cause correct operation with the load at one power factor but incorrect operation due to a change of power factor such as by the connection of

distributed generation below the AVC. It does not necessarily improve the voltage profile of points other than that point, the load centre, used to calculate the compensation parameters.

There is an alternative to the two methods described in section 2.3.4 for operating ULTCs in parallel. The method, negative reactance compounding, uses a form of line drop compensation with negative reactance [55, 56, 59]. This method has been unpopular due to the resultant inaccuracy in control voltage estimation when the load power factor differs from that for which the settings were designed, reports Harlow [57]. It is now recommended for consideration as a useful method for paralleling between transformers where it is not convenient to connect them with a signal wire or if their impedances or tapping ratios differ. Harlow cites improvements in modern sensor accuracy and tighter constraints on load power factor as reason for re-consideration of this technique. Thomson on the other hand argues that the limitation on power factor is a limitation on distributed generation which may be operating to correct for voltage drop along overhead lines.

Other more complex strategies involve manipulating the voltage input to achieve a change in the basic controller behaviour, for example, coordination with a static condenser (section 2.3.5).

Delay timer manipulation - delay inversely proportional to error

The algorithm described in section 2.3.4 does not allow for the magnitude of the voltage error outside the dead-band. The inter-tap delay reduction helps correct a large voltage error quickly. It does not avoid spurious operation due to low voltage errors occurring for periods only slightly longer than the tap operation delay. A system where the tap operation delay is inversely proportional to the voltage error outside the dead-band serves to tap quickly for large errors and slowly for small errors [35, 36]. Example operation of a Calovic controller is shown in 2.7.

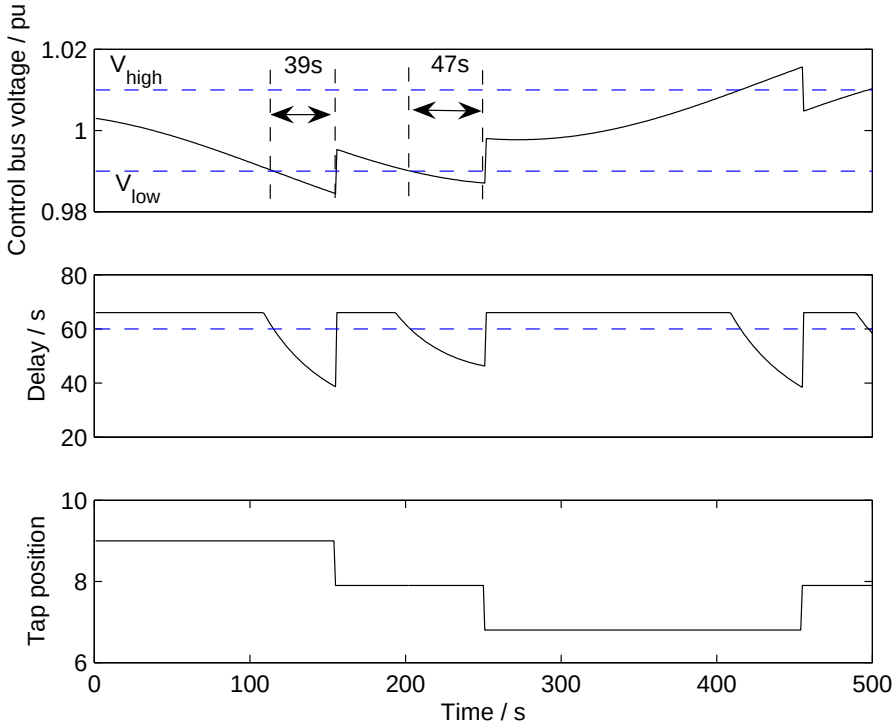

Figure 2.7: *Control voltage and tapping actions due to Calovic's controller.*

2.3.5 More advanced control strategies

In addition to easier adjustment, digital controllers allow the possibility of implementing more complex control strategies and protection rules as required.

Strategies that can be implemented are limited by:

- The cost of the controller.
- The cost and accuracy of input signals.
- Accuracy of system parameters in all operating environments
- The time taken to calculate a decision.
- Accuracy and speed of communication responses required from other devices or operators.

Coordination of generator AVR with a ULTC

Modelling of a system has been conducted by Cartwright *et al.* in which the ULTC operates according to the ability of nearby generation to provide reactive power support [60]. When control voltage is low and the generator AVC cannot provide any more reactive power, the ULTC will tap up and vice versa. The assumption is that a tap action can occur within 5 seconds of the AVC reaching a limit and that there is only 1 signal received by the ULTC by a generator AVC. It seems evident that a fast acting generator AVC will reduce ULTC tapping actions due to transients not caught by the timer delay if the generator AVC is kept away from its control limits.

Present operating practice does not accommodate such interaction. It is historically believed that the operation of the ULTC and the generator Automatic Voltage Controller will result in some kind of conflict or control overlapping with each other [5, 31, 61, 62]. Another area for concern is that with DG in constant voltage mode that subsequent loss of the DG causes significant operational difficulties [63]. For example if a voltage control strategy uses a generator to lift voltage at the end of a long feeder, and that generator is then subject to disconnection, the voltage at the end of the feeder may drop unacceptably low.

Coordination of FACTS devices with a ULTC

A static synchronous compensator (STATCOM) on its own is capable of voltage control by absorbing or generating reactive power as well as real power [64]. The STATCOM is a Flexible Alternating Current Transmission System (FACTS) device.

STATCOMs provide fast acting support though require stored energy to operate in real power support mode. It is desirable that ULTCs perform slow acting voltage control to leave the STATCOM in such a state as to be able to provide maximum fast acting support. Coordination between a STATCOM and a ULTC has been simulated by Paserba [65] with two basic strategies. A trade-off between improving voltage time-series and reducing tap changes of the ULTC was demonstrated. Coordination was achieved by the manipulation of the gain of the voltage error measuring circuit to shift the responsibility for a voltage change from the STATCOM to the slower acting ULTC. In this way, the adjustment for short-term voltage

changes is bourne by the STATCOM and long-term ones by the ULTC.

A similar method is proposed by Kwang Son that coordinates a Static Var Compensator (SVC) with a ULTC in order to maintain the compensation margin of the SVC [66]. The SVC can react to rapid changes in voltage but its compensating current is limited. The compensation margin is maintained by manipulating the delay timing circuit of the ULTC such that the delay is minimised when there is little operating margin left for the SVC and is maximised when there is a large operating margin. As with the STATCOM, the SVC alters the ULTC measured voltage, in this according to how close to its limits the SVC is operating.

Coordination of multiple ULTCs operating in parallel.

It is very common for all but the smallest feeders to have multiple ULTCs working in parallel. There are multiple benefits of having more than one ULTC in parallel:

- The most important is the increased capacity of the combined ULTCs.
- The combined rating can be modified as part of ongoing network planning activities with individual ULTCs being swapped and upgraded as required.
- Maintenance can be scheduled for a ULTC at low load periods allowing the other ULTCs to take the out of service ULTCs share.

The ULTCs may be of the same rating and in the same geographical location. In this case the ULTCs may operate in master-follower mode with one master AVC determining the tap operations the master with the others replicating the operation.

Parallel ULTCs may be of different ratings or be geographically remote. In this case master-follower may not be appropriate and various schemes exist to adequately share duty by examining circulating current between the ULTCs [55, 56].

Parallel ULTCs in the network analysed in this study were of identical rating and tap arrangements. The ULTCs were modelled such that the controller kept the same tap position for each in the set.

Coordination of multiple ULTCs operating in series.

It is recognised that it is beneficial for each delay setting for two or more transformers operating in series to be different [39, 46, 67–69]. The difference ensures that two or more transformers do not react at the same time to a single voltage disturbance. Two transformers acting at the same time in series could cause a voltage error in the opposite direction to that being corrected. This would lead to one or more transformers performing another corrective tap operation with a result of three operations instead of just one to adjust for a change in power flow.

The delay is normally shortest for higher voltage transformers, for example, 45 seconds in the Scottish Power network. Delays of up to 180 seconds are used for lower voltage transformers. The exception to this is when the ULTC is being used to connect generation to the network when a shorter delay is used.

A more sophisticated approach to series ULTC coordination is achieved by blocking. Blocking denotes cancelling tap operations of a ULTC if a higher voltage ULTC in series is about to perform the same operation. The normal rules that demand tap changes according to the voltage error have been combined using fuzzy logic with rules that block tap operations according to the intentions of other ULTCs [70]. The method requires the communication of tap operation intentions between transformers but does not need centralised communication or control.

Figure 2.8 shows that when the 132/33 kV transformer senses the controlled side voltage dipping below its lower limit, it sends a blocking message to the 33/11 kV transformers below it. The 132/33 kV transformer then makes a corrective tap operation after a delay to prevent spurious operation. The block is then lifted. This process reduces the number of 33/11 kV tap operations that result from correcting a voltage error that the 132/33 kV is about to correct itself.

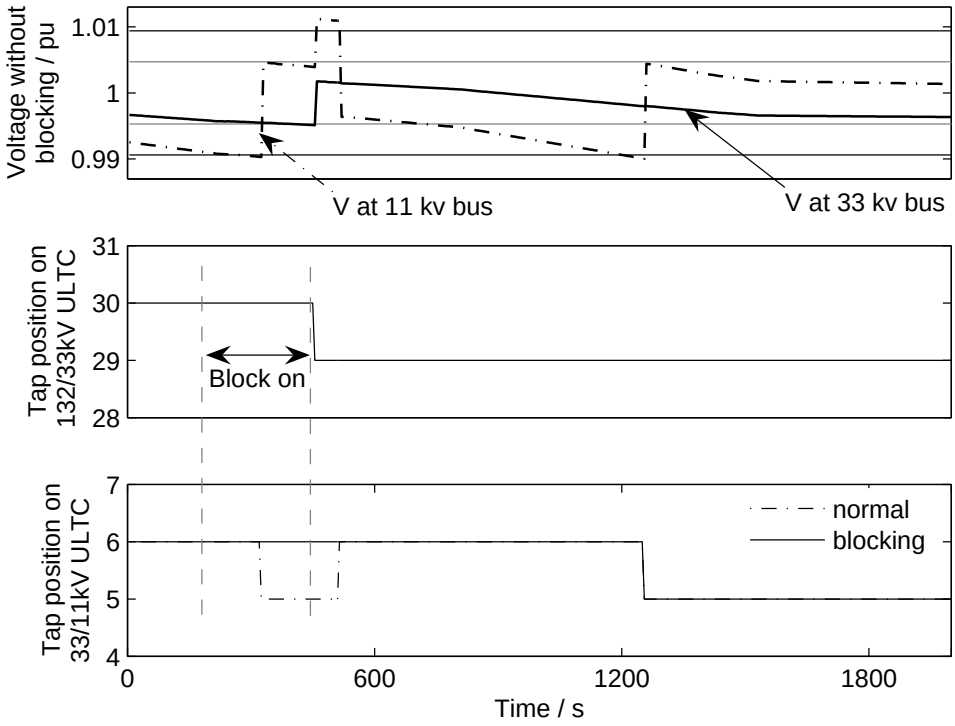

Figure 2.8: *A blocking signal prevents spurious operation of 33/11 kV transformer.*

Coordination of multiple ULTCs in more complex configurations

The paralleling methods suggested in the previous section work if the transformers connect to shared buses both upstream and downstream. Smith *et al.* describe a situation in which the simple blocking rules do not enable optimal behaviour [39].

Consider Figure 2.9. If a disturbance occurs at L2 then all ULTCs observe a voltage change however the duty of responsibility is only on ULTC^{T1} and ULTC^{T2}. Smith proposes a Duty of Responsibility algorithm that takes into account the change in the load experienced by each transformer [39, 67]. A measured load change reduces the time delay imposed on the transformer AVC to operate. The load change at a transformer implies that this transformer has a duty of responsibility to correct any voltage deviation resultant from the load change. Care would need to be taken that given an equal load change on ULTC^{T2} and ULTC^{T3} that the decrease in time delay does not cause conflict with ULTC^{T1}.

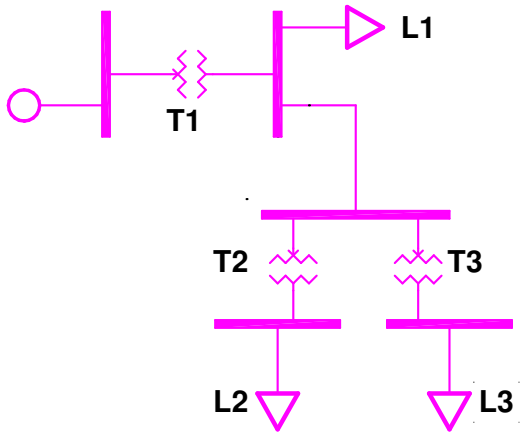

Figure 2.9: *Smith's example network.*

Using voltage prediction.

The imposition of a time delay on voltage tapping actions reduces spurious operation due to transients. The delay corresponds to an implicit assumption that if there is a voltage error for T_d seconds then it will continue to be outwith voltage limits without a correcting action. In other words, the assumption is that the predicted voltage will continue to be outwith limits.

An alternative method to the basic ULTC AVC algorithm described in section 2.3.4 would be to perform a tap operation according to an improved prediction of future voltages. Suzuki *et al.* built auto-regressive moving-average (ARMA) models of near future reactive power and voltage [71]. They made tap changing decisions according to their automatic voltage and reactive power control (AVQC) algorithm. The AVQC algorithm is based on a set of fuzzy logic rules which combine the outputs of the ARMA model to provide a tap operation decision.

At worst, the performance should be as good as the simple assumption made above. If the model was well constructed, the increased amount of information it used to create a voltage prediction should increase the accuracy of the voltage prediction. The assumption here is that as the error of the voltage prediction tends to zero, the performance of the decision algorithm increases monotonically. An example of tap operation according to projected voltages is shown in Figure 2.10.

For network and conditions given in [71], the AVQC algorithm is successful when compared to the basic ULTC AVC. The algorithm avoids the hunting demonstrated at the start of the paper. It is not clear however if the same results might have been achieved by simply widening the voltage limits. Qiang demonstrated in [36] that there are situations in which oscillations cannot be avoided by adjusting the control deadband so the Suzuki solution is of use if it was demonstrated to work on more taxing examples.

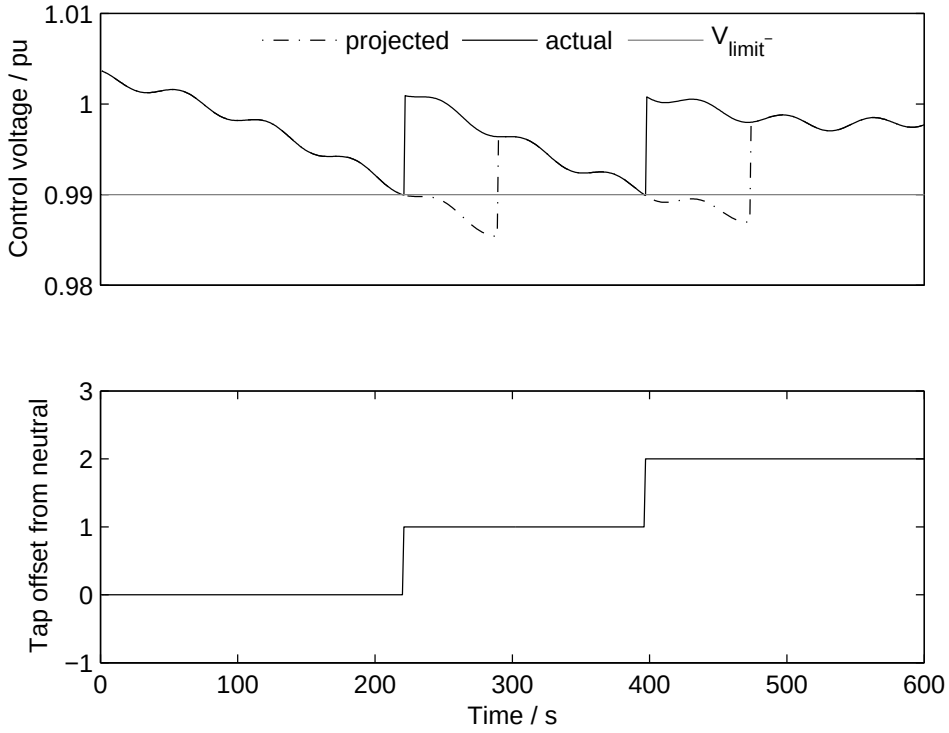

Figure 2.10: *Simple example showing how projected voltage determines control actions to keep voltage close to target voltage.*

Fuzzy Logic

Fuzzy logic is not a control strategy in itself. Fuzzy logic is a method of combining several control rules which may have conflicting goals, and arriving at a decision or measurement.

A simple application of fuzzy logic to ULTC control was simulated by Kasztenny *et al.* [37]. The controller combines rules determining the direction of tap operation according to

measured voltage error with rules determining the time delay again according to the measured voltage error. The performance of the controller is similar to that of the inverse time delay controller described in section 2.3.4. Advantages of the fuzzy logic method are:

1. Rules can be described in natural language and easily translated into fuzzy logic.
2. Many rules can be combined to produce complex behaviour.

In the case of tap-changer control decisions, the fuzzy logic system must ultimately provide a decision at all times as to whether the ULTC is left as it is or whether an up or down tapping operation is required. There is no way to fuzzify the control actions available to the ULTC. The fuzzy logic system can be constructed so as the result can reflect the degree of certainty of a decision. This certainty however can only be interpreted as one of the three control decisions: *stay*, *up* or *down*, that are available. One way of using the certainty of a decision is to introduce a probability that the actions *up* or *down* do not occur that is inversely proportional to the certainty.

2.4 Summary

In future there will be many applications to the DNO to connect generation at the distribution level. Such quantities of generation have a number of effects on the network which may be solved by appropriate installation of protection or network upgrades. This chapter has explored existing ULTC AVC methods and shown that there is considerable potential to mitigate the voltage impact new DG can have on the network. This may be achieved by increased understanding of the operation of ULTCs and appropriate control of the DG.

The next chapter shows the implementation of a method of simulating the operation and interaction of DG with ULTCs. The method takes time series of generation and load magnitude and creates time series of network voltages, power flows and ULTC operation. The algorithms used for ULTC control and for control of the DG are detailed. A method for evaluating the fitness of the network and the DG capacity assigned in terms of voltage control is defined.

Chapter 3
Model Implementation and Evaluation Methods

This chapter presents a method for exercising a network model and observing power flows and voltages in response to the variation of input load and generation over time. Time series define the changing loads and generation for whole days of operation. The network model is generated from a definition file which could define any network. The method can incorporate models of actively controlled network equipment such as ULTCs. This method thus allows the observation of the operation and response of network equipment to time varying load and generation.

Different scenarios can be created by the variation of input files, equipment models, equipment control parameters. The method allows many scenarios to be examined in a single run by the repeated construction and testing of scenarios varying by predetermined parameters.

The observation time series produced by the method are stored in a number of files such that various analyses can be conducted on the observations such as:

- Equipment loading over time.
- Bus voltages over time.
- ULTC tap position over time.
- Total number of tap operations for each ULTC.
- Total energy generated,

These output time series enable a more complex evaluation of system control fitness based on equipment maintenance costs.

3.1 Network simulation

A network model is defined by data such as: busbars, lines, transformers, generators and loads. The simulation in this study, is defined as the encapsulation of the network model inside scripts that can automate the repeated solving of the network model with varying inputs and parameters. The simulation manages the inputs to the network model and stores any required observations from the solved network model.

3.1.1 Time series power flow analysis.

The controllers for ULTCs tested in this study operate on time-scales of the order of seconds, as discussed in section 2.2.1. ULTCs controllers determine discrete control actions with artificial delays imposed between the observation of an under or over voltage condition and action. The controllers are designed to have a wide deadband in their response to voltage measurement such that frequent or opposing action is avoided.

There exist software tools for studying the response of controllers to network conditions such as the dynamic study tool of Power System Simulator for Engineering (PSSE) and SimPowerSystems toolbox for Simulink. These tools include models of closed loop control systems controlling generator AVRs and ULTC controllers. Generator and load models can be provided to determine their response through the simulation. They produce results showing the operation of network equipment and network measurements in millisecond detail. Such software tools produce dynamic network analyses.

A standard power flow calculation produces a network solution for a single point in time. The network is defined with all line parameters, transformer ratios, complex power loads and generation set at the start. The solution is the complex power flow through the defined network with generator voltage angles and bus voltages calculated. The solution includes calculation of reactive power production for constant voltage generators to keep their respective controlled buses at their target voltages subject to generator excitation limits. Extra calculations can be made between iterations in the power flow solution to determine optimal transformer ratios for ULTCs.

The simulation in this study required the implementation of several methods of control for ULTCs and generators to determine their response to the connection of an increased amount of distributed generation. The control methods may include agent type methods where communication between agents is required. The control methods must not be limited by the descriptive power of the dynamic simulation tool. In addition, the generation and load experienced by the network needed to be modified over time according to time series. For this reason, the dynamic network analysis tools available were considered unsuitable for this study.

Consider then a standard power flow calculation. The solution is obtained for a given set of starting conditions. If a load or loads were modified slightly in the solved case and then the network was solved again, the comparison of the two solutions would provide a good indication as to how the network responds to such a change. There is, however, no information available to the solver that the two input network cases are related, they are solved independently. For this reason, such a method is unsuited for the purpose of examining the reaction of a closed loop control system as a result of a load change.

The ULTC control algorithm, however, has an artificially delayed feedback mechanism. Short term oscillations from generator AVRs as a result of a ULTC control action will have dissipated before another action is permitted. The calculation of these oscillations then are not required to model the response of ULTCs to load and generation time series.

The simulation of ULTC operation requires that its control algorithm is presented with network observations at a frequency sufficient that the working of the algorithm is equivalent to that of a real-time model or experiment. The ULTCs operate after time delays of the order 10 seconds and complete a tap change in the order of 1 second. For comparison, dynamic studies generate results using time-steps in the order of 10 ms.

A semi-steady-state method is proposed here that calculates a power flow solution at discrete time-steps based on the network solution at the previous time-step and the adjustment of load and generation according to the input time series. In addition, adjustments can be made to the network model according to the actions of devices such as ULTCs. The actions of such devices are determined according to their observations of the network taken from previous

time-steps.

A number of input data files determine the load and generator complex powers over time. The simulation uses these files to initialise the network and then consequently to modify the network each time-step according to the pre-defined load and generation. The end result of the simulation is a number of data files containing measurements for each time-step as required. Figure 3.1 shows an overview of the simulation in terms of data flow. The Iterative Network Model is examined in more detail in section 3.2.

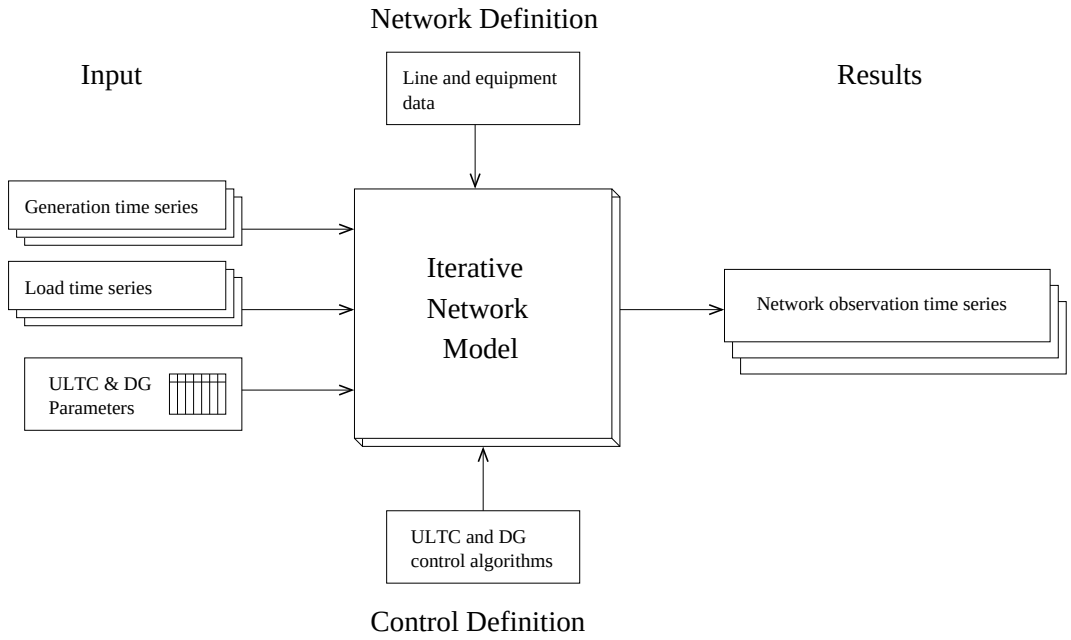

Figure 3.1: *Overview of simulation data flow.*

3.1.2 Discrete step simulation assumptions.

A number of assumptions were made in treating the repeated solution of a network as simulating a continuous system.

The most obvious assumption is that the interaction of the fast-acting generator AVRs with the changing power flows in the network are largely ignored. AVRs adjust the excitation of a machine in seconds to match generator terminal voltage with the target voltage. Their action is a function of a number of time and gain constants.

If properly adjusted the AVR will settle, for example, before a maximum of 4 seconds for a digital control or below 10 seconds for an analogue one [72, 73]. The excitation level will have brought the voltage close to the set point within about half the settling time. For this reason the simulation allows an AVR to adjust its excitation from minimal to maximal in 5 seconds.

It was assumed that the action of AVRs is such that they do not interfere with each other leading to cyclical or overshoot effects.

3.1.3 Network components

The simulation must model relevant network components. The model is generated from a definition file of these components. The key components are busbars, lines, generating plant, transformers, generators and loads. The network definition file contains their individual electrical properties and limits as well as how each connects to the other.

Data was readily available as a definition file for the Scottish Power area that is used in this study. These components were modelled sufficiently for the control methods to be presented with realistic parameters by which they must infer control actions, and for the consequences of such actions to be reflected in subsequent load flow solutions. A run of a simulation is entirely repeatable.

3.1.4 User defined controllers

ULTC AVC

The required input parameter for conventional voltage control by ULTCs is simply the control bus voltage. Refinements include observation of real and reactive power through the transformer. These parameters are available as a result of a power flow solution. In the simulation, a power flow solution is repeatedly obtained from a network model. Before each solution is made, control actions from previous iterations and load and generation changes are reflected in the network model as described in section 3.2.

The following list defines the requirements of the simulation of the automatic voltage control of ULTCs and other controllable network plant.

- The user defined controller is provided with the defined network measurements obtained from the network model at each iteration.
- Available measurements are restricted according to the intentions of the current simulation run.
- The controller produces an action at each time-step. The action is one of the following: “Tap up”, “Tap down” or “No change”. The network model is then updated as required.
- The controller is not limited in computational complexity or resource requirements.
- Inter-controller interaction termed “agent communication” is restricted according to the intentions of the current simulation run.
- The required input parameter for conventional voltage control is the control bus voltage.
- Refinements to the controller may also require observation of real and reactive power through the transformer.

Generator controllers

The model supports user models for the control of DG operation. Control modes modelled include:

PQ Generator in constant power factor mode.

PV Generator in constant voltage mode.

Generation shedding Over-voltage tripping and subsequent reconnection of the generator.

Generation constraint Putting a limit on the maximum real power output of the generator.

3.1.5 Data input and output

The custom simulation software accepts data files that define the network by for example line and network equipment parameters. More detail on the input file format, the `.raw` file, which is used for network definitions in the power flow simulator is found in section A.1.

The simulation accepts load and generation time series to define the load and generation at each time-step. The time series are stored as files containing a row for each value in the series. Two values separated by a tab are used for defining real and reactive components of load or generation.

The simulation software enables the transfer of data between the power flow simulator and the controller models.

The simulation software also stores network parameters at each time-step as a record of the successful run of the simulation. The input `.raw` format is sufficient to record all network data but is not used for the following reasons:

- The state of custom modules would need to be stored separately.
- It is relatively large.
- The format contains many values that do not change during the simulation run.
- The resultant saved data would be difficult to extract data from using standard spreadsheet or graphing software.

The records are separated into files in a form suitable for subsequent analysis. The simulation software only stores required measurements and discards the rest. This is detailed further in section A.2.4.

3.1.6 Network solution

The simulation software ensures that the network is solved at each time-step. This means the solution must converge within reasonable limits in a maximum number of iterations. A

section of code ensures that this happens as described in section A.2.3. Should that code indicate a failed solution, the run exits gracefully, saving network measurements up to the point of failure and allowing the simulation to start a new run with the next set of parameters if specified.

In this way, a large number of scenarios can be simulated in succession, the simulation software starting new runs as defined by the initialisation script. Should a scenario cause the solver not to converge, that run will not be completed but other runs may complete. The results of each run are kept separately.

The next section defines in more detail how the simulation software works and how a simulation run is defined and executed.

3.2 Power System Simulator for Engineering

Power System Simulator^{TM} for Engineering (PSSE) is a commercial power flow package. PSSE is capable of maintaining a network case with line and equipment properties, transformer ratios and load and generation as required.

PSSE provides an Application Programming Interface (API) which enables the user to load, observe and modify a network model maintained in PSSE using code written in Python. The API also allows the code to initiate power flow solutions. It is this API that allows the simulation model built for this study to encapsulate the network model in such a way as to allow the PSSE load flow solvers to operate on network cases repeatedly modified by outside code according to the scenario. Note the distinction between the *simulation* and PSSE; PSSE is always referred to as PSSE; the *simulation* is the combination of PSSE and the external code that *drives* PSSE according to the input data and any custom device models. A more detailed discussion of the use of the PSSE API is provided in Appendix A.

Load and generation scenarios for a day or days are created in advance and along with fixed network parameters. The data is then batch processed by the simulator. User created scripts perform the following functions that are necessary for the observe-update-solve cycle as summarised by the white boxes in Figure 3.2. The pseudocode for a 1 day simulation at

5 second intervals for a single scenario is as follows:

1. Load network data such as branch impedances, loads and generation into the simulator.
2. Solve the network in its present form and ensure convergence.
3. For time = 1 to 17280
    - Observe the solved network.
    - Update network data:
        - According to load and generation time series.
        - According to controller actions.
    - Solve the network using iterative solver and ensure convergence.
4. Exit simulator.

PSSE is capable of providing a solution to the network data in which ULTC winding ratios are set to minimise deviation of bus voltages from their targets. This solution, however, omits the real-time characteristic of all automatic tap-changers. The most important characteristics are the delay between observing a condition that it should act to change and actually acting. This includes any artificial delays used by real transformer controllers. It also ignores that adjustment of tap-position is sequential and usually only reflects local measurements. A real network does not suddenly alter the tap-position of all transformers in an instant.

3.2.1 Custom simulation code using Python

The ULTC delay is implemented in the custom ULTC model, described further in section A.2, in order that the ULTC does not operate too frequently as discussed in Chapter 2. Solution of the network is achieved with the tap ratios fixed according to the network model at each time-step. Operation of the taps is simulated during the Control Algorithms part of the cycle in Figure 3.2 according to algorithms implemented in Python. The algorithm is supplied relevant network details on which to base its operation. The algorithm determines what ratio

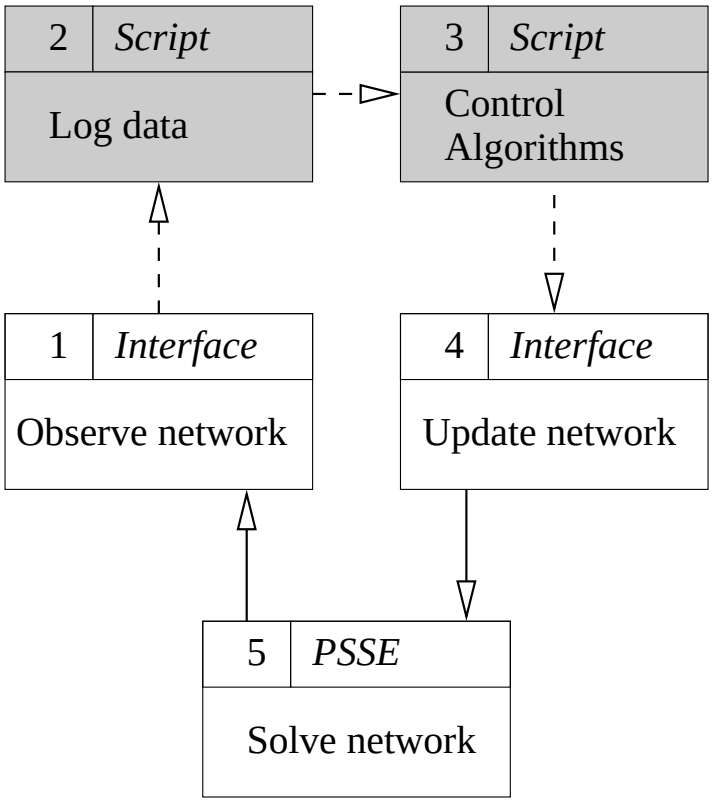

Figure 3.2: *The flow of control in the observe-modify-solve cycle with script activities.*

the tap-changer is set to for the next time-step. The ratio is set during the update part of the cycle. The network is then solved with these ratios fixed at the new values.

The interface to PSSE allows any algorithm to be implemented to control tap-changer action. There are physical constraints such as finite tap ratios and non-zero time for a tap change. The operation of the tap-changer according to these physical constraints on the device is the responsibility of the algorithm or script interfacing with PSSE.

Automation scripts are written in Python, an object-oriented programming language. PSSE can be set to run these scripts, providing an Application Programming Interface (API) with which to modify the network case and run load flow solutions as required. These scripts are responsible for performing a simulation run according to the many possible initialisation parameters such as:

- Network definition file.

- Load profile.
- Generator schedule.
- Generator controller parameters and methods.
- Individual ULTC controller parameters and methods.
- Data to be stored at each time-step for later analysis.

The scripts must also execute the additional tasks every time-step as in Figure 3.2. The tasks shown in the shaded boxes are saving data at each time-step for later analysis and executing the control algorithms. For simplicity of interaction, all code external to PSSE, including implementation of the control algorithms, was written in Python for this project.

The custom code written for this project is split into two distinct types, the *Custom API* and the rest of the simulation code. These are the shaded boxes in Figure 3.3. The *Custom API* is the only code that calls the PSSE API and features an improved technique of error checking which causes the simulation to terminate with notices to the user should the power-flow solution fail to converge. It also simplifies PSSE function calls and provides key data to the rest of the code about the network elements loaded into PSSE. The rest of the code reads in scenario data and then performs the observe-update-solve as described above, using functions supplied by the *Custom API* only.

A more detailed breakdown of the custom code written for the simulator is provided in Appendix A. Figure A.4 in A expands on Figure 3.3 shown here.

3.2.2 Network solution parameters

There are a set of parameters that determine the performance of the load flow methods. The crucial parameters are acceleration factors and the maximum number of solver iterations.

In general, a larger network requires more solver iterations for the solver to converge on a satisfactory solution. A large network, in particular if voltages differ greatly from nominal, requires slow acceleration factors to converge at all.

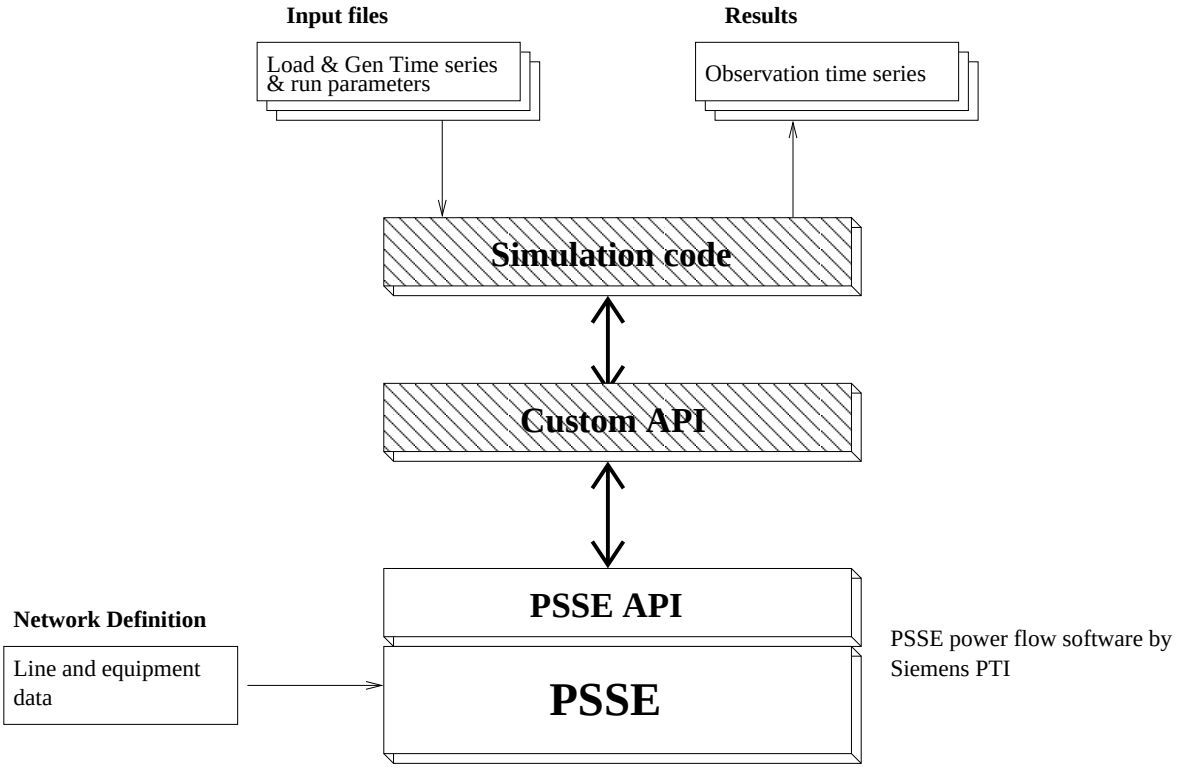

Figure 3.3: *Diagram showing interactions within and between custom Python code (shaded) and PSSE.*

To avoid always using small acceleration factors and a large number of solver iterations, the `solveFixed` method first tries near default acceleration factors (*ACCP*, *ACCQ* and *ACCM*) and the number of solver iterations (*ITMX*) is limited to 300. Should the solver have failed to converge two further attempts are made with different parameters as shown by table 3.1.

Attempt	ACCP	ACCQ	ACCM	ITMX
1	1.0	1.0	1.0	300
2	0.06	0.06	0.06	2000
3	0.01	0.01	0.01	3000

Table 3.1: *Gauss-Seidel solution method parameters*

Should the solver fail at attempt 3 the simulation process exits.

3.3 Load and generation data.

3.3.1 Load data

Typical load data is taken from an Electricity Association spreadsheet with data at hourly or half-hourly bases. The data is split into eight types of load:

- Domestic unrestricted and Economy 7
- Non-Domestic unrestricted and Economy 7
- Non-Domestic load factors 0-20%, 20-30%, 30-40% and >40%

Each type of load is saved as a file containing 48 lines, each line consisting of two values separated by whitespace denoting a complex power value. Each value is the average power for a half-hour period. The complex power values are loaded into the simulation and then are interpolated linearly to produce a value for each time-step in the simulation.

Linear interpolation assumes that the power changes linearly between two half-hour values For example, the daily average load curve for winter is given for domestic and small commercial customers in Figure 3.4.

The proportion of different types of load present must then be given. An aggregated load curve is created by summing all the $type$ curves, weighted by their respective proportions defined by the vector Mix.

$$L_t = \sum_{types} (L_{t,type} \cdot Mix_{type}) \tag{3.1}$$

where L is the load, t is the time-step

This curve is then normalised by dividing each value by the curve's maximum value.

$$L_t^{norm} = L_t / max(real(L)) \tag{3.2}$$

where real(L) is the real values of L.

For example, a load with proportions 3,3,1,1 for: domestic; domestic economy-7; non-domestic and non-domestic economy-7 respectively is shown in Figure 3.5.

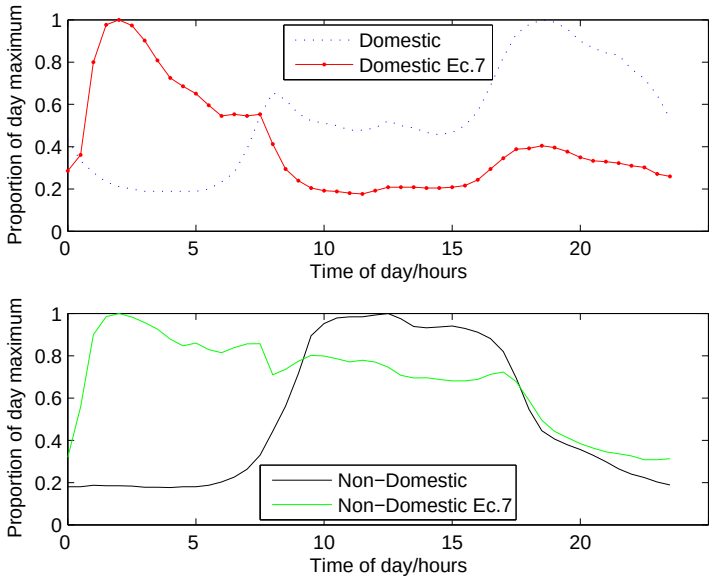

Figure 3.4: *The average load variation due to different customers types during winter.*

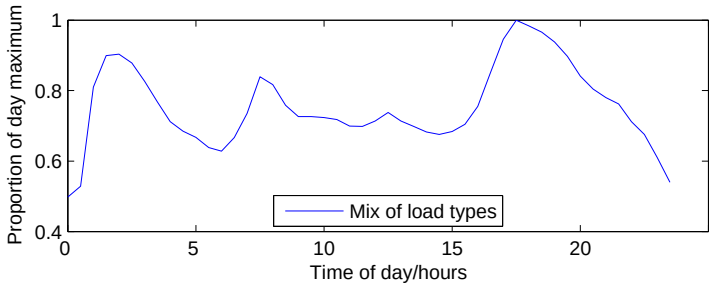

Figure 3.5: *The aggregated load variation due to a mix of load types.*

This normalised curve can then be scaled by multiplying by the the maximum load required on a bus during a day of a simulation run. The result is a time series that is the actual load set for that bus for each time-step in the simulation run.

3.3.2 Generation data

The study has tested the reaction of the distribution network to medium voltage connected variable generation. Although the simulation method is applicable to various types of variable or non-firm distributed generation, wind-powered generation is one of the most common

types with suitable data available.

The study uses data from the Wardlaw community wind farm in Scotland. The wind farm comprises six 3MW turbines, not all of which are necessarily operational at any one time. Figure 3.6 shows the real power output of the wind farm during the period sampled, just under 3 days, with the vertical lines denoting 12 midnight.

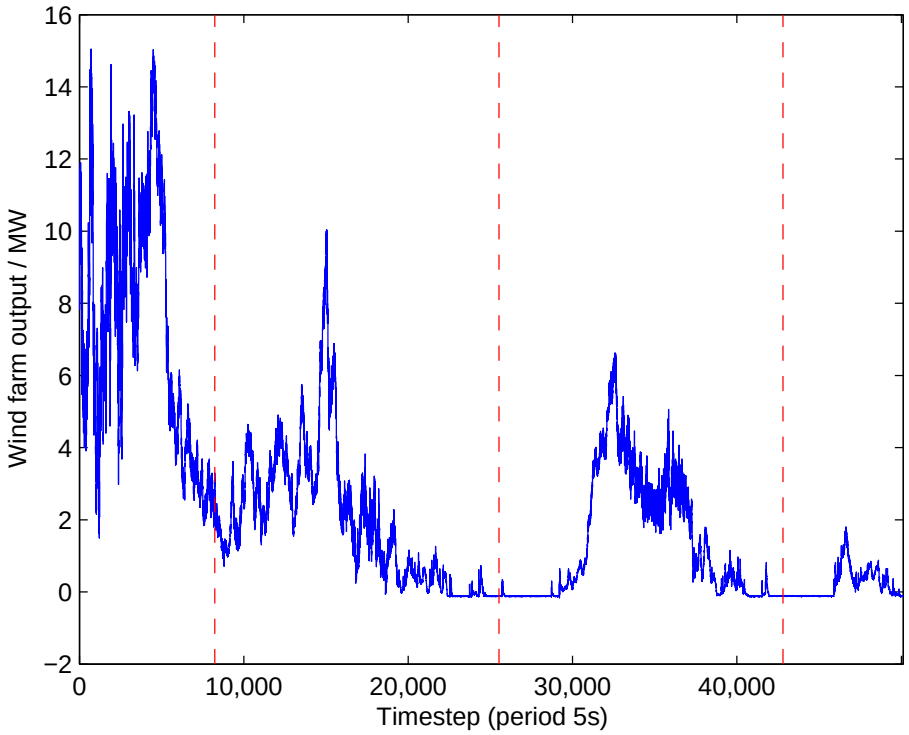

Figure 3.6: *Wind farm real power output for a period just over 2 days in October 2006. The sample period is 5 seconds.*

The wind farm data is split into two 24 hour periods starting and ending at midnight. The data is then normalised like the load data. The normalised curves can be multiplied by the capacity of generation to be connected to a bus to produce the real power output time series of the generation for each time-step. Henceforth these two days of data are called *Wardlaw-day1* and *Wardlaw-day2*.

The data has been recorded with a sample period of 5 seconds. To be sure that ULTC operation due to high frequency variation in DG is properly reflected, the sample period was chosen to be much lower than the delay imposed on ULTC operation. A longer sample

period gives different results. This effect is shown briefly in Appendix B on page 197.

The study typically uses connected generation of maximum output 0.5 to 30 MW depending on the location. The generation curve used for each generator in the simulation is one of the 24 hour normalised curves multiplied by the maximum generation desired for that bus. Note that the wind farm generation is of the order of magnitude of the generation capacities connected in this study.

The reaction of the network is tested with different feeders using different normalised generation curves as a basis for connected generation time series. To achieve this, the study may use a different generation curve on different feeders.

An alternative is to use curves taken with different time offsets from midnight. This simulates geographical dispersion of generation experiencing identical natural resource power, i.e. similar wind speeds, but at different times. An example construction of one curve is that the data may be taken from midnight to midnight in the original *Wardlaw* time series, the other from midnight + 120 seconds to the next midnight + 120 seconds. In this case the latter will be called *Wardlaw-dayN-plus120*.

3.3.3 Generators

DG is connected in this study as either a negative load for PQ mode generation or as a synchronous machine for PV mode generation. The study does not include dynamic simulations or fault current analysis, only load flow calculations. For this reason it is not important how many machines make up the generator connected. The generator is connected with a given real and reactive power output in the PQ case. In the PV case the real power, target voltage and reactive power limits are specified.

It is assumed that all new connected generation will have the ability to control power factor as a Doubly-Fed Induction Generator (DFIG). A DFIG is capable of continuous operation at power factors from 0.95 leading to 0.95 lagging. The Wardlaw DG imports a very small amount of real power during periods of very low wind-speed. It is assumed that if the DG is absorbing real power it does so at unity power factor, that is it does not export or import

reactive power. These assumptions are illustrated in Figure 3.7.

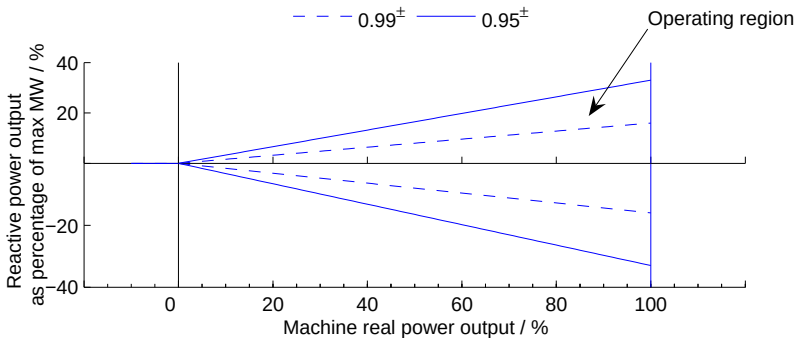

Figure 3.7: *Machine capability diagram of PV mode DG implementation.*

3.4 Voltage controllers.

The following sections detail the operation of different control strategies for ULTCs and DG compared in the subsequent chapters.

This work treats identical parallel transformers as working in master/follower mode where the follower acts in the same time step of the simulation as the master.

3.4.1 Basic voltage regulator

The basic voltage regulator operation outlined in section 2.3.4 is the basis for the ULTC AVR used in this project. The code deciding on whether to initiate a tapping action is contained in the `act` function of the `VoltageRegulator` class. The following pseudo-code is called each time-step where the period of the time-step is *timePassed*:

If $voltage < V^{lowerLimit}$

Set $waiting$ to $True$

Set $operation$ to $tapDown$

Decrease $timer$ by $timePassed$

Else If $voltage > V^{upperLimit}$

Set $waiting$ to $True$

Set $operation$ to $tapUp$

Decrease $timer$ by $timePassed$

Else (voltage within limits)

Reset $timer$ to $OriginalDelay$

Set $waiting$ to $False$

End If

If $waiting$ is $True$ and $timer \leq 0$

Execute tapping operation defined by $operation$

Reset timer to $OriginalDelay$

The `VoltageRegulator` must keep track of the $timer$ value between time-steps.

It can be seen that a tapping operation only occurs if the timer has counted down from $OriginalDelay$ down to zero. The timer only counts down each time-step the voltage is outwith limits. The timer is always left at its maximum value, $OriginalDelay$, if the voltage is within limits.

The tapping operation, $operation$, is executed even if the tap-position is at its limit. The code that $operation$ causes to run will do nothing if asked to tap outside the tap limits. PSSE requires the exact ratio rather than the tap-position at each time-step. To achieve this, each `Transformer` object keeps track of which tap position it is currently on. It only updates the turns ratio in PSSE if it has been requested to tap-up or tap-down. It looks up the associated turns ratio for the new tap position to pass to PSSE from a list of ratios calculated when the object is initialised. The calculation of the list is defined in equation 3.4 in the next section.

Controller parameters

Table 3.2 shows example parameters for ULTC voltage regulators.

From Uncontrolled bus, usually the higher voltage bus.

To Controlled bus, usually the lower voltage bus.

From	To	Base Voltage (kV)	Num taps	Rmax	Rmin	V_+	V_-
35011	35030	132/33	19	1.1	0.8	1.0125	0.9875
35012	35030	132/33	19	1.1	0.8	1.0125	0.9875
35030	67250	33/11	17	1.1	0.9	1.0125	0.9875
66331	66350	33/11	17	1.1	0.9	1.0125	0.9875
66831	66850	33/11	17	1.1	0.9	1.0125	0.9875
66832	66850	33/11	17	1.1	0.9	1.0125	0.9875

Table 3.2: *Voltage regulator parameters in area A.*

Base Voltage The Higher/Lower nominal voltage of the connected buses.

Num taps The number of discrete taps on the controlled transformer for ratio adjustment.

V_+ The upper limit to the controlled bus voltage above which a tap-operation may be initiated.

V_- The lower limit to the controlled bus voltage below which a tap-operation may be initiated.

Rmax The maximum ratio as a product of a fixed ratio.

Rmin The minimum ratio as a product of a fixed ratio.

An important additional parameter, the time delay T, is not readily available for specific transformers. In the Scottish Power network, from which figures the experimentation in Chapter 4 is based, the delay is between 45 and 60 seconds [53].

The transformer ratios TR for each tap position, $n = 1 : NumberofTaps$, are defined by the minimum and maximum ratios of each transformer and the number of taps:

$$StepWidth = (Rmax - Rmin)/(NumTaps - 1) \tag{3.3}$$

$$TR_n = Rmin + (n - 1) \cdot StepWidth \tag{3.4}$$

The data is retrieved during initialisation of the simulation. It is taken from the network case in PSSE via the API. The network case is loaded from a network definition file created from Scottish Power data.

3.5 Generation controllers.

PQ mode generation is implemented by the addition of negative loads to PSSE. PV mode generation is built in to PSSE as a network component. These two modes are implemented as described in section A.2.6.

It is assumed that the DG that is under power factor or voltage control operates as a single machine. Control of individual machines that make up the DG is left to the DG operator. Thus DG added at any bus that is not present in the original data from Scottish Power will be added to the PSSE model in PV or PQ mode as required. All existing generation is in PV mode with constant real power output.

The assumption of the constant power factor generation is that the power factor control of the DG is perfect. A similar assumption is made about the constant voltage DG. It must be noted that PSSE determines reactive power output of each constant voltage DG iteratively by examining power flows and bus voltages of the entire network.

In reality the DG AVR will only react to the voltage at the point of connection. The model used then may be unsuitable for simulations of multiple constant voltage machines connected electrically close to each other, for example on the same bus. For analysis of multiple machine AVR interaction a dynamic study is required. The model is suitable for examining interaction between a single constant voltage machine and its nearby PQ mode DG and ULTCs, as the ULTC time constants are of an order higher.

The above modes can be supplemented by one of the following two generation control algorithms designed to avoid voltage excursions at the connected bus.

3.5.1 Generation shedding algorithm.

This algorithm defines how a generator is shed to avoid the voltage at the point of connection from exceeding limits. The algorithm also defines how the generator may attempt to reconnect.

The algorithm defines the generator to be in one of three states, *In*, *Out* or *Ramping*. *Ramping*

itself has a number of states defined by the time required to ramp up from zero to full capacity. The controller changes state according to the rules in the following pseudocode.

$Capacity$ is the generators capacity in MW, $Ramptime$ is the time to ramp from zero to full capacity power output and $Timeout$ is the time the controller keeps the generator at zero output before attempting to ramp back up to capacity.

Constants $Capacity$, $Ramptime$, $Timeout$

Variables V, $State$, $rampTimer$, $outTimer$

At each time-step, t, first update the $State$ by examining V the voltage at the point of connection, and with reference to timers kept between time-steps $rampTimer$ and $outTimer$.

If already Out then attempt to change to $Ramp$ state. This can be done if the $outTimer$ has timed-out and if the voltage is within limits.

If $State = Out$

If V **is inside limits**

Increment $outTimer$.

If $outTimer \geq Timeout$

Set $State$ to $Ramp$

Set $rampTimer$ to 0

If in the $Ramp$ state then change to In if V inside limits and $rampTimer$ has timed out.

If $State = Ramp$

If V **is inside limits**

Increment $rampTimer$.

If $rampTimer$ **now equal to** $RampTime$

Set $State$ to In.

Always set state to Out if the voltage is outwith limits.

If V **is outwith limits**

Set $State$ to Out

Set $outTimer$ to 0

Having updated the $State$, the current controller state, the output power is determined as a function of P_t, the available power, and the $State$:

If State = Out

Output power is 0.

If State = In

Output power is P_t.

If State = Ramp

Output power is the minimum of P_t and $\frac{rampTimer}{Ramptime}.Capacity$.

Note that the power output at a time-step cannot be greater than that defined by P_t which is fetched from the applicable input time series.

3.5.2 Generation constraint algorithm

The generation constraint algorithm works alongside the shedding algorithm. The state of the shedding algorithm is maintained as above. The real power output of the generator, DG_t is the minimum of that defined by the shedding algorithm and that defined by the present generation cap P^{cap}.

The constraint algorithm is intended to avoid the necessity of entering the tripped state *Out* due to an over-voltage condition. The $VLim^{cap}$ supplied to the constraint algorithm is thus between V^{target} and $VLim^{+}$.

In the event of the terminal voltage exceeding $VLim^{cap}$, the real power output of the generation is constrained or capped. There is no lower voltage limit for the constraint algorithm.

The cap is relative to the generation at the time-step the voltage went above limits. In this way the cap will have a similar level of control during periods of low generation and high

generation. Importantly the cap is not raised unless the available power P_t is at least equal to the cap. In this way the cap is not raised to capacity during short periods of low generation.

Similarly to the shedding algorithm the controller must maintain a number of variables:

Constants $Capacity$, $CapTimeout$, ϵ

Variables Cap, $capTimer$, $capFactor$

ϵ is a hysteresis constant preventing a cap raise when the voltage is close to the limit. The $capFactor$ is the fraction of the existing cap removed from it if the voltage is over the limit. E.g. for a $capFactor$ of 0.1 and an original cap of 14.0 the new cap would be $(1 - 0.1) \cdot 14.0 = 12.6$ if V exceeded $VLim^{cap}$.

At each time-step, t, first update the Cap. The cap is only raised if the available power P_t is at the cap.

If V **is equal to or below** $VLim^{cap}$

If Cap **is less than** $Capacity$ See if Cap can be raised:

If V **is below** $VLim^{cap} - \epsilon$

If P_t **is at least equal to** Cap

Increment $capTimer$

If $capTimer$ **now at least** $CapTimeout$

Set cap to $cap + capFactor$

If the voltage is above the maximum defined for the constraint algorithm then reduce the maximum power allowed by the cap.

If V **is above** $VLim^{cap}$

Set Cap to maximum of $((1 - capFactor) \cdot Cap)$ and zero

The actual power output each time-step is the minimum of the shedding algorithm power and the capped power. The capped power is minimum of P_t and $(Cap \cdot Capacity)$.

3.6 Performance evaluation.

To evaluate the fitness of the network and device control methods, a metric is needed that reflects the extent to which the voltage is kept within limits. This metric is balanced against the number of operations, N_{TC}, required to achieve voltage control in a given time period.

There are two limits that could be used at the voltage levels found on the controlled buses of transformers in this study. The statutory limit is $\pm 6\%$ as required by The Electricity Safety, Quality and Continuity Regulations 2002. The DNOs in Scotland however set themselves a stricter limit for planning purposes of $\pm 3\%$.

An evaluation function has been created for this study which has a voltage history component called the *Total voltage cost penalty* and a component based on the number of tap changes called the *Tap change cost*. The sum of the *Total voltage cost penalty* and the *Tap change cost* is called the *Combined cost penalty*:

$$CombinedCostPenalty = \textit{TapChangeCost} + \textit{TotalVoltageCostPenalty} \tag{3.5}$$

.

It is useful to compare the *Combined cost penalty* with the revenue from generation connected to the distribution network. In this way it can be seen if the *Combined cost penalty* changes in proportion to the generation connected.

To calculate the marginal cost to the system of the effects of increased DG, the *Combined cost penalty* with no DG is subtracted from the *Combined cost penalty* with DG. Note that it is possible to have a marginal cost less than zero if the combined cost penalty with the DG is less than without any DG.

The following sections detail the components of the *Combined cost penalty*. The formulae were implemented in Matlab routines and are run on the result files from the PSSE simulations. Key parameters such as ULTC voltage limits are stored in the results filenames. Some of the routines rely on simple lookup tables that are written for the network being analysed. These could have been automatically generated with the results, but for speed of

implementation they were manually coded for the evaluation routines. The tables required are:

- feeders with their constituent buses.
- buses that have DG connected.
- ULTC bus numbers and the bus numbers of any ULTCs in the feeders below them in the network.

3.6.1 Tap change cost

The *TapChangeCost* is the total number of tap operations in the network being examined in a particular period, multiplied by the cost per tap change. The cost per tap change is based on a transformer overhaul cost and expected life as in section 2.2.1. The cost per tap change is complicated by the cost to generators and consumers of transformer down time. It was assumed that if two or more transformers connect a busbar to the transmission network, then the maintenance penalty (*MP*) will be zero. If only a single transformer provides the connection to higher voltages, it was assumed that all generation will be required to be disconnected during maintenance. The penalty reflects the maximum revenue that could be lost by the generator during this time. It was assumed that the maintenance will be performed at a season of low demand, which will be supplied by back-feeding or closing up normally open inter-connectors between radial feeders.

$$TapOperations = \sum_{t} \begin{cases} 1 & TP_t \neq TP_{t-1} \\ 0 & TP_t = TP_{t-1} \end{cases} \tag{3.6}$$

where TP is tap position.

$$TapChangeCost = (MP + TMC) \cdot \sum_{ULTCs} TapOperations \tag{3.7}$$

where TMC is £0.225, the cost of a single tapping operation based on maintenance costs as discussed in section 2.2.1; MP is the maintenance penalty based on loss of revenue from

disconnected generation during maintenance.

$MP = 0$ if the ULTC is part of a group of two or more parallel transformers, otherwise the cost is calculated as follows:

$$MP = (days \cdot 24 \cdot £(MWh)^{-1})/LifetimeTapOperations \tag{3.8}$$

where $days$ is the number of days required to perform ULTC maintenance, assumed to be 3; $£(MWh)^{-1}$ is £31.72 [74]; and $LifetimeTapOperations$ is assumed to be 100000.

3.6.2 Total voltage cost penalty

The *TotalVoltageCostPenalty* aims to penalise network operation where the voltage on buses exceeds planned limits. The *TotalVoltageCostPenalty* is calculated over a period of operation of a network. The metric should reflect the duration of voltage excursions and the relative importance of the bus on which any excursion occurs during the period of operation.

The *TotalVoltageCostPenalty* should be comparable with the *TapChangeCost*. This is achieved by weighting a voltage excursion with the generation connected below that bus at that time-step multiplied by the average wholesale price of electricity. The *TotalVoltageCostPenalty* then can be considered the cost of the lost opportunity for the generators during periods where the voltage exceeds limits at any point in the feeder.

- Costs due to tap operations.
  - Repair and maintenance.
    - Labour and parts £22.5 per change in 2003 (see section 2.2.1).
    - Transformer disconnection for maintenance penalty.
  - Voltage quality affected by large or frequent voltage steps.
- Costs due to voltage excursions.
  - Revenue lost to tripped distributed generation.
  - Penalties to DNO for exceeding $\pm 6\%$ (or $+10 - 6\% for < 1kV$)

As mentioned earlier, there are costs that are difficult to quantify such as the impact of more frequent maintenance, the impact of more frequent tap changes on nearby connected machines and equipment and the cost of operating at voltages close to legal limits.

The penalty due to voltage excursions is derived as a function of the bus voltage where the function will be called the *barrier function*. The function for the base penalty of the *VoltageCostPenalty*, *VPenalty*, is shown in Figure 3.8 and is defined as follows:

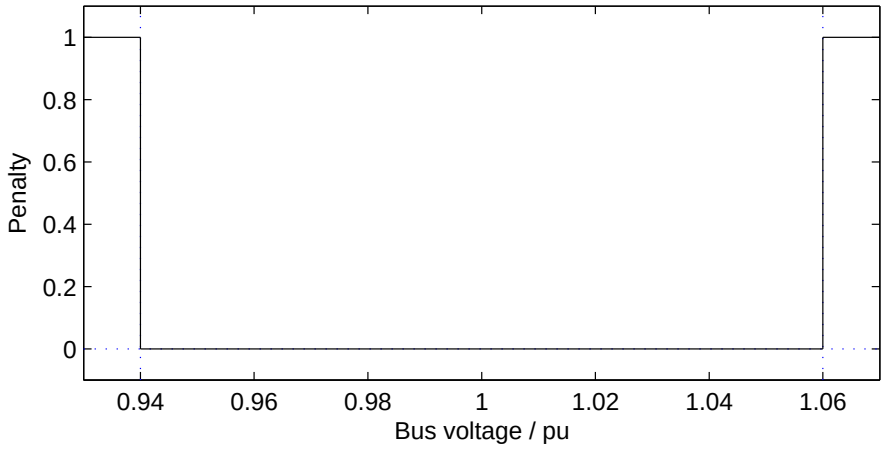

Figure 3.8: *The* VPenalty *function.*

The barrier function gives a zero base-penalty within $\pm 6\%$. Outwith $\pm 6\%$, the base-penalty increases to 1. This reflects that generators that cause a feeder to exceed voltage limits would normally be disconnected. The *VoltageCostPenalty* for that feeder is equal to the lost revenue during the time it would have been disconnected. Note that the penalty does not assume a fixed time for disconnection but penalises every time-step that the voltage exceeds limits with no penalty as soon as the voltage returns within limits.

$$VPenalty_t = \begin{cases} 0 & \alpha(V_t) < 0 \\ 1 & \alpha(V_t) > 1 \end{cases} \tag{3.9}$$

Total voltage cost penalty definition

The method of calculating *TotalVoltageCostPenalty* is defined as follows where vector operations are piecewise such that the binary operator $+$ is defined by:

$$\mathbf{A} + \mathbf{B} = [\mathbf{A}_1 + \mathbf{B}_1, ..., \mathbf{A}_i + \mathbf{B}_i, ..., \mathbf{A}_n + \mathbf{B}_n] \tag{3.10}$$

the unary operator $||$ by:

$$|\mathbf{A}| = [|\mathbf{A}_1|, ..., |\mathbf{A}_i|, ..., |\mathbf{A}_n|] \tag{3.11}$$

and the summation function $\sum$ by:

$$\sum_{x \in \mathbf{X}} \mathbf{A} = [\sum_{x \in \mathbf{X}} \mathbf{A}_{(x,1)}, ..., \sum_{x \in \mathbf{X}} \mathbf{A}_{(x,i)}, ..., \sum_{x \in \mathbf{X}} \mathbf{A}_{(x,n)}] \tag{3.12}$$

For each feeder:

1. Create vectors $\mathbf{BusVoltage}$,$\mathbf{Load}$ and $\mathbf{DG}$ which are the voltage, load and generation at each bus in the feeder over time.

2. Apply barrier function 3.9 to $\mathbf{BusVoltage}$.

$$\mathbf{BusPenalty} = VPenalty(\mathbf{BusVoltage}) \tag{3.13}$$

3. Take the maximum value at each time-step over all $\mathbf{BusPenalty}$ vectors:

$$\mathbf{FeederPenalty} = \max_{FeederBuses}(\mathbf{BusPenalty}) \tag{3.14}$$

   The $\mathbf{FeederPenalty}$ is a time-series of voltage base-penalties which are either 0 or 1.

4. Calculate the $\mathbf{FeederWeighting}$:

$$\mathbf{FeederWeighting} = \sum_{FeederBuses} |\mathbf{Load}| + |\mathbf{DG}| \tag{3.15}$$

   The $\mathbf{FeederWeighting}$ reflects the value of the feeder in terms of DG and Load revenue at each time-step.

5. Calculate the dot product of $\mathbf{FeederPenalty}$ and $\mathbf{FeederWeighting}$:

$$WeightedFeederPenalty = \mathbf{FeederPenalty} \cdot \mathbf{FeederWeighting} \tag{3.16}$$

   The $WeightedFeederPenalty$ is a single scalar value that is the generated electricity and load supplied whilst outside voltage limits.

6. Adjust the weighting of $WeightedFeederPenalty$ by the wholesale electricity price:

$$TotalFeederCostPenalty = \tag{3.17}$$
$$penceMW^{-1}s^{-1} \cdot SamplePeriod \cdot WeightedFeederPenalty$$

   The $TotalFeederCostPenalty$ now reflects the value of electricity generated and supplied on the feeder whilst exceeding voltage limits.

Finally the $TotalVoltageCostPenalty$ is defined by summing the $TotalFeederCostPenalty$ over all feeders:

$$TotalVoltageCostPenalty = \sum_{f \in Feeders} TotalFeederCostPenalty_f \tag{3.18}$$

3.7 A more sophisticated penalty

The barrier function shown in Figure 3.8 does not penalise the operation of the network when the feeder voltages are close to statutory limits. Such a penalty could not distinguish between two strategies that both kept voltages within limits though one might keep voltages closer to unity. An alternative is to create a penalty function that is greatest outwith limits but reduces continuously to zero within limits such as those shown in Figure 3.9. The penalty is greater than zero when the voltage is outside $\pm 3\%$, the DNO planned voltage limits.

The value of this penalty is defined by Equation 3.19 for voltages outwith $\pm 3\%$ but within $\pm 6\%$.

$$\alpha(v) = \frac{1}{\tau} \cdot \big(\ln(v - 0.94) + \ln(1.06 - v)\big) - \big(\ln(0.97 - 0.94) + \ln(1.06 - 1.03)\big) \tag{3.19}$$

τ is a *temperature* coefficient that adjusts the steepness of the curve as shown in Figure 3.9

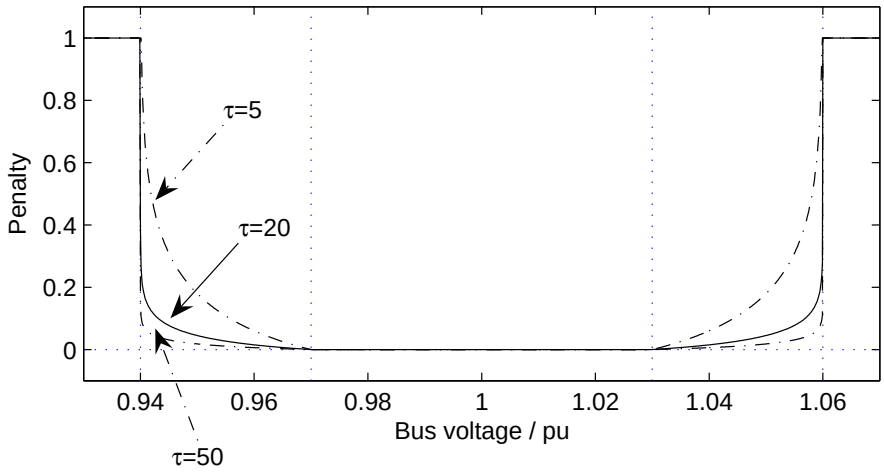

Figure 3.9: *Barrier functions with non-zero penalties close to statutory voltage limits.*

This continuous penalty would be useful in a simulation that iteratively or otherwise, modifies the control strategy in an attempt to arrive at an optimal strategy. This penalty function has not been used in this project however, as the assumptions about the financial cost basis of the straight-sided function cannot be extended to penalising operation within $\pm 6\%$.

3.8 Summary

A method of simulating a network with load and generation changing over time has been presented. The method entails repeated load-flow solution of the network with adjustments for load, generation and tap-changing transformer positions. The simulation uses a power flow solving program in conjunction with Python code to manipulate the load and generation, implement tap-changing transformer ratios and to record required observations.

The voltage control algorithm for the tap-changing transformers has been detailed, as well as two algorithms for the control of generator active power to minimise voltage excursions. Finally, a method of evaluating the fitness of the control algorithms was presented.

The next chapter exercises the simulation method to confirm its correctness. The network studied is introduced and examples are used to demonstrate evaluation of network voltage control performance.

Chapter 4
System Validation and ULTC Study

This chapter describes the emulation of distribution network behaviour in response to time-varying loads and later varying generation. The network behaved in simulation as expected in terms of reacting to time varying loads and distributed generation. The effects of various ULTC AVC operating parameters were explored with the intention of understanding their role as opposed to prescribing optimal settings for the network examined.

Results were produced by repeated power flow solution to simulate time series variation as described in Chapter 3.

4.1 The Network.

The network that was simulated typifies a rural network with potential for further generation in the area [75]. There are a number of grid supply points (GSPs) which are the basis for splitting up the network into six distinct groups of buses named here A, B, C, D, D2 and E. This chapter uses a subsection of this network as shown by Figure 4.1 which comprises of groups A and B.

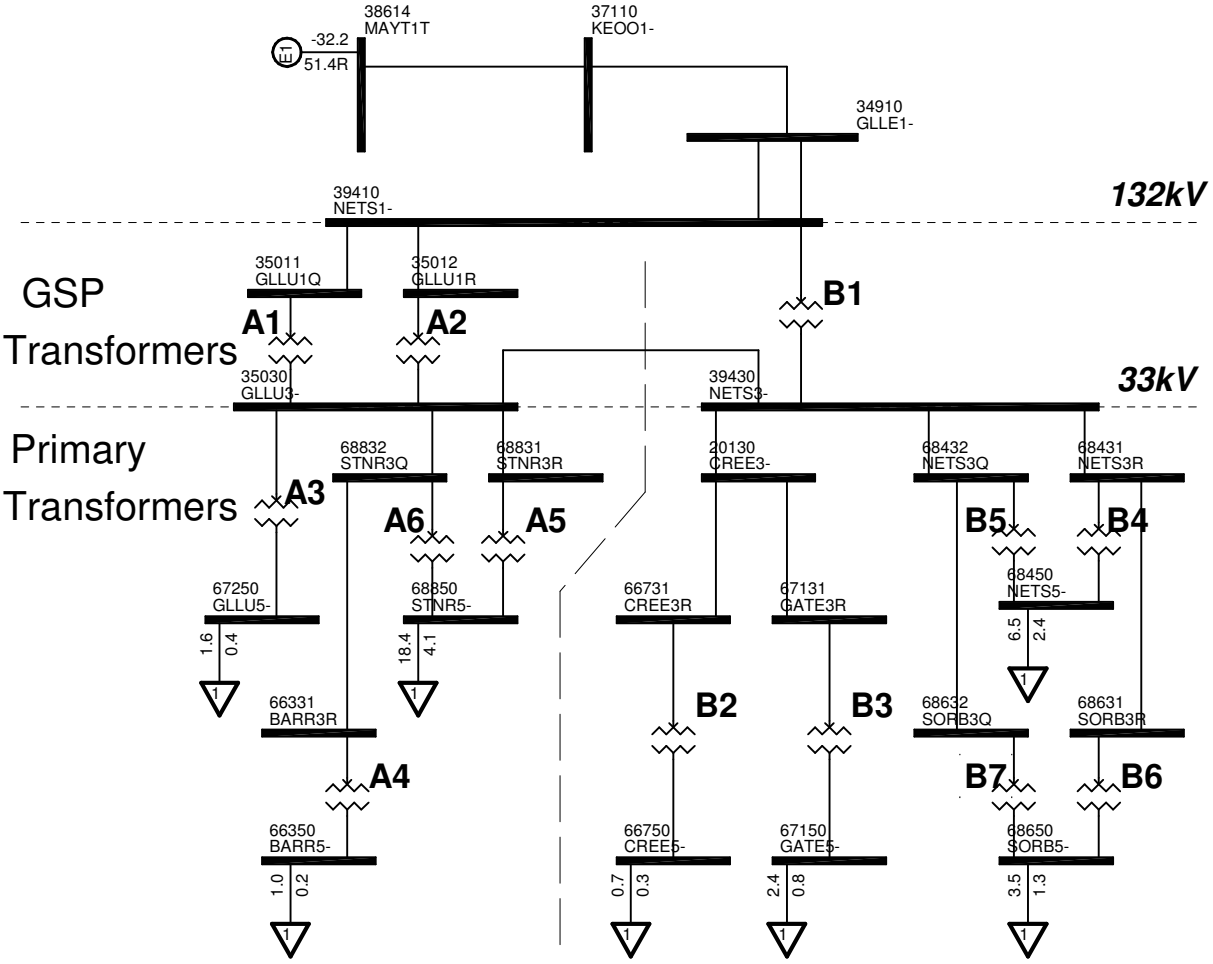

Figure 4.1: *A two GSP area of the Scottish Power Network.*

Above the GSPs are number of hydro plants and a nuclear plant connected to the 132 kV network. The nuclear plant is no longer in operation but at the time at which the network data was collected it was still operating so it was included.

The slack bus was selected as the bus MAYT1T which is adjacent to several of the hydro plants, not shown, that operate to meet local demand in voltage control mode.

The GSPs are regulated by ULTCs from the 132 kV network. The 11 kV substations, the primary substations, are at the ends of long radial feeders. The primary ULTCs regulate the voltage on their LV, 11 kV bus, by adjustment of the turns ratio on the 33 kV side of the transformer. Loads were varied according to simple daily demand profiles as described in section 3.3. No additional generation was connected.

4.2 Operation of under-load tap-changing transformers.

In order to demonstrate the normal operation of under-load tap-changing transformers, the network was simulated for one day using the load curve given in Figure 4.2 to modulate the loads shown in Figure 4.1. The resulting bus voltages and ULTC operations are discussed.

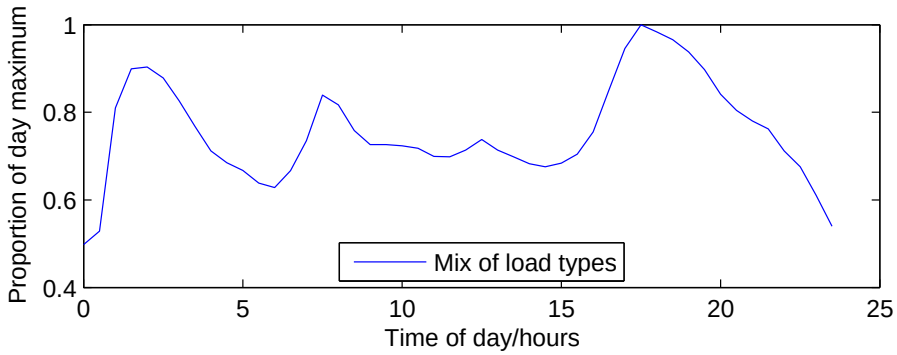

Figure 4.2: *The load variation curve.*

Note that the load curve is normalised. The maximum value of the real and reactive power load at each bus was the maximum winter load as defined by Scottish Power network data. The loads applied at each time-step are these values multiplied by the normalised load curve

as discussed in section 3.3. The term *load bus* applies to the bus on which a load is placed in the *PSSE* case even though this may be a 11 kV bus.

4.2.1 Power flow solutions with simple load variation and fixed tap-changers.

The network case was initialised with tap-positions adjusted for the loads at the first time-step of the 1 day simulation, so as the control bus of each ULTC is close to its target voltage. The simulation was then executed with all ULTCs fixed. Figure 4.3 shows the load bus voltages in area *A*.

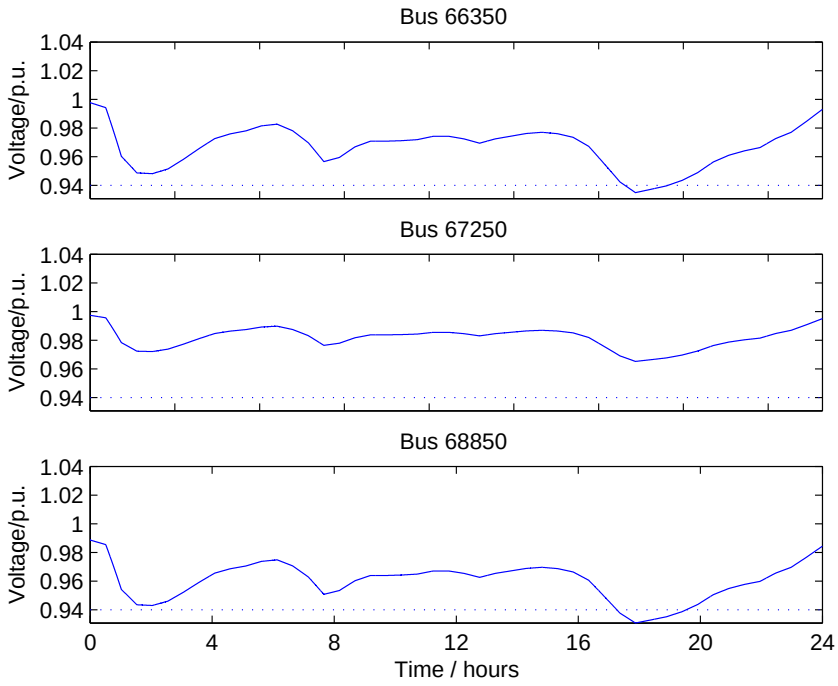

Figure 4.3: *Voltage at the load buses with no ULTC regulation.*

The bus voltages of each bus in the network were observed at each time step and appended to their respective result files. These files were then loaded into MATLAB and are plotted for analysis. At a fixed power factor, as expected, it is shown that the increasing load causes the voltage to drop. The buses shown almost stay within the $\pm 6\%$ statutory limits without any ULTC control though this is not a sufficiently tight limit if the load is in reality comprised

of many loads connected at varying distances from the 11 kV load bus. The further the load from the primary ULTC, the greater is the impedance between the load and the transformer. A greater impedance implies a greater voltage drop between the primary transformer and load. If at full load there is a 4% voltage drop between the substation and load then the ULTC AVC will need to keep the LV bus voltage above nominal - 2% to keep the load bus within statutory limits. As there is usually no active voltage control below the primary transformer, it must control voltage to within tight limits to allow for loads at varying distances and varying magnitudes from the transformer.

Bus 66350 has a small peak load of 0.96 MW. There is a relatively large impedance between it and the GSP. There is a 17.9km and a 19.6km 33 kV line connecting it to the LV side of the GSP transformer. This results in a wider variation of observed voltage than bus 67250.

Bus 67250 shows relatively little voltage variation. It is electrically closer to the GSP than bus 66350 having only a primary distribution transformer connecting it to the GSP transformer by a negligibly short cable. It has a low peak load of 1.6 MW and shows relatively little voltage variation.

Bus 68850 is also close to the GSP but shows a large variation in observed bus voltage. This is because the peak load at 68850 is relatively large at 18.4 MW resulting in a wide load variation through the day.

4.2.2 Tap changer operation with simple load variation.

To keep the voltage closer to 1.0 pu the ULTCs must be allowed to operate. The above simulation was repeated with the automatic voltage control algorithm enabled for all ULTCs. The dead-band was as supplied with the network data. The time delay for each ULTC was 60 seconds.

Figure 4.4 shows the voltage at the load buses. This time the voltage was kept closer to 1.0 pu as expected. Note the sharp changes in voltage. These sharp changes correspond to the tap operations shown in Figure 4.5. At each 5 second time-step, the ULTC AVC checks the control bus voltage and makes adjustments to the turns ratio as appropriate. This results in

different voltages and power flow time series than the previous section.

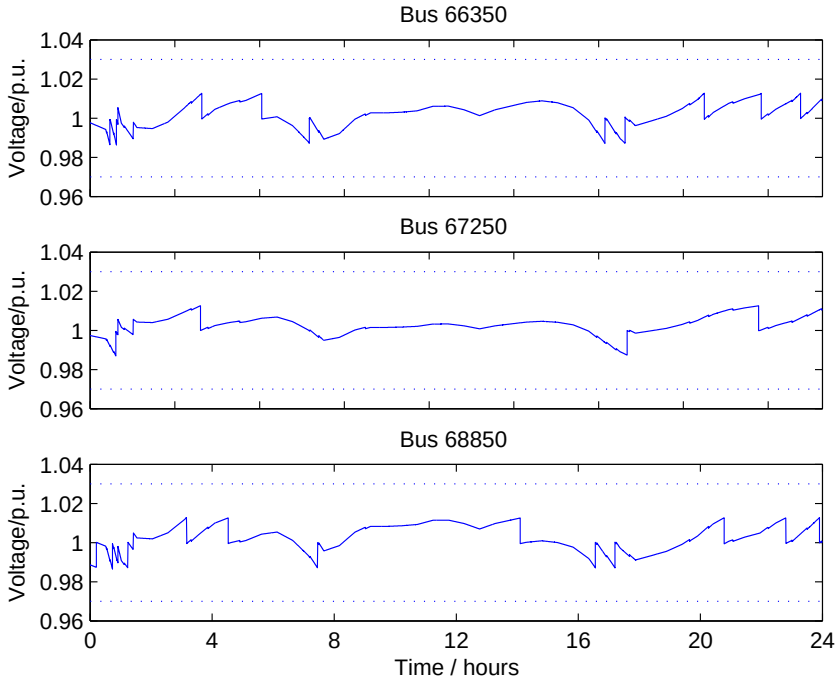

Figure 4.4: *Voltage at the load buses regulated by ULTCs. The dotted lines shown are at 0.97 and 1.03 p.u..*

The tap operations reflect the modulation of the load through the day. As the load increases, the ULTC controllers lower the turns ratio, $N_{HV} : N_{LV}$, by reducing the number of turns on the HV side of the transformer to raise the voltage on the LV side. The peak load occurs just after 16:00 which corresponds with the lowest tap positions of the primary ULTCs as shown in Figures 4.5.

As expected, the primary ULTC A3 (ULTC$_P^{A3}$), the transformer connecting buses 35030 and 67250, shows less activity than the other two ULTCs shown. It was observed earlier that the load bus 67250 shows less voltage variation as a result of load modulation. Consequently less voltage adjustment by tap operation is required to keep the voltage within required AVC voltage limits.

The tap positions of ULTC$_P^{A6}$ are not shown in Figure 4.5 as they are identical to ULTC$_P^{A5}$. The transformers have identical properties and share the same controlled bus in this case.

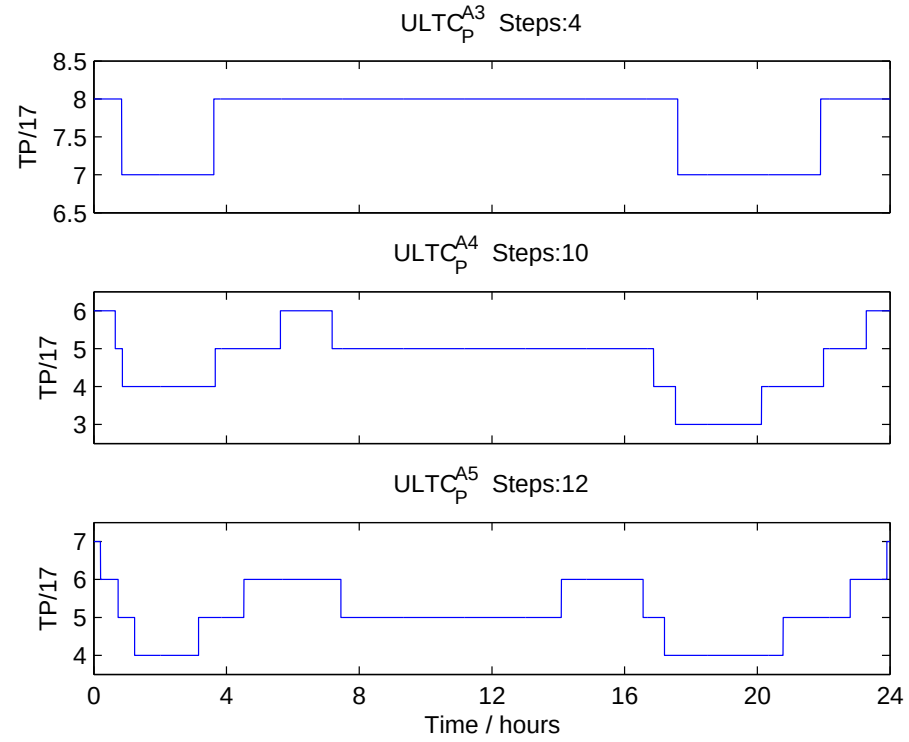

Figure 4.5: *Operation of the primary substation 33 kV/11 kV with load variation.*

ULTC$_{GSP}^{A1}$ and ULTC$_{GSP}^{A2}$ have slightly different properties to each other and the line reactances from the 132 kV bus to their HV sides are different. As a result they show different behaviour as shown in Figure 4.6.

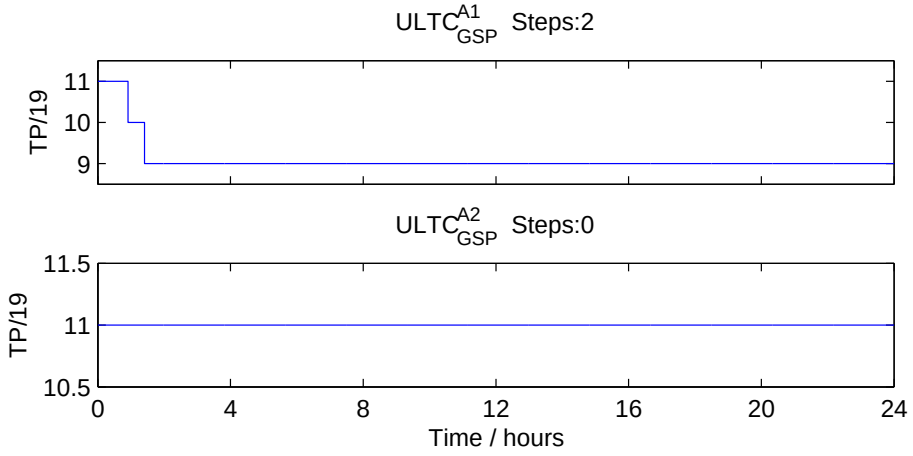

Figure 4.6: *Operation of the GSP transformers 132 kV/33 kV with load variation.*

ULTC$_{GSP}^{A1}$ has slightly tighter voltage limits and consequently acts before ULTC$_{GSP}^{A2}$ when

there is a slow voltage change on the control bus.

The voltage and ULTC tap position time series shown in this section do not end at the same voltage or position as they start, despite the load being equal at the end as the start. The reason for this is that the starting positions for the ULTCs are one of a number of possible configurations that leave the control bus voltages within limits. As the loads change, the ULTCs change tap position according to the algorithm specified. This may leave the tap positions in different positions than the start of the day but still with the controlled buses within limits. Continuing on the simulation further with the load time series repeating each day results in cyclic behaviour with ULTCs in the same position each day at any time of the day.

4.2.3 Adjusting the voltage dead-band.

The voltage dead-band, as described in section 2.3.4, was supplied by the DNO with the rest of the network data for the GSP ULTC$_s$. The voltage dead-band for the primary ULTC$_s$ has been inferred from the step in ratio per tap change as 1.5 times the voltage adjustment due to a single tap operation. The 1 day simulation was repeated with the dead-band increased by a factor of 1.0, 1.5 and 2.0. Figures 4.7 and 4.8 compare the resulting load voltage and tap operations for a single transformer ULTC$_P^{A4}$ with these different factors.

As expected, fewer tap changes are required with a relaxed voltage limit. It could be argued that the original dead-band setting was too strict. As described in section 4.3, the voltage at the primary substation must be kept within strict limits to ensure that each bus that is further away from the GSP stays within statutory limits.

To illustrate the problem of having too small a dead-band the simulation was run with all ULTC dead-bands halved. Figure 4.9 shows that a tap operation to correct the voltage exceeding one limit usually causes the control bus voltage to overshoot the other limit. The repeated overshooting whereby an adjustment is too large to keep the voltage within the dead-band is called hunting. This is observed around hours 07:00 and 18:00.

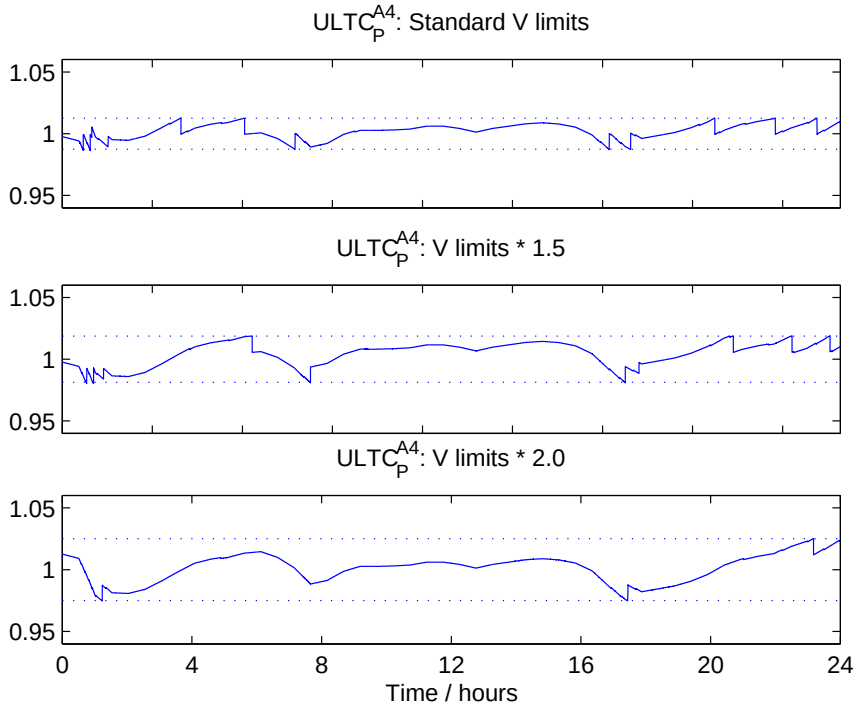

Figure 4.7: *Voltage at bus 66350 for increasing dead-band factors.*

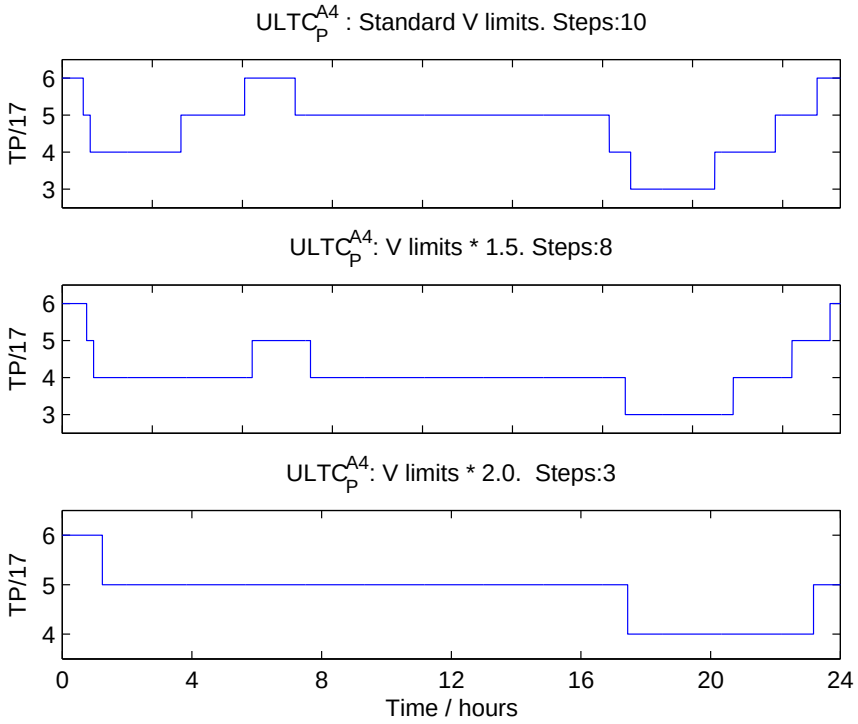

Figure 4.8: *Tap position of $ULTC_P^{A4}$ for increasing dead-band factors.*

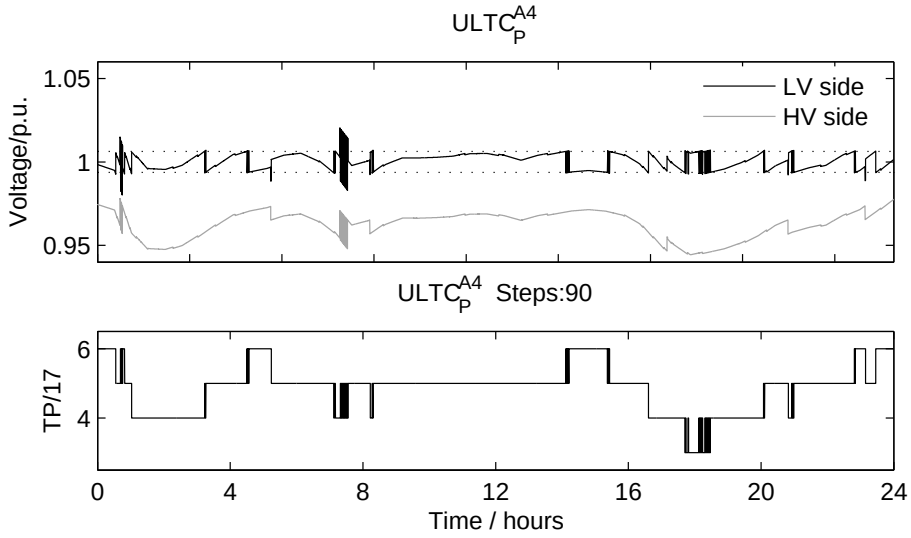

Figure 4.9: *Voltage at bus 66350 and tap positions of ULTC$_P^{A4}$ with voltage dead-band too small.*

4.2.4 Adjusting the time delay.

Figures 4.10 and 4.11 show the load bus voltage of bus 66350 and operation of ULTC$_P^{A4}$ with time delays of 30, 60 and 120 seconds.

Note that with few required tap operations, the time delay has no effect on the total number required. The delay has a small effect on how close the voltage is kept to nominal. The delay is more significant with a more varied power flow through the transformer as seen in the next section.

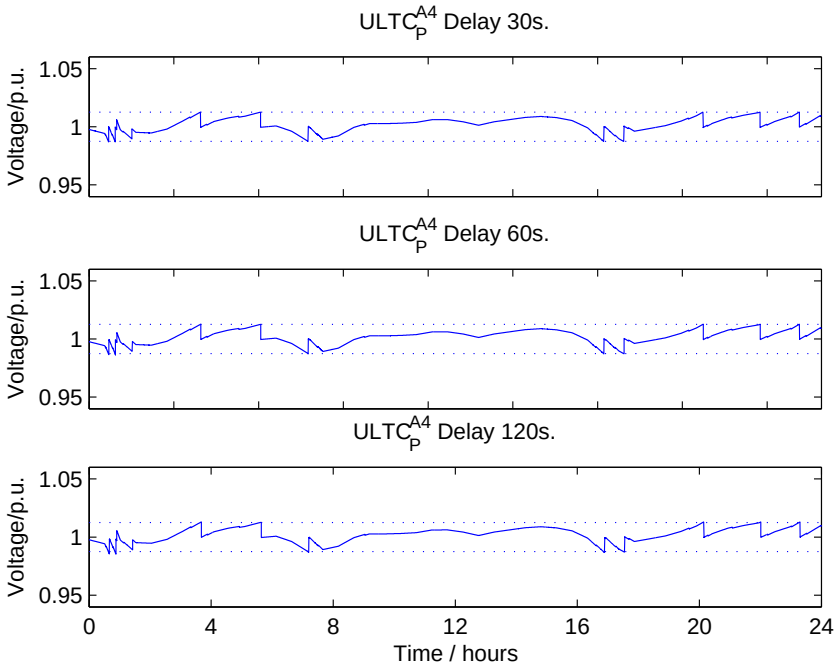

Figure 4.10: *Voltage at bus 66350 as a result of different ULTC delays.*

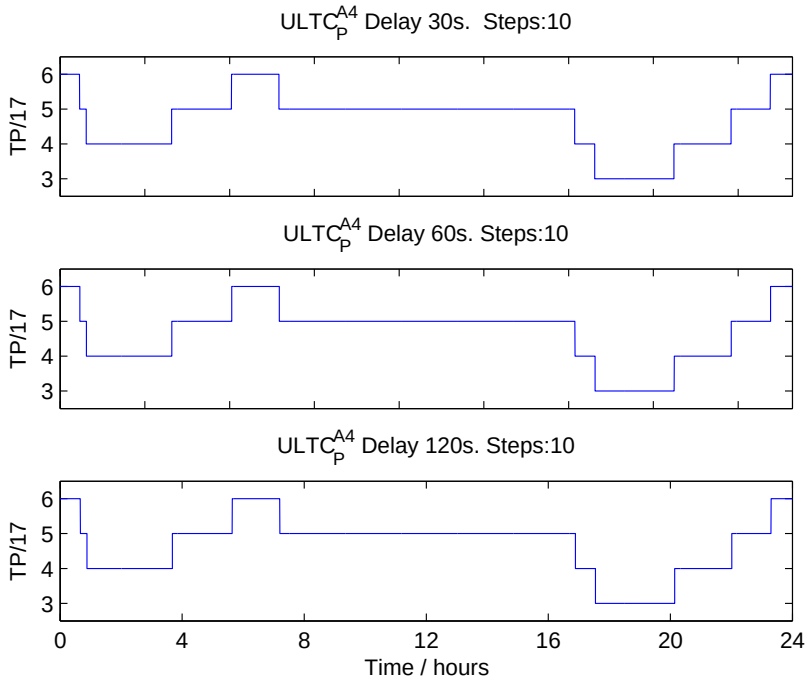

Figure 4.11: *Tap position of ULTC$_P^{A4}$ as a result of different ULTC delays.*

4.2.5 Section summary

This section demonstrated that the time series power flow simulation process produces results consistent with expectations. The interaction of the externally implemented ULTC AVC written for this study is shown to operate as intended. The ULTC AVC controller is shown to control voltage to within the prescribed dead-band.

The voltage dead-band is shown to have a large effect on how close the ULTC AVC keeps the controlled bus to nominal. Small variations in time delay are not shown to affect the performance of voltage control for slowly modulated loads as in this section.

4.3 Network response to increased distributed generation.

The previous section illustrates the basic behaviour of the ULTC AVC and the effect of the delay and voltage dead-band parameters. This section introduces several new elements and considerations to the simulation in order to appreciate the effect of connecting variable generation at 11 kV:

- Non-zero impedance between load and primary distribution transformer.
- Voltage excursions on the high voltage bus of ULTCs.
- Variable generation in PQ mode connected at the primary substation and at the new load buses.
- Unequal time delays at different voltage level ULTCs.
- Alternative ULTC AVC algorithms.
- Variable power factor control of generation.

4.3.1 Voltage at the load.

The previous section showed the successful control of the 11 kV side of the primary distribution transformer using the basic ULTC AVC algorithm. The model, however, fails to reflect that the load is distributed geographically and as such will be connected electrically by varying impedance to the distribution transformers. To more fully appreciate this, the network model was adjusted by the addition of lines and a transformer between the primary substation and the load.

The lines were assumed to be of hard drawn copper type, common in older rural networks. A single $0.15inch^2$ circuit 2km long was used to connect each load bus, with the exception of the largest load at bus 68850 which is assumed to be split into 3 with a $0.15inch^2$ circuit to each. A transformer was included at the load end of the circuit of reactance 1.0 p.u. at a fixed ratio. The transformer tap was assumed to be manually adjusted at the planning stage or seasonally as required. The loads, previously on bus numbers of the form XXX50 are

labelled XXX59 with the intermediate bus before the fixed-tap booster transformers labelled XXX51.

Initialisation of the network case

The secondary substation transformer ratios must be set at the planning stage. The load connected is the mean value of the one day load time series which was described in section 3.3, multiplied by the peak winter value at each bus.

A trial and error process of manual adjustments and load flow solution without tap adjustments was used to arrive at a solution leaving the ULTCs just below a ratio of 1.0 and the load bus voltages at 1.0 p.u. The low ULTC ratio was required to ensure there is room for summer operation when there is less load. The load bus voltages should be close to 1.0 p.u. as the load applied in the tap setting process was the mean for the one day load time series. This allowed for the voltage rise seen at the lower demand periods and the drop seen at the higher demand periods.

The automatic tap assignment feature of the PSSE load flow solver could not be used. The power flow solution failed to converge even at extreme solver parameter settings. At no point in this study was the automatic adjustment of transformers allowed by the PSSE software. Adjustment only occured automatically as a result of the ULTC algorithms in the external simulation code.

The secondary distribution transformers were set as locked. The network definition file, the *.raw* file, had the original ULTCs flagged as in auto-adjust mode. The auto-adjust feature of PSSE was not used but the flag in the *.raw* file allows the external simulation code to recognise which transformers should be controlled by the external code. The secondary distribution transformers have been removed in the final chapters of this study.

Results

Figure 4.12 shows voltage profiles of the three feeders in area A from the 132 kV bus above the GSP to the load buses with the days minimum, mean and maximum load connected. Note

that the three feeders consist of different number of actual buses from the GSP to the load inclusive. For feeder 67259, positions 4,5 and 6 are the same bus. For feeder 68859, positions 5 and 6 are the same bus. With the ULTCs at the same position for each load flow solution, it can be seen that the voltage profile for each feeder varies greatly between the minimum load scenario and the maximum load scenario.

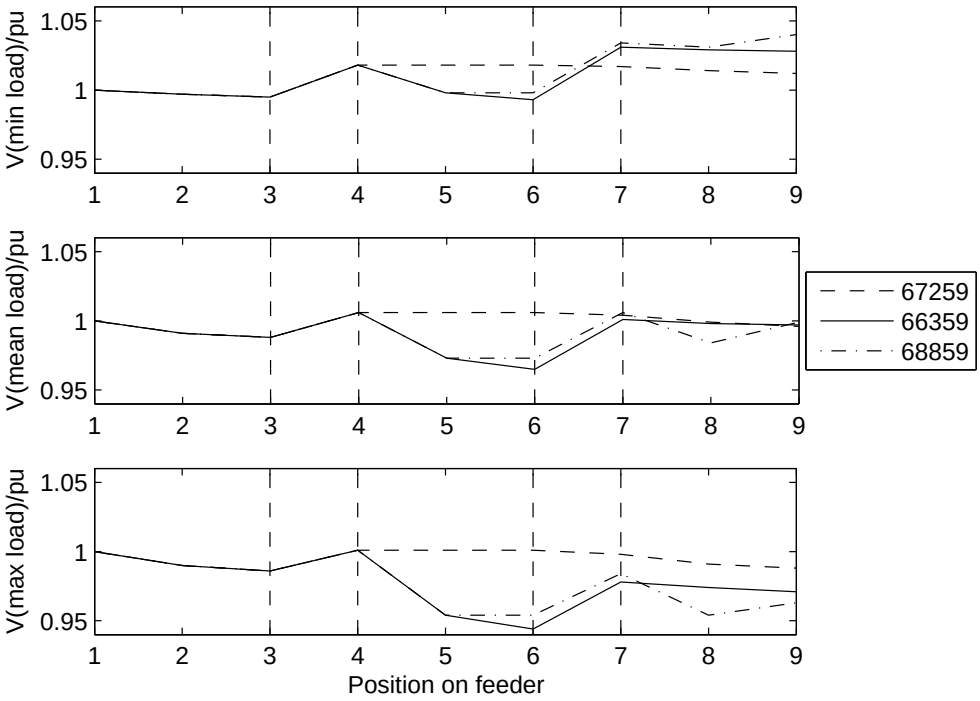

Figure 4.12: *Voltage profile in area A without tap adjustment. Loads are at bus 9 with ULTCs at buses 3-4 and 6-7.*

The reality is better as the ULTC AVCs are able to act to keep the control buses at position 7 within stricter limits. The voltage profiles for the three area A feeders are shown as a result of the ULTCs being allowed to regulate voltage are shown in Figure 4.13.

The buses at positions 4 and 9 are the LV side of the ULTCs on the feeder. The voltage is close to 1 pu as the ULTC AVC action is able to react to the three different load scenarios.

The scatter plots in Figure 4.14 show the voltages at position 7 and 9 from Figure 4.12, this time for areas A and B combined. The plots are the voltages at each bus for each feeder. The circles are used to plot the voltage as a result of minimum summer load, the crosses for

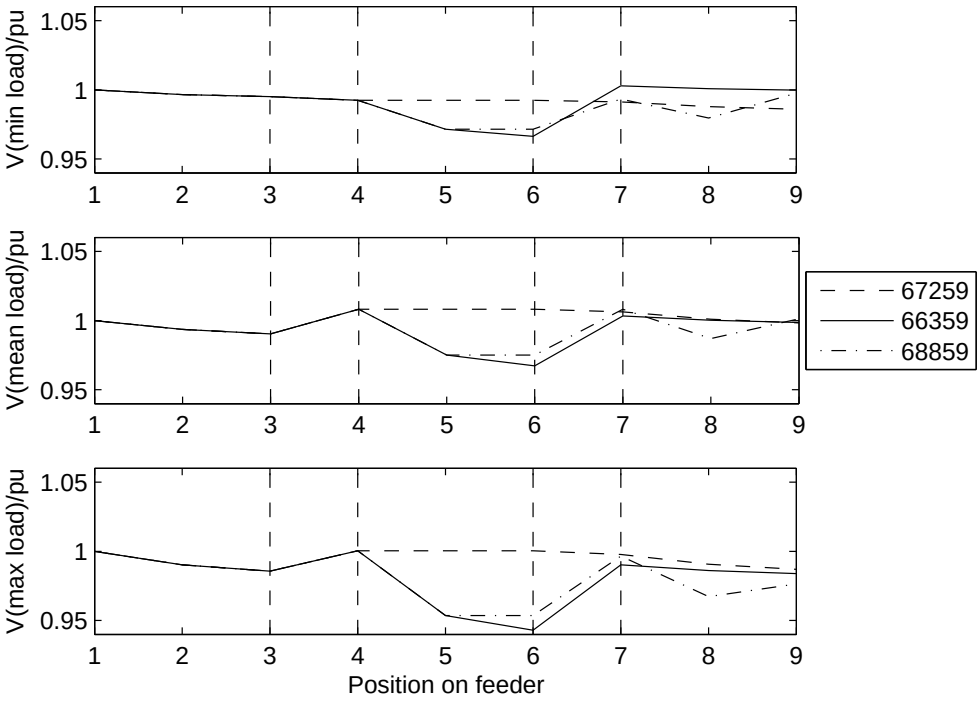

Figure 4.13: *Voltage profile in area A with tap adjustment.*

maximum winter load. There are seven feeders in areas A and B combined thus there are seven circles and seven crosses in each plot.

The first plot is as before, with no AVC control at bus 7. Only the minimum and maximum load scenarios are shown. There is a voltage rise in the minimum load case due to the fixed-tap booster transformer inserted before the load bus in the network case used in this chapter. As the ratio was adjusted for the mean of summer minimum and winter maximum, the voltage is expected and shown to be higher for the minimum load and lower for the maximum load.

The second plot is after a period long enough to allow ULTC AVC control actions. Load bus voltages from different feeders overlap each other. This is because the controlled bus voltage of each feeder's primary ULTC may be anywhere within the ULTCs limits. The load bus voltage can be higher for a higher load if the ULTC tap position happens to be near its upper limit. The bus 9 voltages however are much closer to 1.0 p.u. than in the uncontrolled scenario.

Both plots show an increase in per-unit voltage variation between bus 7 and 9 with slightly

more variation in the uncontrolled case. The load model used characterises the load as constant power with varying voltage when the voltage is above 0.7 per-unit. This assumption will slightly exacerbate the voltage drop or rise seen from the primary transformer to load bus as the voltage tends away from nominal.

The strict limits used in the ULTC control algorithm implementation keep the load bus within a planned voltage limit of $\pm 3\%$.

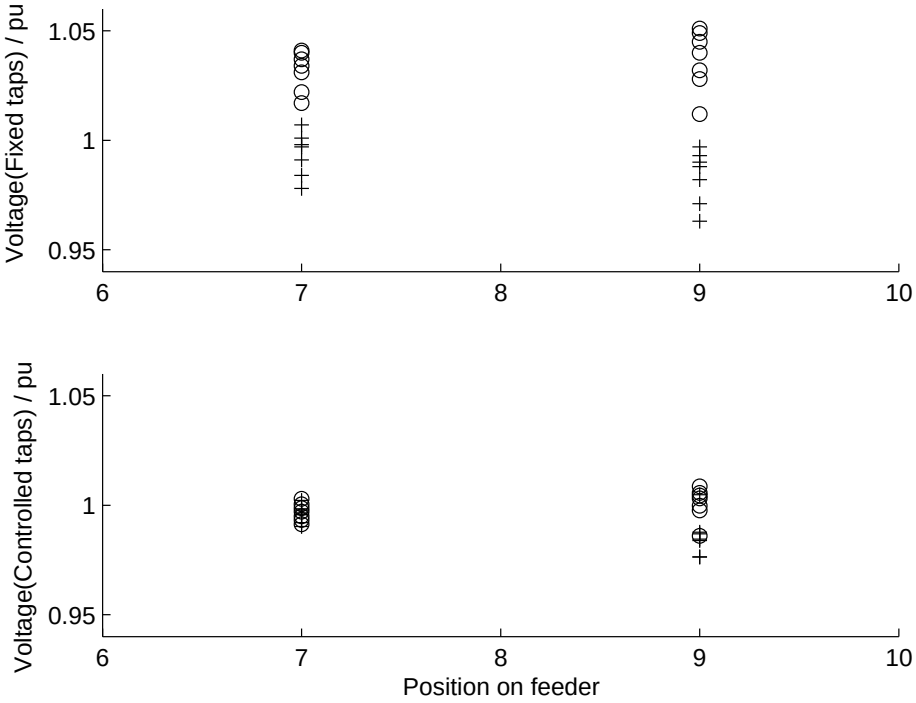

Figure 4.14: *Scatter plot showing spread of voltage variations due to min and max loading. The control buses of the primary transformers are at position 7 and the load buses are at position 9. The $+$ and $\circ$ signs are from maximum and minimum load conditions respectively.*

4.3.2 Additional distributed generation.

Generation added at 11 kV could be connected directly to the primary substation or at the load bus as illustrated in Figure 4.15. The figure shows a primary transformer stepping down from 33kV to 11kV with a fixed boost transformer and 2km line between the LV side of the ULTC and the load as discussed in section 4.3.1.

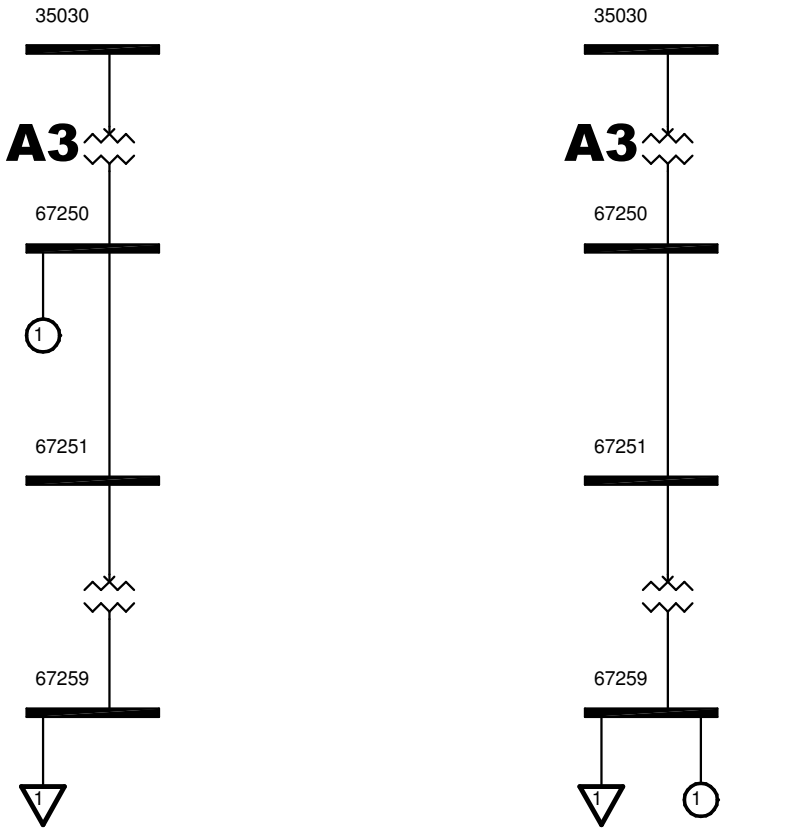

(a) DG connected to primary substation.

(b) DG connected out on load bus.

Figure 4.15: *The possible points of DG connection at 11 kV with feeder 67250 as an example.*

To show the difference in bus voltages between deep connected and load bus connected generation, the simulation was run with varying parameters. A simulation run was conducted for each combination of:

- Minimum or maximum load connected.

- Deep or load bus connected DG.
- DG under each primary substation being a factor of 0.0,0.5,1.0 or 2.0 times the maximum daily load under that substation.

The load and generation was constant through each run with the generation power factor at unity. The simulation was run for a number of time-steps to allow the ULTC AVC to adjust so that their respective control buses where within limits where possible. In this way the run resulted in a steady-state power-flow and tap-position solution.

Figure 4.16 collates the results of the above simulation runs concentrating on the effect on bus voltage at the load and control bus under each primary substation. DG factor defines the real power output of the DG as a multiple of maximum daily load for that feeder. Thus each feeder had a different daily load and DG capacity.

Connecting increasing amounts of generation at the primary substation has little effect on the load bus voltage. So long as the ULTC tap position does not reach the limits of its adjustment range, it can control the LV bus within tight limits leading to little load bus voltage variation.

Connecting increasing amounts of generation to the load bus results in voltage rise on the load bus. Although this can be altered by changing the setting on the fixed tap transformer, this does not mitigate the increased range of voltages observed as a result of increasing generation.

As expected, more generation can be connected at the ULTC LV bus than at a bus connected to the ULTC LV side by a non-zero impedance as in the second case. The variation of voltage rises in each scenarios is due to the different loads on each feeder. The extra impedances connecting each load to the primary transformer were all multiples of a single 2km line as described above, unlike the loads which were determined by the case data.

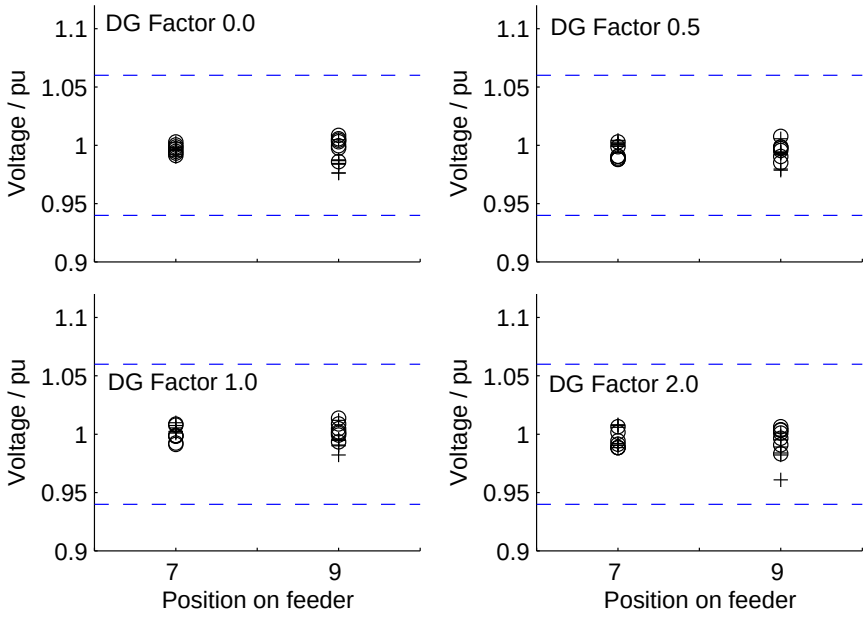

(a) Voltage with DG connected to primary substation.

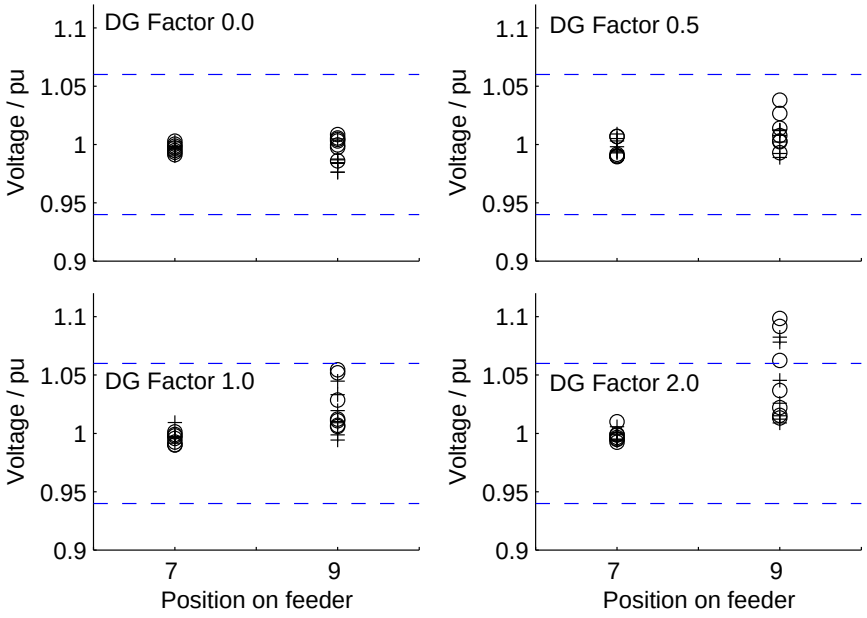

(b) Voltage with DG connected out on load bus.

Figure 4.16: *Voltages at primary substation (7) and load bus (9). DGFactor denotes DG real power connected as a multiple of the load. The + and ∘ signs are from maximum and minimum load conditions respectively.*

4.3.3 Voltage on the transformer buses.

In terms of steady state network behaviour, it appears that a lot more DG could be connected directly to the 11 kV primary substation than in the previous scatter plots. Figure 4.17 is the same as Figure 4.16 but with the ULTC upstream bus voltage plotted.

With a DG factor of 2.0 the upstream bus exceeds or is very close to the statutory limits of $\pm 6\%$ whether the generation is connected deep or on the load bus. The worst instances occur when the minimum load is connected.

These figures show that voltage rise at the point of connection is not the only place where voltage rise due to distributed generation is a concern. The evaluation function in section 3.6 takes into account the voltage of all the buses on a feeder to determine the suitability of the network and generation setup.

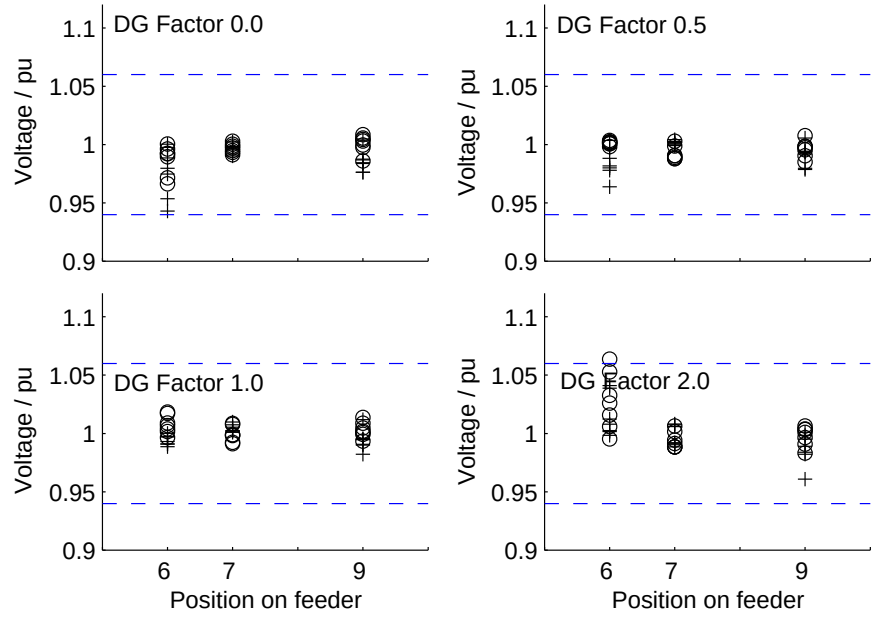

(a) Voltage with DG connected to primary substation.

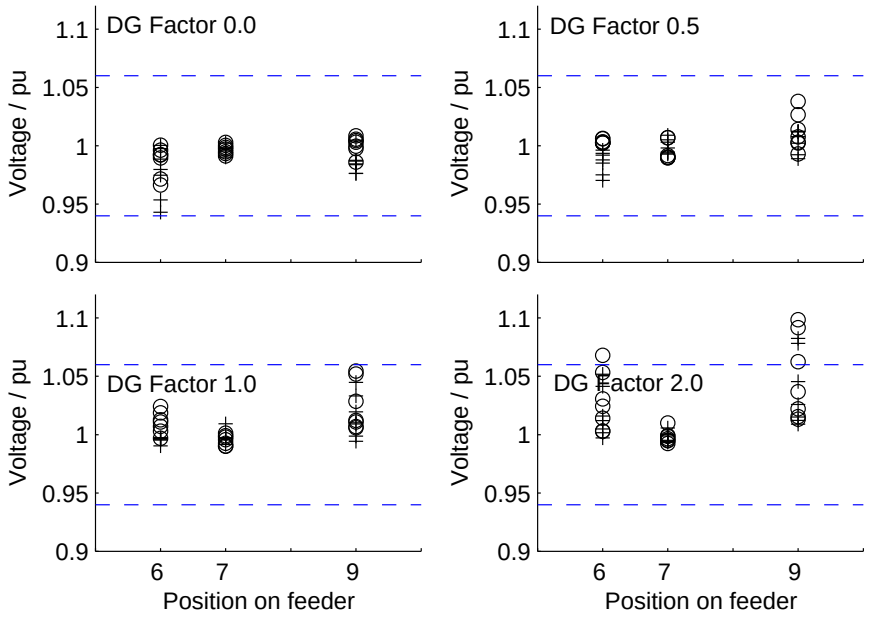

(b) Voltage with DG connected out on load bus.

Figure 4.17: *Voltages at primary substation (6 & 7) and load bus (9). The + and ∘ signs are from maximum and minimum load conditions respectively.*

4.3.4 Tap changer operation with variable DG.

The previous results, shown with added DG, were steady state results. The following results were generated from time series of generation real power output.

Constant power factor mode generation was added to the feeder for ULTC$_P^{A5}$ as seen in Figure 4.15(a). The added generation is referred to as the DG which was connected to the controlled bus of ULTC$_P^{A5}$ to examine its tapping behaviour.

The peak output of the DG is defined in terms of the maximum capacity assigned to bus 68850 at unity power factor as defined in an optimal power flow evaluation of this section of the network by Harrison and Wallace [4]. The output at each time step is defined by the normalised power output curve *Wardlaw-day1* multiplied by the DG peak output as described in section 3.3.2

The resulting ULTC behaviour is shown by its tap positions over time. Figure 4.18 shows the control bus voltage without and then with DG, and below, the tap position of the transformer with and without DG. The limits represented as horizontal lines on the voltage plots are the *VLims* used by ULTC$_P^{A5}$.

Without DG the voltage steps due to tap operations are clearly visible as before. The voltage steps are less clear in the DG case as the voltage is already varying rapidly with DG power output. It can be seen that voltage excursions occur that do not result in a tap operation. This is a result of the time delay parameter, designed to avoid spurious tap operation. The voltage may exceed the operating limit, but only for a few seconds so no tap operation occurs.

It is clear that the frequency of tap change operations increases with the addition of the DG. Some of this increase is due to the highly variable power flow through the transformer. This effect is seen in particular at 14:00.

The addition of time varying DG increases the range of power flows through the transformer. Figure 4.19 shows this for the DG and no DG cases. The negative power flow through the transformer indicates power being exported from the feeder, a situation known as reverse power flow.

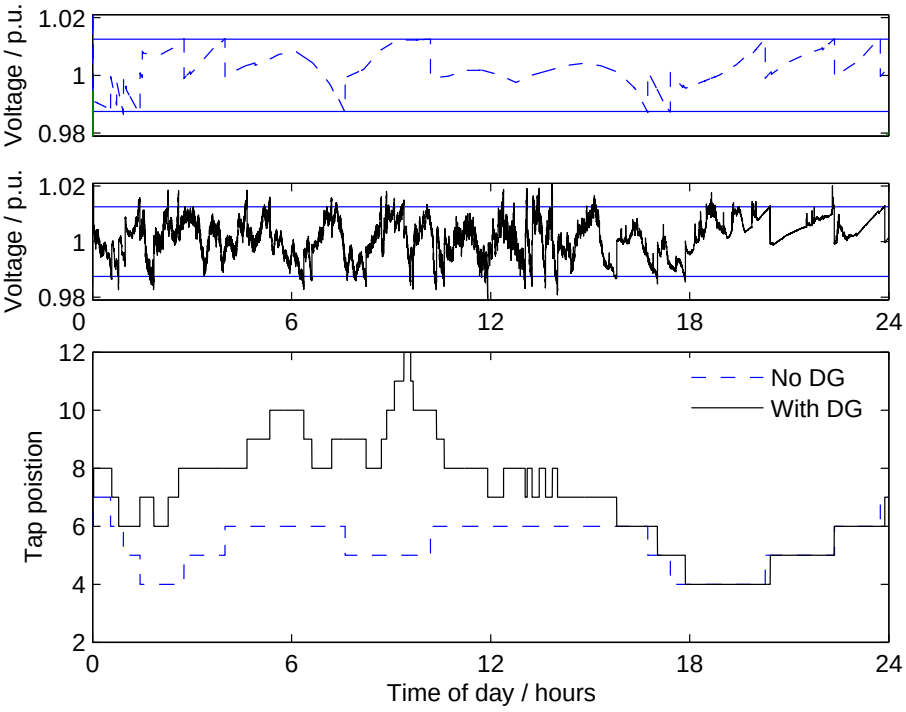

Figure 4.18: *Voltage and ULTC$_P^{A5}$ tap position with generation added deep on the feeder at bus 68850.*

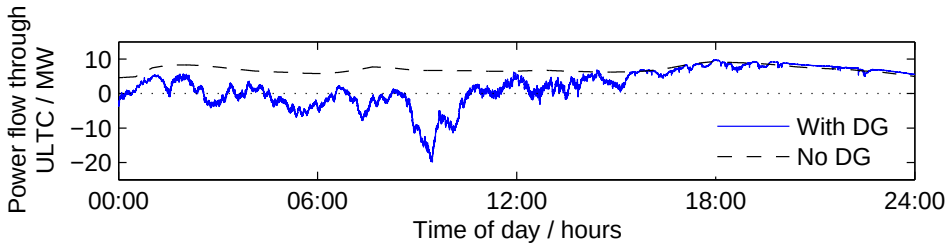

Figure 4.19: *Power flow through ULTC$_P^{A5}$.*

The no DG case shows a positive power flow indicating power is flowing from the HV to the LV side of the primary transformer. The curve is smooth as the variation of load is smooth according to the load time series. The DG case varies between positive and negative. The power flow is positive when the load exceeds generation and negative when the generation exceeds the load. The curve varies rapidly as the aggregate output of several wind turbines in the *Wardlaw-day1* time series is similarly variable.

The increase in range of power flow variation results in an increase in the difference between the minimum and maximum tap position in the day. This range of tap movements is considered unavoidable with respect to improvement of ULTC control parameters. The frequency of tap movements such as the ones around 12:00 may be reduced by adjustment of control parameters as evaluated in the following sections.

Adjusting the delay.

The previous example exhibited a behaviour in which a few tap operations were reversed within minutes of the first operation. These was due to the short term variability of the generation connected.

To test this, the simulation of the previous section was repeated with increased ULTC AVC time delays. Resulting variation in ULTC tap positions are shown in Figure 4.20.

Note the highlighted areas of the plots. The highlighted areas show areas where an increase in ULTC delay has a significant effect on the operation of the AVC. It is shown that an increase in the AVC delay parameter can reduce the number of tapping operations required for voltage control. Doubling the delay reduced the number of tap operations by 18% and tripling the delay reduced the number of tap operations by 30%. The delay causes the AVC to effectively ignore short term voltage variations by only acting when the voltage is outwith limits for a period of time equal to the delay parameter. The longer the delay, the longer the voltage must stay outwith limits before being corrected. The longer the voltage is outwith limits, the stronger is the indication that a tap operation and thus a voltage correction must be made.

The increase in delay has a consequence in the amount of time the ULTC control bus voltage

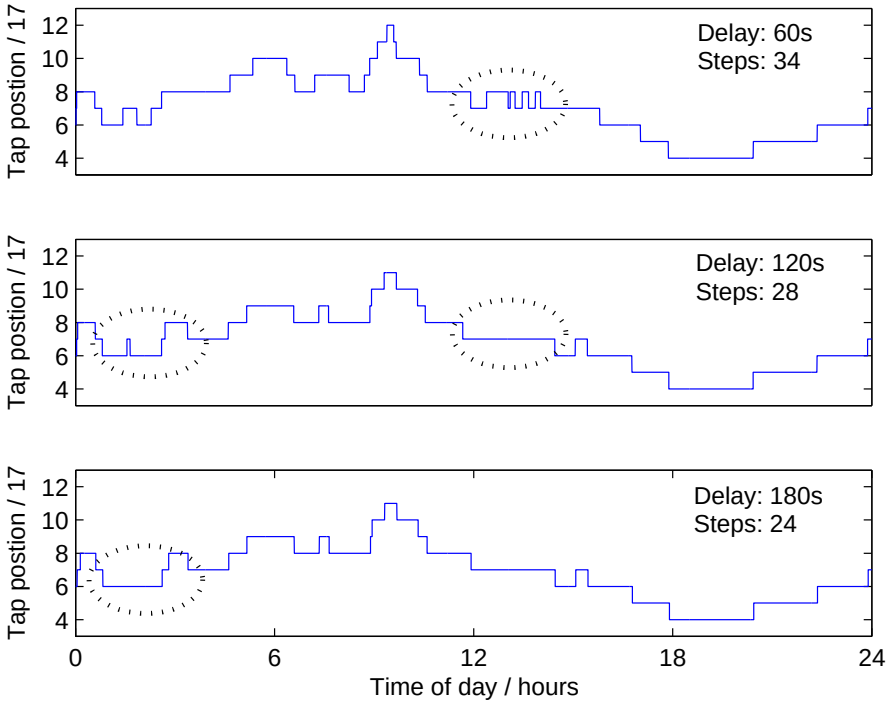

Figure 4.20: *Voltage and ULTC$_P^{A5}$ tap position due to different ULTC delays with generation added deep on the feeder at bus 68850.*

remains outside the ULTC Vlims. This in turn has an effect on the load bus voltage. There is a compromise between delay and voltage control performance that is explored more fully in the next section.

Different delays for different transformers.

To determine the best value for the ULTC AVC delay parameter, the simulation can be run a number of times, each run with a different delay time. As discussed in section 2.3.5 chapter 2, it is desirable to have different delays for transformers in series. To test this, an array of delay values was constructed for the 132/33 kV ULTCs and a separate one for the 33/11 kV ULTCs named $Delays^{132/33}$ and $Delays^{33/11}$.

The simulation was then run with the delay for each voltage level selected from the relevant array. The first simulation shown has no DG connected. It was run for each possible

combination of delays where the arrays are both in the range $(30, 195)$ with a step of 15 seconds.

The results can be visualised by plotting a value obtained from the entire network onto the two dimensions of $Delays^{132/33}$ and $Delays^{33/11}$ giving a three dimensional surface. The value plotted can be any single number reflecting a property of the entire simulation run for that delay combination.

The numbers plotted in Figure 4.21 are the *TapChangeCost* and the *TotalVoltageCostPenalty* for each run. The *TapChangeCost* is a function of the number of tap operations for each ULTC and the associated estimated cost per operation. The *TotalVoltageCostPenalty* is a penalty incurred when any bus on a feeder exceeds the planned $\pm 3\%$ voltage limits. The penalty increases up to the maximum penalty which is if any feeder bus exceeds the statutory $\pm 6\%$limit. The *TapChangeCost* and *TotalVoltageCostPenalty* is described in detail in sections 3.6.1 and 3.6.2.

The two penalties indicate the fitness of the controller and network in terms of their combined ability to keep bus voltages within limits. A high penalty indicates a poor ability to maintain voltage. The two penalties are required as there is a tendency for the reduction of one to be linked to an increase in the other. The goal of maintaining the voltage within limits contradicts the goal of minimising the operation of the ULTC AVC.

Figure 4.21(a) shows that a low delay at the 132/33 kV transformers and a high delay at the 33/11 kV transformers gives the lowest *TapChangeCost*. The *TapChangeCost* is constant for a given DG capacity as exists in this set of results. Thus the lowest *TapChangeCost* amounts to the lowest number of tap operations.

Figure 4.21(b) shows that a low delay at either transformer will minimise the *TotalVoltageCostPenalty*. This indicates that all voltages on all feeders in the simulation run are being kept within planned voltage limits.

The best combination of delays is a trade-off between the *TapChangeCost* and the *TotalVoltageCostPenalty* as shown in Figures 4.21(a) and 4.21(b) respectively. The trade-off is made by weighting the two metrics according to the final cost function as described

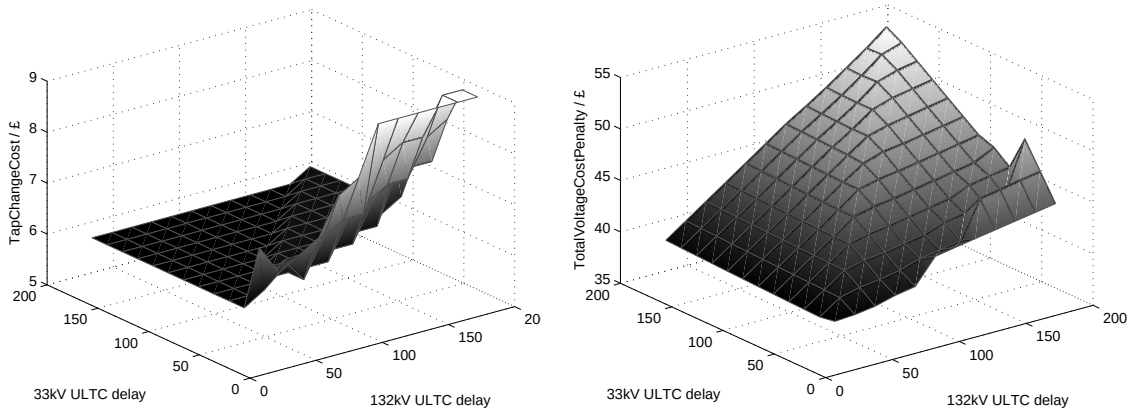

(a) *TapChangeCost*. (b) *TotalVoltageCostPenalty*.

Figure 4.21: *Cost components of a 1 day simulation with no DG. Both delay axes are in 15s intervals from 30s to 195s inclusive.*

in section 3.6 of chapter 3. The cost function for all combinations of $Delays^{132/33}$ and $Delays^{33/11}$ is shown in Figure 4.22.

There is an easily discernible ridge along the line of equal delays. This confirms the rule discussed in section 2.3.5 that suggests that the time delays should be different from each other for two ULTCs in series. The GSP ULTC delay dominates the cost function. For GSP delays of 30 seconds, there is little to differentiate between the primary ULTC delay settings.

Subsequent simulations have used a 45 and 60 second delay for GSP and primary ULTCs respectively. These values are consistent with Scottish Power's settings and with studies finding that unequal delays give the best performance [53, 69].

A similarly constructed plot is shown in Figure 4.23. The data is from a set of simulations described in chapter 5. A large amount of DG, termed DG_{max} is connected at unity power factor to the network as detailed in that chapter. The figure serves as an indication that optimal delay settings are dependent on the amount of DG connected. The graph shows an optimal area for delay settings where the evaluation function is minimised. Unlike the previous scenario, the optimal settings are for equal delays in both GSP and primary ULTCs.

The optimal setting exists in a shallow optimal area with 90,90. The method of varying

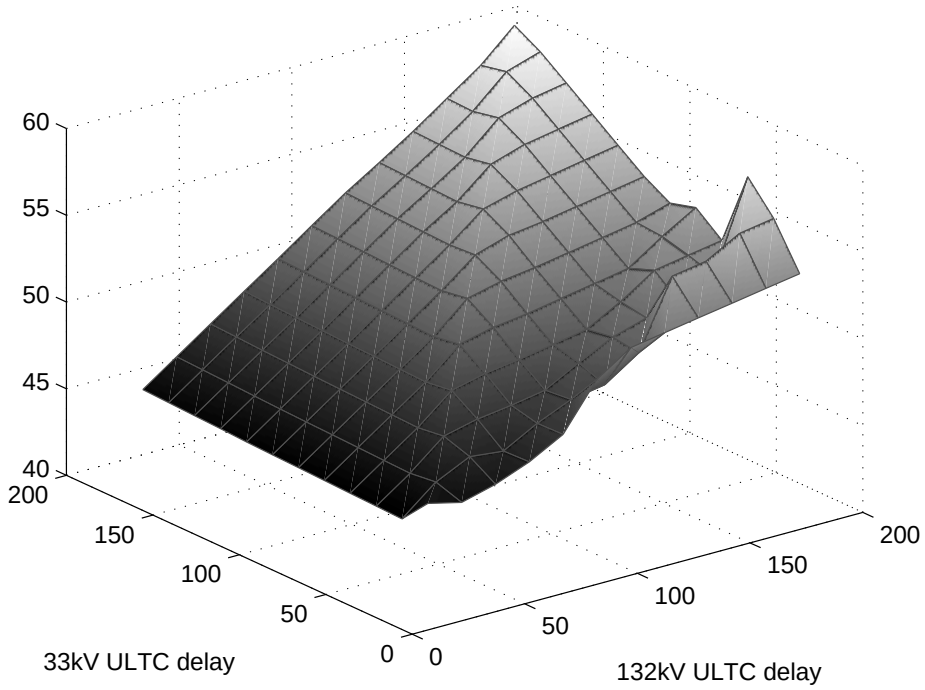

Figure 4.22: TotalVoltageCostPenalty + TapChangeCost *of a 1 day simulation with no DG.*

all GSP ULTC time delays and all primary ULTC time delays together ignores the likelihood that different feeders are best suited to different delays. Using all the same delays, 90 seconds appears to be the best compromise for both GSP and primary ULTCs. The fact that they are the same for both and the lack of a ridge or trough indicates that the high variation of the DG may mask the problems caused by equal delay settings.

4.4 Chapter summary

An area of the Scottish Power network was introduced as the basis for the simulations in this project. The network comprises two GSPs and a number of rural radial feeders. The simulation method has been used in a number of scenarios to verify the semi-steady state method and introduce the different time series that have been examined in subsequent chapters. The implementation of ULTC control behaves as expected.

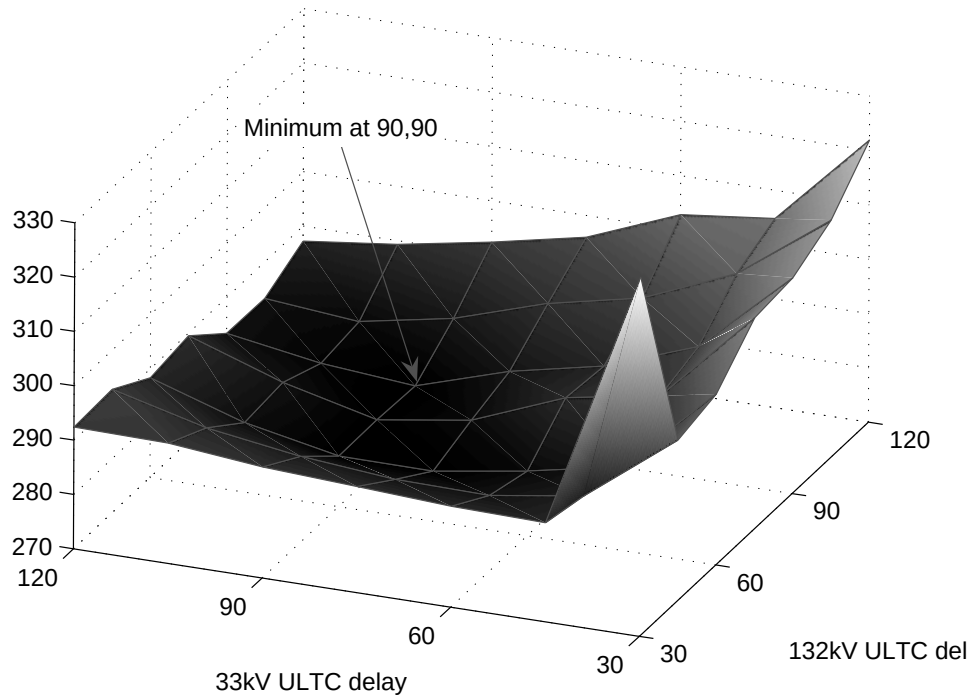

Figure 4.23: TotalVoltageCostPenalty + TapChangeCost *of a 1 day simulation with* DG_{max}.

The controller parameters have been explored to further confirm the implementation. It is shown that the dead-band in the voltage measurement part of the ULTC must be sufficiently large to avoid hunting and sufficiently small to keep voltages close to the target voltage.

The *TapChangeCost* and *TotalVoltageCostPenalty* were used to show the voltage control fitness of a scenario. These metrics are used extensively in subsequent chapters. The metrics were used to explore the time-delay parameter of the ULTC controller. The scenarios tested did not demonstrate a clear rule to determine the best time delay settings. Subsequent chapters will thus use 45 and 60 second delays for GSP and primary ULTCs respectively. These delays are as used by Scottish Power and are not contradicted by the limited findings in this chapter.

The next chapter outlines the connection options for distributed generation and demonstrates the fitness of a number of combinations of connection choices.

Chapter 5
Connecting Fixed Power Factor DG

Chapter 4 demonstrated the simulation of ULTCs over a 24 hour period. Simulation results were obtained by repeated load flow solution as described in Chapter 3.

This chapter reports the use of the above techniques to demonstrate the impact of various DG scenarios on the Dumfries and Galloway (D&G) network. The D&G network information is accurate for the 132 kV and 33 kV part of the network. The 33 kV/11 kV transformer parameters and 11 kV line parameters have been assigned with reference to typical equipment parameters as discussed in section 4.1. Note that some modifications have been made to the network in the next chapter. In this chapter, the target voltage for all load buses was 1.0pu. This was achieved in the no DG case by the manual setting for the winter and summer cases, of a fixed transformer below the primary transformer. The transformer was then fixed for all scenarios.

Keeping the target voltage for all load buses the same allows the application of the evaluation function to the network with a narrow voltage target. Chapter 6, however, uses an evaluation method using only statutory limits.

In this chapter, all connected generation was required to be in strict power factor control mode or PQ mode. Most of the assumptions made are discussed in Chapter 3 with additional assumptions noted as necessary.

The scenarios tested are among the permutations of the following parameters.

- Feeder to which DG is connected.
- Connection voltage.
- Maximum power output of DG.

- Power output time series.
- Power factor.
- Generation events such as ramping up or rapid loss of DG overlaid on the power output time series.
- ULTC operating parameters T_d and V_{lim}.

The scenarios tested are not exhaustive, even given the few parameters above. The scenarios do highlight the key concerns and impacts of DG.

5.1 Construction of the scenario

5.1.1 Feeder selection

The network shown in section 4.1 on page 67 has feeders of different properties. Some feeders have a low impedance between the load bus and the grid supply point (GSP) and are termed *strong* feeders. Other, usually smaller loads, have higher impedances between them and the GSP. These are *weak* feeders.

This study initially examines the placement of DG in three different feeders, a *strong* feeder, a *medium* feeder and a *weak* feeder as shown in Figure 5.1.

Finally the study reports generation placed on all feeders in proportion to the maximum DG that can be connected according to an optimal load flow solution.

5.1.2 Connection voltage

The network used in the simulation has three nominal voltage levels: 132 kV, the sub-transmission voltage in Scotland; 33 kV and 11 kV.

The connection of generation at 132 kV is not considered in this study.

DG was connected at 33 kV at the high voltage (HV) side of primary transformers (ULTC$_P$).

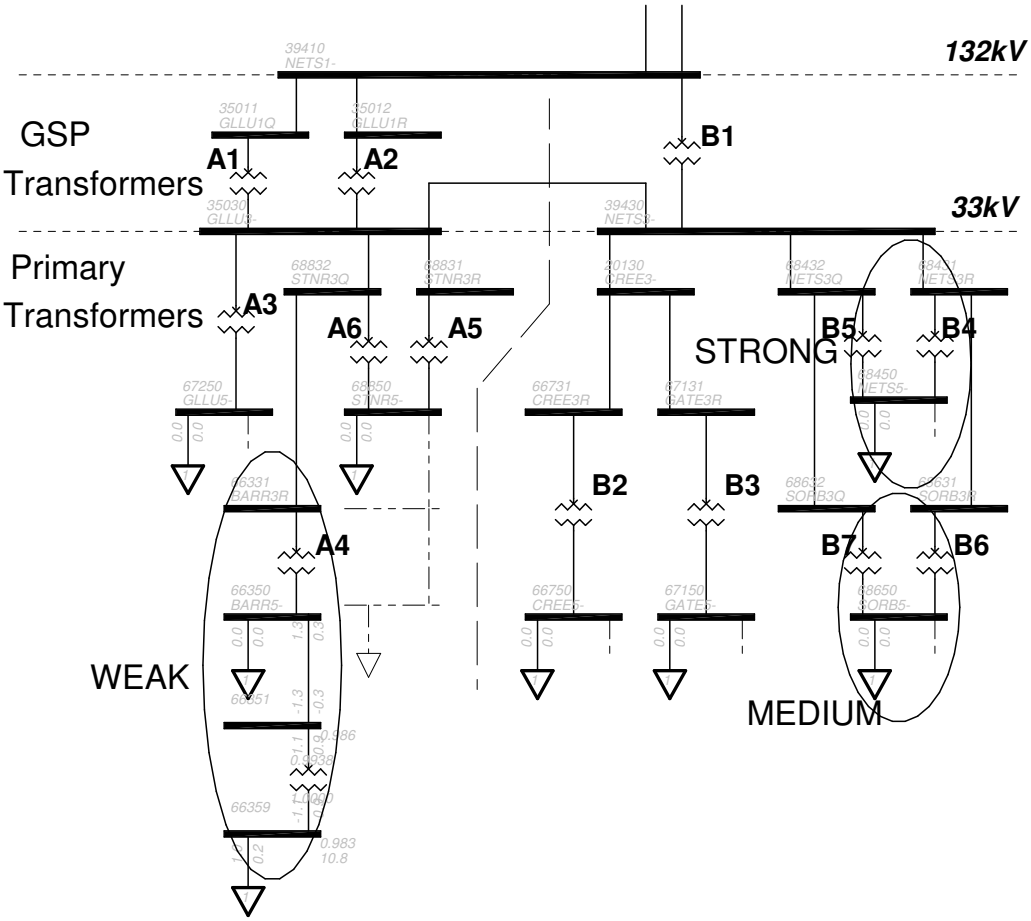

Figure 5.1: *Network diagram with three key feeders highlighted.*

DG was connected at 11 kV at the low voltage (LV) side of the primary transformers and on the load bus distant from the primary transformers as shown in section 4.3.2 in Figure 4.15

5.1.3 Power output time series

Several one day power output time series will be used to simulate the connection of DG as described in section 3.3.2 page 50.

The time series contain steady outputs, linearly ramping outputs and rapidly varying outputs. The linearly ramping time series allows clear observation of the network adjusting to generation changing smoothly over time. The rapidly varying time series allows evaluation of the network as a result of realistic outputs of generation. Key scenarios were also tested

with a *Generation event* as described in section 5.1.6 to simulate connection or rapid disconnection of a DG source.

5.1.4 Maximum power output of DG

The power output time series are a vector *F* in the range $(0, 1)$ with the $max(F) = 1$. The actual power output vector for a day's simulation is obtained by multiplying the time series with the maximum power output by the DG, the DG's capacity. To test the ability of the network to absorb new DG the maximum power output for each simulation was the capacity of the new DG.

The study identified the optimal placement of DG, maximising total connected DG whilst meeting thermal and voltage constraints. This was achieved by repeated optimal load flow solutions and increasing generation by representing it as negative load shedding. The load curve used in this study is for winter load so the 100% load and unity power factor results were used for DG_{max}.

The connected capacity will be a function of DG_{max} found in the Harrison study [4]. The function is given by:

$$DGCapacity_F = DG_{max,F} \cdot DGFactor \tag{5.1}$$

where F is the feeder and $DGFactor$ is the multiplier used for the scenario.

In many circumstances the maximum connected DG is roughly the local load plus the primary transformer rating. This is an intuitive steady state result as the exported power would be the power rating of the transformer. The study identified, however, buses that are constrained by the connection of DG nearby and cannot support the capacities suggested by such a simple approximation and thus some resulting capacities do not follow that approximation.

The optimal power flow method demonstrated the worst cases in terms of equipment loading and voltage rise. This study demonstrates a time series analysis method which shows that greater capacities can be connected subject to dynamic generator constraints and shows the associated loss of revenue of such a scheme.

5.1.5 Power factor

DG_{max} was calculated by taking the maximum of three scenarios each with all generation connected at different power factors. The power factors were 0.95 lagging (0.95^{-}), unity (1) and 0.95 leading (0.95^{+}). These correspond to the approximate operating range of Doubly-Fed Induction Generators (DFIGs) [30]. It is recognised that generation operating at a slightly leading power factor is likely to be most favourable for the connection of larger amounts of DG [30].

Scenarios were created for five different power factors: 0.95^{-}, 0.9875^{-}, 1.0, 0.9875^{+} and 0.95^{+}. In terms of reactive power output, 0.9875^{-} is half way between 0.95^{-} and unity. Likewise generation operating at 0.9875^{+} absorbs half as much reactive power as at 0.95^{+}.

5.1.6 Generation events

The power output time series combined with the maximum power output for the DG combine to create the actual power output for the connected DG during the simulation period. These power output vectors define normal operation of the DG. It is desirable to examine the effect of less frequent events such as the following:

1. Full loss of DG. No fault condition.
2. Temporary loss of DG followed by re-start and re-connection.

These events are created by multiplying the normal power output vector element-wise with the vectors described by Figure 5.2.

5.1.7 ULTC operating parameters

The ULTC has two adjustable parameters according to the simple automatic voltage regulation algorithm described in section 3.4.1. The parameters are delay and deadband.

Section 4.3.4 demonstrated a method to search for optimal delay settings. The ULTCs were simply split into those with HV side at 132 kV and those with HV side at 33 kV. In the

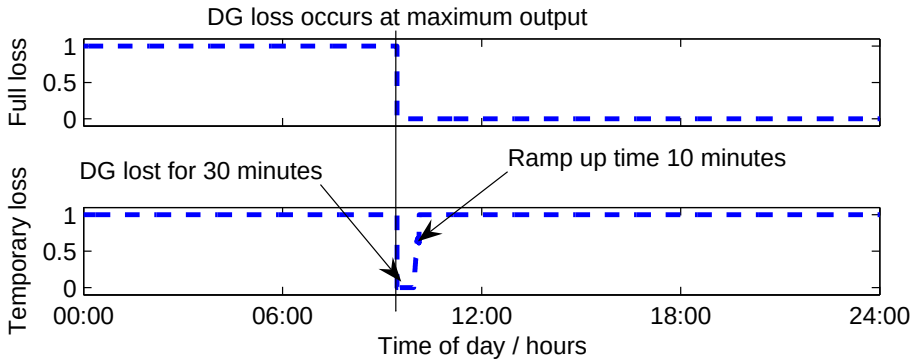

Figure 5.2: *The three events imposed on normal generation vectors.*

network examined this is equivalent to splitting into GSPs and the primary transformers. As identified in section 2.3.5 the delay settings of two or more ULTCs in series are ideally set differently.

Due to the limited data available to optimise the ULTC settings in section 4.3.4, the approximate values used by Scottish Power [53] were used in this study. The HV ULTCs have the shorter delay of 45s and the LV transformers 60s.

Deadband parameters are available for the GSP ULTCs in the D&G network. The deadband parameters for the LV ULTCs were approximated from typical operating parameters as discussed in section 4.2.3.

5.1.8 Scenario parameter summary

Table 5.1 summarises the features of a scenario. The study will not be exhaustive of these combinations as there are 720 combinations of them just adding generation to one bus.

5.2 Investigation of DG connected in PQ mode.

This section reports the effect of DG in an area with previously no DG. The network used was as described in section 4.1 differing only in the amount and position of connection of DG. The generation was kept connected according to the scenario, despite any voltage violations

Feeder	$V_{Connection}$	Max P_{gen}	Time series	Power factor	Events	ULTC Parameters
strong *medium* *weak* *all*	33 kV 11 kV(deep) 11 kV(shallow)	varies	*Wardlaw-day1* *Wardlaw-day2* *flatMax* *ramp*	0.95^{+} 0.9875^{+} 1.0 0.9875^{-} 0.95^{-}	*none* *lossFull* *lossTemp*	Fixed T_d and V_{lim}

Table 5.1: *Summary of scenario parameters.*

that may occur. The evaluation methods described in section 3.6 have been used to assess the connection of extra DG.

Each subsection primarily investigates one variable of the scenario but may vary others in order to explore the impact of the variable.

5.2.1 The effect of feeder selection.

Different feeders can support differing amounts of generation according to line and equipment thermal limits and consumer voltage rise. The capacity of generation that will be connected at each of the three feeders selected for examination is a multiple of DG_{max}. The power factor of the DG will be at unity as was used in the calculation of DG_{max}.

Firstly, the simulation is run with the DG connected on the LV bus of the selected feeder ULTCs with a steady generation profile. This profile provides the maximum power output throughout the period of the simulation. The simulation demonstrates the ability of the network to adequately control bus voltages for any of the load busbars for the given connected power. The load varies according to the time series used for all loads in this study.

The three feeders selected differ in the impedance between the LV side of the primary transformer and the 132 kV network. The impedances give an indication as to the effect on voltage rise the DG will have. The impedances were calculated with the tie between the two 33 kV busbars directly under the two GSPs open. Despite this simplification they give

an indication as to the relative "strength" of connection of each feeder.

The first group of simulations shown had the same amount of DG connected to all three feeders equal to the DG_{max} for the weakest of the three feeders. This simulation demonstrates the differing ability of different feeders to *absorb* DG. To emphasise this point, for this simulation only, the ULTCs are fixed throughout the simulation.

Figure 5.3 shows the feeders' load bus voltage levels with the voltage without DG shown as reference.

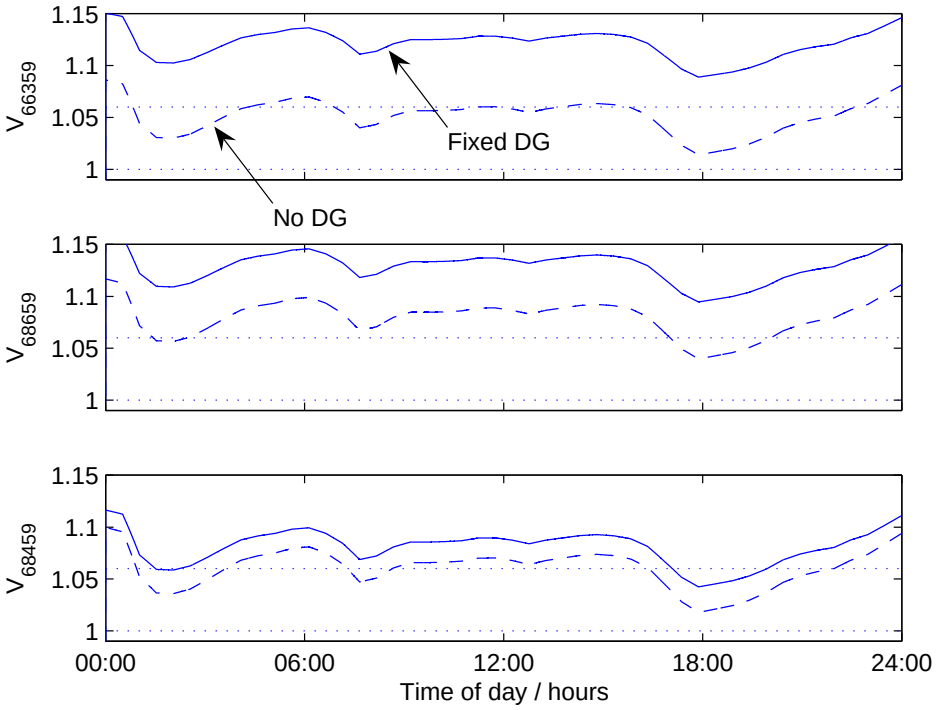

Figure 5.3: *11 kV bus voltage of the three selected feeders with and without the fixed DG connected and ULTCs stationary.*

It is clear that the voltage is unacceptable, but it demonstrates the rise due to the DG is least in the most strongly connected feeder, more in the medium one and a little more in the weak feeder.

Next, the feeders had DG connected equal to their respective (DG_{max}) values. A different run

of the simulation was made for each feeder with the other feeders having no DG connected.

With the tap positions suited to no DG connected, the immediate connection of (DG_{max}) results in a rapid sequence of tapping actions to restore the voltage. All other generation time series start with less than maximum DG. These time series require only a few adjustments of the ULTC position. The evaluation method ignores the cost of the adjustments in the first minutes of the simulation.

Figure 5.4 shows the operation of each feeders' ULTC in response to the changing load with DG_{max} connected at fixed output with the no DG response as reference. Figure 5.5 shows load bus voltage for the same scenario.

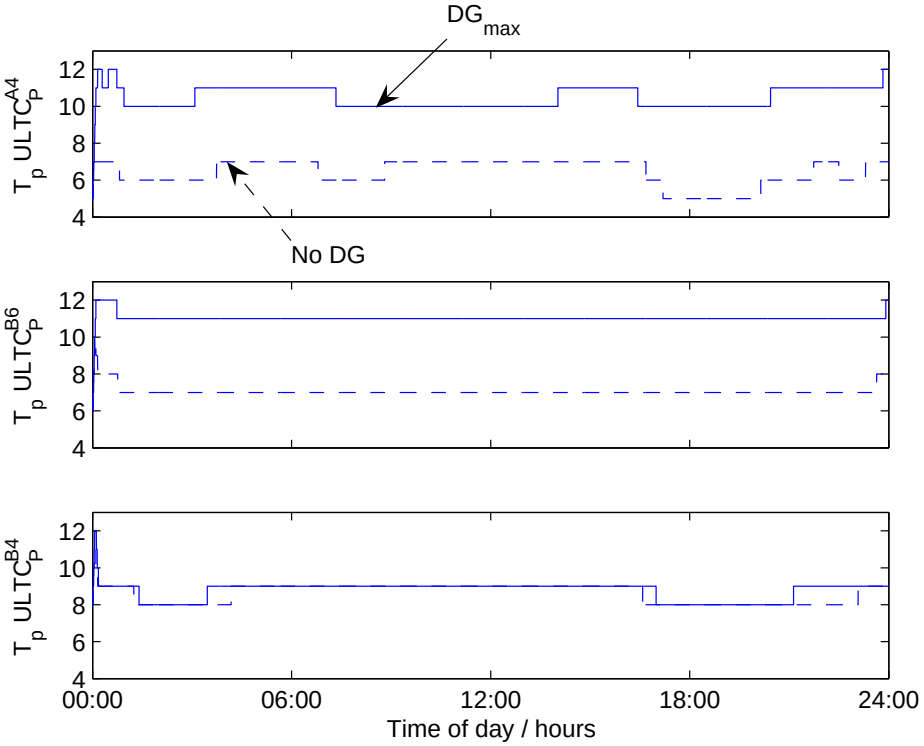

Figure 5.4: *Response of the ULTC$_P$s to the changing load with DG_{max}.*

Figure 5.4 shows few tapping operations at the primary ULTCs of each feeder. As expected with steady generator real and reactive power output, the tap changing behaviour of the primary ULTCs is similar with and without the DG. The main difference observed in both the *weak* and *medium* feeder is the average tap position. The ULTCs operate at the start of

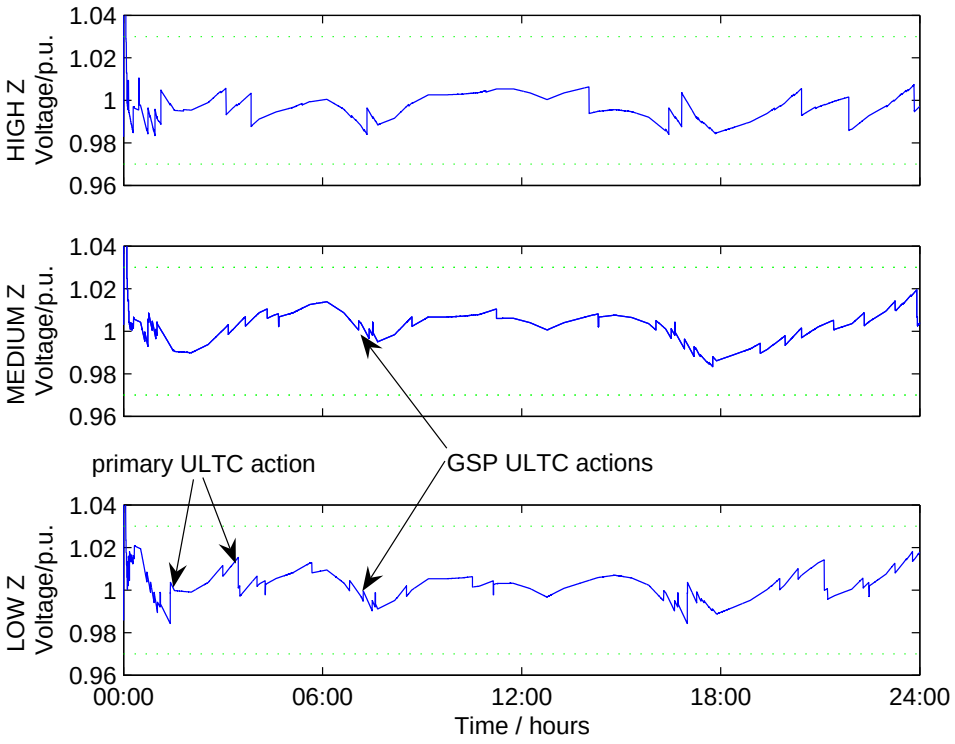

Figure 5.5: *Load bus voltage as a result of changing load and ULTC voltage regulation with DG_{max} for three different feeders.*

the day according to whether there is DG or not and then operate to control voltage changes due to the load throughout the day.

Figure 5.5 shows small voltage steps up and down frequently for the LOW and MEDIUM impedance feeders. This is as a result tapping actions of the GSP ULTC transformer for area B. Note that the network is capable of maintaining the 11 kV load bus voltage well within the prescribed planned $\pm 3\%$ as expected.

Figure 5.6 shows the percentage primary ULTC loading over time for the feeders with DG connected.

Each feeder has a thermal limit dictated by the line and transformer thermal limit. The thermal limits are seasonally dependent and also have a steady state rating and a cyclic rating. The 33 kV/ 11kV primary transformer has been added to each feeder in the model derived from the Scottish Power network data according to typical transformer parameters. For this reason the

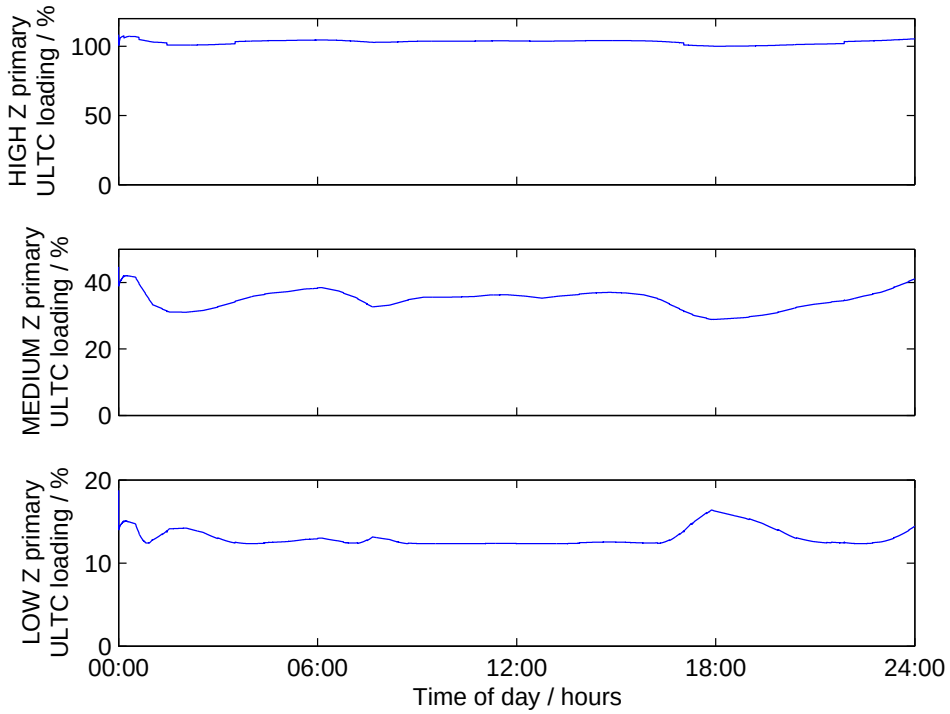

Figure 5.6: *Line loading with DG_{max} for the three feeders.*

imported/exported power along the feeder is compared to the actual line rating of the feeder as supplied by Scottish Power.

The percentage transformer loadings are lowest for the *strong* feeder, the one with lowest impedance. These feeders are good candidates for even more DG in terms of thermal rating but may be limited by the ability of the area as a whole to maintain voltages within limits.

5.2.2 The effect of connection level.

Similarly to the connection of DG to different feeders, the level at which DG is connected affects its impact on the feeder. The three connection levels identified, on the HV side of ULTC$_P$s, on the LV side of ULTC$_P$s and "out on" the 11 kV load bus all have differing impedances between the DG and the transmission network and between the DG and the load.

Three simulations were run with DG on the high impedance feeder. DG_{max} was connected in the three different places identified: *Out* on the load bus, the LV side of ULTC$_P$s and the

HV side of ULTC$_P$s. The generation time series used was *Wardlaw-day1*.

The feeder's grid transformer (ULTC$_{GSP}$) and primary transformer (ULTC$_P$) operations hardly vary between the different positions as seen in Figure 5.7.

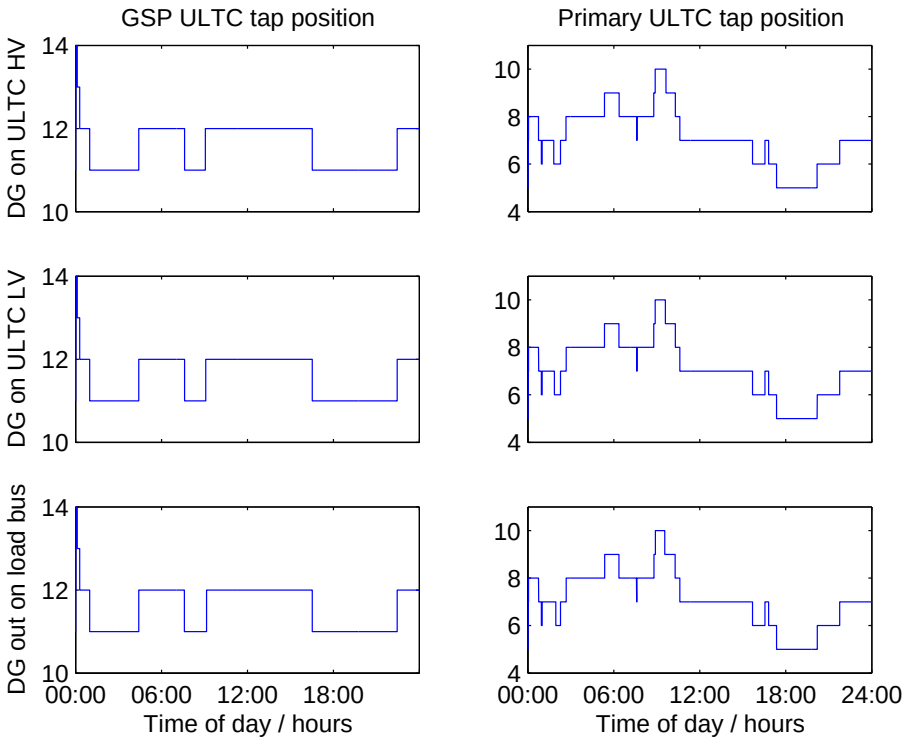

Figure 5.7: *GSP and primary ULTC tap position with* Wardlaw-day1 DG_{max} *connected at different voltage levels.*

The patterns of operation are identical between connection level scenarios. There are slight variations in exact timing of each operation. The resultant load bus voltage time series in Figure 5.8 differ between connection points as expected. The load bus voltage is higher when it has DG connected to it. The amount of voltage rise changes as the DG output changes. This makes it harder for the ULTC to regulate voltage such that the load bus is within limits.

The line loading for the line feeding the primary substation is very similar for all three connection points and is shown in Figure 5.9.

The line loading over time only shows a peak of 50% of the steady state rating of the line. Note the low line loading between 12:00 and 18:00. During this period the generation nearly

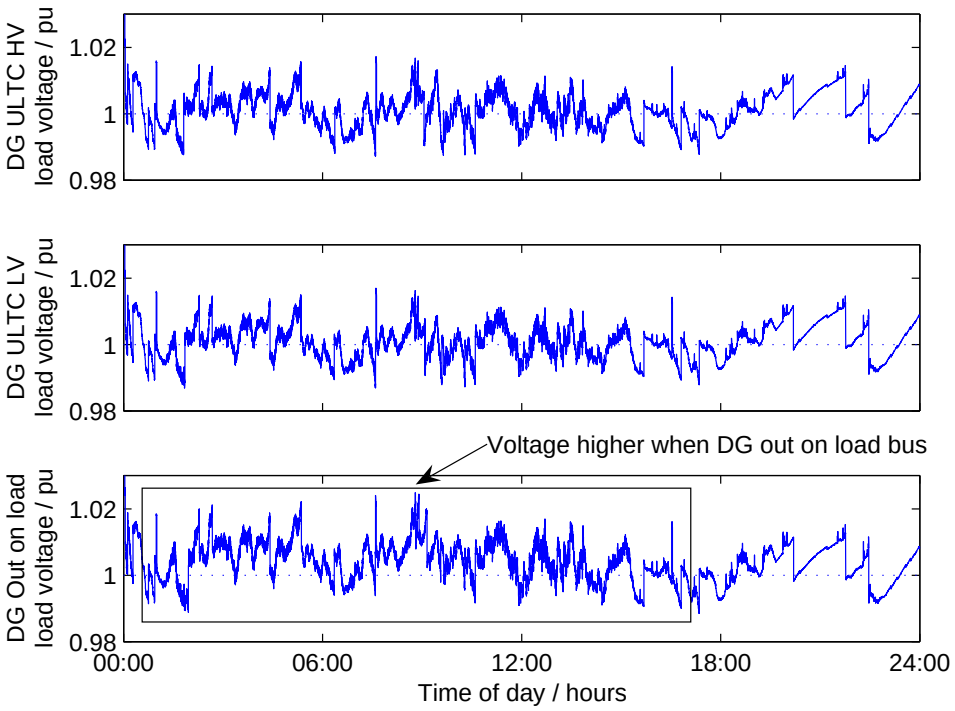

Figure 5.8: *Load bus voltage with* Wardlaw-day1 DG_{max} *connected at different voltage levels.*

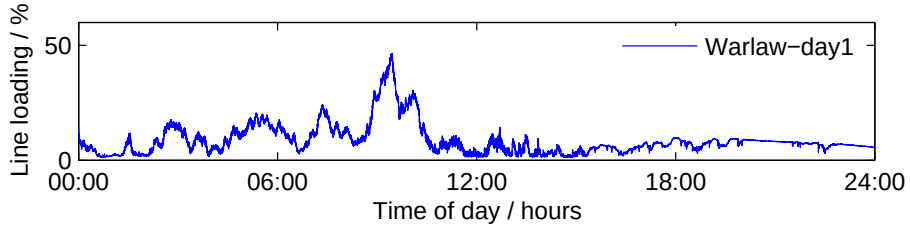

Figure 5.9: *Line loading with* DG_{max} *connected on the HV side of* $ULTC_P$.

matches the load. The smoother line loading between 18:00 and 24:00 occurs during a period mainly of no generation. This results in a smoother voltage time series during this period as shown in Figure 5.8.

The transformer reached a higher loading as a percentage of its rating than the line but is discussed further with respect to the next simulation.

The next result shows a marked difference between connection levels. This time DG with the

Wardlaw-day1 time series was connected at each of the three voltage levels in three simulation runs. This time, $DG_{2 \cdot max}$ is connected each time.

The first two figures, 5.10 and 5.11 show that with connection at HV/LV ULTC$_P$ results in adequate control of the load bus voltage.

Figure 5.10 shows that with the DG all connected at the load bus, a voltage rise occurs bringing the voltage up to the planned $\pm 3\%$ limits. There is little difference in load bus voltage between the scenarios connecting on the HV side ULTC$_P$ and on the LV side.

Figure 5.11 shows that connection on the HV side of ULTC$_P$ results in a slightly more extreme voltage profile for the HV side of the transformer. This is not translated into a load bus voltage rise due to transformer tap operation.

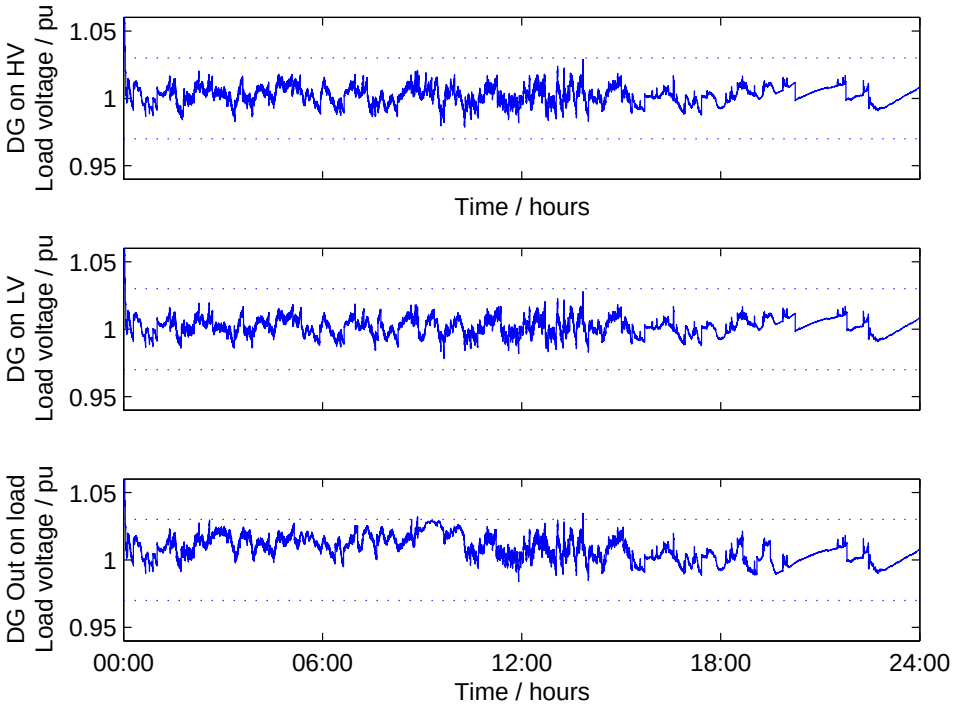

Figure 5.10: *Load bus voltage for high Z feeder and* $DG_{2 \cdot max}$ Wardlaw-day1.

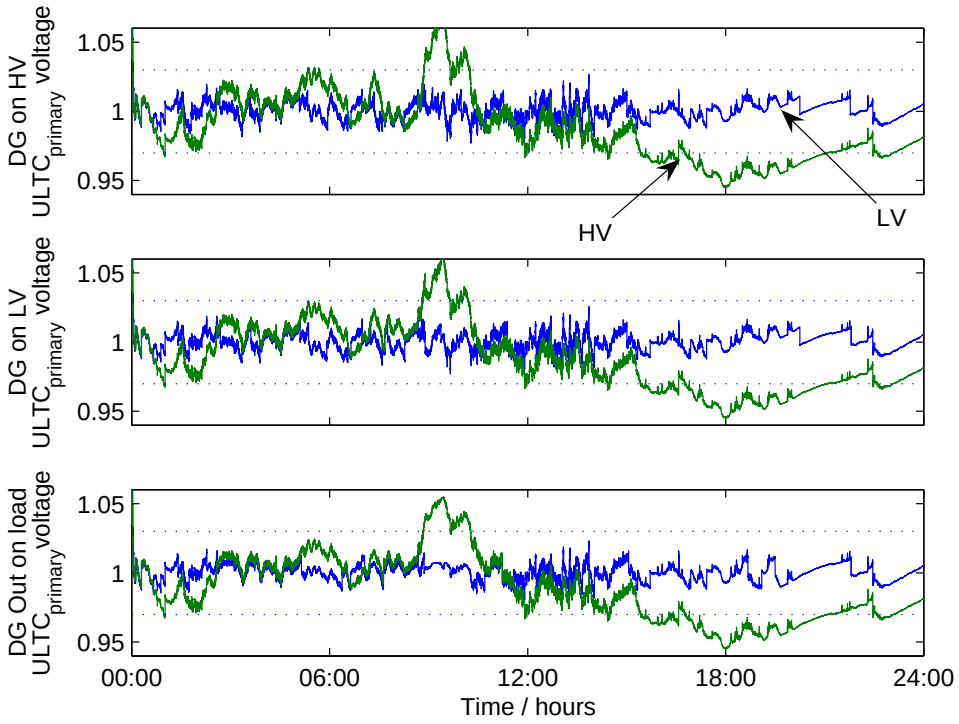

Figure 5.11: *$ULTC_{primary}^{HV/LV}$ voltage for high Z feeder and $DG_{2 \cdot max}$* Wardlaw-day1.

Figure 5.12 shows ULTC$_{GSP}$ tap operations as a result of the connection of $DG_{2 \cdot max}$ at the three positions.

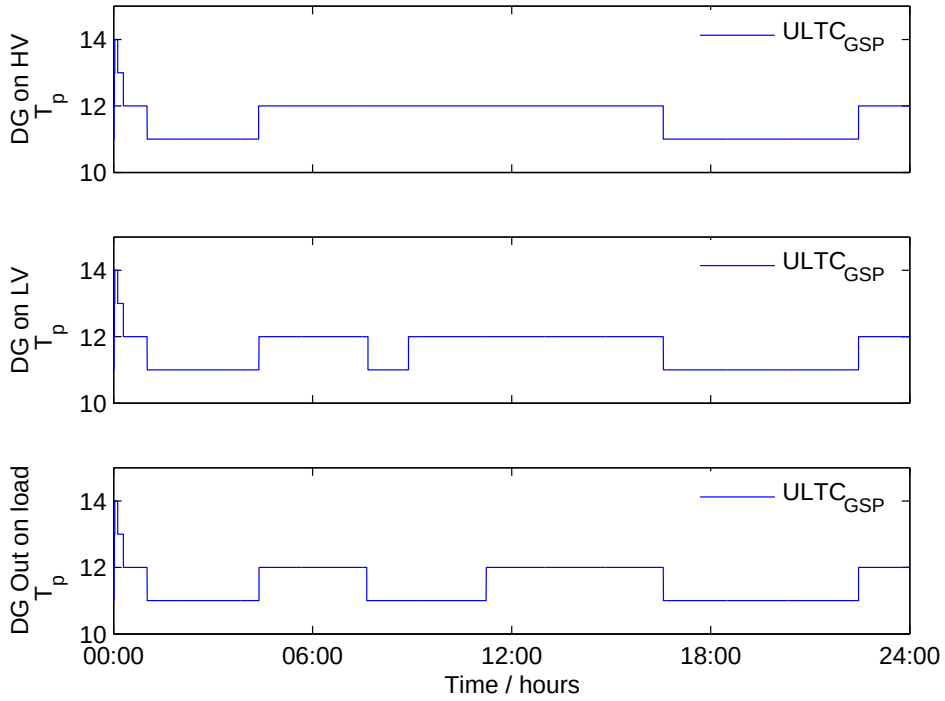

Figure 5.12: *Tap position of ULTC$_{GSP}$ for high Z feeder and $DG_{2 \cdot max}$ connected with* Wardlaw-day1 *time series.*

As expected there is little change between the cases. This is explained by Figure 5.14 later on page 114. The power flow seen by ULTC$_{GSP}$ differs only slightly between the three positions.

The operation of ULTC$_P$ shows a marked difference depending on the voltage level at which the DG is connected, as shown in Figure 5.13. The scenarios were all with two times DG_{max} ($DG_{2 \cdot max}$). The ULTC$_P$ exhibits a greater number of tap changes when the DG is connected on the LV side of the ULTC than out on the load. The ULTC$_P$ responds with even greater activity when the DG is connected to the HV side of the ULTC. This is explained by the effect described above that the connection of DG on the HV side results in a greater range of voltages on the HV side than if the DG is connected below the ULTC. A greater range of voltages on the HV side translates into a greater range of voltages on the LV side resulting in more tap operations to correct it.

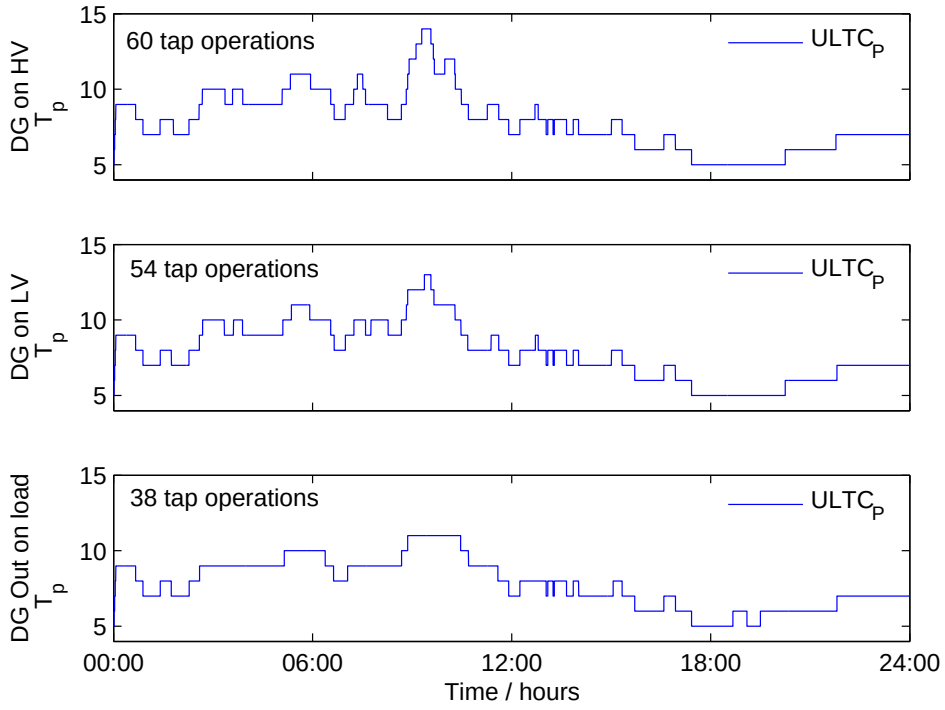

Figure 5.13: *Tap position of ULTC$_P$ for high Z feeder and $DG_{2 \cdot max}$* Wardlaw-day1.

Figure 5.14 shows the difference in line loading between the three cases. Line loading is measured in MVA and thus includes the real and reactive components of power flow. ULTC operation affects the reactive power flow in the feeder. As the three scenarios exhibit different ULTC behaviour, in particular different extremes of tap position, the line loading above the ULTC is similarly affected by the reactive power term.

Figure 5.15 shows the difference in transformer loading between two of the connection cases. Naturally with much greater DG capacity than load, the transformer loading is greater if the DG is connected on its low voltage side. Connection on the load bus results in slightly less ULTC loading when the feeder is exporting power. This is due to 11 kV line losses.

Nameplate ratings of transformers can be exceeded for short durations. The extent to which it can be exceeded is largely determined by the temperature rise in the transformer. Transformer temperature is a function of: ambient temperature; transformer rating and construction; and the power flow over time through the transformer.

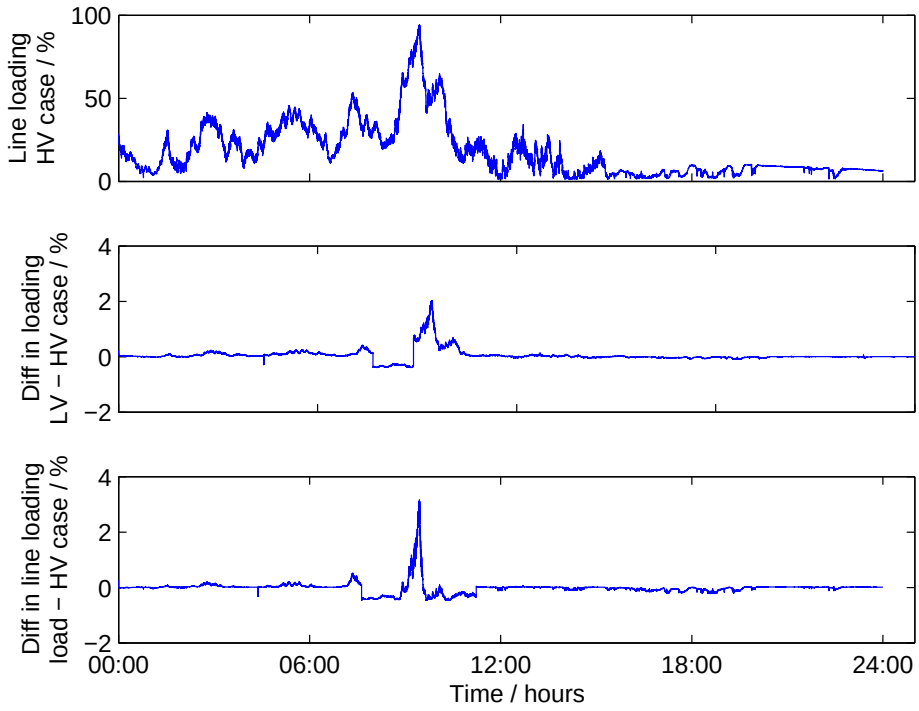

Figure 5.14: *Line load due to $DG_{2 \cdot max}$ connected to HV side of $ULTC_P$. Also shown are the difference to this curve from DG connected at LV and off on load.*

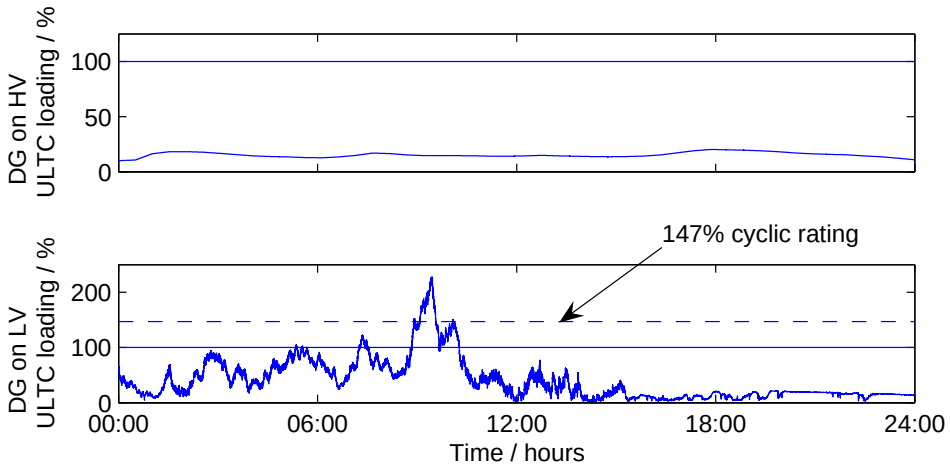

Figure 5.15: *$ULTC_P$ loading in HV and LV connected DG cases.*

In normal cyclic duty the British Standard Institution's Code of Practice 1010 recommends that transformer current should not exceed 150% of nameplate rating [76].

Cyclic ratings can be determined for a transformer even after installation by transformer modelling. An EA Technology case study demonstrated up to a 47% greater cyclic rating than nameplate rating [77] for a GSP transformer. This rating is indicated on the figure for reference.

A study by Mott MacDonald for The Carbon Trust and the Department of Trade and Industry [30] illustrates typical amounts of DG that can be connected depending on the connection point in the feeder. Where 1.8MW can be connected out on 11 kV, 5MW can be connected to the LV side of the primary ULTC and greater than 10MW can be connected to the HV side of the primary ULTC. This approximation is taken as a ratio of 1:3 for DG capacity remote from the LV side of the ULTC to the DG capacity connected directly to the LV bus of the ULTC for a given amount of DG connected to a feeder. The 1:3 ratio is adopted in this study to determine the placing of DG on a feeder where the capacity connected to the feeder as a whole is of interest.

5.2.3 Power factor and voltage rise.

The power factor of DG has a large effect on local bus voltages. Choosing a leading power factor is a method to reduce voltage rise by absorbing VArs and thus improve the ability of the network to accept DG. This section shows that this can also increase ULTC operation in cases where the generation output varies over short time periods such as cases with wind powered generation.

Two load scenarios were simulated, one a steady minimum summer load, the other a steady maximum winter load. Each load scenario was simulated with DG out on the load, modulated according to the ramping output profile at one of five different power factors: 0.95lag, 0.9875lag, unity, 0.9875lead and 0.95lag. The time of day was thus not strictly important but a semi-steady state simulation allowed for operation of tap changers and was otherwise useful in showing the progression of bus voltage with DG change.

The load bus voltage is shown in Figures 5.16 and 5.17.

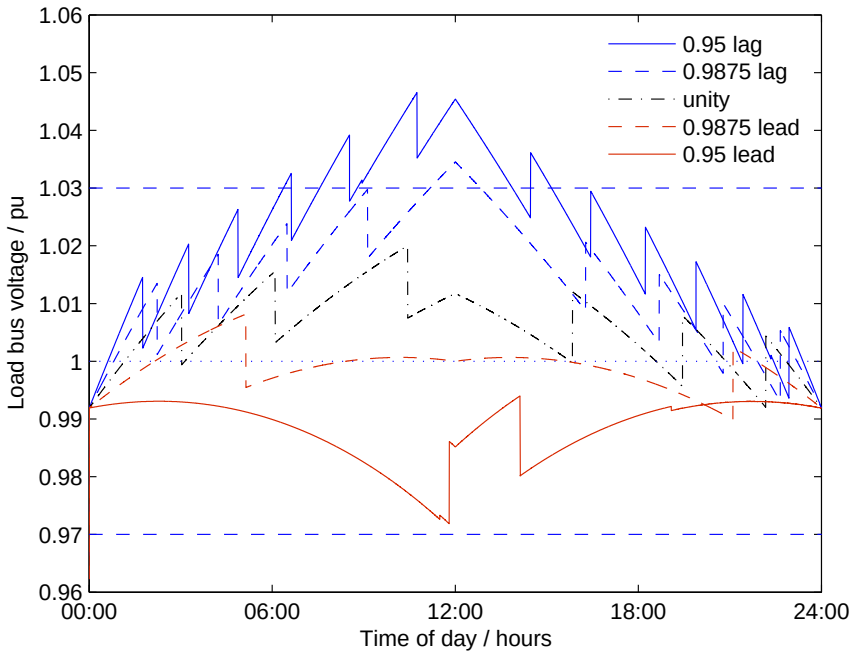

Figure 5.16: *Load bus voltage as a result of minimum summer load and DG_{max} connected at the same bus with 5 different power factors.*

The voltage time series observed is similar for both winter and summer scenarios. With a lagging power factor, the primary ULTC makes many voltage corrections. The load bus moves from absorbing VArs to exporting VArs as the generation increases in the first part of the simulation up to 12:00. This raises the load bus voltage and thus the LV side of the primary transformer. The transformer AVC then repeatedly corrects this voltage rise.

The number of tapping operations reduces as the amount of VArs the DG exports is reduced. The two scenarios with DG at a leading power factor required the same amount of correction. Note that in the 0.95 leading case, the correction was for an under-voltage. The increasing real power output of the DG tends to raise the load bus voltage but the proportionate increase in VAr absorption lowers the voltage. Small voltage steps are visible. These are as a result of automatic GSP ULTC adjustment.

Increased reactive power generation on top of real power generation also causes greater voltage rise on the HV side of the primary transformer as seen in Figures 5.18 and 5.19.

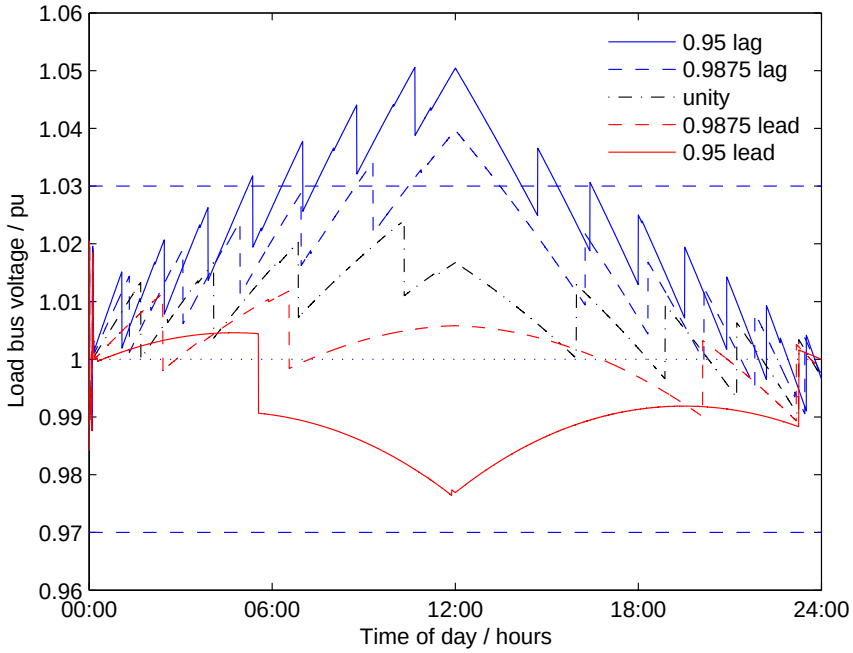

Figure 5.17: *Load bus voltage as a result of maximum winter load and DG_{max} connected at the same bus with 5 different power factors.*

These observations support the strategy of operating DG at a leading power factor as opposed to unity or a lagging power factor. In the extreme lagging p.f. case, the voltage is caused to exceed the statutory upper limit of $+6\%$ pu. The increased load in winter is not sole cause of the large difference in the voltage on the HV side of the ULTC between the two figures. The ULTC$_{GSP}$ is at a different tap setting and voltage on the LV side of the ULTC$_{GSP}$ is lower in the winter case, hence the voltage on the HV side of the ULTC$_P$ is lower.

One reservation about operating DG at a leading power factor is illustrated in Figure 5.20. It is shown that when the DG is operating at a leading power factor, the extra imported reactive power causes slightly increased line loading. Only the two most extreme power factors tested are shown as the difference is slight. In addition to increased line loading, the leading power factor also adds to the reactive power requirements of the feeder. If it is the policy for all DG to be operated with a leading power factor then the reactive power requirement would have to be met by larger plant.

The difference in tap position that connecting DG makes compared to having no DG is very

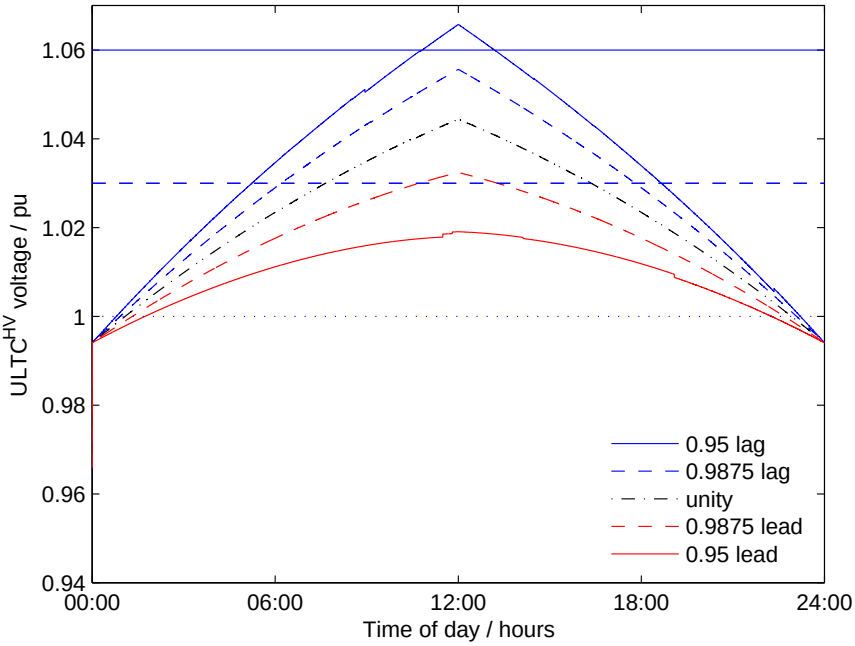

Figure 5.18: *$ULTC_P^{HV}$ bus voltage, minimum summer load and DG_{max} connected out on the load bus.*

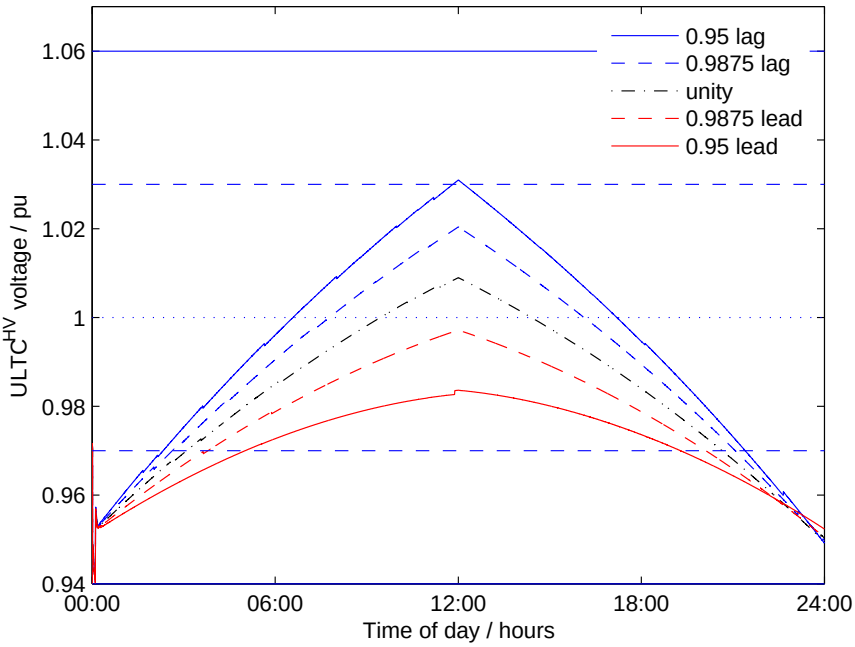

Figure 5.19: *$ULTC_P^{HV}$ bus voltage, maximum winter load and DG_{max} connected out on the load bus.*

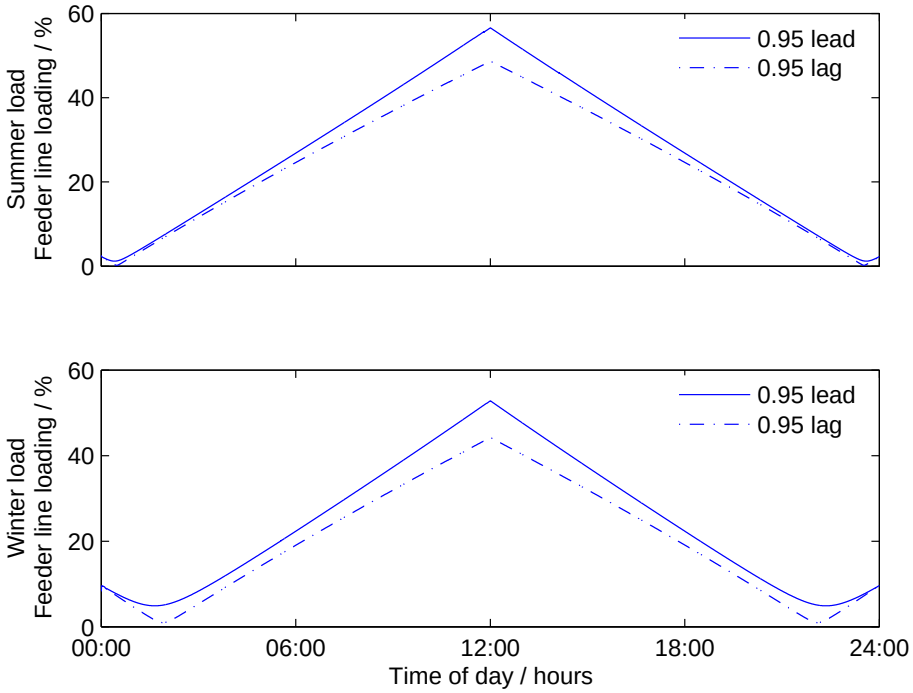

Figure 5.20: *Feeder line loading at two different power factors.*

important when it comes to assessing loss of generation events as explored in section 5.1.6. If the tap position differs greatly between having DG connected and not, then the unplanned disconnection of the generation will cause an undesirable large voltage step and then a number of subsequent tapping operations.

5.2.4 Varying output with different generation profiles.

Sample frequency

As shown in previous sections, DG varying on a short time scale can affect the amount of tap operations performed by the ULTCs. The extent to which time-scale of power output fluctuation affects tap operation was explored.

$DG_{2 \cdot max}$ was connected to just the low and medium impedance feeders. The power output time series used for the DG was different for each graph in each figure. The first graph in each figure used *Wardlaw-day1* for the DG output profile. The second graph had a power output time series generated by creating a half hour moving average of *Wardlaw-day1* and then under-sampling it with a sample period of half an hour. This second time series is the equivalent time series that would be generated by a monitoring device producing only a half hourly measurement. Such devices sample voltage at a much shorter period than half an hour and then average the results to give half-hourly data.

The resulting time series of tap positions is shown in Figures 5.21 and 5.22 for feeder B1.

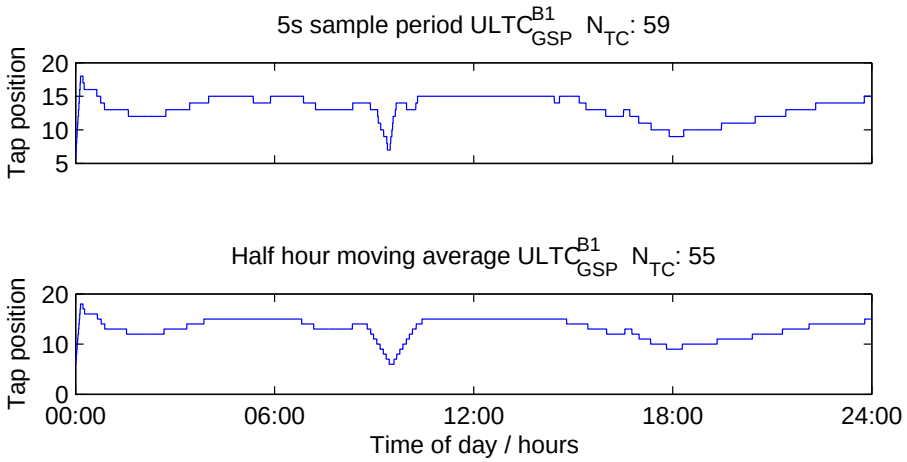

Figure 5.21: *The effect on ULTC$_{GSP}$ tap operations of DG output data sample period.*

The time series of tap positions for the GSP and primary ULTCs on feeder B1 differ between the two sampling frequencies. The difference is not as marked as might be expected, but clearly the primary transformer shows reduced operation with the smoothed curve. ULTC$_{GSP}$ shows similar operation as the range of the two curves is the same. Much of the ULTC$_{GSP}$

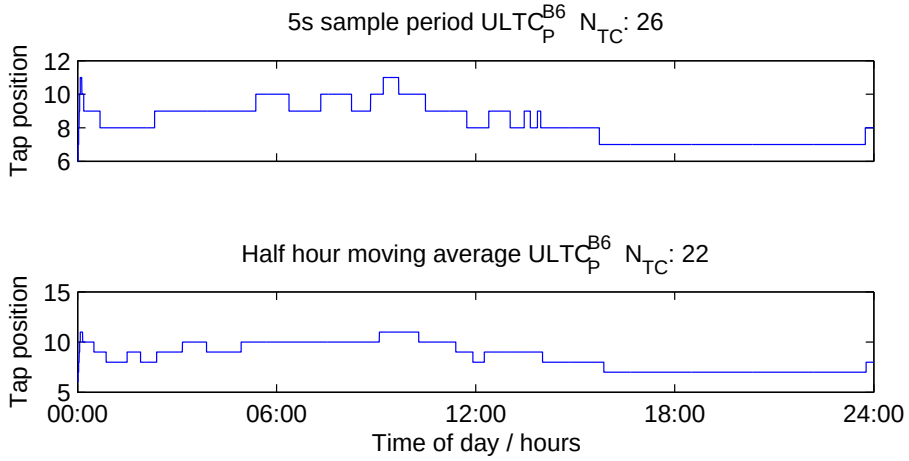

Figure 5.22: *The effect on $ULTC_P$ tap operations of DG output data sample period.*

operation handles the slower change in load and hence voltage. The time series simulations in this study needed to use the higher frequency input time series in order to fully model the operation of ULTCs in response to the higher frequency power fluctuations seen at DG such as wind farms.

Geographical dispersion

In this study so far, all DG in the network has been varied by the same time series. In reality, even if all the DG was from the same resource such as wind, the power outputs from these geographically dispersed wind farms would not be synchronised. The aggregation of such sources will lead to a smoother total power export time series. This section, however, tests the hypothesis that if each generator follows different time series then the changing power flows to and from each feeder could cause increased ULTC tapping operation to maintain voltages within limits.

The following Figures 5.23 and 5.24 both used the Wardlaw data; however in the second and third plot of each of these, the medium impedance feeder was given an output profile offset from the original *Wardlaw-day1* by 300 s or 1200 s. These offsets correspond to the propagation of a change in wind speed between the medium and low impedance feeder occurring at 10 ms^{-1} over distances of 3 km and 12 km respectively.

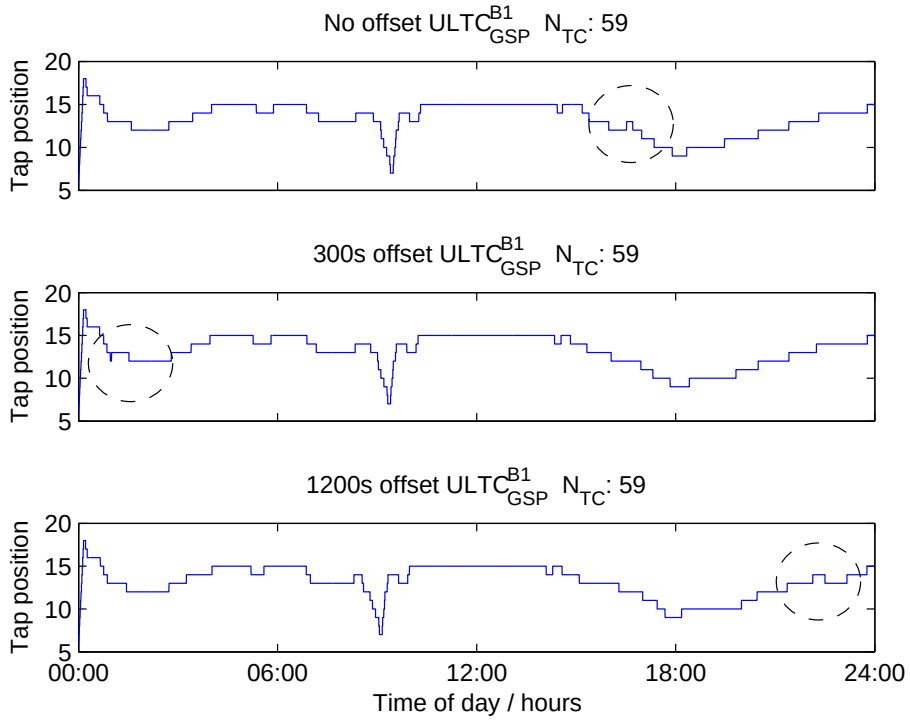

Figure 5.23: *Tap operation due to offset generation time series for ULTC$_{GSP}$.*

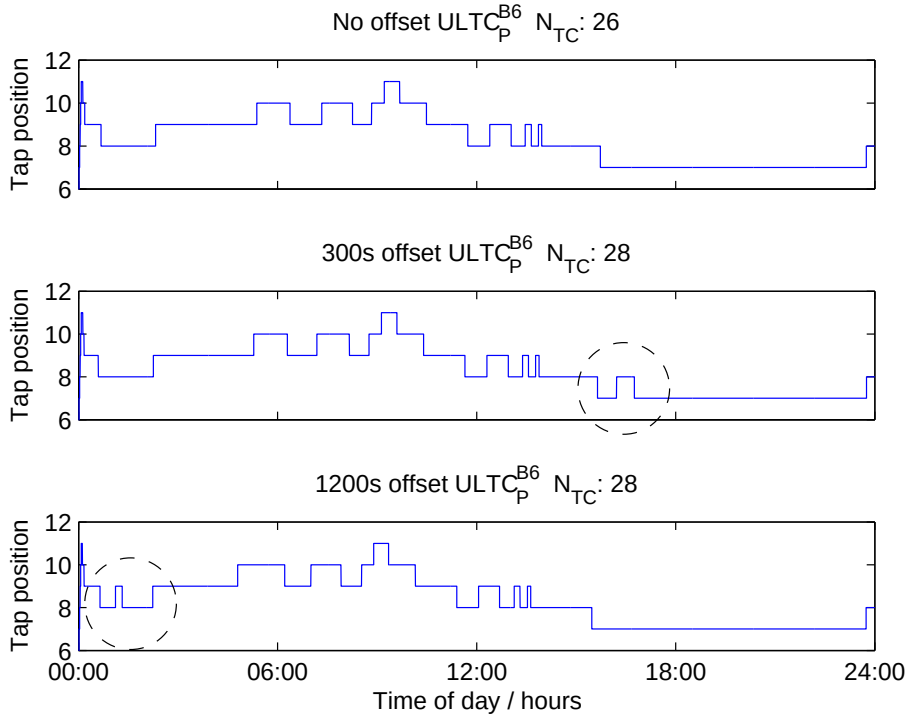

Figure 5.24: *Tap operation due to offset generation time series for ULTC$_{P}$.*

Differences between the scenarios are circled. There is however no significant difference in the number of ULTC$_{GSP}$ or ULTC$_P$ tapping operations.

5.2.5 Testing for maximum capacity.

The previous section demonstrated how different factors affect the impact of DG on voltage and ULTC operation. After selecting the most desirable options, the capacity of the DG is varied to demonstrate cost and benefits of different amounts of generation. As a starting point, DG was connected to each feeder in the network with capacity as defined by the peak load, optimal power factor scenario. Two power factors were used for the DG, unity and 0.9875 leading which seemed most favourable in previous sections. The power output time series used was *Wardlaw-day1*.

As a result of examining the thermal branch loading, two further simulation runs were conducted with DG_{max} multiplied by 120% and 140%. Note that the area of the network simulated has two GSP transformers. These transformers and the respective feeders connected below them are named areas A and B.

Figure 5.25 plots the evaluation of the three scenarios with increasing DG at unity and leading power factors respectively.

The first column: Absolute Penalties

The first column shows the *TotalVoltageCostPenalty* and *TapChangeCost* for areas A and B as described in section 3.6 on page 60 for one day of simulation. *Tap cost* denotes the cost of the total number of tap changes *TapChangeCost*. The cost per tap change assumes disconnection of DG when overhauling a feeder connected by a single ULTC in addition to the basic cost of maintenance.

The absolute penalties increase with the amount of DG connected. The area A plot shows that increasing DG connected at unity power factor above DG_{max} results in a significant rise in *TotalVoltageCostPenalty* with *TapChangeCost* rising only slowly. The cost of the effect on bus voltages with increasing DG outweighs the cost of the change in the number of tap

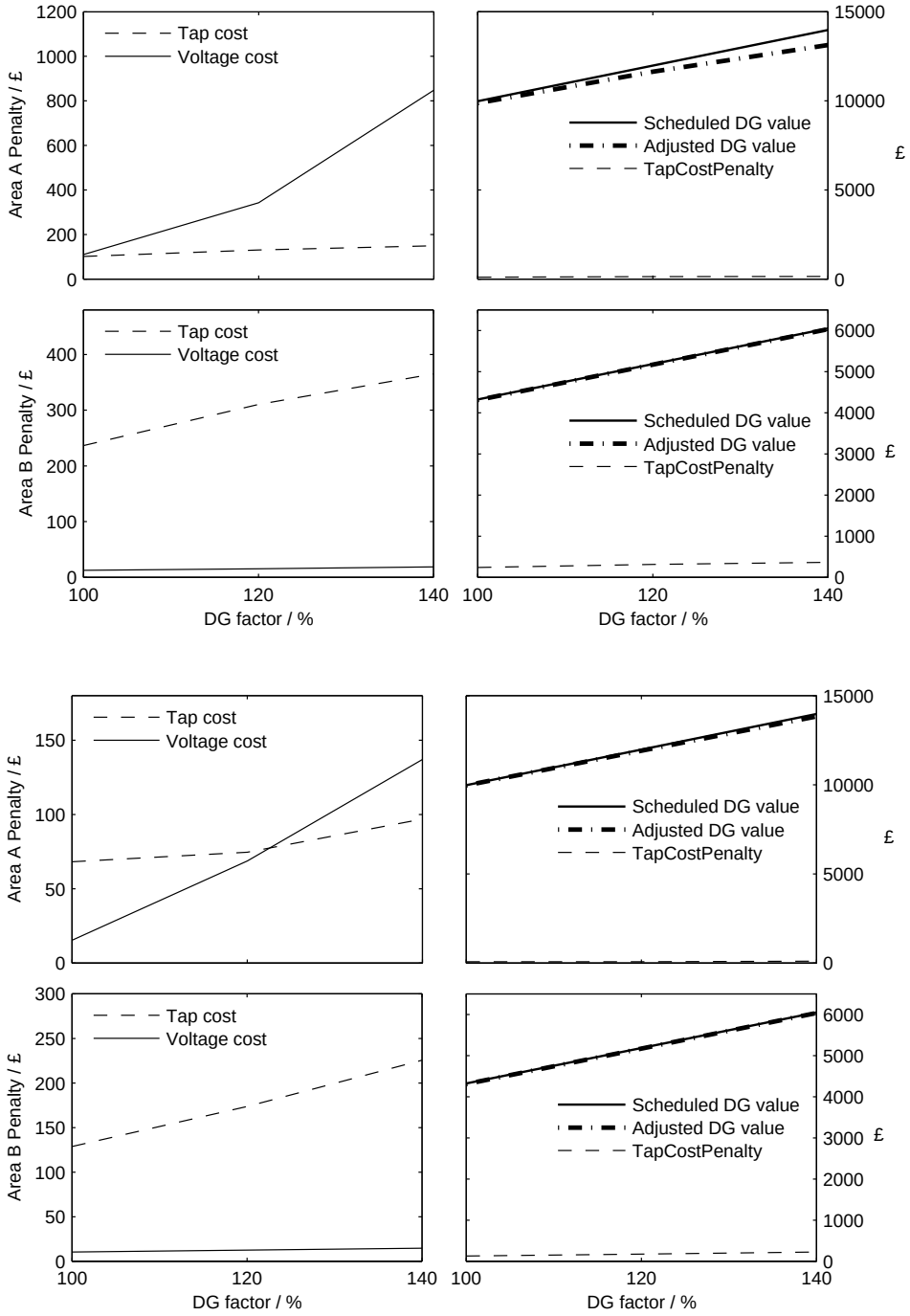

(b) DG connected at 0.9875 leading.

Figure 5.25: *Cost penalties for 3 amounts of* Wardlaw-day1 *DG in areas A and B.*

operations required. This is largely due to the over-voltages experienced on the HV side of primary ULTCs as a result of exporting power from feeders.

The result for area A with DG connected at a leading power factor is markedly better. The import of reactive power keeps voltage rise down thus reducing the *TotalVoltageCostPenalty*. In addition the *TapChangeCost* is reduced. Any fluctuations of real power output correspond to a proportionate fluctuation in reactive power import, reducing the fluctuation of bus voltages as shown in section 5.2.3. Less fluctuation in bus voltages means a reduction in the number of tapping operations.

The *TapChangeCost* is of the order of the DNO interim charge. The charge is supposed to cover operation and maintenance of the whole distribution network, not just that of ULTCs. The *TapChangeCost* was calculated for 2003, whereas the interim charge is for 2005 which would suggest the *TapChangeCost* would be even greater relative to the interim charge using 2005 figures if available. The *TapChangeCost* is exaggerated in these graphs as it includes the cost of tapping operations with no DG. The *TapChangeCost* includes the cost of compensating DG for disconnection during ULTC maintenance which the DNO interim charge does not.

The first column: Differences in penalties by area

In both areas the increase in DG resulted in increasing penalties and the connection of DG at a slightly reactive power factor reduced these penalties. The areas differ in that in area A the greatest penalty arises from DG causing voltages to exceed the planned voltage limit of $\pm 3\%$. In area B, the cost of tap operations dominates any voltage control problems.

The ULTC$_{GSP}$ in area B has a relatively fine degree of control for a tap changer and as such reacts frequently to changing power flows and their consequent effects on voltage. In the DG_{max} scenario, the HV winding ratios of ULTC$_{GSP}^{A1}$ and ULTC$_{GSP}^{A2}$ vary from 0.9667 to 1.0167 in 3, 1.66% steps with a total of 13 tapping actions. This is in contrast to ULTC$_{GSP}^{B1}$ which varies from 0.9500 to 1.0063 in 9, 0.625% steps with a total of 107 tapping operations. The *TapChangeCost* is thus high in area B due to the GSP tapping actions. The fine degree of control and lower connected capacities do however result in a lower number of tap operations

for the primary transformers.

In addition the area B has a higher *TapChangeCost* as its GSP ULTC consists of only a single transformer which is more heavily penalised according to the *TapChangeCost* definition. To be precise, for the DG_{max} scenario, the *TapChangeCost* definition assigns a cost of £0.23 to each tapping operation of a GSP transformer in A but a £1.83 to a tapping operation in the GSP for B.

The *TotalVoltageCostPenalty* does not increase significantly in area B with increased DG, nor does it decrease significantly with connection at a leading power factor. The total connected capacity of DG in area B is much lower, limited by the thermal limits of ULTC_{GSP}^{B1}. Thus for similar line and transformer characteristics in area B feeders, there is less voltage drop or rise caused by the import or export of power in the feeders.

The second column: Penalties compared to revenue

The second column has plotted the potential revenue from the DG in each area. The revenue is the electricity generated for the day multiplied by the mean wholesale electricity price for 2003. In addition, the revenue with the *TotalVoltageCostPenalty* subtracted is shown. The *TotalVoltageCostPenalty* is a penalty whose value is based on lost revenue. The adjusted value represents the revenue from generation that did not cause voltage excursions from statutory limits.

For comparison the *TapChangeCost* is plotted with the two revenue values. The *TapChangeCost* is very small compared even to the adjusted revenue. Thus if the DNO were able to apportion the cost of extra tapping operations due to connected DG the costs could be passed to the DG. The significance of *TapChangeCost* is shown more clearly by plotting the penalty as a proportion of revenue.

Penalties as proportion of revenue

Figure 5.26 shows the combined penalties of areas A and B as a percentage of revenue over the 3 scenarios. The penalties used in the calculations have subtracted the

TotalVoltageCostPenalty calculated with no DG. In this scenario is £35.33 per day for the combined cost penalty. The values are for areas A and B combined. The tap cost component is given for the combined cost penalty and also has £35.33 subtracted from the *TapChangeCost* as the only cost associated with the no DG case is the *TapChangeCost*. In this way they are marginal penalties due to DG connection.

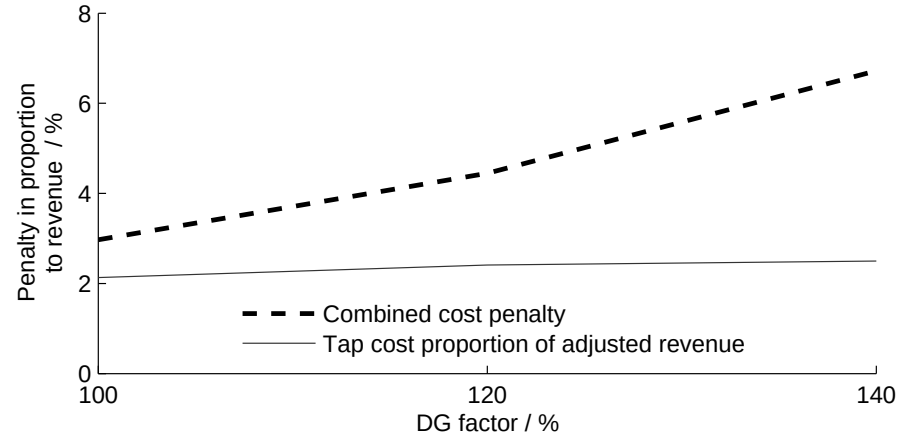

(a) DG at unity power factor.

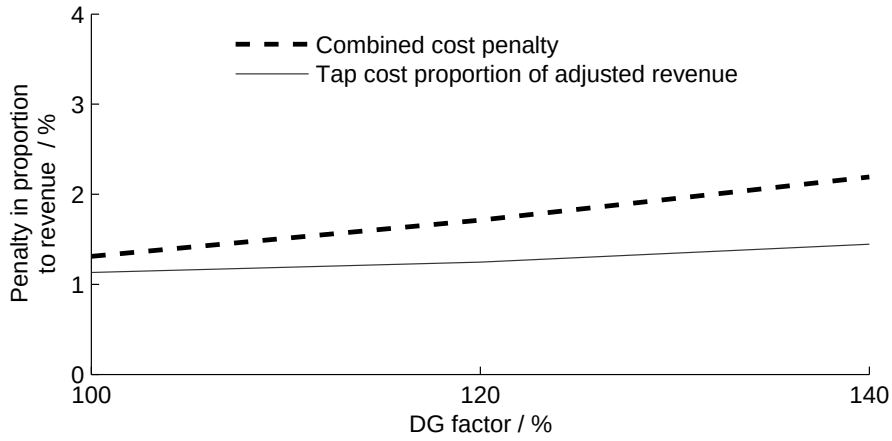

(b) DG connected at 0.9875 leading.

Figure 5.26: *Marginal penalties as a percentage of revenue for* Wardlaw-day1.

The two plots differ in the fixed power factor at which the DG is connected. At both power factors the percentage combined cost penalties increase with increased DG.

The *TapChangeCost* is defined such that a proportion of transformer maintenance costs are

proportionate to the frequency of tap operation. The tap cost component is thus of use for assessing the increased maintenance cost of ULTCs as a result of the connection of DG.

The *TotalVoltageCostPenalty* component denotes a measure of the reduction of generation that would ideally be imposed given adequate abilities of the DG to estimate the state of the feeder beyond its connection point and constrain real power output accordingly. The amount of reduction used in the calculation is the total output of the DG in the feeder during times where feeder voltages are outside limits.

The combination of the *TotalVoltageCostPenalty* and the *TapChangeCost* in the combined cost penalty are a measure of cost to the system for the connection of DG. The system in this case is the DNO and the generators. The combined cost is independent of how such costs are or should be apportioned between the parties within the system. When given as a proportion of revenue, the combined cost indicates the proportion of potential revenue lost to the penalties due to over-voltages in a feeder and to the increased cost of ULTC maintenance. The combined cost not only increases in absolute terms with increased DG capacity, but it also increases as a percentage of the revenue when the DG is connected at unity power factor. The combined cost as a percentage of revenue is lower when the DG is connected at a slightly leading power factor though similarly to the unity power factor case, the percentage combined cost doubles from the 100% DG_{max} case to the 140% DG_{max} case.

Reactive power import

The combined cost of DG operating at a leading power factor is lower than when operating at unity. The lower costs are a result of variable reactive power imported by the DG. The reactive power flow through the primary ULTC without DG is from the HV to LV side. With the addition of DG operation at a leading power factor, this increases the reactive power flow and thus increases transformer loading. This is of concern as transformer loading is a limiting factor, even though it is not reflected in the cost penalty. The $DG_{max \cdot 140\%}$ case with DG at a leading power factor results in one ULTC exceeding the cyclic limit, 150% of the nameplate rating, discussed in section 5.2.2.

Wardlaw-day2 results

The set of simulations has been repeated for *Wardlaw-day2* power output data.

First the absolute penalties are compared between the two *Wardlaw* generation time series. The difference between scenarios and areas is similar for DG at unity and leading power factors. The same observations for the two power factors also apply to *Wardlaw-day2*.

In area A the *TotalVoltageCostPenalty* is much higher due to *Wardlaw-day2* though the *TapChangeCost* is lower. Voltage control is at its limits in area A for *Wardlaw-day1* and with *Wardlaw-day2* the generation output varies near its capacity for much longer so the HV sides of primary transformers stay out of voltage limits for longer and some load buses reach their upper voltage limits.

The transformer loading time series reveals the difference between the two days in power exported from the feeder and thus voltage rise down the feeder. The power export time series and corresponding HV and LV voltages for ULTC_P^{A4} are shown in Figure 5.28 for DG connected at unity power factor.

The peak in export power in *Wardlaw-day1* is much more short-lived than in *Wardlaw-day2*. Correspondingly the voltage rise on the HV side of the primary ULTCs stays higher for longer for the *Wardlaw-day2* scenario and consequently the *TotalVoltageCostPenalty* is higher for *Wardlaw-day2*.

The *TapChangeCost* is lower as there are fewer larger power swings in the *Wardlaw-day2* scenario. Although high frequency power swings are more noticeable in the *Wardlaw-day2* scenario causing many tapping operations this is not as significant as the less frequent but larger power swings.

The *TapChangeCost* is slightly lower in area B in the *Wardlaw-day2* scenario. The main difference is the fewer operations of the GSP transformer which as already mentioned is penalised quite heavily. Although the *TapChangeCost* in area B is lower, as a percentage of revenue it increases more noticeably in the *Wardlaw-day2* scenario as shown in 5.29. The smaller power swings due to *Wardlaw-day2* become larger as the capacity of the DG increases. As they exceed 100% of DG_{max} the swings in power flow become larger and the

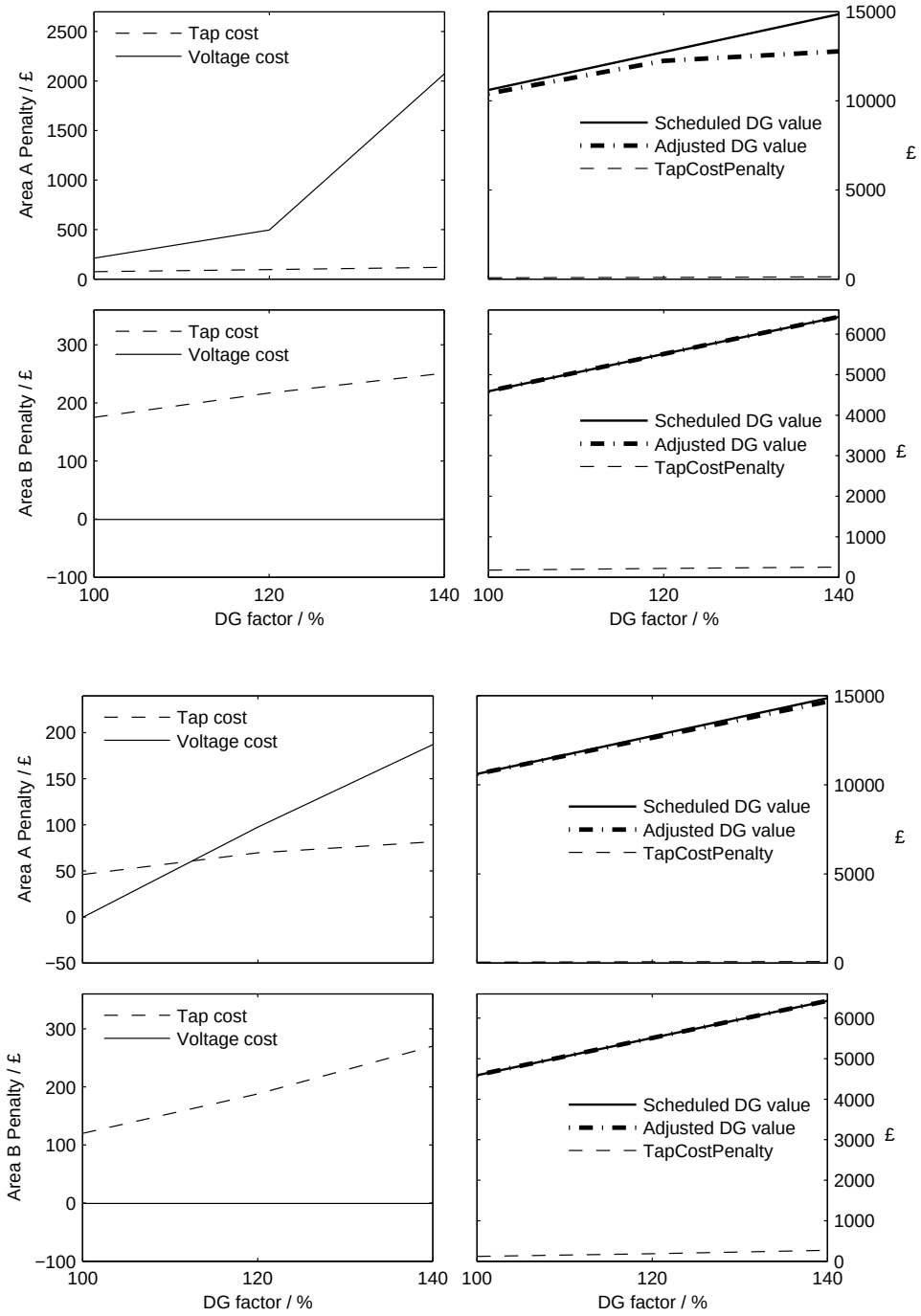

(b) DG connected at 0.9875 leading.

Figure 5.27: *Cost penalties for 3 amounts of* Wardlaw-day2 *DG in areas A and B.*

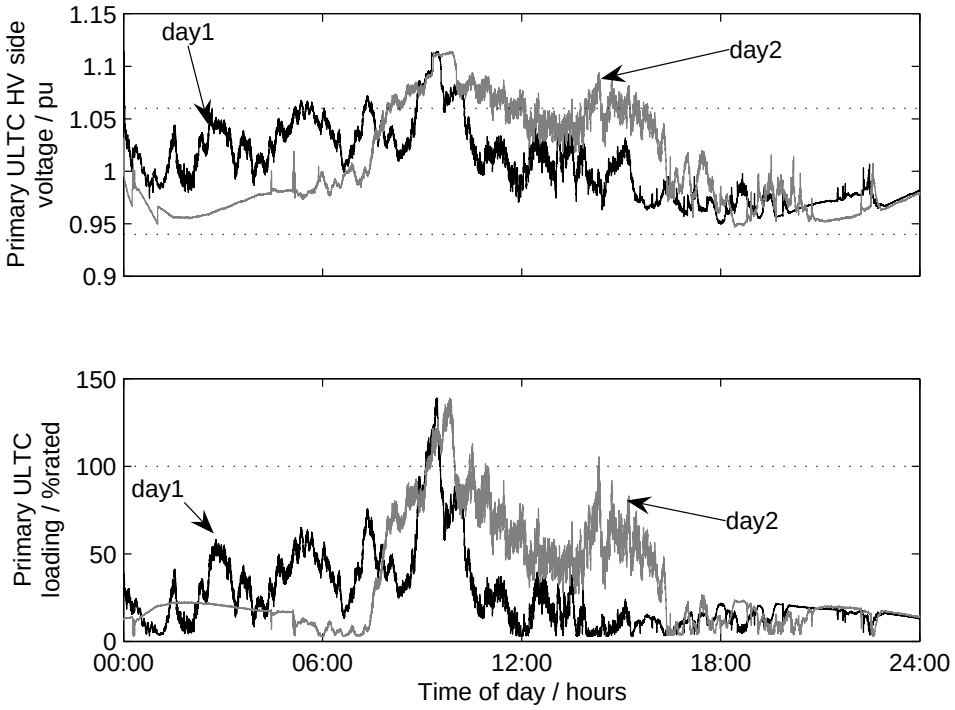

Figure 5.28: *Top, voltage on the HV side of the primary transformer on feeder 66350 for each day at unity power factor; Bottom, primary transformer loading on feeder 66350.*

GSP ULTC must compensate for the resulting voltage changes.

As noted there is a greater absolute combined cost penalty for areas A and B in *Wardlaw-day2* than in *Wardlaw-day1*. There is also an increase in energy exported and thus revenue of approximately 10%. The increase in combined cost is greater and thus the percentage contribution of the DG to the combined cost is greater for *Wardlaw-day2*.

5.2.6 Unplanned outages

Having determined an upper bound to the amount of DG that can be connected according to the scenarios above, it is important to the operation of the distribution network what happens in the event of a failure of the generation plant. As discussed in section 5.2.3, such a failure could cause a large voltage step.

A large voltage step is undesirable. Quoting the G59/G75 working group of the Distribution

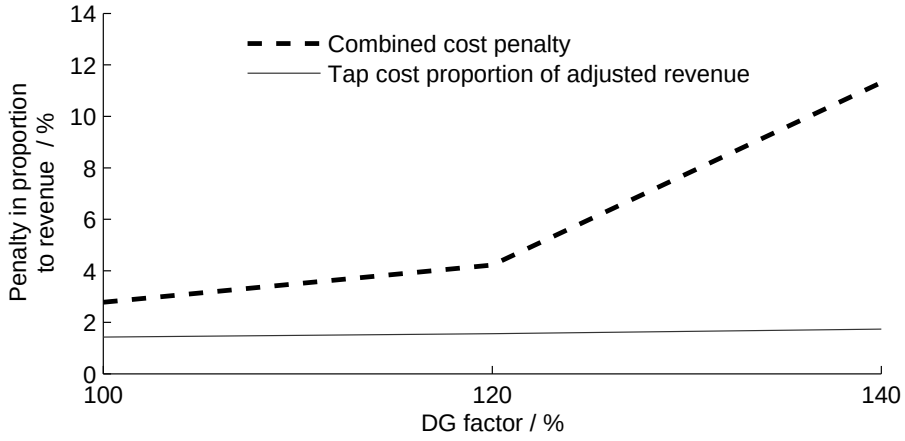

(a) DG at unity power factor.

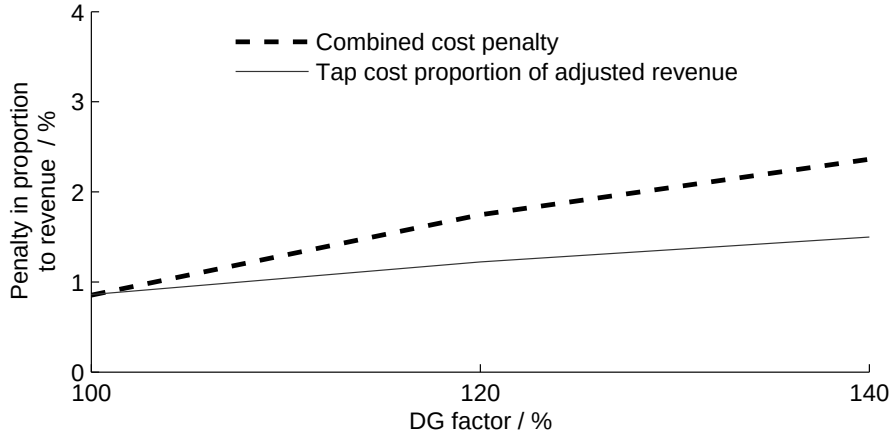

(b) DG connected at 0.9875 leading.

Figure 5.29: *Marginal penalties as a percentage of revenue for* Wardlaw-day2.

Code of Licensed Distribution Operators of Great Britain [22]:

> Typical limits for Step Voltage Changes caused by the connection and disconnection of Generating Plants from the Distribution System, should be $\pm 3\%$ step for infrequent planned switching events or outages (in accordance with Engineering Recommendation P28) and $\pm 6\%$for unplanned outages such as faults. These limits are applicable to Step Voltage Changes as defined in this Recommendation and should not be exceeded unless agreed with the DNO first, who will consider the impact of possible variations on existing customers.

The two *Wardlaw* time series have been modified according to the full-loss and

temporary-loss filters shown in section 5.1.6. The resulting time series are shown in Figure 5.30.

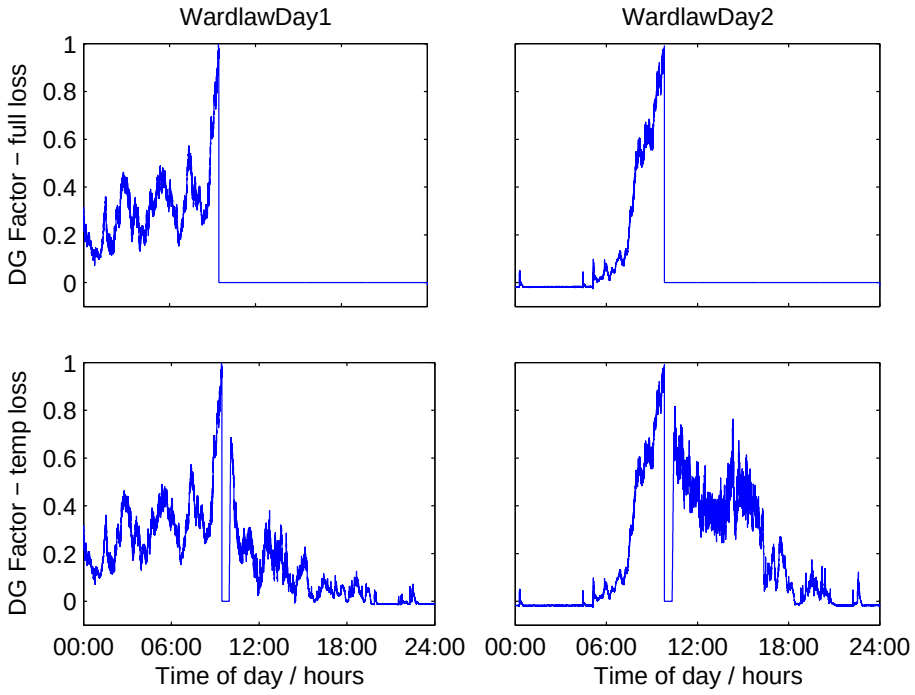

Figure 5.30: Wardlaw-day1 *and* Wardlaw-day2 *time series in* fullLoss *and* tempLoss *scenarios.*

These time series are input to the simulation with DG set to DG_{max}. Firstly, the impact of *Wardlaw-day1-fullLoss* and *Wardlaw-day1-tempLoss* on the operation and bus voltages of ULTC$_P^{A5}$ is shown in Figures 5.31 and 5.32.

The loss of generation results in a large voltage change. The change is outside the $\pm 6\%$ allowed by the G75/1 recommendations. The ULTCs operate to bring the control voltage within limits.

Once this is done, the ULTCs operate as the no DG scenario in the *fullLoss* case and as in the *Wardlaw* scenario in the *tempLoss* case.

The simulations are repeated with the DG operating at a power factor of 0.9875 leading. Figures 5.33 and 5.34 show the resulting voltage and primary transformer time series for feeder 68850.

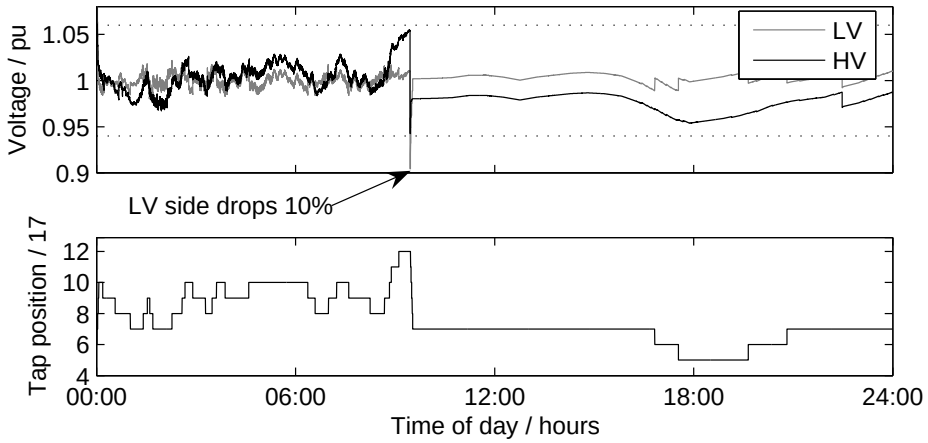

Figure 5.31: *ULTC$_P^{A5}$ HV and LV voltage and tap position due to full loss scenario 1 at unity power factor.*

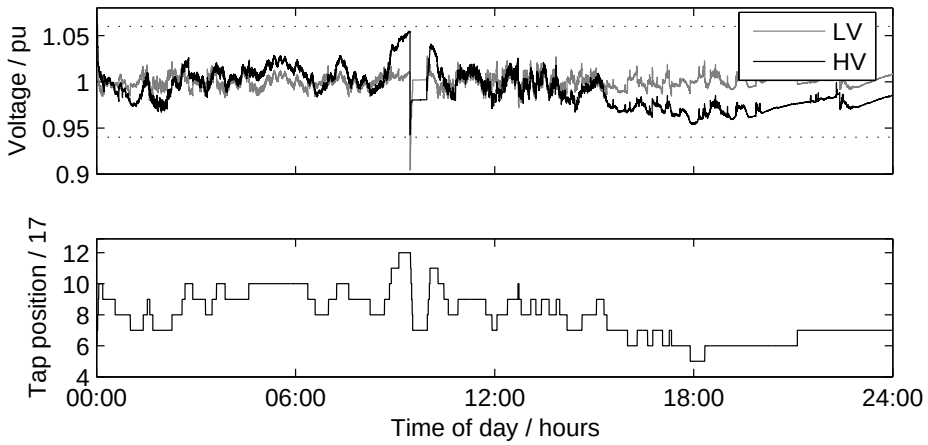

Figure 5.32: *ULTC$_P^{A5}$ HV and LV voltage and tap position due to temporary loss scenario 1 at unity power factor.*

With generation operating at a leading power factor the voltage step is much smaller. The import of reactive power being proportional to active power results in less of a voltage rise when the DG is at its capacity than when operating at unity power factor. When the DG is suddenly lost as in this case, as the voltage rise already corrected for by the primary ULTC is less, the voltage step is less and also the ULTC requires less operations to restore the correct voltage.

The 4% step is outside the "infrequent planned switching events or outages" limit of $\pm 3\%$

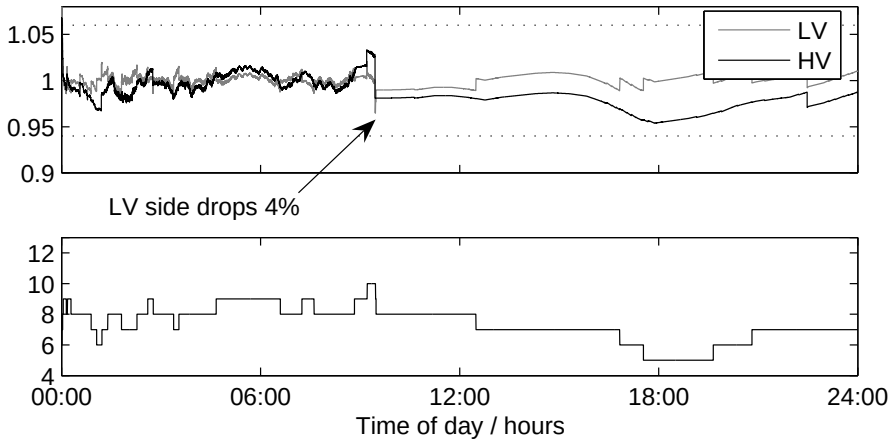

Figure 5.33: *ULTC$_P^{A5}$ HV and LV voltage and tap position due to full loss scenario 1 at leading power factor.*

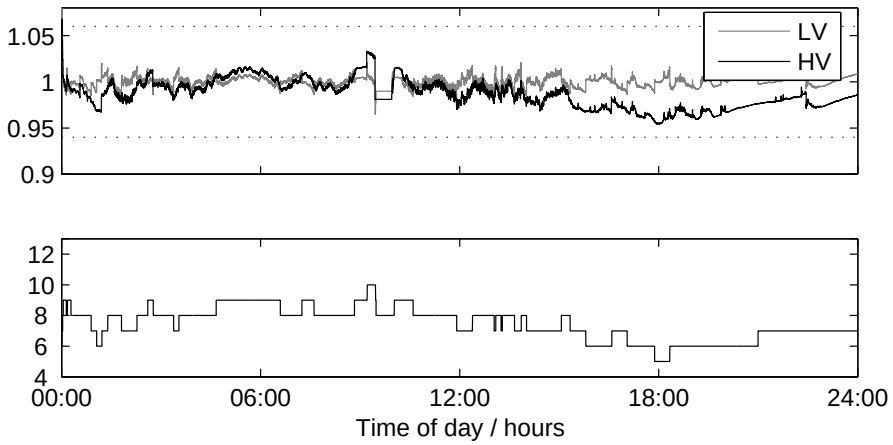

Figure 5.34: *ULTC$_P^{A5}$ HV and LV voltage and tap position due to temporary loss scenario 1 at leading power factor.*

quoted on page 132. The loss of generation scenario here involves the loss of generation across the distribution network. Investigation into the loss of generation in chapter 6 uses the loss of the largest generator on the network as the worst case.

5.2.7 Summary

The simulation method and evaluation function has been exercised on a number of scenarios. Some scenarios tested were designed to show the simulation model performed according to expectations and achieved this. Other scenarios pushed the distribution network to its limits showing how the ULTC react to such a situation. The simulation method has been shown to be able to include the effects of multiple generation time series on the network.

A number of factors are demonstrated that increase the number of tap operations required to control voltage within limits in the distribution network. The number of operations increases with capacity of DG, impedance between DG and 132 kV network, intermittency and outage events. The connection of DG further from the transmission network is dominated by thermal limits with a slight increase in reactive power requirement for unity or leading power factor connected generation.

The *TapChangeCost* and *TotalVoltageCostPenalty* indicate the cost of tap operations and a crude measure of generation curtailment. The combination of the two metrics as *Combined cost penalty* has been used to compare scenarios in terms of the fitness of the network to maintain voltage levels. This metric has indicated that the *TapChangeCost* is a small percentage of the revenue from the generation.

Of concern, however, is the ability of the distribution network equipment to maintain acceptable voltages. The operation of DG at a slightly leading power factor results in less voltage variation due to variation of active power generation. The leading power factor also reduces step voltages that arise due to sudden loss of DG. The disadvantage of such as strategy is increased transformer loading and increased reactive power requirements of the lower voltage end of feeders with DG connected.

The next chapter shows how the three methods of control of variable DG described in Chapter 3 can reduce the combined *TapChangeCost* and *TotalVoltageCostPenalty* for a given power factor and thus minimise the costs and negative impacts associated with such non-firm generation connecting to the distribution network.

Chapter 6
Connection of DG with Active Control.

Chapter 5 used a penalty evaluation function, *TotalVoltageCostPenalty*, to explore the effects of different DG connection strategies and scenarios. The final two sections showed the fitness of the network of connecting the DG_{max} scenario in normal operation and with an outage event. This chapter demonstrates three methods of DG control described in section 3.5 that are implemented and tested with the scenarios from chapter 5. The methods show a reduction in *TotalVoltageCostPenalty* compared to leaving the DG in power factor control with unconstrained real power output.

Two key changes are made to the network simulation from previous chapters.

It was ascertained that the ULTC dead-band parameters used by Harrison in the study of the network used in this project were different to those used in the previous chapter. A simulation was run with the results in Appendix C on page 199 that indicate that the parameters used in the Harrison study have a marginally lower associated *TotalVoltageCostPenalty*. In the interests of continuity and because the values perform marginally better, they will be used for this chapter.

Secondly, a modification has been made to the network below the primary transformer. The load was previously connected via a 2km line and boost transformer. The boost transformer has been removed. Generation connected at 11 kV away from the transformer can now be connected either on the load bus or on a separate 2 km line.

The four locations for DG are now as shown as loads on Figure 6.1. The actual load is indicated by the non-zero load.

In section 5.2.2 it was stated that DG is added to a feeder by apportioning it in a 1:3 ratio between the capacity of DG connected to the remote point from the LV side of the ULTC and the LV bus of the ULTC itself. With the two remote points of connection, the 1:3 ratio was

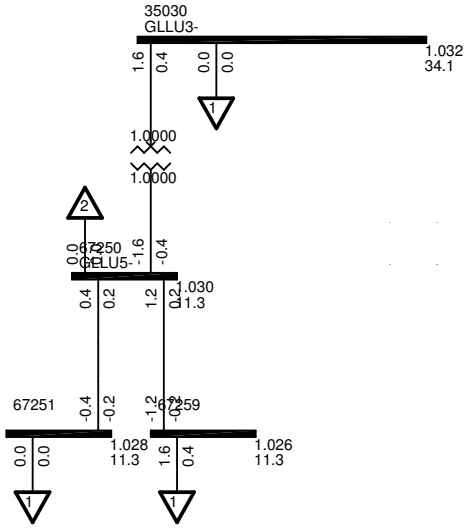

Figure 6.1: *The four possible connection points of DG around a primary substation.*

maintained and the two remote points were split 3:2 between the dedicated DG line and the line feeding the load bus.

The key tests from chapter 5 were repeated with the new network model and ULTC parameters. Again 100%, 120% and 140% of DG_{max} is connected. DG at unity power factor results are shown in Figures 6.2 to 6.5.

There are differences between these results and those on page 124.

The results shown here for both the *Wardlaw-day1* and *Wardlaw-day2* scenarios show a lower *TotalVoltageCostPenalty* for area A and a lower *TapChangeCost* for area B. The impact of that on the penalties expressed as percentages are as follows. For day one, the combined cost penalties increase from 3 to 6.5% for the three DG amounts in Chapter 5. In this chapter they increase from 2 to 5.5%. For day two the Chapter 5 combined cost penalties increased from 2.5% to 12%. In this chapter they increase from 2 to 9%. Despite the differences in resulting combined cost penalties, it is possible to compare the three DG control methods in this chapter to the PQ case by comparing to the results shown here.

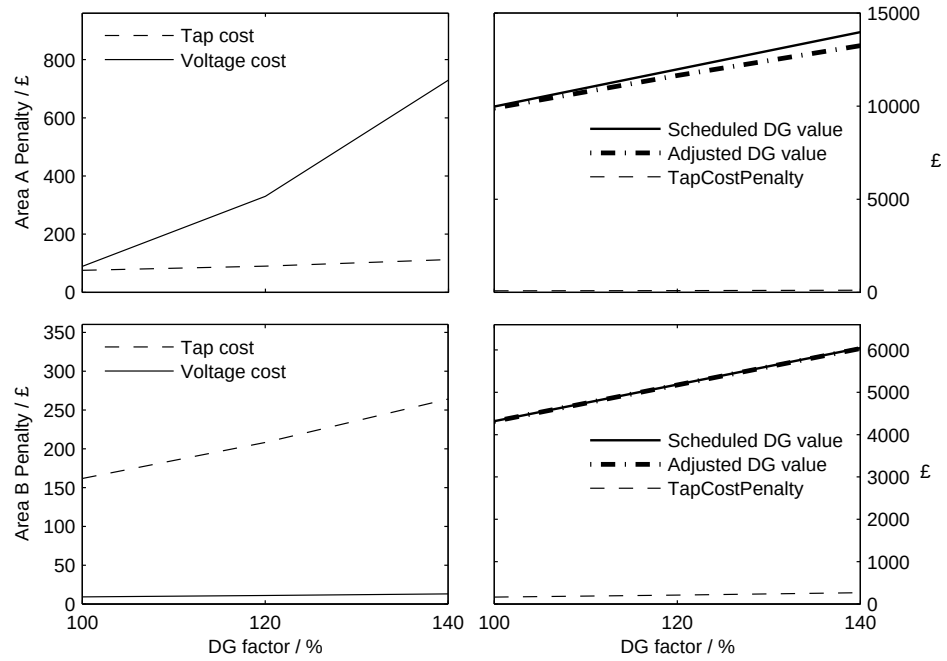

Figure 6.2: *Penalty for 3 DG scenarios in areas A and B. DG is* Wardlaw-day1 *at unity p.f..*

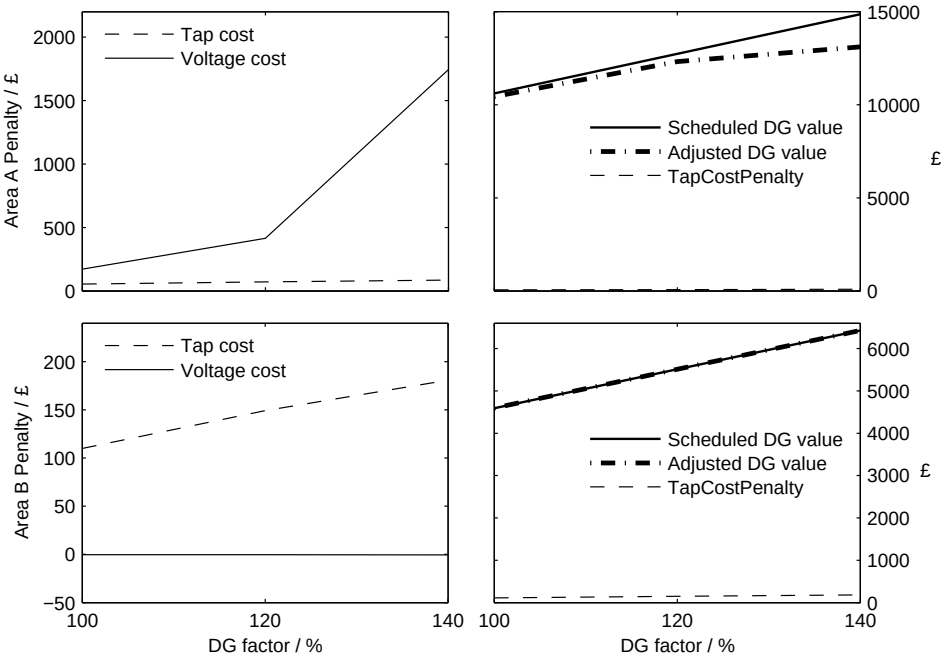

Figure 6.3: *Penalty for 3 DG scenarios in areas A and B. DG is* Wardlaw-day2 *at unity p.f..*

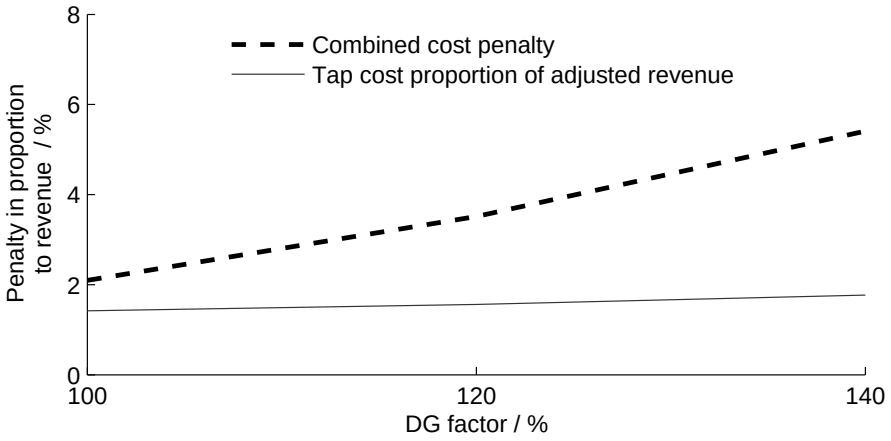

Figure 6.4: *Marginal penalties as a percentage of revenue.* Wardlaw-day1

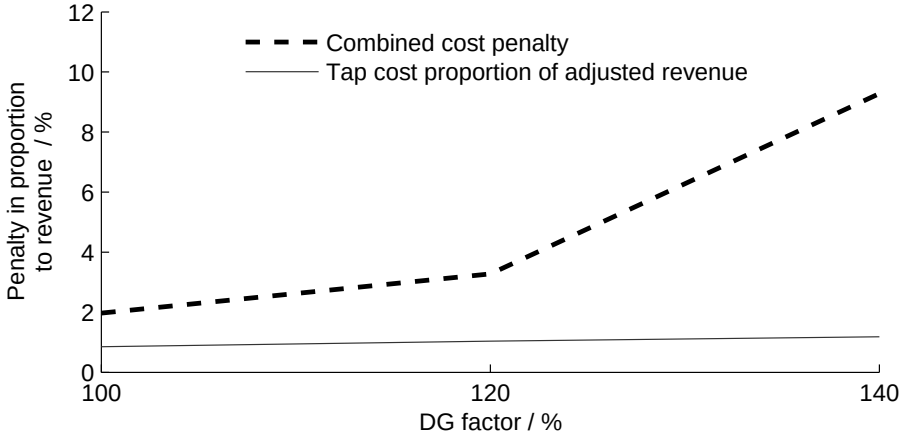

Figure 6.5: *Marginal penalties as a percentage of revenue.* Wardlaw-day2

6.1 PQ mode DG connected with voltage limit.

In the previous chapter, section 5.2 showed that the connection of DG can cause voltage violations. These violations may be violations of statutory limits or violations of operating limits imposed by the DNO to ensure supply quality and ensure compliance to the statutory limits. In this section, the DG will be shed if it exceeds the limit imposed for the bus it is connected to.

The three DG_{max} scenarios were repeated with the shedding algorithm detailed in section 3.5.1 on page 56. The three scenarios were repeated with *Wardlaw-day1* and *Wardlaw-day2* power production time series. The DG was connected at the DNO preferred, unity power factor, for comparison with the PQ mode results in the previous section.

As a reminder, the algorithm states that any bus violating set limits will have its DG, but not load, reduced to zero. The limits used are $\pm 3\%$. Following a disconnection, the DG will try to reconnect after a delay of 10 minutes. It will ramp up to its output according to the scenario over time.

The evaluations of the simulations are given in Figures 6.6 to 6.9. The marginal penalties give an indication as to the contribution of DG to the cost of tapping operations during the period simulated. The combined cost represents the system cost of the connection strategy, that is the loss of potential revenue due to voltage violations and the cost of tapping operations. The tap cost as a percentage of adjusted revenue is a measure of the ULTC maintenance costs if passed on to the generator, as a percentage of the generator adjusted revenue where the adjusted revenue is the potential revenue less the penalty due to voltage violations.

There is little difference in any of the penalty measures between the generation shedding algorithm and the standard fixed power factor mode.

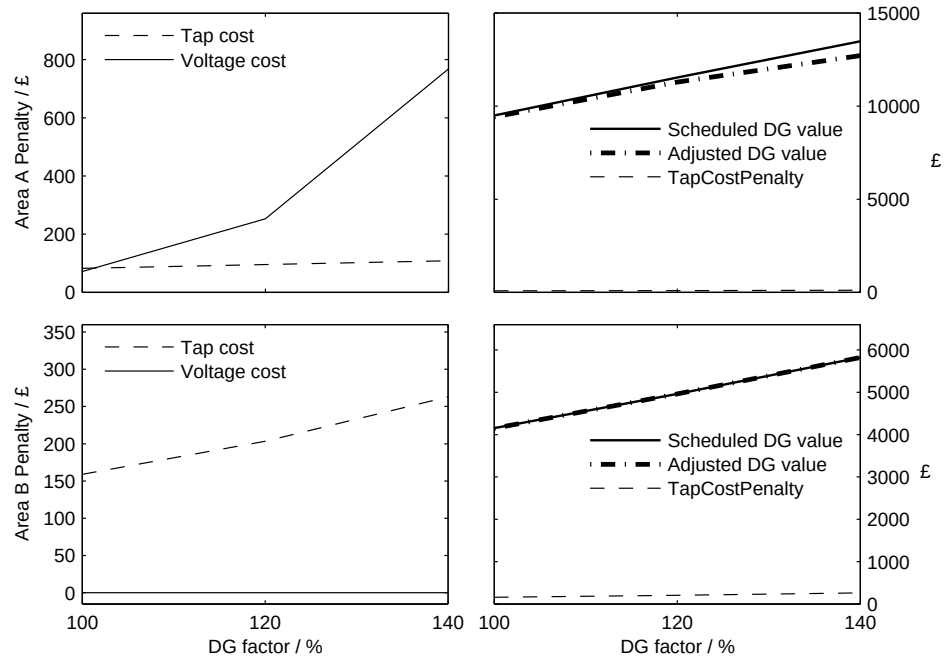

Figure 6.6: *Penalty for 3 DG scenarios in areas A and B with shedding.* Wardlaw-day1

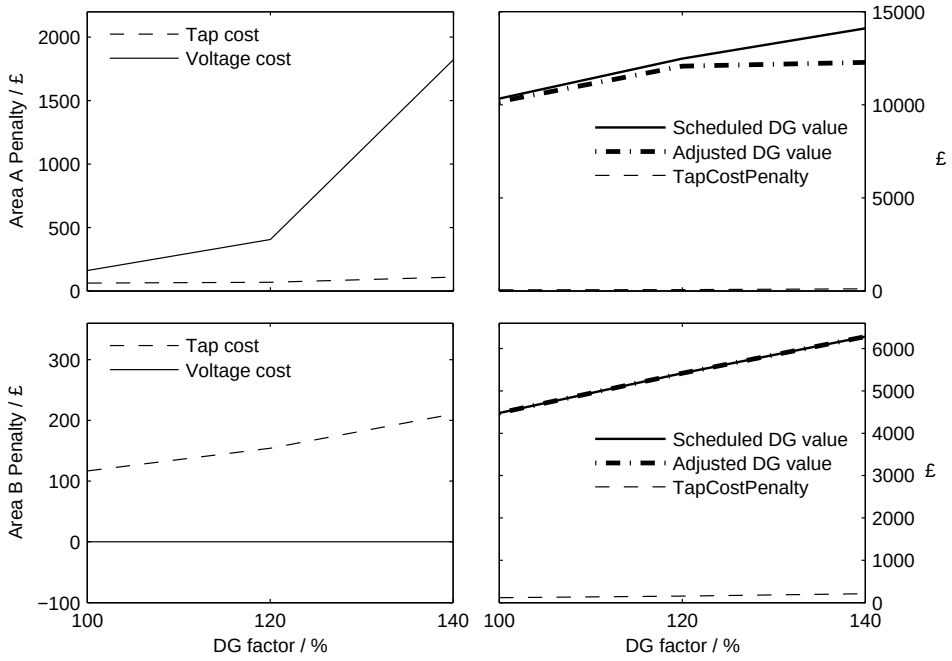

Figure 6.7: *Penalty for 3 DG scenarios in areas A and B with shedding.* Wardlaw-day2

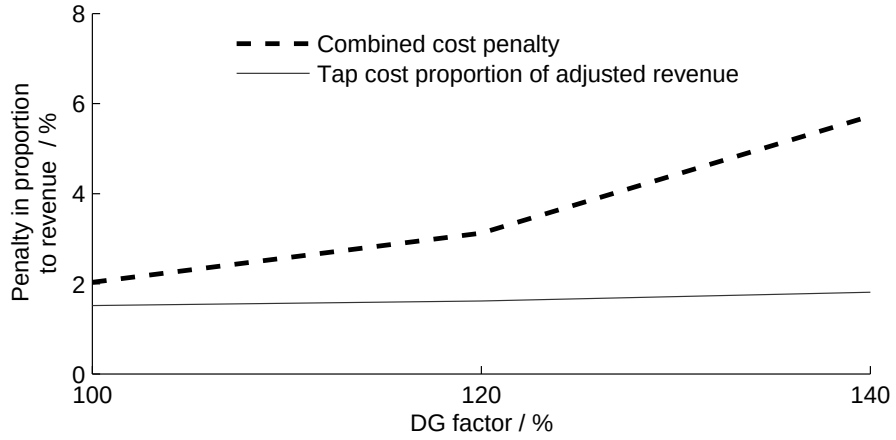

Figure 6.8: *Marginal penalties as a percentage of revenue with shedding.* Wardlaw-day1

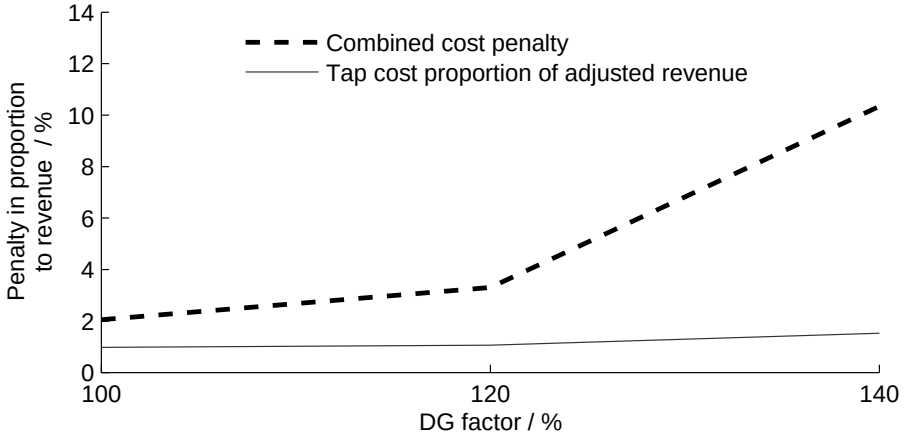

Figure 6.9: *Marginal penalties as a percentage of revenue with shedding.* Wardlaw-day2

There is however a difference in operation. The power output of DG on feeder 68850 is shown for *Wardlaw-day2* with an increase on DG_{max} of 40% in Figure 6.10.

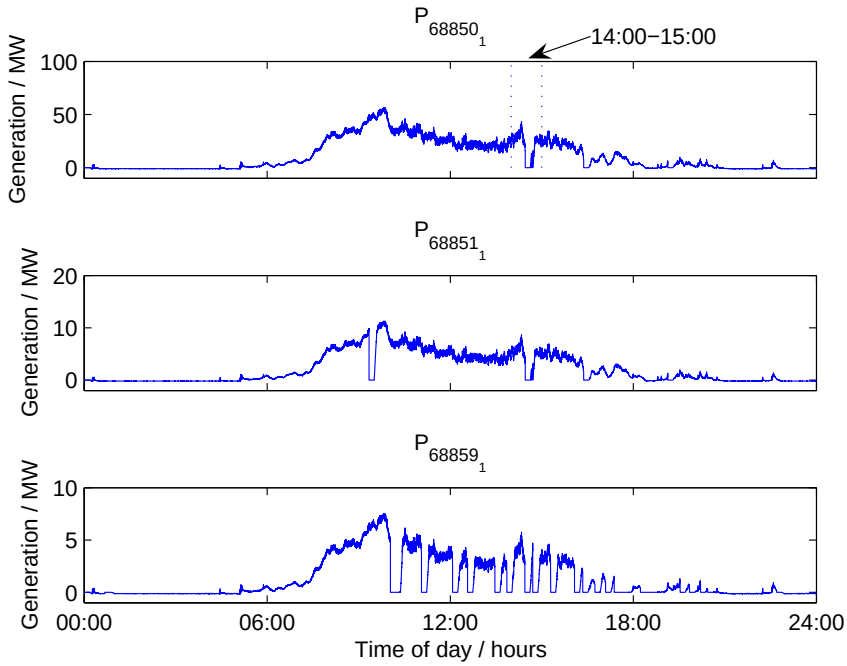

Figure 6.10: *The three connected generators on feeder 68850. Even the DG on the ULTC LV bus activates generation shedding.*

The action of the shedding algorithm is evident. The impact of the generation shedding affects the voltage level up the feeder. The act of a full disconnection of generation at times of near maximum generation unsurprisingly causes large voltage fluctuations as seen in Figure 6.11, though these are slightly masked by the variation due to the Wardlaw generation time-series. The operation of the primary transformer can be seen correcting the voltage for the no-generation state.

A shortfall of the algorithm is that it only looks at the connecting bus voltage to determine whether the generation should be shed. As discussed in the previous section, the HV side of the primary transformers spend a long period over the statutory voltage limits. The generation however is all on the LV side, connected directly and at the end of 2 km lines. Thus the generation is causing over-voltages further up the feeder as the power is exported up towards the transmission network but the local voltage is not necessarily over itself and thus the generation does not respond.

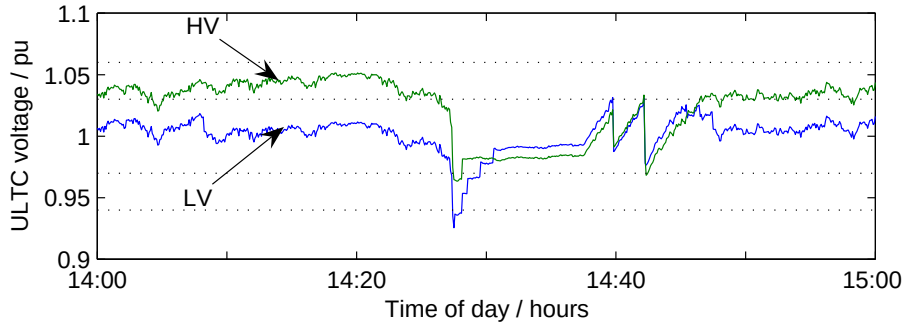

Figure 6.11

The very slight improvement in cost penalty is accompanied by a slight decrease in revenue as some of the generation is shed.

6.2 PQ mode DG connected with curtailment algorithm.

The previous sections (5.2 and 6.1) showed that change in power flows brought about by the connection of DG can cause voltage violations. To avoid this the DG can be shed. As a consequence this can have a drastic effect on the network power flows and require a number of corrections by ULTCs to restore voltages. Another control algorithm has been developed for this study, working with the shedding algorithm as a backup it is able to reduce the impact of mismatched generation and load.

The power limiter imposes a dynamic cap on the maximum output allowed by the DG. The cap is tightened as the connecting bus voltage gets close to the upper voltage limit for that bus. Following a return of the connected bus voltage, the cap is incrementally released should the DG already be generating up to the cap. The DG curtailment algorithm is defined in detail in section 3.5.2.

The three DG_{max} scenarios are repeated with the curtailment algorithm. The DG is connected at the DNO preferred, unity power factor, for comparison with the PQ mode results in the previous section.

Figures 6.12 and 6.13 show a reduction in combined cost compared to the original unlimited DG results of Figures 6.2 to 6.3. The improved reduction in combined cost comes with less lost generation than the voltage shedding case.

The total energy exported to the network by the DG in the most extreme $DG_{max} + 40\%$ case was 1302.6 MWh for day 1 and day 2 combined. The shedding algorithm caused the loss of 3.9% of that energy with no noticeable improvement in combined cost. The curtailment algorithm caused a limitation of production of 2.2% with a noticeable improvement in combined cost. This is reflected in the graphs showing the combined cost due to the DG as a percentage of revenue in Figures 6.14 to 6.15.

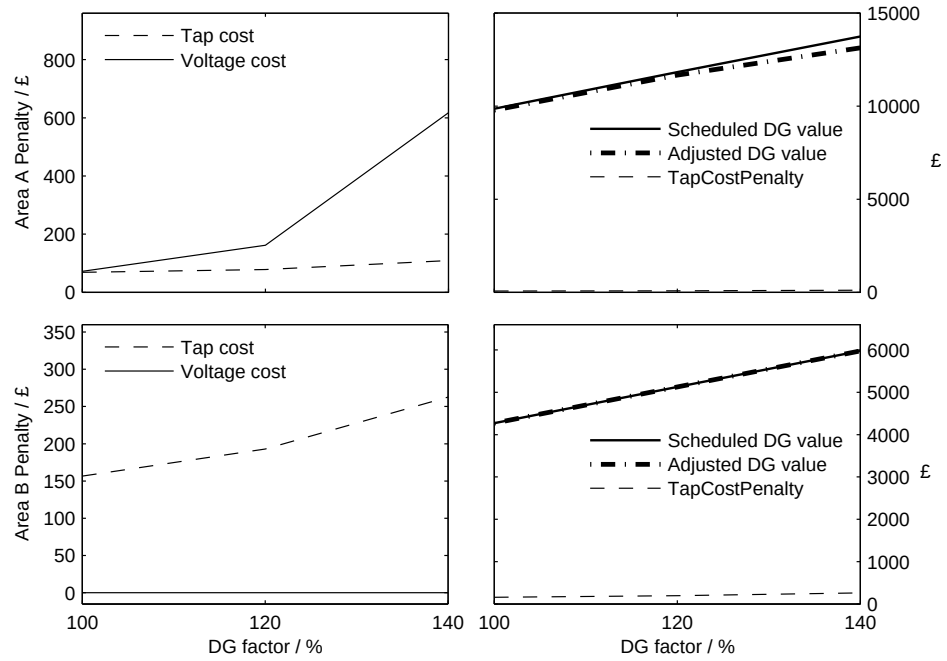

Figure 6.12: *Penalty for 3* Wardlaw-day1 *DG scenarios with DG curtailment.*

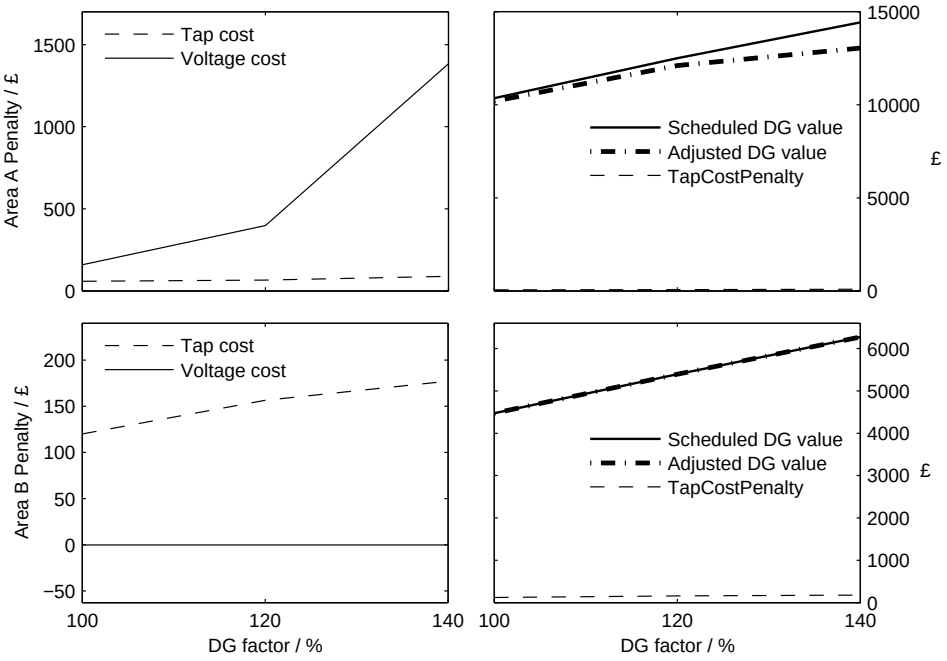

Figure 6.13: *Penalty for 3* Wardlaw-day2 *DG scenarios with DG curtailment.*

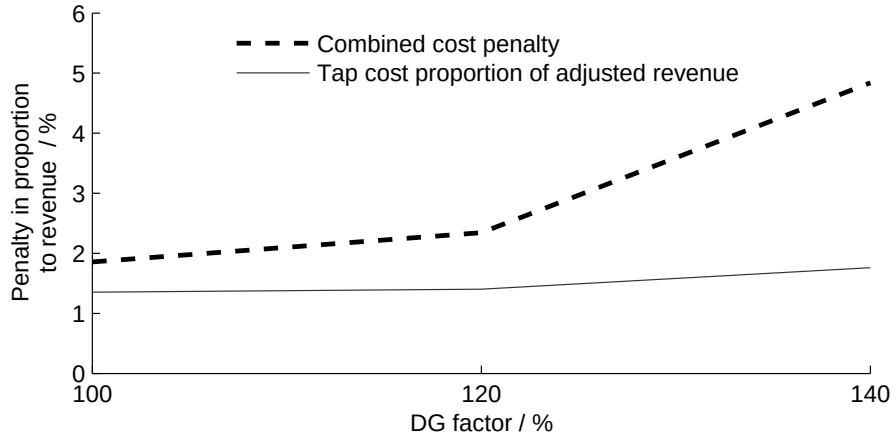

Figure 6.14: *Marginal penalties as a percentage of revenue with DG curtailment.* Wardlaw-day1

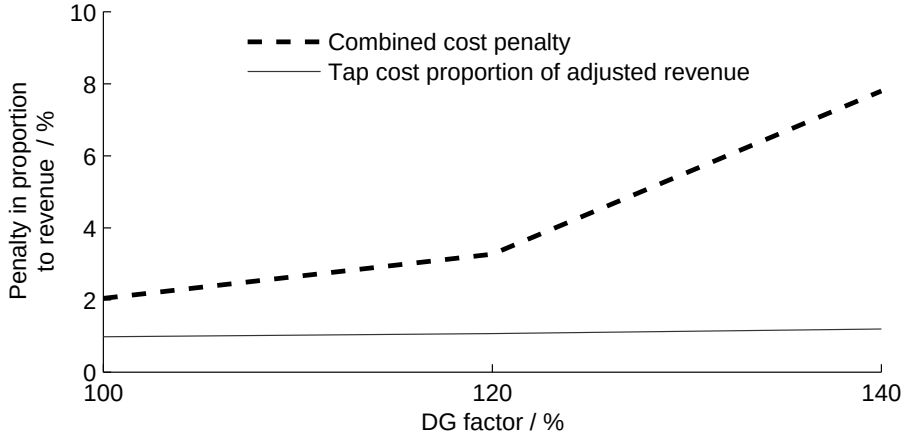

Figure 6.15: *Marginal penalties as a percentage of revenue with DG curtailment.* Wardlaw-day2

6.3 DG connected in PV mode.

The final method of DG control simulated is the standard PV mode control with assumptions as described in section 3.5. As discussed, the simulation does not dynamically model the operation of the generator AVR. For this reason the simulation does not model any generator interactions that may occur if they are electrically close. If they have similar time constants it is possible that without communication the generators could work against each other, one producing VArs with the other absorbing.

A maximum of one generator in PV mode is added per feeder in this section. Although caution is observed here when adding PV generation, it is common to see load flow solutions with multiple PV generators. Indeed above the GSPs in this simulation are a number of hydro plant in PV mode maintaining 132 kV voltage with the help of tap changing transformers. When multiple generators are on the same busbar, they are grouped as a *Plant* in PSSE, which has an associated scheduled voltage. The case examined only includes multiple units that are identical. PSSE adjusts each generator on the busbar so that they share the load and thus have identical outputs.

The runs in this section were all conducted with the DG_{max} scenarios with DG controlled by the shedding algorithm operating at the statutory $\pm 6\%$limits. The amount of voltage control available for PV mode DG is limited by power factor as described by Figure 3.7 on page 53. The power factor range in these results is either 0.9875 leading/lagging or 0.95 leading/lagging.

The bus that the PV mode generation is connected to also is regulated by the primary transformer. The transformer voltage limits are set equidistant from 1.0pu so the voltage set-point of the transformers is 1.0pu. The set-point of the generation is the same as the ULTC.

Again *Wardlaw-day1* and *Wardlaw-day2* was used as the basis of generation time series for all DG. All PQ DG is disconnected should the connecting bus voltage exceed the statutory $\pm 6\%$limits and re-connected when the voltage is within limits by the strategy demonstrated in section 6.1.

6.3.1 PQ mode DG with PV support

The first simulation shown has all DG operating in PQ mode except the largest generating buses in each of the areas A and B which are buses 68850 and 68450 respectively. The generators connected to these buses operated between a 0.9875 leading and a 0.9875 lagging power factor. The results of the 3 DG_{max} scenarios are shown in Figures 6.16 to 6.18.

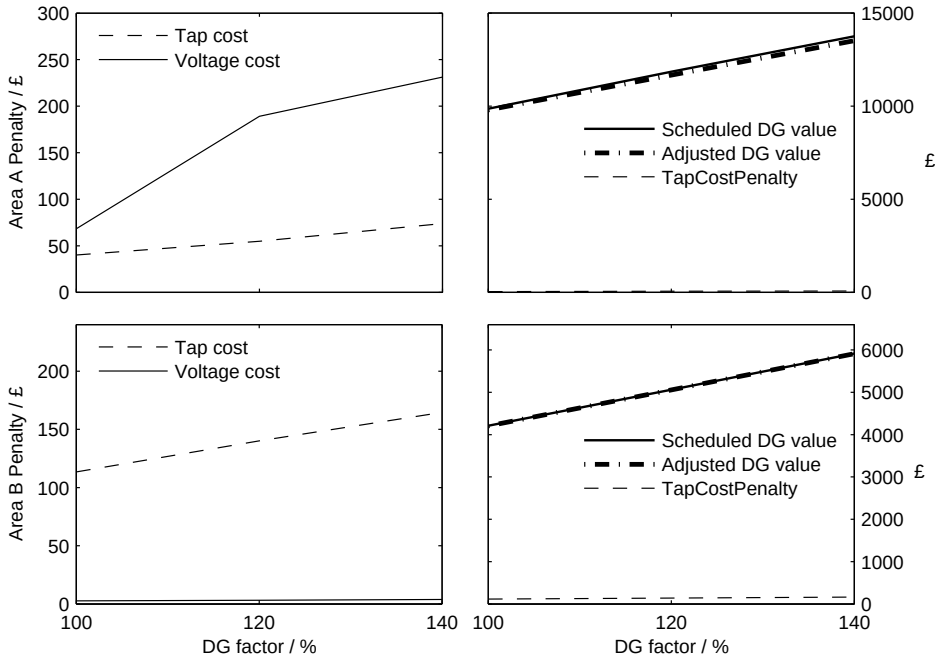

Figure 6.16: *Penalty for 3 scenarios in areas A, B each with PV control.* Wardlaw-day1

The combined costs are clearly lower with this control method. Both the *TapChangeCost* and *TotalVoltageCostPenalty* are lower compared to any of the previous control methods. 1.2% of the generation is shed in days 1 and 2 combined which is lower than both other generation control methods. These observations are confirmed by Figure 6.18 showing the combined cost as percentage of revenue for days 1 and 2.

A closer look at area A

Feeder voltages and transformer operations are shown to help understand how the PV mode generation improves voltage quality and reduces tap changes. The most marked improvement

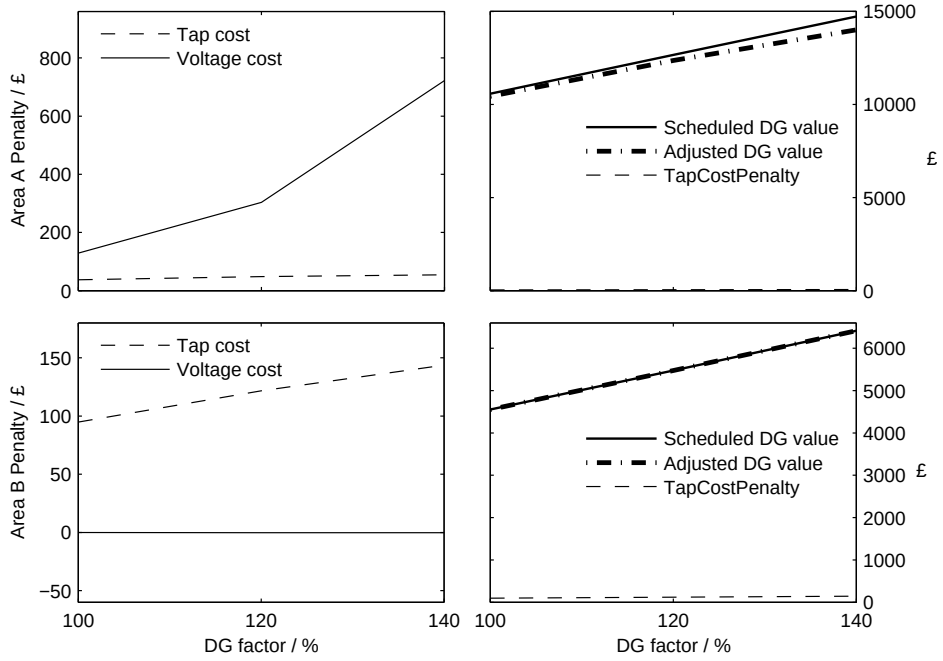

Figure 6.17: *Penalty for 3 scenarios in areas A, B each with PV control.* Wardlaw-day2

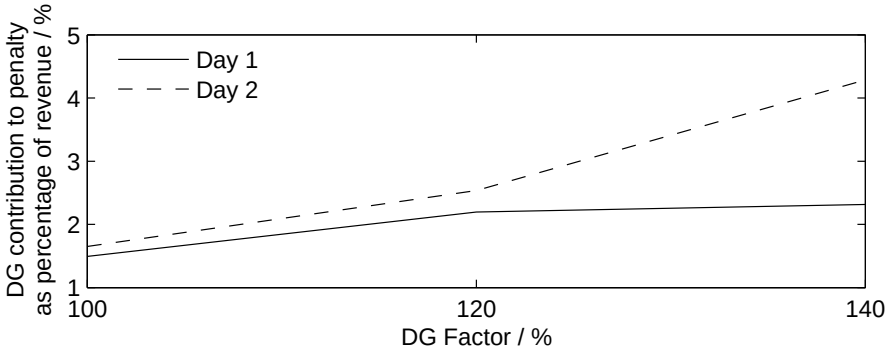

Figure 6.18: *Marginal penalties as a percentage of revenue each with PV control.*

is observed in the $DG_{max} + 40\%$ case. The operation of the three primary transformers in area A are shown in Figure 6.19. The figure compares operation with DG fixed at unity power factor and with the PV mode setup.

The tap position time series of the primary has improved in two ways. Firstly, time series is smoother in the PV case, that is, there is a reduction in the number of tap operations that are reversed shortly after being made. Secondly, the range of tap positions during the day is

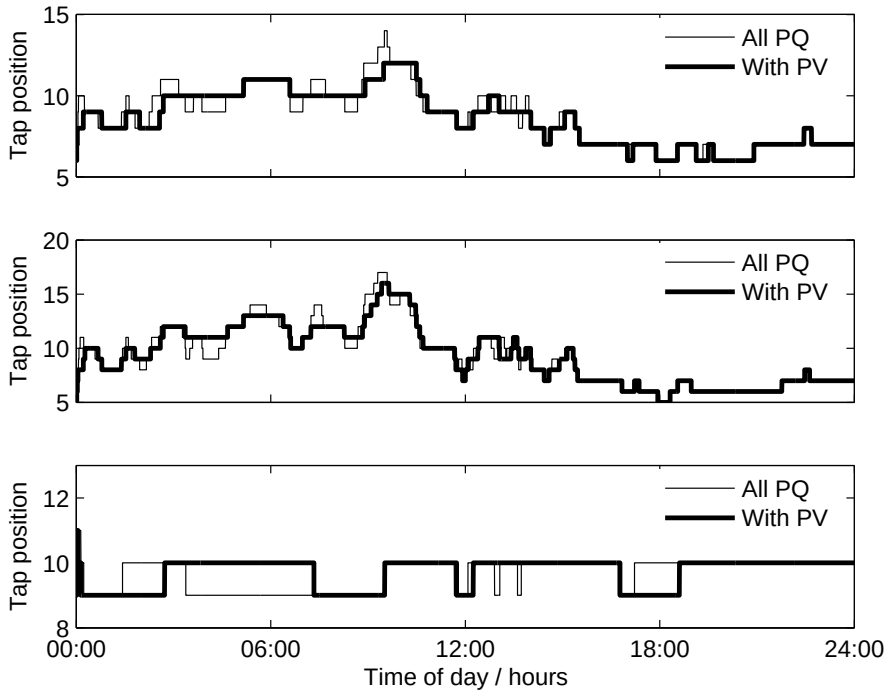

Figure 6.19: *Tap position of primary ULTCs for feeders 68850, 66350, 67250 in area A for* Wardlaw-day1 .

reduced in PV mode. The two characteristics combine to cause a lower *TapChangeCost* and less step voltages caused by tap operations.

Note how the middle plot, the tap position time series for ULTC_P^{A4}, is improved. The PV DG is not directly connected to the feeder but as a result of its actions, it keeps bus 68832 at a more constant voltage. The 66350 feeder shares bus 68832 with feeder 68850 and thus benefits from voltage control in that latter.

It is shown in Figure 6.20 that in PV mode the voltage of the primary transformer LV side is kept much closer to the target voltage of 1.0 pu. This in turn causes less variation in the voltage at the load as shown in Figure 6.21.

An obvious consequence of the voltage being kept close to 1 pu on the LV side of a ULTC is that the ULTC does not need to change tap position. Thus whilst the PV DG is within reactive power limits it completely stops the operation of the ULTC to which it is closely connected. This could lead to a reliance on the DG for voltage control that could cause large voltage excursions in the event of a loss of that DG. This is tested in section 6.3.4.

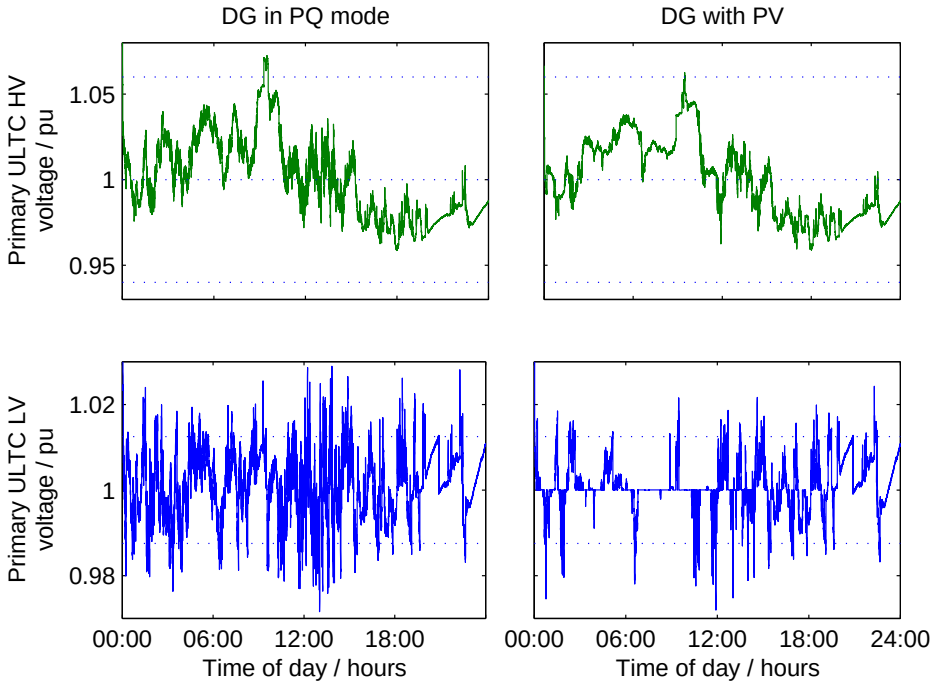

Figure 6.20: *HV and LV voltage of primary on feeder 68850. Statutory limits are shown on HV plots and ULTC dead-band on LV plots.*

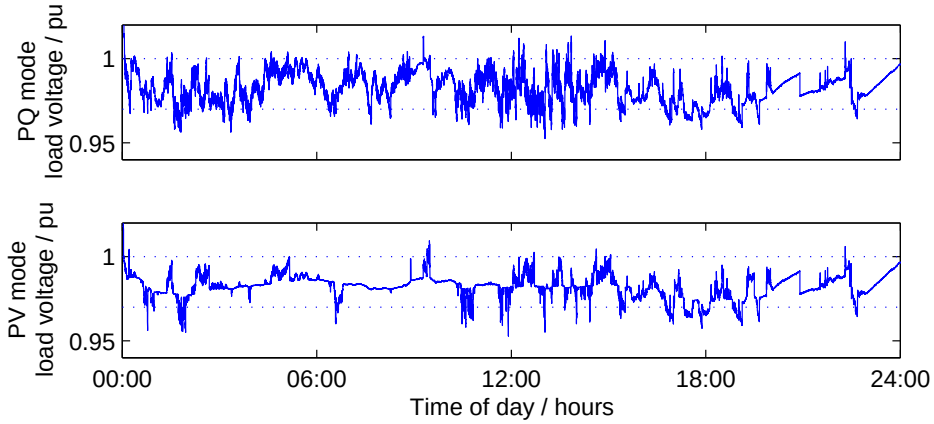

Figure 6.21: *Load bus voltage in PQ and PV scenarios with lower planned voltage limit of* -3% *shown.*

The number of tap operations made by the GSP transformers in area A are not reduced by the PV scenario for *Wardlaw-day1* as shown in Figure 6.22. Some short term operation is smoothed out but additional operations occur in the middle of the day. These operations coincide with peak real power output of the DG.

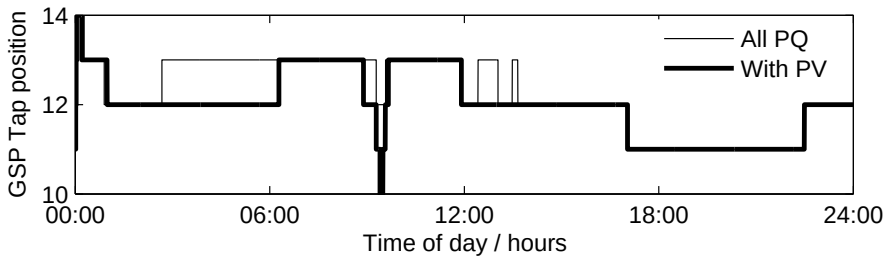

Figure 6.22: *Tap position of GSP transformers for area A.*

The PV mode does not prevent all tapping operations in ULTCs A5 and A6 as the DG repeatedly reaches its lower reactive power limit, or in other words its maximum Q import. In PV mode the generator on bus 68850 is absorbing VArs when at peak power output. This is shown in Figure 6.23. The reactive power limits Q_{min} and Q_{max} at a time-step are proportional to the real power output at that time-step.

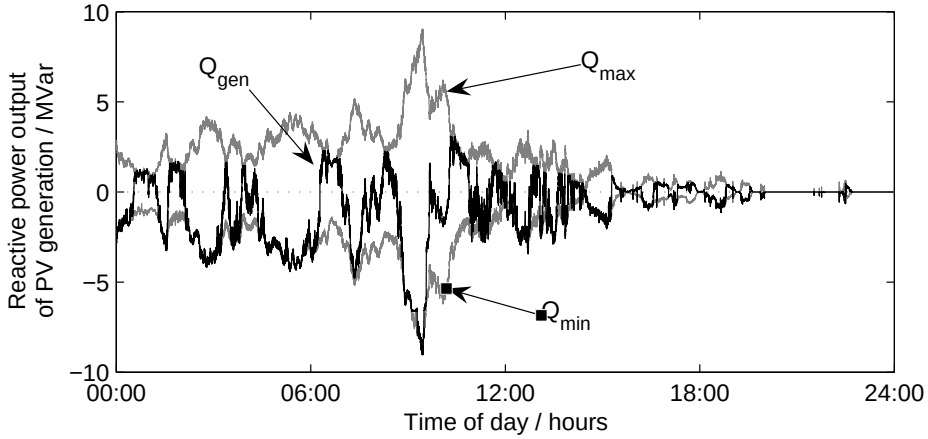

Figure 6.23: *Reactive power import/export by generator at bus 68850.*

The generator at 68850 has 58% capacity of all DG in area A and thus impacts on bus voltages in A. The import of so much reactive power during peak generation periods, as shown in

Figure 6.23, causes the voltage on the GSP LV side to drop, requiring correction as shown by Figure 6.24.

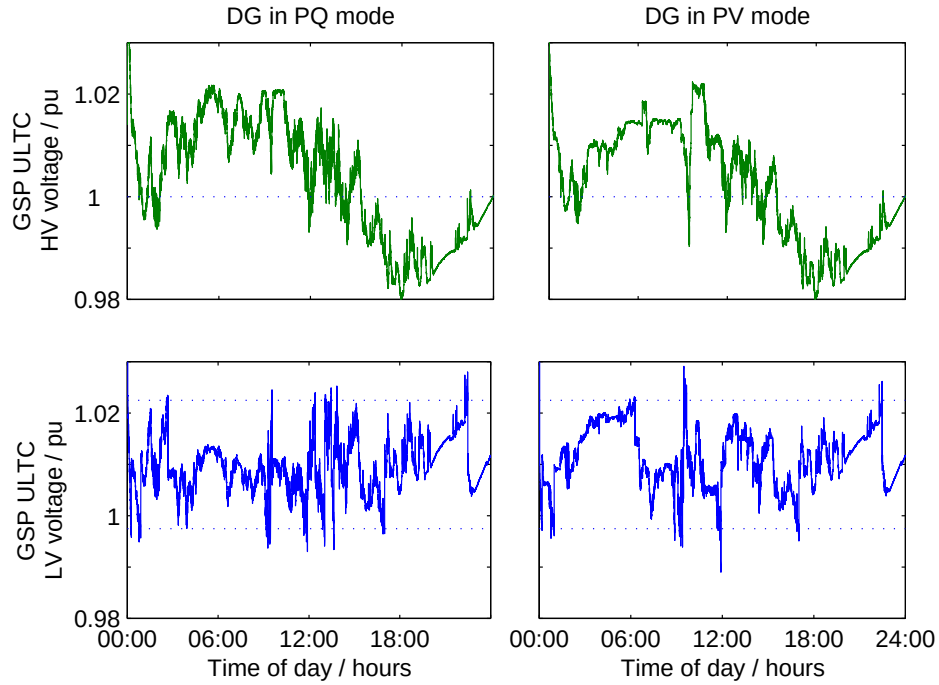

Figure 6.24: *HV and LV voltage of GSP on feeder 68850. Statutory limits are shown on HV plots and ULTC dead-band on LV plots.*

The power spike in the *Wardlaw-day1* time series is short lived and thus the GSP must reverse its tap operations. This spike in the GSP tap position time series adds little to the combined cost though. The GSP consists of two parallel ULTCs resulting in a low per-operation cost as maintenance should be possible without interfering with normal operation of the network in low power flow periods.

A closer look at area B

The feeder with the largest DG in B was selected to have DG connection in PV mode with all other DG in PQ mode. That feeder is also the lowest impedance feeder and already required only a few tapping operations even in PQ mode. The PV mode reduced these slightly, with a knock-on effect of greatly reducing the GSP ULTC operations and operations of neighbouring

feeders. This is shown as a table of tap operations for *Wardlaw-day1* and *Wardlaw-day2* with DG at unity power factor except for two in each area being in PV mode with the 0.9875^{-} to 0.9875^{+} power factor range.

Scenario		Tap operations by ULTC code				
		B1	B2	B3	B4/B5	B6/B7
Day 1	All PQ	105	9	12	7	35
	PV Strong	63	9	10	5	29
	PV Medium	73	11	10	7	17
Day 2	All PQ	71	9	10	5	25
	PV Strong	55	9	10	7	21
	PV Medium	69	9	12	7	17

Table 6.1: *140% case DG area B tap operations where PV Strong and Medium are scenarios with area B PV connected to 68450 and 68650 respectively.*

The third and sixth row have DG at busbar 68650, the medium impedance feeder in area B in PV mode instead of 68450 the least impedance feeder. Putting the DG at 68450 reduced the feeders primary tap operations as intended. The scenarios reduced the overall combined cost penalty in both days by approximately 0.2%. This improvement was modest due to the scenario not reducing GSP tap operations.

Aside from allowing multiple DG in each area being in PV mode, there are many combinations of which DG to give voltage control, however they won't be explored further as the immediate benefit of employing PV mode DG is thus far demonstrated.

DG operates in both leading and lagging power factor when in PV mode

As shown in the previous sub-section, the PV mode DG in area A repeatedly reaches its lower reactive power limit and can no longer keep the LV side of the primary transformer down. The PV mode does not cause DG to operate solely in a leading power factor. Figure 6.25 shows the PV mode DG in areas A and B for *Wardlaw-day1* and *Wardlaw-day2* time series.

The area A PV generation operates at a leading power factor during its peak power output in an attempt to compensate for the large amount of DG in that area.

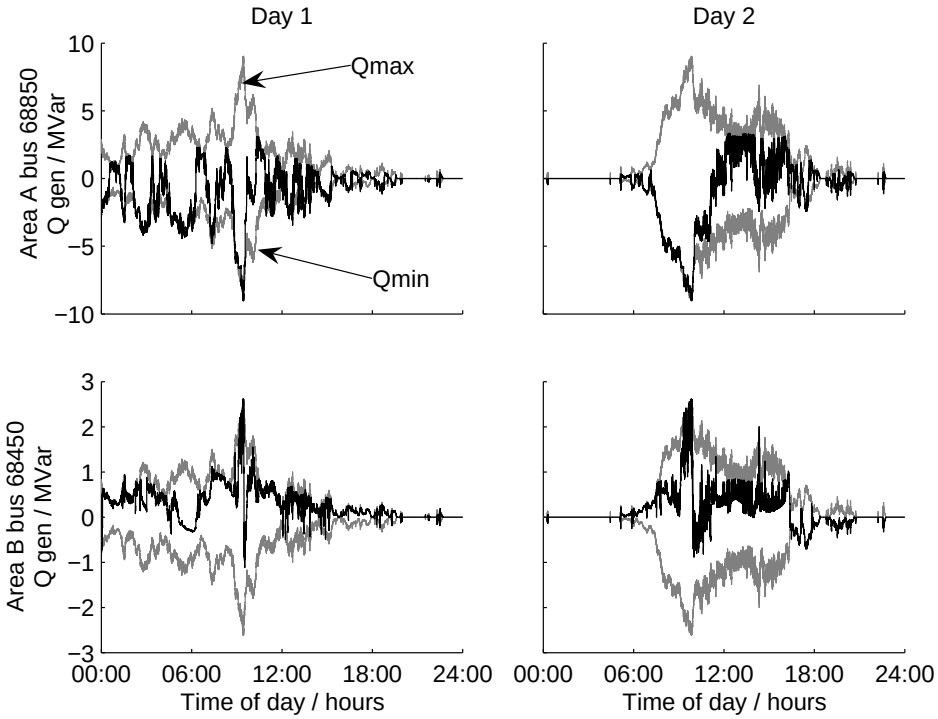

Figure 6.25: *Reactive power output of PV mode DG in areas A and B for* Wardlaw-day1 *and* Wardlaw-day2.

The results for area B show the PV mode DG operates mainly at a lagging power factor within its reactive power limits. For this reason the voltage is kept steady during the period of rapid power output change in the afternoon of *Wardlaw-day2* reducing primary ULTC tap operations.

6.3.2 A combination of PV and PQ leading generation

Operating the two larger DG in PV mode, the PV support scenario, is an improvement on them all being in PQ mode at unity. The *CombinedCostPenalty*, however, is greater in the PV support scenario than in the scenario where all DG is in PQ mode with a slightly leading power factor. The 140% DG_{max} case in the PV support sceanrio of the previous section results in 2.2% and 4.2% for the combined cost as percentage of revenue for the PV mode in days 1 and 2 respectively. This was shown in Figure 6.18. The figures for operation of all DG in a slightly leading power factor mode are a much lower 1.5% and 1.9% for days 1 and 2

respectively as previously shown in Figures 6.4 to 6.5. The leading fixed power factor mode is better than the limited PV mode in both the number of tap changes seen over the two days and in terms of the number of voltage excursions. The slightly leading power factor PQ mode has already been shown to be superior in terms of voltage control and number of required tapping operations to the unity PQ mode.

The largest two DGs are again operated in PV mode with all other DG in PQ mode at 0.9875 reactive power factor. The simulation is run for *Wardlaw-day1* and *Wardlaw-day2* and the results combined to give a cost penalty as a percentage of the two days revenue combined. This is shown in Figure 6.26.

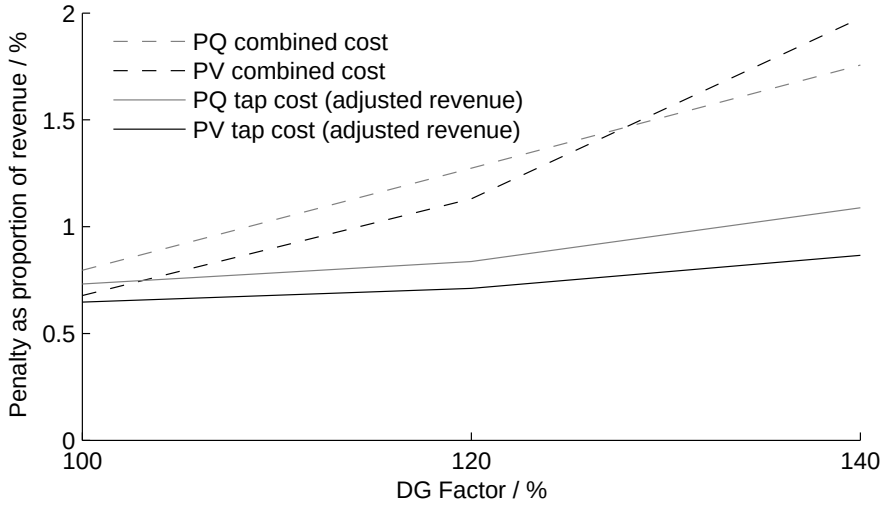

Figure 6.26: *The tap cost as a percentage of adjusted revenue is shown for the PQ mode at 0.9875 leading p.f. and for the PV mode as described. The results are for days 1 and 2 combined. Also shown are the combined costs.*

With all PQ generation at a leading power factor the PV mode shows improvement on the all leading PQ mode in the tap cost as a proportion of adjusted revenue as well as combined cost. Operating the PQ DG such that it absorbs reactive power in proportion to its real power output reduces the voltage rise problem, as shown in earlier sections, with the PV mode DG providing extra control and a positive reactive power output when required.

6.3.3 Increased reactive power capability

The last set of results with only one PV mode generator in each area has the power factor limits of the PV mode DG expanded to the 0.95 leading/lagging. These limits are typical of the latest DFIG wind turbines. The results are plotted alongside the previous results for comparison in Figure 6.27.

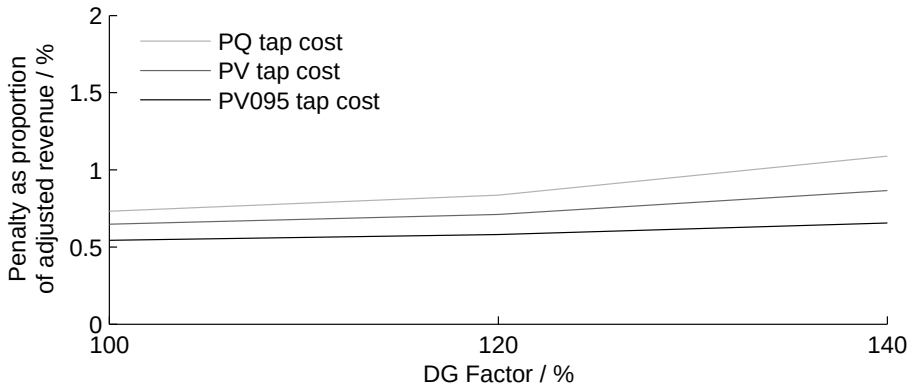

Figure 6.27: *Combined cost as a percentage of revenue is shown for: the PQ mode at 0.9875 leading p.f.; PV mode with p.f. limits* $0.9875^{\pm}$ *(PV) and PV mode with p.f. limits* $0.95^{\pm}$ *(PV095). Also shown are the respective tap costs as a proportion of adjusted revenue.*

This setup leads to a better relative tap cost than the PQ setup and the previous PV setup. The increased range of reactive power output of the PV mode DG increases their ability to moderate voltage changes due to real power output fluctuation.

6.3.4 Loss of generation in PV mode

The most favourable PV scenario with reactive power $0.95^{\pm}$ is selected for comparison with the PQ mode scenario with power factor 0.9875 leading. A generator is disconnected should its connecting bus exceed the statutory $\pm 6\%$ per-unit voltage. Both scenarios use *Wardlaw-day1* time series filtered by *FullLoss* for bus 68850 and the *Wardlaw-day1* time series for all other generation. The capacity of generation is defined by $DG_{max \cdot 140\%}$.

Figures 6.28 and 6.29 show the voltage at the bus in question as well as the primary transformer ULTC$_P^{A5}$ tap position. The LV side of ULTC$_P^{A5}$ is bus 68850, the bus from which

the DG disconnects at its peak output.

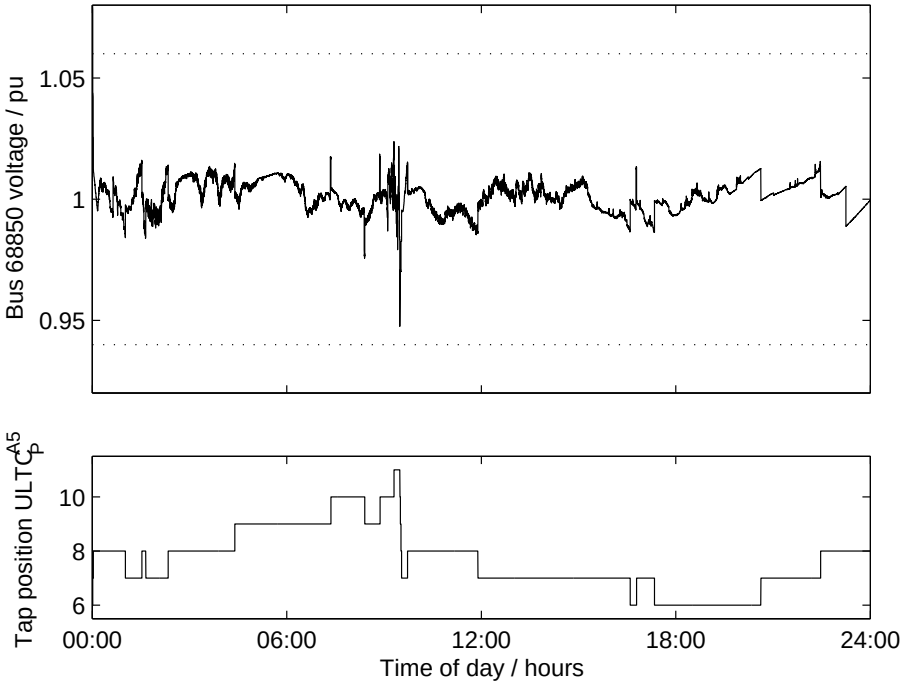

Figure 6.28: *Bus voltage and primary transformer tap position as a result of PQ DG loss at 68850.*

The PQ scenario results in a 2% upward voltage spike. A number of tap operations are required however, to restore the voltage as the tap position is four stops away from the position at which it would operate without the DG. A number of tap operations are forced on neighbouring feeders which are shortly corrected as feeder 68850 settles.

At the time of disconnection the PV scenario shows a significant 6% upward voltage spike. This is as a result of the loss of the reactive power absorption of the generator at that point. The spike is greater than in the PQ scenario as the PV mode DG is operating at its maximum reactive power absorption at a 0.95 leading power factor. The primary transformer reacts but the action is reversed as the GSP transformer compensates.

The reactive power absorption was at its limit with the generator effectively operating at 0.95 leading. Thus the PV mode DG was absorbing twice the reactive power as the PQ mode transformer at the point of power loss.

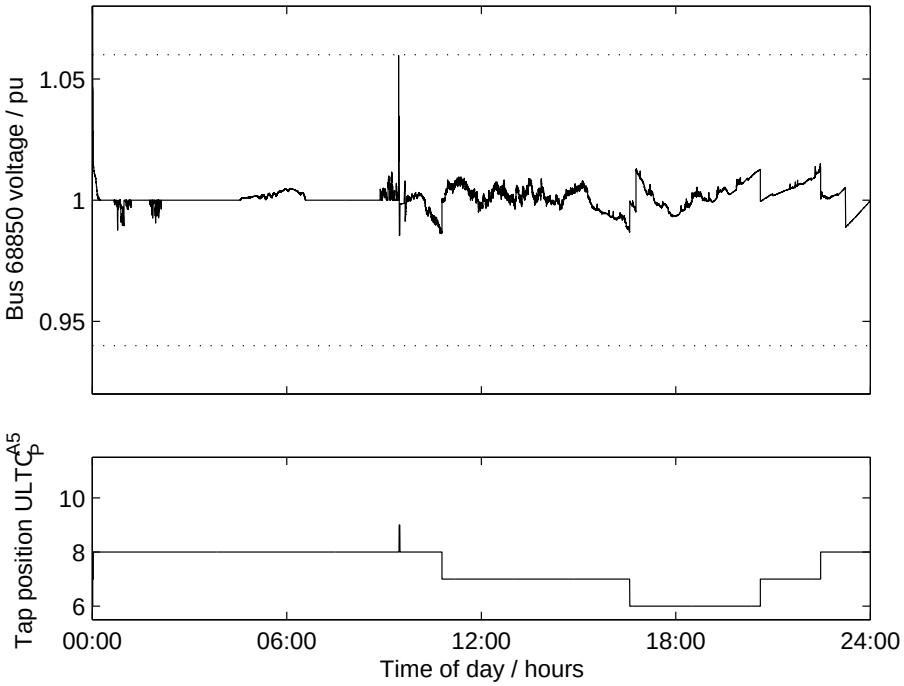

Figure 6.29: *Bus voltage and primary transformer tap position as a result of PV DG loss at 68850.*

In both cases the large amount of generation lost leads to very similar corrective action by the GSP transformer. The GSP transformer ultimately leads to the correction of the voltage.

The 6% voltage spike is undesirable and would lead to penalties to the DG operator that would have been avoided if the generation was absorbing less reactive power such as in the slightly leading PQ mode. It remains to be answered whether the likelihood of such a rapid loss of generation, and consequently reactive power support, outweighs the benefits gained by operating in voltage control mode. The 6% spike would not have occured if the voltage control mode was constrained to $0.9875^{\pm}$ so the likelihood of such a loss of DG occuring at peak output must be balanced with the reduction in tap operation due to the greater range of control of the PV at $0.95^{\pm}$.

6.3.5 Increased prevalence of PV mode generators

Each feeder has three points of connection for generation. Generation connected to the LV side of primary transformers by a negligible impedance has an obvious target voltage that is the target voltage of the transformer AVR. Two scenarios were tested where the DG connected to the LV side of the primary ULTC in each feeder was in PV mode. The reactive power limits were defined by a power factor of ± 0.9875 for one and ± 0.95 for the other. The PQ mode DG was all at a 0.9875 leading power factor.

Figure 6.30 shows the resulting tap cost penalties as a percentage of adjusted revenue, that is the *TotalVoltageCostPenalty* subtracted from the potential revenue. Five curves are plotted to link the results to the previous sections. The top dashed line is the percentage tap cost for the scenario with all DG at a slightly leading, fixed power factor (PQ). The light and dark dot-dash lines are results from simulations in which only the largest generator in each area is in voltage control mode whilst the rest in the area are in the slightly leading PQ mode. The reactive power limits of the PV mode generators are defined by minimum and maximum power factors $0.9875^{\pm}$ and $0.95^{\pm}$ for the light and dark dot-dash lines respectively. The light and dark solid lines are results from this section in which PV mode generation is connected in each feeder again with power factor ranges $0.9875^{\pm}$ and $0.95^{\pm}$ for the light and dark lines respectively.

For each power factor range, the scenarios with PV mode generation connected on each feeder result in a lower tap cost than their respective per area scenarios. The PV generator on each feeder reduces the number of tapping operations on the respective feeder primary ULTCs. In the case of only one PV mode generator per area, the main gain is a reduction of tapping operations of the primary ULTC on which the PV generator is connected as well as smaller reductions in neighbouring feeders due to the smoothing of the voltage on the HV side of their primary ULTCs.

The main contributor to the high tap cost penalty is the GSP in area B as it is penalised for being a single ULTC. The area B GSP (ULTC_{GSP}^{B1}) accounts for 62% rising to 70% of the area A and B tap costs combined, from the DG_{max} scenario to the $DG_{max \cdot 140\%}$. As the PV strategies mainly reduce primary ULTC operation, the reduction in the cost of tap operations

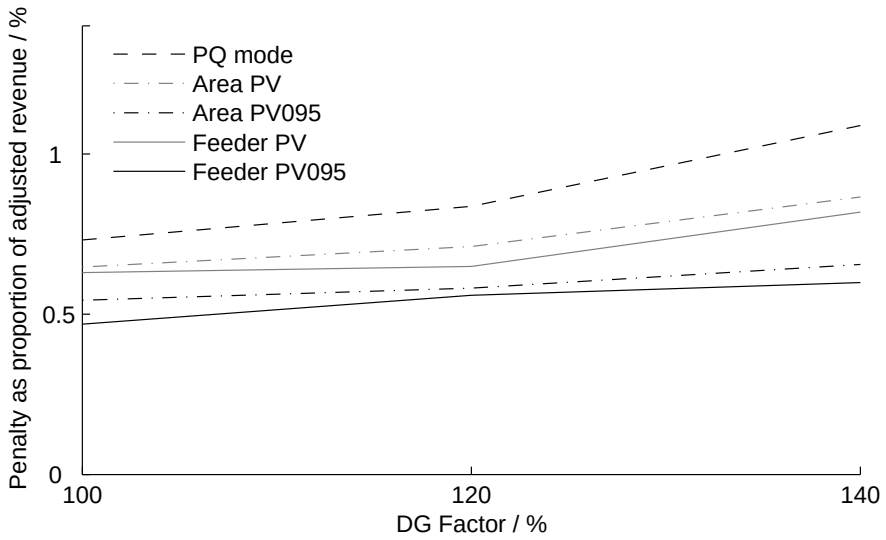

Figure 6.30: *Contribution to penalty as a percentage of revenue for different PV control scenarios.*

is less for area B than in area A due to the high cost of GSP ULTC operations in area B. The reduction is up to 52% in A for the $DG_{max \cdot 140\%}$ case and 38% in B.

The tight reactive power limits on the PV mode generators with power factor $0.9875^{\pm}$ mean that they can never absorb more reactive power than in the PQ scenario with fixed power factor of 0.9875 leading. This scenario then will fare better as a result of the loss of a single generator than when that generator had a greater reactive power range for voltage control but was the sole generator in PV mode. The strategy of a PV generator in each feeder with power factor $0.9875^{\pm}$ exhibits the same 6% voltage spike on loss of generation as in the previous section.

The 6% voltage spike is only seen when the large added generator in area A is suddenly disconnected. The generator comprises 58% of generation in area A. The final strategy shown is to take advantage of the larger reactive power limits on all DG added to the network except for the large generator in A which is constrained to a power factor $0.9875^{\pm}$. The result is a marginal percentage tap cost comparable to the feeder or area strategies with PV generation at $0.95^{\pm}$ power factor as shown in Figure 6.31.

The voltage spike on disconnection of the largest DG in A is less than 1% which is similar

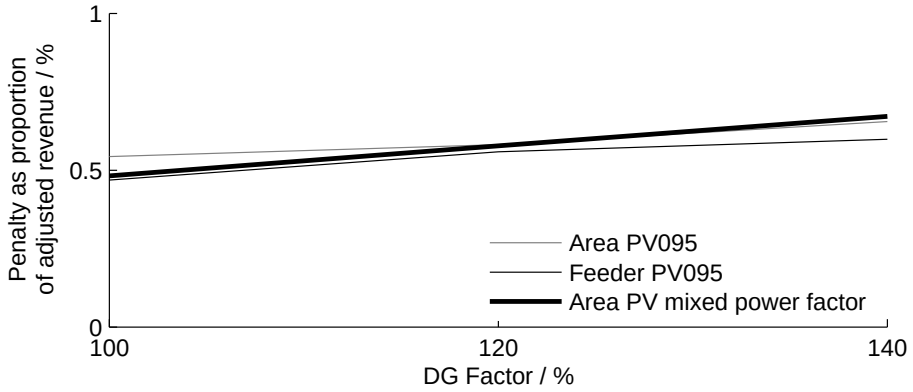

Figure 6.31: *Tap cost percentage of PV mode DG on each feeder with mixed power factor limits is similar to limits of* $0.95^{\pm}$ *for all DG.*

to the PQ mode with the benefit of greatly reduced tap operation of the primary ULTCs and the resultant reduced percentage tap costs as previously indicated. The voltage spikes of the other, smaller, DG in A and B result in small voltage spikes even though they have larger reactive power ranges.

6.4 Summary and discussion.

This chapter demonstrated the effect on ULTC operation of DG connected at a fixed power factor with the real power output controlled by one of two algorithms intended to avoid voltage violations in the feeder. The algorithms make a small improvement to the combined cost penalty incurred but as a result of a lower amount of energy exported, the combined cost penalty as a percentage of revenue is slightly higher.

The introduction of key PV mode generation with the tighter reactive power limits results in a 20% reduction in DGs marginal *TapChangeCost* over the best PQ mode operation for the $DG_{max\cdot 140\%}$ scenario. PV mode generation with the larger reactive power limit results in a 35% reduction in the DGs marginal *TapChangeCost* over the best PQ mode operation. The PV mode generation resulted in a larger voltage step when the PV and PQ modes of operation are compared with a generator outage event occurring at peak output. The PV mode scenario resulted in less overall network and ULTC disturbance other than the short-lived spike and

similarly to the PQ mode did not violate statutory limits.

A more distributed approach to voltage control with more modest reactive power limits results in up to a 25% reduction in marginal *TapChangeCost* over the PQ mode. This approach excels in the loss of generator scenario as the reactive power import or export is not so great that the loss of one generator results in a large voltage step. The distributed approach with larger reactive power limits suffers from the same problem of the voltage step due to the loss of the largest generator. A compromise was demonstrated setting the larger generator to a tighter reactive power limit resulting in a small voltage step on disconnection but an improvement on DG marginal *TapChangeCost* of 35%.

The PQ mode and the mixed limit PV mode tap penalties are shown in Figure 6.32 along with operation and maintenance component of the Distribution Use of System charges applied to generators connecting in the UK after April 2005. The charges were split into three parts, the first and second parts based on the cost of system reinforcement, the third to cover operation and maintenance of the distribution network set at £1 per kW installed capacity. It is the third part which is shown here.

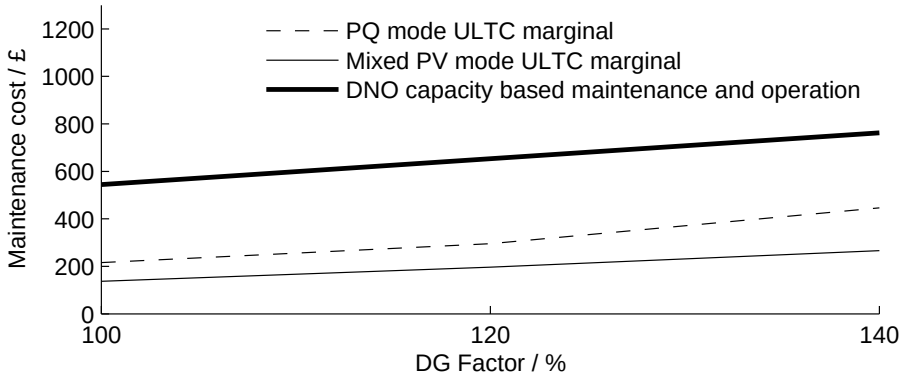

Figure 6.32: *Tap cost of mixed PV mode, PQ mode and the DNO capacity based maintenance charge.*

The DNO maintenance charge was calculated at a time when DG was connected at a fixed power factor. Given the assumption that by examination of the graph, that 50% of the DNO maintenance charge is for transformer maintenance, it can be deduced from the marginal tap cost reduction of 35% that mixed PV mode would save 17.5% of the DNO maintenance

costs. If this saving was passed on directly to the generator, this would mean a yearly charge of 82.5 pence per kW installed capacity instead of £1. In addition, the system reinforcement requirements may be less depending on the case. The PV control method will reduce the need for reinforcement for reasons of voltage control and voltage rise due to connected DG. The method will not reduce the need for reinforcement where the MVA rating of connecting transformers and lines are the limiting factor nor the need to ensure all protection is suited to the bi-directional power flow associated with the connection of large amounts of DG.

Chapter 7
Discussion of Results and Conclusions

This study was motivated by the desire to increase the economic and technical feasibility of the connection of DG in the distribution network. Two recent projects conducted at the University of Edinburgh provided direction to the study. The first project used optimal power flow techniques to study the maximum connection of generation in an example rural network, the second designed and modelled a novel reactive power controller for a distributed generator to maximise the capacity that could be connected to existing networks without detriment to voltage quality. The first project examined steady state network power flow whilst the second used dynamic network and generator models. This study demonstrated a technique using multiple steady-state power flow calculations to simulate a time-varying network model with custom scripts to control time-dependent network components, in this case under-load tap-changing transformers (ULTCs). Through the simulation of a number of network scenarios which were based on the first study, a number of generator control methods inspired by the second study were evaluated with attention to the effect on network voltages and to the change in frequency of ULTC operations. Evaluation functions were developed and used to evaluate network-wide control strategies, penalising bus voltage excursion and ULTC operation. The result showed that a reduction in system costs can be achieved using a strategy that requires some generators to be in voltage control mode.

7.1 Chapter summary

Chapter 1 stated the motivation behind the project: the increased demand for connection of DG and the desirability of minimising the cost of connection. The project objective was thus to maximise connection of DG using existing network equipment and lines. The increased operation and hence maintenance costs of the ULTC was stated as one factor that limits the acceptability of connection of generation at the distribution level. The thesis of this work

was that simple methods exist to reduce the maintenance costs of the ULTC resulting from increased DG.

Chapter 2 described in more detail the operation of the distribution network and the requirements of Distribution Network Operators. It was stated that increased connection of DG is possible with expensive network upgrades but that other methods also allow satisfactory connection of DG without upgrades. The ULTC and its control methods were described in more detail so that its operation could be modelled and evaluated.

A description of the simulation of ULTC operation over time in a rural network was given in Chapter 3. The method applied a power-flow solver repeatedly on a network case with external code updating the network model between solutions. This resulted in time series of ULTC tap position and network flows and voltages. The ULTC control algorithm was defined as well as an evaluation formula that was applied to the results after completion of each simulation.

The ULTC control method was verified in Chapter 4 by its application to a rural network. The response of the network and the ULTCs was observed in response to time-varying load and later also time-varying generation. Control parameters of the ULTC were varied to illuminate the working of the control algorithm and to show that existing settings are reasonable. The evaluation function described in Chapter 3 was demonstrated as a way of obtaining improved parameters for the ULTC control algorithm.

Chapter 5 listed the various connection topologies for generation and demonstrated network operation for a number of them. High penetration of DG was simulated and the connection points and operating parameters demonstrated further. The connection of DG in a fixed power factor (PQ) mode was evaluated including the observation of the network, in particular voltage step changes, in response to the sudden loss of generation.

Chapter 6 applied two real power curtailment algorithms to the scenarios of chapter 5 in an attempt to improve the cost penalties used to evaluate the system cost of increased generation. Finally, DG was connected in voltage control (PV) mode. Extensive simulations were carried out comparing the system cost of PV mode generation with the best PQ setup. PV control was shown to be an improvement on the PQ mode when distributed through the distribution

network.

This chapter describes the content of the thesis; the extent to which it answers the thesis statement; the contribution to knowledge and further study that is required.

7.2 The strengths and limitations of the approach

This study simulated a typical distribution network over a time-scale much longer than a typical dynamic study but with the sufficient modelling of time-dependent components such as load, generation and ULTC operation. PSSE, an industry standard power flow solver, was chosen for speed of implementation and for confidence in the results. The main limitation of this approach is the lack of detail in the generator AVR model and thus the inability of the approach to show the operation of the AVRs over suitable time-scales. Although the approach cannot demonstrate dynamic adjustment of the system to a large step in power output from a generator, it will indicate the best state the system can be in given the change in power flow and current tap positions of the ULTCs. The delay used in the ULTC control algorithm is an order of magnitude larger than the time taken for a generator AVR to settle following a large step in output power. The time-step chosen is larger than the AVR settling time but smaller than the ULTC delay used in the ULTC control algorithm. Thus the generator AVRs are assumed to have settled between time-steps . For these reasons the method is sufficient for the analysis of the ULTC interactions with generator AVRs and with each other.

The simulation approach allows custom code to be written to model any component of the network. Code was written to model ULTC operation as well as to update generator and load data according to input data files. The method also allowed the manipulation of parameters, such as generator reactive power limits, at run-time as opposed to requiring adjustment of the original input network data file. The changes made are saved as part of the simulation management script on completion of the simulation.

The custom code maintained a copy of relevant network parameters using an object-oriented style of programming with an instance of a network component for each component loaded into PSSE that is either manipulated or controlled by external code or needs to be monitored

by the external code. This means that there is much replication of network data in that it exists in PSSE itself and in the custom code. This did not cause computer memory problems with the number of buses in the order of tens or hundreds but could be a disadvantage with larger networks and more complex custom models. The replication reduces the number of calls to the PSSE API, speeding up the simulation process. The classes written to define network components can be included in and extended by other classes allowing more complex control rules and interactions as required for future work.

The ULTC model used throughout this study is sufficiently detailed to indicate the effect of power fluctuations on tap operation frequency. However, the use of the time-step of five seconds masks the inaccuracy of the analogue timing circuits used in most existing transformer AVCs. The situation that the simulation may fail to model is when two nearby ULTCs operate at the same time-step. In reality one may operate first and the resulting reactive power flow changes would then affect the control rule of the other. As a tap change takes a number of seconds however, the effect of the tap change in reality might not be observable for a number of seconds after the AVC has made a tap change decision by which time the hypothetical nearby ULTC AVC has also made its decision. In this sense then, the five second period is sufficient to indicate the frequency of operation of ULTCs.

The construction of the evaluation function used to indicate increased system costs of additional DG relies on a number of assumptions. The base cost of a tapping operation is calculated as a function of expected operations between maintenance intervals and from an estimate of maintenance costs. Both of these values will vary depending on operational practices and the size and model of transformer installed. The ULTCs in this study were on transformers whose capacity was between 5MVA and 60MVA and a varied number of total tap positions from 17 to 49. The other component of a tap cost operation is the assumed loss of revenue during transformer maintenance. DG is assumed to be ordered to disconnect during transformer maintenance of the feeder which connects it to the transmission network where only a single transformer provides the connection. The loss of revenue included in the tap cost is based on the generator operating at capacity for the duration of the maintenance but in reality this may be much lower with a typical capacity factor for wind of 30% for example. The final figures for system cost savings are thus only indications but the evaluation function

is still useful for comparison between different strategies. Lastly, the mean tap cost assumes that the rate of degradation of the transformer and contacts is independent of the frequency of operation and of the transformer loading at the moment of operation.

It was decided to obtain real data of a frequency suited to testing the sensitivity of ULTCs to realistically rapid power fluctuations. The source was a wind farm of capacity 18 MW which experienced a maximum power output of 15 MW over the period sampled. The power output is the sum of the output of up to six wind turbines. The output power of the generators in the study varied from 0.2 MW to 40 MW in the case of the largest generator in area A as shown in Figure 7.1 The smaller generators would exhibit more rapid power

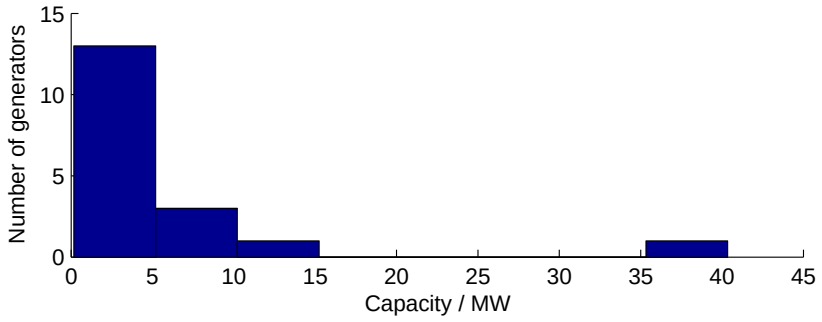

Figure 7.1: *Histogram of DG maximum output in the DG_{max} scenario.*

fluctuations than the source as they would be comprised either of smaller machines with a lower angular momentum that smooths out rapid wind fluctuations or of a farm with fewer machines. The larger generator would be made up of more machines which would have the effect of smoothing the short-term fluctuations of the power output. With regard to the smaller generators, the simulation thus under-estimates the increase in tapping operations due to short-term fluctuations. On the other hand, as the DG outputs are synchronised instead of varying geographically, this over-exaggerates tap operation. The single larger generator than the source data would be expected to exhibit slightly less short-term output power fluctuations, which again would over-exaggerate tapping operations.

7.3 Addressing the thesis

This study has demonstrated that the operating costs of distribution network equipment in terms of transformer maintenance increases with the connection of DG. It was shown, however, that this increase is a small percentage of the revenue from exported energy, before taking into account incentives for renewable generation. The fear of high costs resulting from ULTC interaction and competition was seen to be unfounded in all of the cases shown. Given the capital cost and maintenance cost of transformers according to the Scottish DNOs SP and SSE, it would be economically efficient to use existing equipment wherever possible, even if it means much shorter maintenance intervals for automatic tap-changing equipment.

The operation of selected DG in voltage control mode was shown to be preferable to constant power factor mode. The voltage control mode did not cause conflict with transformer tap-changer operation. Operation of a large generator with a wide reactive power capability in PV mode did result in some dependency on the DG for voltage control. The loss of such large plant could result in a voltage step or spike at the limit of G75/1 recommendations. The probability of such a loss of generation may be small enough such that the benefits of increased voltage control outweighs the negative impact of a large voltage step to voltage regulation.

A strategy of assigning only limited reactive power ranges to the larger generator removed the problem of the voltage step. With the PV mode plant distributed throughout the network, this strategy also improved on the increased cost associated with connecting the generation in constant power factor mode by 35% in terms of marginal ULTC maintenance costs.

A novel method of simulating the operation of ULTCs over time has been demonstrated. It benefits from the ability to apply alternative control algorithms for ULTCs and generators. The algorithms are independent of proprietary scripting languages but were implemented in Python, an open source, object-oriented and complete programming language. The complexity of such algorithms are limited only by the computational power of the machine on which the simulation is run. For example a module was written that allows the simulation of the communication of short messages between ULTC and generation controllers. The module allowed for the variation in reliability and speed of the communication medium. Another

module allows the creation of control rules in fuzzy logic. This technique has the advantage that a number of potentially conflicting goals and data sources, such as the requirement to control local voltage and to respond to a communication, can be combined to provide a decision.

7.4 Impacts of the study

The study has demonstrated that the increased transformer maintenance costs associated with additional generation connected in the distribution network are small compared to the revenue generated and the cost of network upgrades often associated with new generation. The increased cost in terms of transformer maintenance in the scenarios shown are in Table 7.1 to be of the order of £100 a day for the distributed PV method. This amounts to £36,500 increased maintenance per year for the connection of 100 to 140 MW capacity of wind generation. It is a small amount when compared to the cost of a single grid transformer (£0.5 to 1.0 million with £56,000 yearly charges to the former [44, 45]) and the cost and planning difficulties associated with longer lines. Note, however, that the *TapChangeCost* is based on 2003 estimates whereas the SP and SSE charges are 2007.

	DG_{max} £	$DG_{max} \cdot 120\%$ £	$DG_{max} \cdot 140\%$ £
PQ unity	401	518	643
PQ 0.9875 leading	251	330	482
PV mixed	188	251	328

Table 7.1: TapChangeCost *for different DG capacity and connection strategies over two days.*

The total *TapChangeCost* over the two different days of operation can be compared between the PV strategy and the PQ strategy. The *TapChangeCost* for the PV strategy with $DG_{max} \cdot 120\%$ is the same as the *TapChangeCost* for DG_{max} connected in PQ mode with a slightly leading power factor. In other words, for the same maintenance costs, 20% more DG can be connected in the PV mode than the PQ mode. Compared to connecting DG_{max} in PQ mode at unity power factor, the PV strategy results in a lower *TapChangeCost* for an additional 40%

of capacity. No more than 40% was evaluated as this resulted in the GSP ULTCs exceeding 150% of their MVA rating.

Increased transformer maintenance can be a barrier to the connection of more DG. With greater knowledge of the effect of DG on ULTC operation, the additional maintenance costs can be estimated and apportioned appropriately. Transformers that are liable to suffer greatly increased ULTC operation as a result of DG can be identified. The role of such transformers can then be supported by upgrading the transformer, requiring increased voltage control from DG or limiting the connection of highly variable DG as appropriate.

Greater capacity for the connection of plant using existing transformers was demonstrated allowing higher levels of renewable generation and geographically dependent plant such as combined heat and power plant. Increased ULTC maintenance can be minimised by enabling DG to operate in voltage control mode with strict power factor limits. The narrow power factor range required for beneficial voltage control from DG minimises the cost for asynchronous generators such as Doubly-Fed Induction Generators as it minimises the rating of the power electronic converters used. The narrow power factor range recommended in this study for PV DG and the slightly leading power factor PQ mode also limits the voltage step experienced on the feeder should the DG be suddenly disconnected, for example due to a fault. This allows a greater capacity of DG to be connected for a given maximum acceptable voltage step if these recommendations are followed as opposed to connection at a fixed unity power factor.

The study considers a small part of a paradigm of active management of the distribution network. The paradigm sees greater control of components of the distribution network to bring about more flexible voltage and frequency control to both accommodate new load and generation and to maximise the use of existing equipment. The paradigm is often associated with large amounts of communication between the controlling components. This thesis demonstrates a method that at its simplest does not require additional communication equipment.

7.5 Suggestions for further work

A disadvantage of using a wide power factor range for generators in PV mode was shown to be the risk of voltage steps due to loss of generation. Greater proportionate reactive power limits for generators whilst operating below nominal capacity could be allowed. These would maximise the voltage regulating ability of the generator at lower real power outputs, without the associated risk of large voltage steps present when operating generation close to capacity.

The risk of voltage steps due to sudden loss of DG could also be reduced by coordination of voltage control between the PV mode generator and the ULTC controller as discussed in section 2.3.5. Such coordination would allow the ULTC to perform larger voltage adjustments with the DG AVR performing smaller ones. In this way the DG can be operated within tighter reactive power limits such that a sudden change in available power and hence reactive power control does not lead to excessive voltage steps. The greater reactive capability could be limited to certain circumstances such as large changes in available power or according to instructions from some form of hierarchical control system of the distribution network. This method is an ideal step towards more flexible distribution network management as communication is only required between the generating plant and the transformer substation. The communication requirements themselves are likely not to require continual data to central controllers and need no dedicated data connections. Messages might be sent by a generator AVR agent to the ULTC control agent for example, indicating when a generator AVR changes from being well within reactive power limits to being close to a reactive power limit. As shown in Figure 6.25, this occurs only a few times daily requiring only a few simple messages to a single pre-determined recipient.

A curtailment algorithm was demonstrated that sensed the voltage at the point of connection and limited reactive power accordingly. The simulation method used could be easily extended to model remote bus voltage measurement and the creation corresponding algorithms for generation curtailment and target voltage where appropriate.

A major limitation to the export of power from variable generation is a function of the thermal rating of the lines and transformer connecting it to the higher voltage network, and the local load. An extension of the ULTC and DG coordination strategy is for the ULTC

to communicate according to its loading and operating temperature. In this way, larger capacities of DG can be connected with the condition that they can be curtailed according to network conditions, local load and neighbouring generating plant. The efficacy of such a method can be evaluated by the addition of a time-dependent thermal model of lines and transformers.

7.6 Thesis Conclusion

A novel method has been demonstrated to model the operation of ULTCs subject to time varying network power flows. An evaluation function has been constructed that can be used to compare different distribution network operating strategies and DG penetration levels in terms of ULTC maintenance costs. The strategy of allowing automatic voltage control by the larger generators in the distribution network results in lower maintenance costs than requiring DG to be in constant power factor mode.

Appendix A
Detail of the implementation of the simulation model using PSSE and Python.

Power System Simulator^{TM}for Engineering (PSSE) is a commercial power flow package. PSSE is capable of maintaining a network case with line and equipment properties, transformer ratios and load and generation as required.

The network case is created by PSSE from a network definition file. It has a number of formats for saving and loading network models. The one used in this study is one of the three *.raw* formats discussed further in section A.1. The *.raw* format uses whitespace, integer and decimal numbers and a few keywords to define a network model. As such the file is *human readable* and can be modified in a text editor as required. Some user defined code uses the data in the *.raw* file to build up the parts of the simulation external to PSSE that are described below.

A.0.1 Power flow automation

As described above, a power flow solution is repeatedly obtained from a network model. Before each solution is made, control actions from previous time-steps and load and generation values for the current time-step are reflected in the network model.

To simulate tap-changer operation over a period of one day requires 17280 completions of the observe-update-solve cycle. It would thus be infeasible to perform these cycles by manual operation of the load flow software.

The package provides an Application Programming Interface (API) which enables the user to load, observe and modify the model maintained in PSSE using code written in Python. The API also allows the code to initiate power flow solutions. It is this API that allows the simulation to encapsulate the network model in such a way as to allow the PSSE load flow

solvers to operate on network cases repeatedly modified by outside code according to the scenario. Note the distinction between the *simulation* and PSSE; PSSE is always referred to as PSSE; the *simulation* is the combination of PSSE and the external code that *drives* PSSE according to the input data and any custom device models.

Load and generation scenarios for a day or days are created in advance and along with fixed network parameters. The data is then batch processed by the simulator. User created scripts perform the following functions that are necessary for the observe-update-solve cycle as summarised in Figure A.1. The pseudocode for a 1 day simulation at 5 second intervals for a single scenario is as follows:

1. Load network data such as branch impedances, loads and generation into the simulator.
2. Solve the network in its present form and ensure convergence.
3. For time = 1 to 17280
    - Observe the solved network.
    - Update network data:
        - According to load and generation time series.
        - According to controller actions.
    - Solve the network using iterative solver and ensure convergence.
4. Exit simulator.

PSSE is capable of providing a solution to the network data in which ULTC winding ratios are set to minimise deviation of bus voltages from their targets. This solution, however, omits the real-time characteristic of all automatic tap-changers. The most important characteristics are the delay between observing a condition that it should act to change and actually acting. This includes any artificial delays used by real transformer controllers. It also ignores that adjustment of tap-position is sequential and usually only reflects local measurements. A real network does not suddenly alter the tap-position of all transformers in an instant.

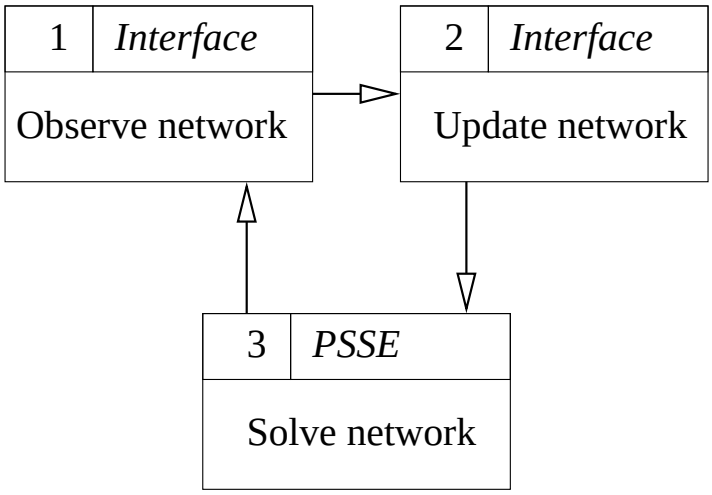

Figure A.1: *Flow of control in the observe-modify-solve cycle.*

The delay is implemented in the custom ULTC model, described further in section A.2, in order that the ULTC does not operate too frequently as discussed in chapter 2. Solution of the network is achieved with the tap ratios fixed according to the network model at each time-step. Operation of the taps is simulated during the observe-update part of the cycle according to algorithms implemented in Python. The algorithm is supplied relevant network details on which to base its operation. The algorithm determines what ratio the tap-changer is set to for the next time-step. The ratio is set during the update part of the cycle. The network is then solved with these ratios fixed at the new values.

The interface to PSSE thus allows any algorithm to be implemented to control tap-changer action. There are physical constraints such as finite tap ratios and non-zero time for a tap change. The operation of the tap-changer according to these physical constraints on the device is the responsibility of the algorithm or script interfacing with PSSE.

Automation scripts are written in Python, an object-oriented programming language. PSSE can be set to run these scripts, providing an Application Programming Interface (API) with which to modify the network case and run load flow solutions as required. These scripts are responsible for performing a simulation run according to the many possible initialisation parameters such as:

- Network definition file.
- Load profile.
- Generator schedule.
- Generator controller parameters and methods.
- Individual ULTC controller parameters and methods.
- Data to be stored at each time-step for later analysis.

The scripts must also execute the additional tasks every time-step as in Figure A.2. The tasks shown are saving data at each time-step for later analysis and executing the control algorithms. For simplicity of interaction, all code external to PSSE, including implementation of the control algorithms, was written in Python for this project.

The object-orientated nature of Python allows the implementations of controllers to be extensible; for distinct controllers to have access to limited input data and to allow a simulation setup to be copied and re-used with minor modifications as required.

A.1 Python and the PSSE API

The API is made available by PSSE to the programmer as an object. A software object is a collection of functions and variables which may themselves be objects. The API is implemented in Python, an object-oriented programming language.

The PSSE API is organised as a collection of functions [78]. There are a number of types of function used in this study. Most functions either modify a network value or PSSE parameter, or return a network value or PSSE parameter value. Other functions request that PSSE performs a calculation such as the load flow solution.

The functions all belong to the API object called “psspy”. According to Python programming syntax, calling a function contained in an object is performed as follows:

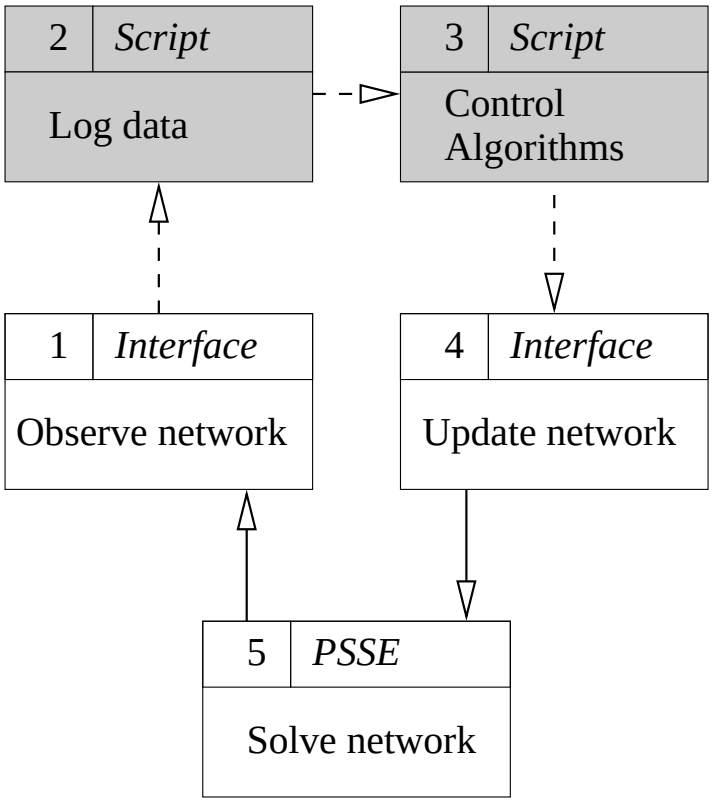

Figure A.2: *The flow of control in the observe-modify-solve cycle with script activities.*

```
returnValue = psspy.functionName(parameters)
```

where `returnValue` stores the value or values returned from the call and `functionName(...)` is the name of the desired function with the required zero or more parameters supplied in `parameters`.

The current network data loaded into PSSE is called the "current case". The current case is divided into different network component types. Each component type is divided into rows, one for each component. This structure maps to the structure of PSSE network definition files. Each row of the definition file is a separate network component except transformers which use 3 or 4 rows for their definition. The rows are grouped in the file according to the component type.

An extract from a *.raw* file, the network definition file format used in this study, is shown in Figure A.3.

Note that each component definition starts with a reference to one or more bus numbers that define(s) its position. The file is edited with removed rows signified by "...".

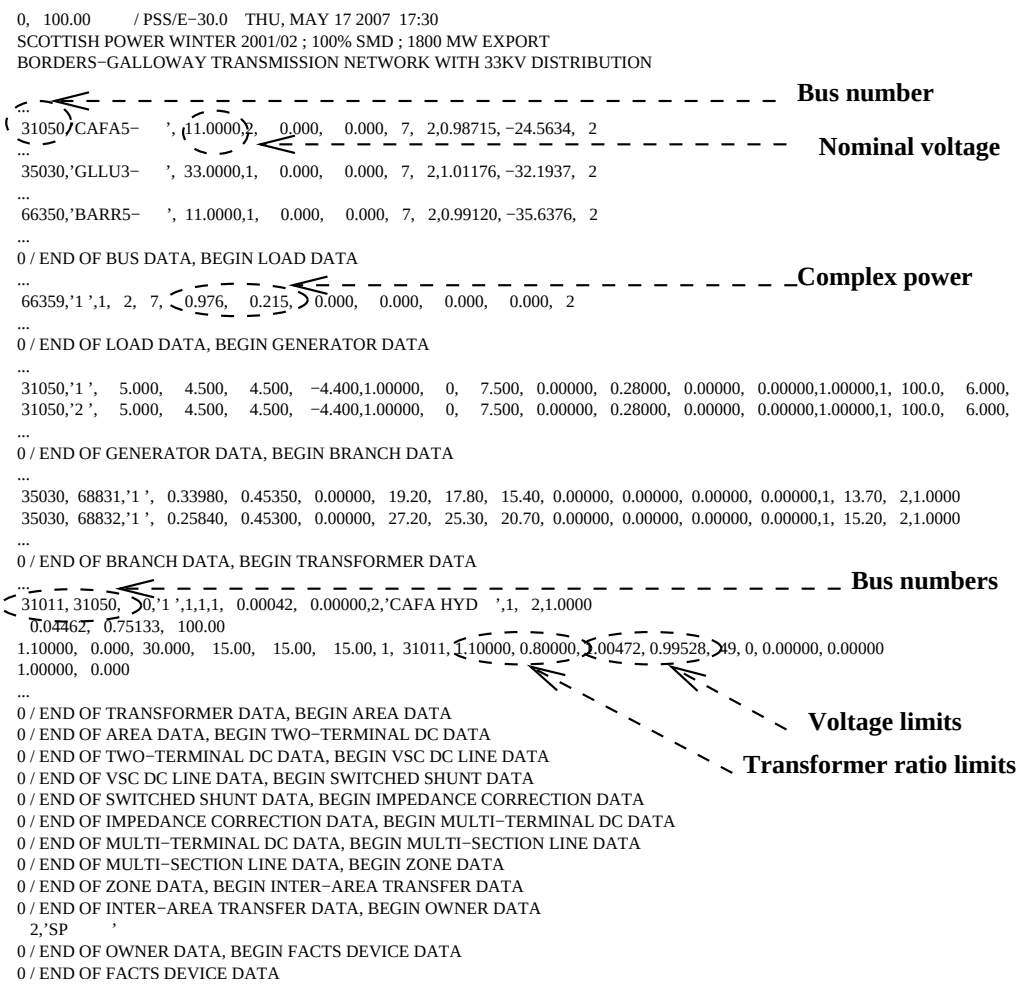

Figure A.3: *Raw file.*

In addition to groups of values mapping to network components there are groups of values that describe collections of other network components. Each row or item in the "Plants" collection object defines the properties of all generators at each bus. For example each generator is be given the same voltage set point by specifying it in the "Plants" collection. The "Plants" collection is accessed using the `psspy` method `plant_data`.

A.1.1 Set functions

The set functions refer either to network values or calculation parameters. A distinct function is provided for each network component type such as `bus_data(...)` for setting the parameters of existing buses and `load_data(...)` for setting the parameters of any loads connected to the buses.

When modifying or setting a value of an existing network component in PSSE, all the parameters for the component must be supplied to the relevant function in one go. To make this a little easier the API accepts a value called the default value signifying that the existing value be used. The supplied default value must match the type of the argument it is being substituted for. PSSE supplies two default values, `_i` for integers and `_f` for floating point numbers. The PSSE documentation clearly states which parameters are of each type.

For example to set the bus type code to `2` for bus `35030` the programmer would use the following syntax:

```
error = psspy.bus_data(35030,
                       [2,_i,_i,_i],
                       [_f,_f,_f,_f,_f],
                        "")
```

where: `error` is an integral error code returned by the API which is equal to zero if no error occurred; `_i` is the default value for integers; `_f` is the default value for floating point values.

A.1.2 Get functions

There are get functions to retrieve the values of network data loaded into PSSE or to retrieve PSSE parameters. Similarly to the set functions, a distinct function is provided for each network component type. For example, `busdat` is the function that gets a parameter of existing buses.

Unlike set functions, the get functions only return one value per call. To retrieve a particular value, the name of that value is passed as a function argument. For example, to retrieve the

base or nominal voltage of a bus the following function call is made:
`error, nominalVoltage = psspy.busdat(busNumber, 'BASE')`.

Functions in Python may return more than one value. The get functions return a collection of values called a tuple. Python syntax allows the assignment of all return values to a variable when it becomes a tuple type. Alternatively, as in the example above, the return values are assigned to two variables, each one being of the type of each value returned assuming there are the same number of return values as assignment variables. In this way both `error` and `nominalVoltage` are modified or instantiated by the "busdat" function call.

A.1.3 Error values

Note that both the get and set type functions return an error value which is an integer. The onus is on the programmer to include code to check its value. The convention for the PSSE API is for a value of zero to mean that the function call was successful. Non-zero values mean different things according to the function. The meaning of the values is provided in the documentation accompanying PSSE [79]. For example, a common error is a "Bus not found" error meaning that the bus number supplied in the function call does not exist in the current case.

The simulation code written for this project ensures all returned error values are always checked and turned into Exceptions as required according to section A.2.7.

A.1.4 Executing user-defined code in PSSE

The simplest method of executing user-defined code is to open the PSSE graphical user interface (GUI) and select "Run Auto" in the command line interface labelled "CLI"[80]. In effect this imports the selected file/module with the API object `psspy` in the scope of the imported module. The module is thus able to assume the existence of an object called `psspy` when called from PSSE. It can then execute the API functions stored in the `psspy` object.

A.2 Organisation of Python simulation and controller code

A simulation of a network over time using the method described in Figures A.1 and 3.2 is termed a simulation run. A simulation run involves repeating the five main stages in addition to any initialisation required at the start and clean-up code required at the end. It is desirable that simulation runs be made with parameters as follows:

- Demand time series.
- Generation time series.
- Network definition files.
- Control algorithm implementation selection and parameters.
- Subset of network data to be recorded at each time-step.

For this reason the simulation code was separated into a distinct main experiment initialisation file containing the specific parameters for the desired run, and other files that are included by the main file containing code usable by any setup file.

Taking advantage of the object-oriented paradigm adopted by Python, most of the reusable code created for the simulation is packaged into classes. A class is simply a collection of code that defines objects that are created at runtime like the "psspy" object that contains the PSSE API functions. The object can then be used to perform the required tasks. The property of class inheritance has been used to advantage where appropriate. This allowed the re-use of code common to all classes.

The classes fall into areas of responsibility with the `Class` names of those classes as listed below. Nesting of class names indicates inheritance which allows the child class to inherit code written for the parent class.

- Providing a simple method of maintaining network component values.
  - `PSSE_Bus`

  - `PSSE_Branch`
  - `PSSE_Files`

- Performing and initialising current run.
  - `Simulation_Run`
  - `Simulation_Iteration`
  - `PSSE_LoadFlow`

- Storing run data at each time-step.
  - `Files`

- Implementing ULTC control algorithms.
  - `Agents`
    - `VoltageRegulator`
    - `CalovicVoltageRegulator`
    - `CommAgent`
      - `FuzzyAgent`
  - `Fuzzy`
  - `Communicator`
  - `Multicaster`

In addition the following classes provide functionality used by the simulation classes:

- `Exceptions` provides improved error handling
- `Useful` implements essential mathematical functions such as interpolation

The data flow between key classes, PSSE and the input and results files are shown in Figure A.4.

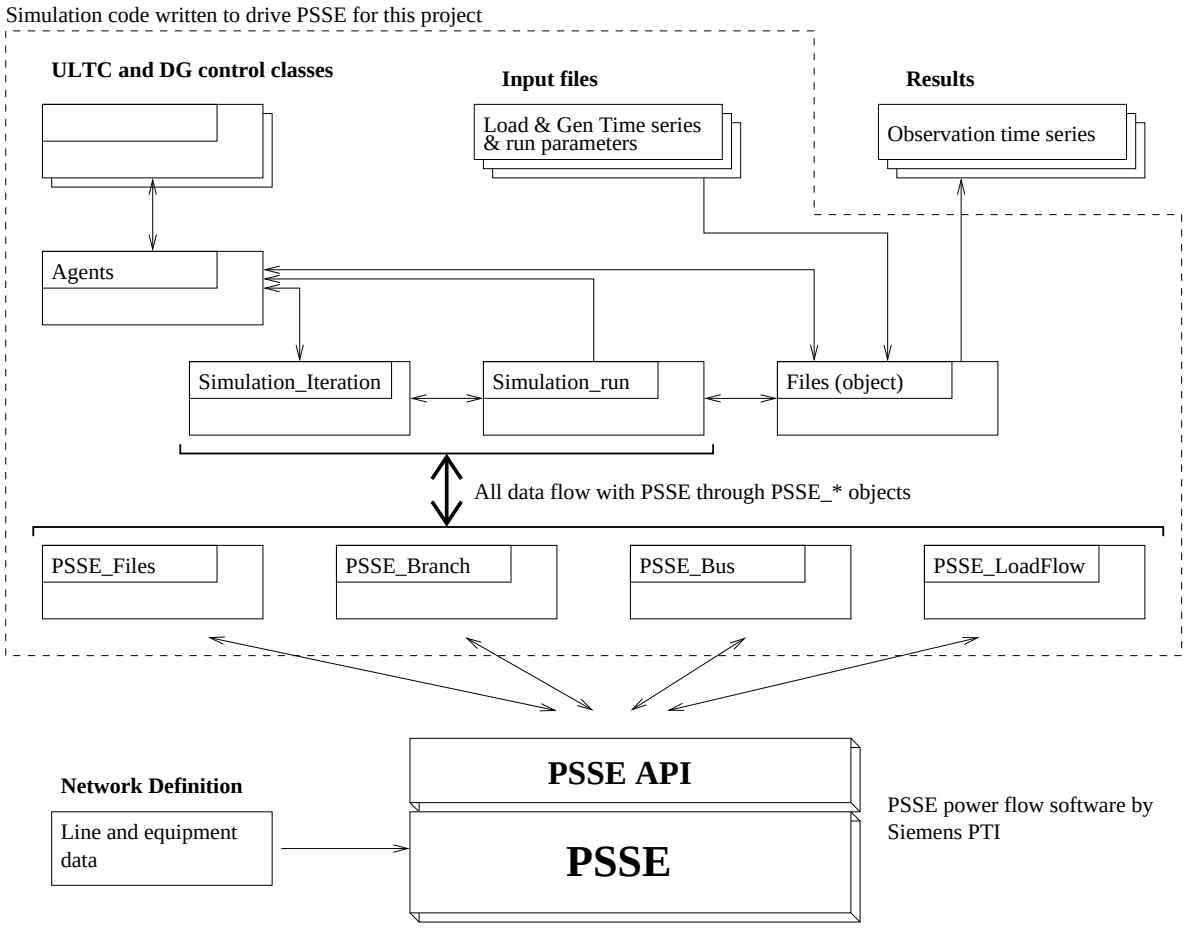

Figure A.4: *Diagram showing interactions within and between custom Python objects and PSSE.*

A.2.1 Providing a simple method of maintaining network component values

During a single time-step of the simulation, it is possible that a parameter of a network component is used several times. To minimise API function calls it is desirable to store the result of a single call for repeated use. In addition, the primitive error reporting method used in the API requires a call to check the error message after each API call.

To simplify algorithm implementation it was appropriate to take advantage of the object-oriented paradigm of Python and the associated error handling using “Exceptions”.

For every network element in the study that is to be monitored or modified at each time-step, an object is created. At each time-step the object ensures it reflects the same values as the PSSE element. It also modifies PSSE elements according to input time series and agent decisions. The error value returned by each API function call is checked and handled appropriately as discussed in section A.2.7

The `Bus` and `Branch` objects are used to illustrate the above points. The `Bus` object is required to update its voltage at each time-step. All network elements are referenced by either one or two bus numbers. The `Branch` elements are referenced by the start and end bus numbers of the each line. A `Branch` object contains a reference to the relevant two `Bus` objects. The voltage at the busbars at each end of the line is found by following the reference to each `Bus` object in the `Branch` object and looking up the stored value found there.

In addition to objects containing references to other objects, the use of hierarchy further justifies the object paradigm. For example the `Transformer` class extends the `Branch` class. Thus when a `Transformer` object is created, the same method is used to fetch its terminal voltages as for the `Branch`. The `Transformer` class in addition provides functionality to get and set the transformer tap ratio as appropriate.

All elements referenced by one bus number such as `Load` and `Machine` contain an instance of the `Bus` class. This is illustrated in Figure A.5. To check the voltage in a `Load` object, the `getVoltage` method of the `Bus` object is called. For example `v = myLoad.bus.getVoltage()`.

All elements referenced by two bus numbers such as `Transformer` extend the `Branch` class. This is illustrated in Figure A.6. An example usage of such inheritance is that to examine the voltage of a bus in a `Transformer` object, the following syntax is used: `v = myTransformer.bus1.getVoltage()`. A `Transformer` object inherits `bus1` and `bus2` from the `Branch` class definition.

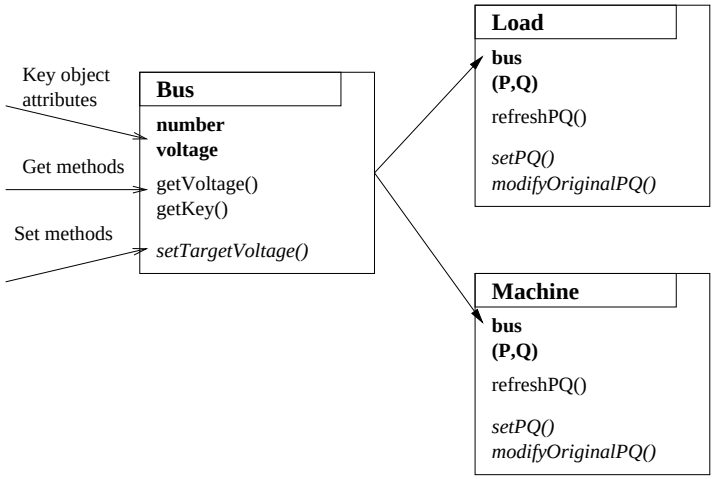

Figure A.5: *Class structure and important access methods of "single bus" objects.*

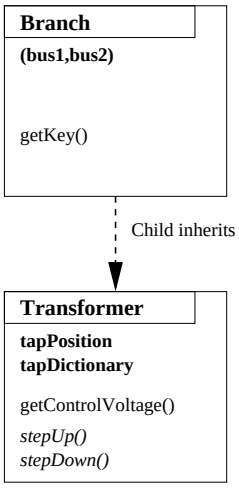

Figure A.6: *Class hierarchy and important access methods of "two bus" objects.*

A.2.2 Performing and initialising current run

The module SimulationRun contains the class definition `SimulationRun`. It takes amongst others the following initialisation arguments:

- The `psspy` object supplied by PSSE.
- The bus numbers of various network elements observed and controlled during each time-step.

- The type of controllers used for different network elements.
- The objects used to store results.

On initialisation the object builds all the required objects for the simulation. Each `PSSE*` object is supplied a pointer to the `psspy` object so that PSSE API function calls can be performed as required. A loop is then executed that repeatedly performs a time-step cycle using the object created by the `SimulationIteration` class definition.

Care was taken to handle exceptions as discussed in section A.2.7. Multiple `SimulationRun` objects may be created, one following the other on completion of a cycle for each time-step. If one run fails the simulation continues with the next one.

The `nextIteration` method of the `SimulationIteration` object is repeatedly called with the time passed since the previous time-step as its argument. `SimulationIteration` ensures the following:

1. Load demand and generator real power are set from the input time series for this time-step.
2. The resulting network is solved using the required PSSE solver via the `PSSE_LoadFlow` module.
3. PSSE solver output to the command window is suppressed during normal operation.

The module `PSSE_LoadFlow` contains methods requesting that PSSE solves the current case.

The `Transformer` objects are initialised in `SimulationRun` so that they reflect the starting positions of the ULTCs.

After initialisation, tap-position changes are only initiated by the ULTC controller for each transformer as described in the second observe-modify-solve cycle illustrated by Figure 3.2 in section A.0.1. The load flow solution is thus obtained with the tap positions fixed so that PSSE does not itself adjust any transformer ratios during the load-flow solution of the network.

The method written to achieve this is `solveFixed` which sets PSSE solver parameters as descibed in section A.2.3.

A.2.3 Network solution parameters

There are other parameters than the tap-fixing option, that determine the performance of the load flow methods. The crucial parameters are acceleration factors and the maximum number of solver iterations.

In general, a larger network requires more solver iterations for the solver to converge on a satisfactory solution. A large network, in particular if voltages differ greatly from nominal, requires slow acceleration factors to converge at all.

To avoid always using small acceleration factors and a large number of solver iterations, the `solveFixed` method first tries near default acceleration factors (*ACCP*, *ACCQ* and *ACCM*) and the number of solver iterations (*ITMX*) is limited to 300. Should the solver have failed to converge two further attempts are made with different parameters as shown by table A.1.

Attempt	ACCP	ACCQ	ACCM	ITMX
1	1.0	1.0	1.0	300
2	0.06	0.06	0.06	2000
3	0.01	0.01	0.01	3000

Table A.1: *Gauss-Seidel solution method parameters*

Should the solver fail at attempt 3 the simulation process exits.

A.2.4 Storing run data at each time-step

The most important class definition in the `Files` module is the `DirectoryStore` class. The `DirectoryStore` object ensures a directory exists for saving data to numerous files. It is initialised with an indicator of each object it is required to save data from in a particular directory. In addition, it is initialised with the required variable names of each object that

should be stored. The variable names are supplied as a list of strings matching the variable in the object.

Files for each object-value pair are created separately in above directory. The filename is derived from the object method `key()` defined for this type of purpose. The function `key()` returns a string containing the defining bus number or numbers as well as other information as appropriate.

For example a `DirectoryStore` object could be created for a number of lines needing real and reactive power flows recorded. The object would create a directory `Lines` in the results folder and inside that a number of files. The list of variable names supplied to the object would be `['P', 'Q']`. The directory structure created would look like this:

- `ResultsFolder`
  - `Lines`
    - `P_BusA_BusB_1.dat`
    - `P_BusA_BusC_1.dat`
    - `P_BusA_BusC_2.dat`
    - `Q_BusA_BusB_1.dat`
    - `Q_BusA_BusC_1.dat`
    - `Q_BusA_BusC_2.dat`

The required values are stored at each time-step by calling the `appendMembers()` method which does not itself require arguments. Each value is appended to its respective file as a new line. Multiple columns are created where the value appended is a complex number. Floating point numbers are stored to 5 decimal places.

For a simulation run with 17280 time-steps, each `.dat` file would contain 17280 lines. These files can then be imported easily into graphing packages. In this study MATLAB was used.

A simulation may result in millions of disk writes. This is made feasible by the sufficient cacheing of the disk-write operations performed by the built-in Python `write()` function found in the `os` module.

A.2.5 Implementing ULTC control algorithms

A general class `Agent` in module `Agents` is tasked with holding the reference to the object the agent is to control, called the device. The `Agent` object also ensures that that device reflects the current case in the method `act()`. The `act()` method is intended to be called at each time-step and includes any code that that `Agent` should execute each time-step.

The algorithms for two different types of ULTC controller are described in section 3.4. The class definitions `VoltageRegulator` and `CalovicVoltageRegulator` both extend the `Agent` class. Both classes define the method `act()` which first calls the `Agent` method `act()` and then follows class specific code. Both classes maintain a record of the time passed since the last tap operation and use this with the control voltage of the associated device to make the next tap decision. The tap decision is acted upon by a call to the `tapUp()` or `tapDown()` methods of the associated `Transformer` object as required.

A.2.6 Implementing generator control modes

The generator control modes, *PQ* and *PV* are implemented by the creation of an object for each generator of the classes `PQMachine` and `Machine` respectively. Both objects allow the modification of real power output.

`PQMachine` references a `Bus` object and creates a new `Load` object for the bus. A constant power factor mode machine is not available in PSSE. The `PQMachine` acts by controlling the load on the referenced bus except that the complex power value for the load supplied to PSSE is negative that of the required generation. The power factor of the machine can be specified at initialisation or be supplied each time the real power output is specified.

`Machine` references a `Bus` object and manipulates any machines connected to the reference bus in PSSE. The machine reactive power output is determined by the PSSE power flow solver according to the target voltage and reactive power limits. The `Machine` object can be used to alter the target voltage, reactive power limits and its real power output.

A.2.7 Additional module: Exceptions

Exceptions are an important part of many modern programming languages. Exceptions are "raised" when certain errors occur. Rather than explicitly store the error or success message from a function call, it can be caught by an "except" clause.

The function call must have been in the body of a corresponding "try" clause. Once the exception is caught in the "except" clause, the programmer may require the program to perform any task including exiting the program or raising further exceptions. If the function call was not inside a "try" clause, or if a further exception is raised in the "except" clause, more distant enclosing "try" clauses are sought. Should the exception occur with no enclosing "try" clause then the exception terminates the program with a detailed message of where the exception occurred.

Python provides a class for the exception object called `Exception`. It also provides other classes that extend `Exception` that signify particular errors. For example a `KeyError` exception is thrown when there is an attempt to access a indexed data-structure with a non-existent key.

The following code illustrates the use of "try" and "except":

```
try:

...

  try:
    #attempt to create a new directory
    os.mkdir(resultsDir)
  except OSError,(code,message):
    #if OSError code is not 17 then raise the OSError again
    if code != 17:
      raise OSError(code,message)
    #if OSError code is 17 then directory exists so do nothing
```

```
...

except Exception,message:
#if an Exception occurs execute required code,
#then re-raise Exception
  print 'This is a message.'
  raise Exception
```

The programmer may implement further exception classes extending `Exception` or other exceptions as appropriate. Custom exception classes have been created for this simulation in the "Exceptions.py" file which is thus the module "Exceptions".

In the simulation, calls to PSSE API functions are performed by objects with the definition in files starting `PSSE`. Every time an API function call is made, the error value returned is checked. Should the error value be greater than zero a custom exception is thrown. Most of the custom exceptions are of type `PSSEException` or `PSSEWarning`. If an error occurs as a result of a call to a load flow solver another exception `PSSESolverException` is raised. In addition to the exception type, a message is included which has been derived from the PSSE API user manual. In this way the simulation can catch certain types of exceptions and perhaps continue simulation after certain code is performed. If the situation is not retrievable the exception "bubbles-up" the execution stack until the program is forced to quit. This is invaluable for providing information as to whether the error occurs in the PSSE program, perhaps as a result of exceptional network values, or whether the error is in the control implementation.

A.2.8 Additional module: Useful

The "Useful.py" file contains some mathematical functions that were unable to be imported when running the Python scripts via PSSE due to errors during execution. Importantly an interpolation function and some improved collection types have been implemented.

The interpolation function allows the user to specify the time between each time-step. If the

load and generation time series have a different frequency then a new series is inferred using linear interpolation. For example, a steady generation time series can be defined using a two line file, each line having the required steady value.

A dictionary class is implemented that can be constructed with a default value. Normally a dictionary "value" is associated with a "key" which acts as an index. If the "key" is not present, the dictionary returns the default "value". This is useful for example when a minority of transformers have a specified controller type and the user wishes all other transformers to have a default type.

Appendix B
Supplementary results for Chapter 3

Figure B.1 shows three results of simulating the connection of DG to two points on a 11kV feeder. The DG output is varied according to three different data sets. The graphs show the tap operations made by the feeder's primary transformer in response to the connected load and DG. The output of the DG each time-step is determined by a different method for each graph.

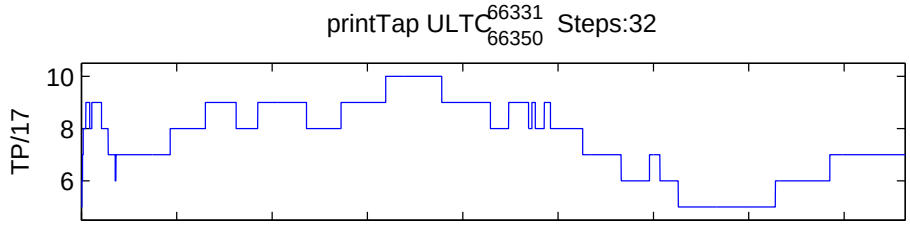

(a) Original windfarm real power output, day 1.

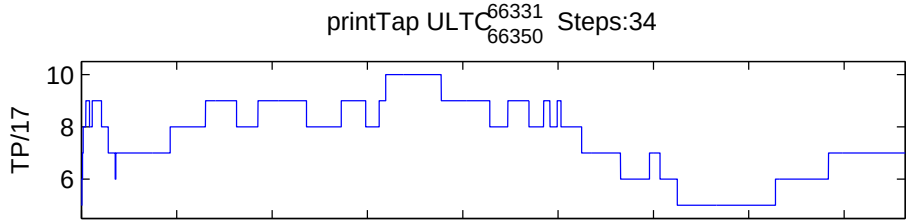

(b) Day 1 data undersampled. 120s sample period. Converted to 5s sample period by linear interpolation between data points.

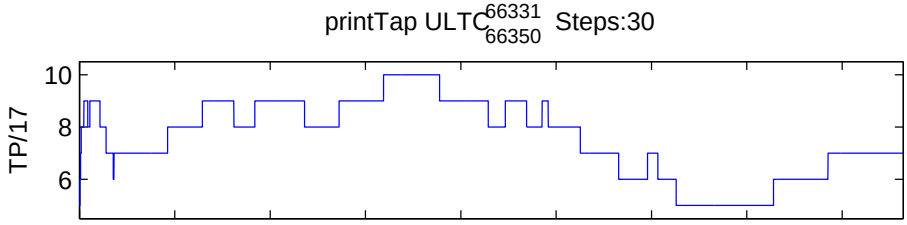

(c) Day 1 data averaged over 120s intervals. 120s sample period. Converted to 5s sample period by linear interpolation between data points.

Figure B.1: *Three plots showing ULTC tap position over a 1 day period when presented with different versions of the same data set.*

Appendix C
Supplementary results for Chapter 6

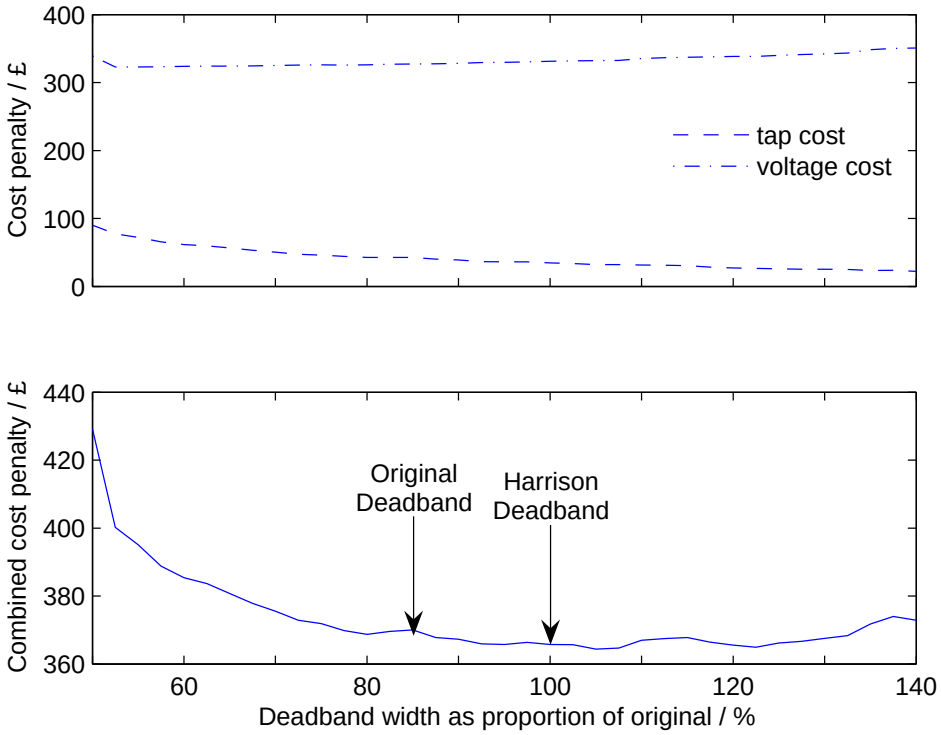

Figure C.1: *Cost penalty as a result of varying voltage dead-bands.*

References

[1] Energy Information Administration - Office of Integrated Analysis and Forecasting - U.S. Department of Energy, "International energy outlook 2006." http://www.eia.doe.gov/oiaf/ieo/ reprot number DOE/EIA-0484(2006).

[2] The DTI - UK, "Energy: its impact on the environment and society." http://www.dti.gov.uk/publications/ URN 02/1055, 2002.

[3] G. Harrison and A. Wallace, "Maximising distributed generation capacity in deregulated markets," in *Transmission and Distribution Conference and Exposition, 2003 IEEE PES*, vol. 2, pp. 527–530 vol.2, 2003.

[4] G. Harrison and A. Wallace, "Optimal power flow evaluation of distribution network capacity for the connection of distributed generation," *Generation, Transmission and Distribution, IEE Proceedings-*, vol. 152, no. 1, pp. 115–122, 2005.

[5] A. Wallace, A.R.; Kiprakis, "Reduction of voltage violations from embedded generators connected to the distribution network by intelligent reactive power control," *Power System Management and Control, 2002. Fifth International Conference on (Conf. Publ. No. 488)*, pp. 210–215, 17-19 April 2002.

[6] A. Kiprakis, *Increasing the capacity of distributed generation in electricity networks by intelligent generator control*. PhD thesis, University of Edinburgh, 2005.

[7] R. Finnie, "Securing a Renewable Future: Scotland's Renewable Energy." http://www.scotland.gov.uk/Publications/2003/03/16850/20554, March 2003. ISBN 0-7559-0766-3.

[8] Scottish Parliament, "Reports of likely windfarm development "overstated"." News Release http://www.scotland.gov.uk/News/Releases/2005/02/14120838, February 2005.

[9] C. Foote, G. Burt, I. Elders, and G. Ault, "Developing distributed generation penetration scenarios," in *Future Power Systems, 2005 International Conference on*, pp. 6 pp.–, 2005.

[10] R. Dodds, "Small generators-the connection to the public electricity network," in *Combined Cycle/Cogeneration Systems, IEE Colloquium on*, pp. 5/1 – 5/5, March 1995.

[11] K. Jarrett, J. Hedgecock, R. Gregory, and T. Warham, "Technical guide to the connection of generation to the distribution network: Appendix c." http://www.dti.gov.uk/publications/ URN 03/1631, February 2004.

[12] C. Masters, "Voltage rise: the big issue when connecting embedded generation to long 11 kv overhead lines," *Power engineering journal*, pp. Page(s): 5–12, February 2002. 00990181.pdf.

[13] The DTI for UK, "Digest of United Kingdom energy statistics." The Stationery Office, PO Box 29, Norwich NR3 1GN or `http://www.dti.gov.uk/energy/inform/dukes/index.shtml`, 2003.

[14] P. Glendinning, "Potential solutions to voltage control issues for distribution networks containing independent generators," in *Electricity Distribution, 2001. Part 1: Contributions. CIRED. 16th International Conference and Exhibition on (IEE Conf. Publ No. 482)*, vol. 4, June 2001.

[15] I. E. Consulting, M. C. for Electrical Energy, and UMIST, "Ancillary service provision from distributed generation." `http://www.dti.gov.uk/publications/index.html`, 2004.

[16] T. Boehme, A. R. Wallace, and G. P. Harrison, "Applying time series to power flow analysis in networks with high wind penetration," *Power Systems, IEEE Transactions on*, vol. 22, no. 3, pp. 951–957, 2007.

[17] N. Jenkins (working group secretary), "Cired working group no 4 on dispersed generation, preliminary report for discussion of." CIRED 1999, Nice, 2 June, June 1999. wg_04.

[18] Office of the Deputy Prime Minister UK, "Planning policy statement 22: Renewable energy." `http://www.communities.gov.uk/index.asp?id=1143909`, August 2004.

[19] T. Eberly and R. Schaefer, "Voltage versus var/power-factor regulation on synchronous generators," *Industry Applications, IEEE Transactions on*, vol. 38, no. 6, pp. 1682–1687, 2002.

[20] G. Strbac, N. Jenkins, M. Hird, P. Djapic, and G. Nicholson, "Integration of operation of embedded generation and distribution networks," Final report K/EL/00262/REP, UMIST and Manchester Centre for Electrical Energy, May 2002. kel00262.pdf.

[21] A. Collinson, F. Dai, A. Beddoes, and J. Crabtree, "Solutions for the connection and operation of distributed generation," Tech. Rep. K/EL/00303/00/01/REP URN 03/1195, EA Technology Ltd, 2003. kel00303.pdf.

[22] G59 G75 working group of the Distribution Code Review Panel, "Voltage step changes." `http://www.dcode.org.uk`, February 2007.

[23] A. Larsson, "Flicker emission of wind turbines during continuous operation," *Energy Conversion, IEEE Transaction on*, vol. 17, no. 1, pp. 114–118, 2002.

[24] N. Jenkins, R. Allan, P. Crossley, D. Kirschen, and G. Strbac, *Embedded Generation*. The IEE, 2000.

[25] C. Chell, "Fault level assessment: experience in distribution systems," in *Fault Level Assessment - Guessing with Greater Precision?, IEE Colloquium on*, pp. 6/1–6/4, January 1996.

[26] J. Fan and Z. Bo, "Modelling of on-load tap-changer transformer with variable impedance and its applications," in *Energy Management and Power Delivery, 1998. Proceedings of EMPD '98. 1998 International Conference on*, vol. 2, pp. 491–494 vol.2, 1998.

[27] K. Jarrett, J. Hedgecock, R. Gregory, and T. Warham, "Technical guide to the connection of generation to the distribution network." `http://www.dti.gov.uk/publications/` URN 03/1631, February 2004.

[28] Her Majestys Stationery Office - UK, "The electricity safety, quality and continuity regulations 2002." `http://www.uk-legislation.hmso.gov.uk/` ref: 2002 No. 2665.

[29] T. Burton, D. Sharpe, N. Jenkins, and E. Bossa, *Wind Energy Handbook*. Wiley, 2001.

[30] M. MacDonald, "The Carbon Trust & DTI renewables network impact study annex 3: distribution network topography analysis.," Tech. Rep. URN 03/1898/AN3, The Carbon Trust & DTI, 2003.

[31] J. Crabtree, Y. Dickson, L. Kerford, and A. Wright, "Methods to accommodate embedded generation without degrading network voltage regulation," Tech. Rep. ETSU K/EL/00230/REP, EA Technology, 2001. kel00230.pdf.

[32] H. Saadat, *Power System Analysis*. McGraw-Hill Higher Education, 2002.

[33] K. Harker, "Power system commissioning and maintenance practice," *IEE Review*, vol. 44, no. 5, pp. 221–221, 1998.

[34] Central Electricity Generating Board, *Modern Power Station Practice*, vol. 4. Pergamon, 1982.

[35] M. S. Calovic, "Modeling and analysis of under-load tap-changing transformer control systems," *IEEE Trans. on Power Apparatus and Systems*, vol. PAS-103, pp. 1909–1915, July 1984.

[36] W. Qiang, D. H. Popovic, and D. J. Hill, "Avoiding sustained oscillations in power systems with tap changing transformers," *International Journal of Electrical Power and Energy Systems*, vol. 22, pp. 597–605, 2000.

[37] B. Kasztenny, E. Rosolowski, J. Izykowski, M. Saha, and B. Hillstrom, "Fuzzy logic controller for on-load transformer tap changer," *Power Delivery, IEEE Transactions on*, vol. 13, pp. 164–170, January 1998. 00660874.pdf.

[38] M. Larsson, “Reduce tap changer wear and tear.” Transmission and Distribution World, April 1998. http://tdworld.com/mag/power_reduce_tap_changer/index.html.

[39] C. Smith, M. Redfern, and S. Potts, “Improvement in the performance of on-load tap changer transformers operating in series,” in *Power Engineering Society General Meeting, 2003, IEEE*, vol. 3, pp. –1910 Vol. 3, 2003.

[40] Electric Power Research Institute Inc., “Contact wear indicators for load tap changers and circuit breakers.” http://www.epri.com, 2003.

[41] B. Handley, M. Redfern, and S. White, “On load tap-changer conditioned based maintenance,” *Generation, Transmission and Distribution, IEE Proceedings-*, vol. 148, no. 4, pp. 296–300, 2001.

[42] H. Haring, “On-load tap changers current experience and future developments,” in *Developments On-Load Tapchangers: Current Experience and Future, IEE European Seminar on*, pp. 2/1–2/5, 1995.

[43] M. Redfern and W. Handley, “Duty based maintenance for on-load transformer tap changers,” in *Power Engineering Society Summer Meeting, 2001. IEEE*, vol. 3, pp. 1824–1829 vol.3, 2001.

[44] Scottish Hydro-Electric Transmission Ltd, “Statement of scottish hydro-electric transmission ltd’s basis of its transmission owner charges.” http://www.ofgem.gov.uk/Networks/Trans/ElecTransPolicy/Charging/Documents1/16890-2107b.pdf, April 2007.

[45] SP Transmission & Distribution, “Statement of the basis of transmission owner charges.” http://www.ofgem.gov.uk/Networks/Trans/ElecTransPolicy/Charging/Documents1/17054-21506_SPT.pdf, April 2007.

[46] J. Fan and S. Salman, “The effect of integration of wind farms into utility network on voltage control due to the co-ordination of avc relays,” in *Advances in Power System Control, Operation and Management*, vol. 1, pp. 260–265 vol.1, 1997.

[47] F. Jiang, S. K. Salman, V. Elaveeti, and R. Gupta, “Improvement of automatic voltage control of on-load tap-changer transformer in a distribution system with embedded generators,” in *proceedings of the 36th Universities Power Engineering Conference*, 2001.

[48] S. Salman and I. Rida, “Ann-based avc relay for voltage control of distribution network with and without embedded generation,” in *Electric Utility Deregulation and Restructuring and Power Technologies, 2000. Proceedings. DRPT 2000. International Conference on*, pp. 263–267, 2000.

[49] D. Bassett, "Control of tap change under load transformers through the use of programmable logic controllers," *Power Delivery, IEEE Transactions on*, vol. 8, pp. 1759 – 1765, October 1993. 00248283.pdf.

[50] J. Harlow, "Load tap changing controls as a power system nerve center," in *Transmission and Distribution Conference, 1994., Proceedings of the 1994 IEEE Power Engineering Society*, pp. 619–624, 1994.

[51] P. Okanik, B. Kurth, and J. Harlow, "An update on the paralleling of oltc power transformers," in *Transmission and Distribution Conference, 1999 IEEE*, vol. 2, pp. 871–875, 1999.

[52] Econnect Ltd, "Active local distribution network management for embedded generation." `http://www.dti.gov.uk/publications/index.html`, 2005.

[53] G. Kelly. Personal communication, May 2004. gordonkellymail.txt.

[54] Beckwith Electric Company, Application Engineering, "M-0067e tapchanger control." `http://www.beckwithelectric.com`.

[55] Beckwith Electric Company, Application Engineering, "Introduction to paralleling of ltc transformers by the circulating current method." `http://www.beckwithelectric.com`.

[56] T. E. Jauch, "Advanced transformer paralleling." `http://www.beckwithelectric.com`.

[57] J. Harlow, "Lets rethink negative reactance transformer paralleling," in *Transmission and Distribution Conference and Exposition, 2003 IEEE PES*, vol. 2, pp. 434–438 vol.2, 2003.

[58] E. Lakervi and E. Holmes, *Electricity distribution network design*. Peter Peregrinus Ltd., 2003.

[59] M. Thompson, "Automatic-voltage-control relays and embedded generation: Part 2," *Power Engineering Journal*, pp. 93–99, June 2000.

[60] P. Cartwright, L. Holdsworth, J. Ekanayake, and N. Jenkins, "Co-ordinated voltage control strategy for a doubly-fed induction generator (dfig)-based wind farm," in *Generation, Transmission and Distribution, IEE Proceedings-*, vol. 151, pp. 495 – 502, July 2004. CoordinatedVoltageControlStrategyDFIG.pdf.

[61] B. Delfino, G. Denegri, A. Invernizzi, and S. Massucco, "Voltage regulation issues in a deregulated environment," in *Transmission and Distribution Conference and Exposition, 2001 IEEE/PES*, vol. 1, pp. 264–269 vol.1, 2001.

[62] I. El-Samahy and E. El-Saadany, "The effect of dg on power quality in a deregulated environment," in *Power Engineering Society General Meeting, 2005. IEEE*, pp. 2969–2976 Vol. 3, 2005.

[63] R. Dugan and T. McDermott, "Operating conflicts for distributed generation on distribution systems," in *Rural Electric Power Conference, 2001*, pp. A3/1–A3/6, 2001.

[64] E. Larsen, N. Miller, S. Nilsson, and S. Lindgren, "Benefits of gto-based compensation systems for electric utility applications," *Power Delivery, IEEE Transactions on*, vol. 7, no. 4, pp. 2056–2064, 1992.

[65] J. Paserba, D. Leonard, N. Miller, S. Naumann, M. Lauby, and F. Sener, "Coordination of a distribution level continuously controlled compensation device with existing substation equipment for long term var management," *Power Delivery, IEEE Transactions on*, vol. 9, no. 2, pp. 1034–1040, 1994.

[66] K. Son, K. Moon, S. Lee, and J. Park, "Coordination of an svc with a ultc reserving compensation margin for emergency control," *Power Delivery, IEEE Transactions on*, vol. 15, pp. 1193–1198, October 2000. 00891502.pdf.

[67] C. Smith, S. Potts, and M. Redfern, "Simulation studies of oltc transformer avc relays operating in series using a rtds, real time digital simulator," in *Developments in Power System Protection, 2004. Eighth IEE International Conference on*, vol. 2, pp. 619–622 Vol.2, 2004.

[68] F. Carbone, G. Castellano, and G. Moreschini, "Coordination and control of tap changers under load at different voltage level transformers," in *Electrotechnical Conference, 1996. MELECON '96., 8th Mediterranean*, vol. 3, pp. 1646 – 1648, May 1996.

[69] M. Larsson and D. Karlsson, "Coordinated control of cascaded tap changers in a radial distribution network," 1995.

[70] M. Larsson, *Coordination of cascaded tap changers using a fuzzy-rule-based controller*, vol. 102, pp. 113–123. Amsterdam, The Netherlands, The Netherlands: Elsevier North-Holland, Inc., 1999.

[71] M. Suzuki, E. Morima, T. Minakawa, and K. Sato, "Coordinated avqc operations of ehv transformer's tap changer by fuzzy expert control system," in *Power System Technology, 2002. Proceedings. PowerCon 2002. International Conference on*, vol. 3, pp. 1679–1684 vol.3, 2002.

[72] R. Schaefer, "Excitation control of the synchronous motor," *Industry Applications, IEEE Transactions on*, vol. 35, no. 3, pp. 694–702, 1999.

[73] A. Godhwani, M. Basler, K. Kim, and T. Eberly, "Commissioning experience with a modern digital excitation system," *Energy Conversion, IEEE Transactions on*, vol. 13, no. 2, pp. 183–187, 1998.

[74] OXERA Consulting Ltd, "Technical guide to the connection of generation to the distribution network: Appendix c." `http://www.dti.gov.uk/publications/` URN 03/1631, September 2004.

[75] G. Harrison and A. Wallace, "Maximising distributed generation capacity in deregulated markets," *IEE Proceedings*, vol. 152, pp. 115 – 122, Jan. 2005. 01393425wallace.underscore.harrison2005.pdf.

[76] D. Harrison, "Loading capabilities of large power transformers," *Power Engineering Journal [see also Power Engineer]*, vol. 9, no. 5, pp. 225–230, 1995.

[77] P. Brown and J. White, "Determination of the maximum cyclic rating of high-voltage power transformers," *Power Engineering Journal [see also Power Engineer]*, vol. 12, no. 1, pp. 17–20, 1998.

[78] Shaw Power Technologies Inc., *Online Documentation - PSS/E 30: PSS/E Application Program Interface*, August 2004.

[79] Shaw Power Technologies Inc., *Online Documentation - PSS/E 30: PSS/E IPLAN Program Manual*, August 2004.

[80] J. B. O'Donnell, "Using python to automate psse." `http://www.see.ed.ac.uk/~jbo/PSSE_Python/index.html`, 2004. Work in progress.